

# **The Small Ubiquitin-related modifier (SUMO) regulates *Drosophila* NF- $\kappa$ B signaling**

**A thesis**

**Submitted in partial fulfilment of the requirements**

**of the degree**

**Doctor of Philosophy**

**By**

**Sushmitha Hegde**

**20152016**



**Indian Institute of Science Education and Research, Pune**

## Certificate

I certify that the original work presented in this thesis titled 'The Small Ubiquitin-related modifier (SUMO) regulates *Drosophila* NF- $\kappa$ B signaling' was carried out by Ms. Sushmitha Hegde at IISER, Pune, under my guidance, from August 2017 to July 2022. The work presented here or a part of it has not been included in any other thesis submitted previously for the award of any degree or diploma from any other University or institution.



Girish Ratnaparkhi

Thesis supervisor

12.07.2022

## Declaration

I declare that this written submission represents my ideas in my own words, and where others' ideas have been included, I have adequately cited and referenced the original sources. I also declare that I have adhered to all academic honesty and integrity principles and have not misrepresented, fabricated, or falsified any idea/data/fact/source in my submission. I understand that violation of the above will be cause for disciplinary action by the Institute and can also evoke penal action from the sources, which have thus been appropriately cited, or from whom proper permission has not been taken when needed.



Sushmitha Hegde

12.07.2022

## Acknowledgments

“Did I test the hypothesis, or did the hypothesis test me?”

-Anon

I am grateful to my supervisor Dr. Girish Ratnaparkhi for his constant support, advice, and patience during my Ph.D. study. He has always been approachable, attentive to ideas and results, and provided immense freedom to conduct my research. His encouragement and kindness were instrumental in keeping me motivated through the peaks and troughs of my research journey. I thank him for the constant reaffirmation of the joy and beauty of stories.

I thank my research advisory committee members, Dr. L.S Shashidhara and Dr. Jomon Joseph, for their timely suggestions and for keeping my research on track. The inputs provided by Dr. Deepti Trivedi, NCBS *Drosophila* facility, were invaluable in designing the gRNA and ssODN for the CRISPR-Cas9 experiment. I thank Dr. Richa Rikhy, Dr. Girish Deshpande, and Dr. Anuradha Ratnaparkhi for the fruitful discussions. I also thank Dr. Kundan Sengupta and Dr. Nishad Matange for providing exposure to exciting and diverse science during my initial years at IISER. I thank members of the fly facility, Microscopy facility, and Mass spectrometry facility for aiding in the smooth execution of my experiments. I thank the amicable non-teaching staff of the Biology department for their support in facilitating hassle-free research.

I was lucky to have congenial work colleagues in the GR lab. I thank them for the enriching work experience. Special thanks to Amar for mentoring me during the initial years and being a keen sounding board for my work later. His unbiased and valuable advice on all things will be missed. Warm thanks are owed to Roopali and Swati for the “big picture” discussions providing much-needed perspective during trying times.

This journey would have been impossible without the support from my wonderful parents, Mr. Rajaram Hegde and Mrs. Sukanya Hegde, brother Supraj Hegde, and extended family. I thank them for their empathy and for being there for me despite not completely understanding the nature of my work or its demands.



I would like to thank the batch of Integrated Ph.D. 2015 for all the fantastic memories. Big thanks to my friends Aparna and Meenakshi, who have been unwavering constants throughout my Ph.D. Aparna has always been a compassionate listener and an accomplice through thick and thin. Her positive outlook made her the go-to person to discuss anything under the sun. My Ph.D. experience was better for having known her. Meenakshi has pushed me to do better and has always been a reliable accountability buddy. I will miss them dearly.

Like Ulysses' legendary voyage to the island of Ithaca, my Ph.D. gave me a marvelous journey without which I would not have set out. There were Lastrigonians and Cyclopes but also mother of pearl, ebony, and coral. And I wouldn't have it any other way.

## Synopsis

The nuclear factor- $\kappa$ B (NF- $\kappa$ B) family of transcription factors plays crucial roles in cell survival and immunity. In *Drosophila*, the two major NF- $\kappa$ B signaling cascades, Toll and IMD, deploy the NF- $\kappa$ B effectors Dorsal/Dif and Relish, respectively. The Toll pathway has also been co-opted for embryonic development in addition to immunity. Post-translational modifications (PTMs), such as phosphorylation, ubiquitination, and, more recently, SUMOylation, have been shown to determine the outcome of NF- $\kappa$ B signaling. The Small Ubiquitin-related modifier (SUMO) is a polypeptide modifier conferring diverse fates to target proteins, affecting the activity, localization, and interaction potential of proteins. Few studies have explored the physiological consequences of SUMOylation of specific proteins in a living organism due to challenges presented by genetic manipulation and subsequent phenotypic analysis. As part of my doctoral research, I have dissected the functional consequence of SUMOylation of two proteins, Dorsal (DL) and Casp (Casp), in two distinct NF- $\kappa$ B signaling cascades.

Since the site of SUMO conjugation for DL was known, I began my study by engineering a fly line expressing the SUMO-conjugation resistant DL<sup>K382R</sup> variant using CRISPR-Cas9 gene editing. This fly line was homozygous viable and was evaluated for defects in embryonic patterning and immunity. Early development proceeded normally in these mutant flies. Interestingly, we observed differences in embryonic viability between the *dl*<sup>K382R</sup> mutants and wild-type animals in the context of DL haploinsufficiency at higher temperatures. Unlike their wild-type counterparts, the *dl*<sup>K382R</sup> mutants fared better and completed the developmental program. An *in-situ* hybridization experiment for DL targets and a quantitative 3'-RNA sequencing indicated that the rescue was due to a better transcriptional activity of DL<sup>K382R</sup>. Therefore, we inferred that SUMO dampens transcriptional activity in the embryo during genetic and environmental perturbations.

Next, I evaluated the larval immune response in these mutants. In the cellular response, the population of crystal cells, platelet-like cells necessary for wound healing, was dramatically increased. In the humoral response, Toll-specific antimicrobial peptides (AMPs) were upregulated. An analysis of DL localization in the

fat body, a key site of AMP production, paradoxically determined that DL<sup>K382R</sup> was less abundant in the nuclei. An assay of the protein levels of Cact, a cytoplasmic inhibitor and transcriptional target of DL, indicated higher levels in the fat body. Additionally, a mathematical model supports the notion that SUMO regulates DL at the transcriptional level to modulate the observed outcomes. Taken together, we conclude that SUMO attenuates DL activity in both developmental and immune contexts.

Having established roles for SUMO in Toll/DL signaling, we turned our attention to the role of SUMO in modulating the function of Caspar (Casp), a negative regulator of IMD signaling. Previous studies in the lab identified the site of SUMO modification, and the fly line harboring the *casp*<sup>K551R</sup> mutation was created. The SUMO-conjugation resistant *casp*<sup>K551R</sup> flies exhibited an altered lifespan but did not demonstrate immune phenotypes, evaluated by a bacterial clearance assay. Additionally, we were unsuccessful in our attempts to identify SUMOylated Casp in the fly upon an immune challenge and a heat shock. The putative role of SUMO in regulating Casp function in *Drosophila* lifespan warrants further investigation.

During our investigation into Casp, we realized that little is known about its molecular function in immunity or otherwise. We uncovered a novel maternal role for this protein and investigated embryonic phenotypes further to understand Casp function. Using a robust hypomorphic allele transheterozygous with a *Casp* deficiency, we found that embryos lacking *casp* do not progress to gastrulation. Mass spectrometric analysis of the Casp interactome indicated a repertoire of interactors unique to Casp and conserved with the mammalian ortholog. Evaluation of the topmost interactor, the transitional endoplasmic reticulum ATPase (TER94), revealed functions in the early embryo as well. Loss of *casp* and *ter94* in the embryo resulted in aberrant nuclear division, cytoskeletal assembly, and primordial germ cell formation. A preliminary analysis of animals lacking functional Casp domains suggests a critical role for the Casp-TER94 axis in mediating embryonic development.

## Publications

1. **Hegde, S.**, Sreejan, A., Gadgil, C. J., & Ratnaparkhi, G. S. SUMOylation of Dorsal attenuates Toll/NF- $\kappa$ B signaling. *Genetics*.
2. Tendulkar, S., **Hegde, S.**, Garg, L., Thulasidharan, A., Kaduskar, B., Ratnaparkhi, A., & Ratnaparkhi, G. S. (2022). Caspar, an adapter for VAPB and TER94, modulates the progression of ALS8 by regulating IMD/NF $\kappa$ B-mediated glial inflammation in a Drosophila model of human disease. *Human Molecular Genetics*.
3. **Hegde, S.**, Soory, A., Kaduskar, B., & Ratnaparkhi, G. S. (2020). SUMO conjugation regulates immune signalling. *Fly*, 14(1-4), 62-79.

## Table of contents

Chapter 1: An introduction to SUMO and NF- $\kappa$ B signaling.....	16
1.1 Abstract.....	16
1.2 What is SUMO conjugation? .....	18
1.3 What is the effect of SUMO conjugation on the substrate? .....	20
1.4 SUMO in host defence .....	22
1.5 SUMOylation regulates Toll/TLR signaling.....	24
1.6 SUMOylation regulates TNF/ IMD signaling.....	29
1.7 Aim of the study.....	35
1.8 References.....	36
Chapter 2: SUMOylation of Dorsal attenuates Toll/NF- $\kappa$ B signaling; a developmental perspective .....	50
2.1 Abstract.....	50
2.2 Introduction .....	51
2.3 Results .....	52
2.3.1 Generation of a genome-edited <i>dl</i> <sup>K382R</sup> mutant.....	52
2.3.2 Early development proceeds normally in <i>dl</i> <sup>SCR</sup> embryos .....	55
2.3.3 Haploinsufficiency of <i>dl</i> is rescued in <i>dl</i> <sup>SCR</sup> embryos .....	57
2.3.4 DL <sup>SCR</sup> supports the developmental program under haploinsufficient conditions. .....	59
2.3.5 DL <sup>SCR</sup> is a stronger transcriptional activator than DL <sup>WT</sup> under conditions of haploinsufficiency.....	63
2.4 Discussion.....	67
2.5 Materials and Methods .....	68
2.6 References.....	72
Chapter 3: SUMOylation of Dorsal attenuates Toll/NF- $\kappa$ B signaling; an immune perspective.....	81

3.1 Abstract.....	81
3.2 Introduction .....	82
3.3 Results .....	82
3.3.1 SUMO restrains DL activity in the larval immune response.....	82
3.3.2 Dynamics of nuclear import of DL <sup>SCR</sup> in the larval fat body .....	87
3.3.3 A mathematical model to investigate the activity of SUMOylated DL .....	90
3.4 Discussion .....	93
3.5 Materials and Methods .....	97
3.6 References.....	101
Chapter 4: SUMOylation of Caspar, a negative regulator of IMD .....	106
4.1 Abstract.....	106
4.2 Introduction .....	107
4.3 Results .....	112
4.3.2 Altered lifespan in <i>Casp</i> <sup>K551R</sup> mutants. ....	117
4.3.3 Bacterial clearance remains unchanged in <i>Casp</i> <sup>K551R</sup> mutants .....	118
4.3.4 A possible maternal role for Casp? .....	119
4.4 Discussion .....	120
4.5 Materials and methods .....	121
4.6 Contributions/Notes:.....	122
4.7 References.....	123
Chapter 5: Caspar is a maternal effect gene required for early development .....	130
5.1 Abstract.....	130
5.2 Introduction .....	131
5.3 Results .....	133
5.3.1 <i>Casp</i> <sup>lof</sup> is a robust hypomorphic <i>Casp</i> allele.....	133
5.3.2 Casp function is required for early embryonic development.....	135
5.3.3 Casp interacts with TER94 and VAP in the early embryo .....	137

5.3.4 TER94 is required maternally .....	138
5.3.5 Caspar regulates primordial germ cell number.....	141
5.3.6 Function of Casp domains.....	143
5.4 Discussion .....	144
5.5 Materials and methods .....	147
5.6 References .....	150
Copyright Permissions .....	159
Appendix I: validation of SUMO targets in the 0-3 h embryo.....	159
I.1 Introduction .....	160
I.2 Results .....	161
I.2.1 RNAi-based knockdown of SUMO cycle components.....	161
Table 1: Lines tested for Maternal knockdown of SUMO cycle elements.....	162
Table 2: Lines tested for knockdown of SUMO/ SUMO cycle components in the embryo. ....	163
I.2.2 Proteins in <i>Drosophila</i> axis patterning events as potential SUMO targets.....	164
Table 3: Potential SUMO Targets in early <i>Drosophila</i> development. ....	164
I.2.3 14-3-3 $\epsilon$ is SUMOylated <i>in bacto</i> .....	166
I.2.4 dUbc9 is SUMOylated <i>in bacto</i> .....	167
I.3 Discussion.....	169
I.4 Materials and methods .....	170
I.5 Contributions/Notes:.....	172
I.6 References .....	173
Appendix II: SUMOylation of DL; a contrasting tale of the UAS-GAL4 system.....	175
II.1 Introduction .....	175
II.2 Results .....	175
II.2.1 Validation of transgenic constructs.....	175
II.2.2 DL <sup>K382R</sup> mutants are defective in DV patterning.....	176

II.2.3 DL <sup>K382R</sup> fails to enter the nucleus .....	178
II.2.4 DL <sup>K382R</sup> is unstable in the 0-3 hr embryo .....	179
II.2.5 DL <sup>K382R</sup> retains its function in the presence of a wild-type Dorsal .....	180
II.3 Discussion .....	181
II.4 Materials and methods .....	182
II.5 Contributions/Notes: .....	184
II.6 References .....	184
Appendix III: SUMOylation of DL and the stress response in adults .....	186
III.1 Introduction .....	186
III.2 Results .....	186
III.2.1 Toll signaling in adult <i>d/SCR</i> animals .....	186
III.2.2 <i>d/SCR</i> animals succumb to infection .....	188
III.2.3 <i>d/SCR</i> animals are sensitive to starvation .....	189
III.3 Discussion .....	189
III.4 Materials and Methods .....	190
III.5 Notes: .....	191
III.6 References .....	191



## List of figures

Fig. 1.1. SUMO Conjugation of a substrate protein. ....	19
Fig. 1.2. SUMO targets in immune signaling. ....	23
Fig. 1.3. Mechanistic models for SUMO regulation of Toll/TLR signaling. ....	26
Fig. 1.4. Mechanistic models for SUMO Regulation of IMD/TNF signaling. ....	31
Fig. 2.1. Creating the <i>dI<sup>K382R</sup></i> mutant using the CRISPR-Cas9 system. ....	53
Fig. 2.2. <i>dI</i> transcripts express at similar levels in <i>dI<sup>WT</sup></i> and <i>dI<sup>SCR</sup></i> . ....	54
Fig. 2.3. SUMO conjugation is dispensable for embryonic development. ....	56
Fig. 2.4. <i>dI<sup>SCR</sup></i> is haplo-sufficient. ....	58
Fig. 2.5. Haplo-sufficiency of the <i>dI<sup>SCR</sup></i> allele. ....	59
Fig. 2.6. DL activity is altered in the SUMO-deficient mutant. ....	62
Fig. 2.7. The DL gradient visualized with a DL antibody in <i>control</i> , <i>dI<sup>WT</sup>/Df</i> , and <i>dI<sup>SCR</sup>/Df</i> embryos. ....	63
Fig. 2.8. DL <sup>SCR</sup> displays higher transcriptional activity. ....	64
Fig. 2.9. Quantitative changes in the transcriptome of embryos laid by <i>dI<sup>SCR</sup></i> mothers .....	66
Fig. 3.1. DL <sup>SCR</sup> is a robust immune effector in the larva. ....	84
Fig. 3.2. <i>dI<sup>1</sup></i> is a S317N mutant and is resistant to Toll signaling. ....	85
Fig. 3.3. Crystal cells in <i>dI<sup>SCR</sup></i> , <i>dI<sup>1</sup>/dI<sup>SCR</sup></i> , and <i>dI<sup>4</sup>/dI<sup>SCR</sup></i> larvae. ....	86
Fig. 3.4. AMPs are upregulated in <i>dI<sup>SCR</sup></i> animals. ....	87
Fig. 3.5. DL <sup>SCR</sup> is responsive to Toll signaling in the larval fat body. ....	89
Fig. 3.6. Cact levels are elevated in <i>dI<sup>SCR</sup></i> animals. ....	90
Fig. 3.7. Mathematical model to understand roles for SUMOylated DL. ....	91
Fig. 3.8. DL SUMOylation attenuates Toll signaling. ....	94
Fig. 4.1. Casp is a FAF1 ortholog. ....	108
Fig. 4.2. FAF1 domains and modifications modulate function. ....	109
Fig. 4.3. FAF1 interacts with polyubiquitinated proteins, VCP, and VAP. ....	110
Fig. 4.4. SUMO predictions for Casp. ....	111

Fig. 4.5. Immunoprecipitation of Casp with a Casp-specific antibody. ....	113
Fig. 4.6. Evaluating SUMOylation of Casp under conditions of immune stress. ....	116
Fig. 4.7. Attempt to detect SUMOylated Casp in response to heat stress. ....	116
Fig. 4.8. Confirming the presence of the K551R mutation in the CRISPR-Cas9 Casp gene-edited lines. ....	117
Fig. 4.9. SUMO-conjugation-resistant Casp mutants exhibit altered lifespan. ....	118
Fig. 4.10. Bacterial clearance is comparable across control and SUMO-conjugation-resistant Casp mutants. ....	119
Fig. 4.11. Casp is deposited maternally. ....	120
Fig. 5.1. Patterning in the fly. ....	132
Fig. 5.2. Casp <sup>lof</sup> is a hypomorphic Casp allele. ....	134
Fig. 5.3. Casp assists in progression to gastrulation. ....	136
Fig. 5.4. Casp <sup>lof</sup> /Df embryos display nuclear division and cytoskeletal defects. ....	136
Fig. 5.5. TER94 and VAP33 are major interactors of Casp. ....	138
Fig. 5.6. TER94 is required maternally. ....	140
Fig. 5.7. Casp influences PGC number. ....	142
Fig. 5.8. Casp domain deletions and their predicted interaction dynamics. ....	144
Fig. 5.9. Global ubiquitination profile in <i>casp<sup>lof</sup></i> and <i>ter94<sup>i</sup></i> embryos. ....	146
Fig. I.1. Maternal knockdown of SUMO components. ....	161
Fig. I.2. Early embryonic lethality was observed upon the knockdown of SUMO cycle components. ....	164
Fig. I.3. SUMOylation predictions for 14-3-3 $\epsilon$ . ....	166
Fig. I.4. 14-3-3 $\epsilon$ is SUMOylated in a bacterial SUMOylation assay. ....	167
Fig. I.5. SUMO predictions for dUbc9. ....	168
Fig. I.6. dUbc9 is SUMOylated in a bacterial SUMOylation assay. ....	169
Fig. II.1. Validation of <i>UAS-dl</i> constructs. ....	176
Fig. II.2. DL <sup>K382R</sup> animals are defective in DV patterning. ....	177
Fig. II.3. DL <sup>K382R</sup> is undetectable in the ventral nuclei. ....	178

Fig. II.4. DL <sup>K382R</sup> is degraded in the embryo. ....	179
Fig. II. 5. DL <sup>K382R</sup> can carry out its function in the presence of wild type Dorsal. ....	181
Fig. III.1. Toll signaling in <i>dI<sup>SCR</sup></i> animals. ....	187
Fig. III.2. <i>dI<sup>SCR</sup></i> animals are susceptible to infection. ....	188
Fig. III.3. <i>dI<sup>SCR</sup></i> animals are susceptible to starvation. ....	189

## Chapter 1: An introduction to SUMO and NF- $\kappa$ B signaling

### 1.1 Abstract

Post-translational modifiers (PTMs) are critical drivers and attenuators of signaling cascades. The NF- $\kappa$ B signaling cascade has been well studied in the context of immunity and inflammation. PTMs transduce signals initiated at pattern recognition receptors on the cell surface, which recognize the pathogen. These signals reach the transcriptional master regulators that switch on/off genes essential for the host defense. In this chapter, I introduce functional roles for a PTM, small ubiquitin-like modifier (SUMO), in regulating NF- $\kappa$ B signaling in *Drosophila*. I list known SUMO substrate proteins in the core signaling pathways and discuss, using the few mechanistic studies that exist, the effect of SUMO conjugation on signaling and possible molecular models that explain SUMO regulation.

**Keywords:** Immunity, PTM, signal transduction, SIM, Ubiquitin, Activation

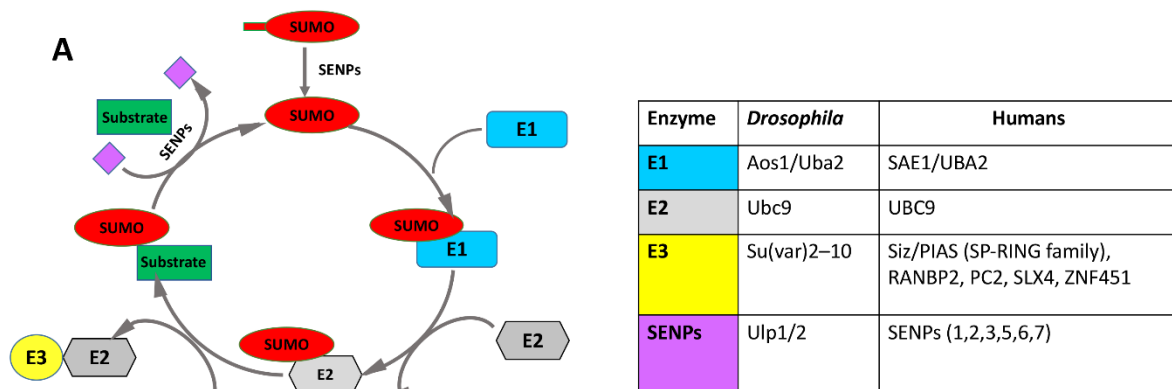
Proteins undergo post-translational modifications (PTM). The PTMs modifying the substrate protein can modulate its structure, folding, stability, dynamics, function, or location. The effect of the PTM on the substrate protein is often context-dependent, with the kind of PTMs or the timing or location of a modification affecting function in a differential manner. PTMs come in all shapes and sizes with various chemical groups. PTMs can be small such as phosphate, intermediate in size, such as lipids, or large such as attachments of sugar polymers (Garcia, 2019; Harding & Crabbe, 1991; Voet et al., 2006; Walsh et al., 2005). Proteins can themselves modify other proteins by conjugating to specific side-chains. The best-studied examples of protein modifiers are Ubiquitin-like proteins (UBLs), which include a diverse group of proteins with a Ubiquitin fold, inclusive of Ubiquitin, Nedd8, ISG15, FUB1, UBL5, URM5, SUMO, ATG8/12 and many others (Cappadocia & Lima, 2018; Eifler & Vertegaal, 2015; van der Veen & Ploegh, 2012; Vierstra, 2012). The protein PTMs conjugate a wide variety of protein substrates, primarily targeting lysine side chains. Considering the large variety of PTMs, the large number of proteins that they target, and the growing evidence that each substrate protein is a target of multiple PTMs, a functional landscape for each protein can be envisaged, where its native unconjugated state can be tweaked in a multitude of ways depending on the sequence and combination of PTMs. At this point, with the advent of high throughput proteomics, researchers are generating lists of proteins that are post-translationally modified. Still, functional implications of the effect of a single PTM on protein function, leave alone the combinatorial/sequential effects of multiple PTMs, are far from being completely understood.

The Small Ubiquitin-like modifier (SUMO) (Hay, 2005), initially christened as Smt3 (Suppressor Of Mif Two 3 Homolog 1) (Johnson et al., 1997; Matunis et al., 1996; Melchior, 2000; Meluh & Koshland, 1995; Saitoh et al., 1997; Seufert et al., 1995; Wilson, 2017) is a PTM distinct from its more famous cousin Ubiquitin, with which it shares a common fold, but <20% sequence identity. SUMO maturation, conjugation, and de-conjugation require a distinct set of enzymes that do not appear to overlap with any other UBL (Geiss-Friedlander & Melchior, 2007; Hay, 2005; Melchior, 2000; Talamillo et al., 2008; Vierstra, 2012) (Fig. 1.1A). Proteomic studies indicate that SUMO modifies 10-20% of the proteome, depending on the context (Golebiowski *et al.* 2009; Tammsalu *et al.* 2014; Hendriks *et al.* 2017; Pirone *et al.* 2017).

## 1.2 What is SUMO conjugation?

SUMO conjugation, or SUMOylation, involves the covalent attachment of the C-terminal carboxyl of the polypeptide chain to the  $\zeta$  amino group of a lysine residue on the substrate by an iso-peptide bond. SUMO, synthesized as an inactive precursor, is matured with the aid of Sentrin-specific proteases (SENPs) (Hay, 2005, 2013; Mukhopadhyay & Dasso, 2017), also called ubiquitin-like specific proteases (ULPs), exposing a diglycine motif at the SUMO C terminus (Fig. 1.1). Activation occurs at an active cysteine residue of the heterodimeric E1 complex of activating enzymes (SAE1/SAE2) accompanied by ATP hydrolysis.

SUMO is then transferred to the cysteine of the single E2 SUMO-conjugating enzyme, Ubc9, which mediates SUMO conjugation to the target lysine with SUMO E3 ligases (Geiss-Friedlander & Melchior, 2007; Hay, 2005) providing specificity in the cell. SENPs act as both deconjugases and maturases, though they exhibit specificity for particular SUMO isoforms (Kunz et al., 2018). Other SUMO deconjugating enzymes like DES1/2 and USPL1 have recently been discovered, though their functions in SUMO maturation are minimal (Nayak & Müller, 2014).



**B**

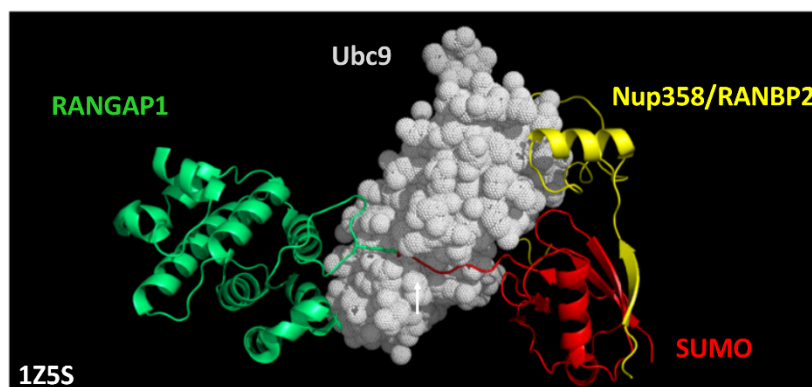


**Fig. 1.1. SUMO Conjugation of a substrate protein.**

A. The SUMO conjugation/de-conjugation cycle. The addition and removal of SUMO to a target substrate are under enzymatic control. The first step is the maturation of SUMO by an endoprotease, named sentrin-specific protease (SENPs) or Ub-like specific protease (ULP) that exposes the C-terminal di-glycine motif. Next, the E1 heterodimer engages with SUMO via a thioester linkage and subsequently hands it over to the E2 enzyme. The E2 then interacts with the substrate and catalyses the conjugation of the C-terminal COOH of SUMO to a specific lysine side-chain of the substrate. This conjugation step may be either enhanced or directed by a E3 'ligase' enzyme. Tabulated on the right hand side are proteins involved in regulating the SUMO cycle.

B. Crystal structure (1Z5S;(Reverter & Lima, 2005)) of SUMO conjugated to RANGAP1 (substrate) by the E2 (Ubc9), with Nup358 acting as an E3 ligase. The structure shows the interaction between the substrate (RANGAP1) and Ubc9, as well as the cleft/tunnel (white arrow) in Ubc9 that holds the C-terminal GG tail of SUMO for conjugation with the lysine side chain of RANGAP1. The figure was generated using coordinates from the PDB using PyMol (The PyMOLMolecular Graphics System, Version 1.5.0.4 Schrödinger, LLC).

A SUMOylated substrate is deconjugated with the aid of SENPs, making it available for a new conjugation cycle (Fig. 1.1A). Genomes of organisms such as *S. cerevisiae* and *Drosophila* have a single SUMO gene, while mammals have five SUMO paralogs (Citra & Chiocca, 2013; Liang et al., 2016). A major targeting motif for SUMO is the lysine residue in the core sequence  $\psi$ -**K**-X- $\alpha$  or its inverted variant  $\alpha$ -X-**K**- $\psi$ , with  $\psi$  representing a hydrophobic amino acid, usually isoleucine, leucine or Valine and  $\alpha$  representing a negatively charged side chain, usually glutamic acid or aspartic acid. Other 'extended' variants of this canonical conjugation motif have also been defined (Beauclair et al., 2015), which allows the prediction of target lysines for experimental testing. Studies over the last decade have confirmed that prediction accuracy hovers at ~50%, suggesting that lysines within non-canonical motifs are also routinely SUMOylated. At this point, we do not entirely understand the molecular basis of motif recognition (Cappadocia & Lima, 2018). The first crystal structure of the complex of E2/E3/Substrate/SUMO1 was solved by Christopher Lima's group (Reverter & Lima, 2005) (Fig. 1.1B) and subsequently followed by other structures (PDB: 3UIO, 3UIN) that uncovered molecular interactions between these molecules. These structures confirm that the E2 (Ubc9) brings together the substrate (RANGAP1) with SUMO. The conjugation event occurs in a deep groove in Ubc9 (arrow, Fig. 1.1B). Nup358/RanBP2 stabilizes the complex and enhances SUMO conjugation, acting as an E3.

### 1.3 What is the effect of SUMO conjugation on the substrate?

The power of SUMO conjugation lies in the versatility that it affords to the biological function of its substrate. For example, SUMO may change the conformation of a protein upon binding, exemplified by the human thymine DNA glycosylase. This SUMO1-modified protein displays altered DNA binding without limiting its enzymatic activity, allowing it to dissociate from DNA (Steinacher & Schär, 2005). SUMO can also decide the fate of a protein by competing with modifications like ubiquitination, acetylation, or methylation at the identical lysine residue. In the case of hormone receptors like Glucocorticoid receptor (GR) or Androgen receptor (AR), the SUMO-modified lysine competes with ubiquitin, affecting the rate of turnover (Chymkowitch et al., 2011). In this way, changes in turnover can affect transcriptional output. In other instances, like the SUMO modification of c-Jun and c-Fos, components of the AP-1 dimer, the half-life may remain unaltered, but transcriptional activity is reduced (Bossis et al., 2005; Müller et al., 2000). Biochemical analysis of non-SUMOylatable c-Fos suggests that accumulation at the promoters may be altered to fine-tune gene regulation, though the exact mechanism remains to be ascertained (Tempé et al., 2014). These examples demonstrate that SUMO modification of a subset of transcription factors (TFs) plays a crucial role in their regulation. Though SUMO negatively regulates the majority of TFs, a fraction is also positively regulated. The heat shock factor HSF1 is SUMO modified upon heat stress, enhancing DNA binding (Hong et al., 2001). SUMOylation is also known to alter the subcellular localization of proteins. One example is the transcription factor Medea (Med), the *Drosophila* ortholog of Smad4. SUMOylation of Med promotes nuclear export and hence negatively regulates Dpp signaling in the embryo (Miles et al., 2008).

Identifying a hydrophobic motif, designated SUMO-interacting motif (SIM) or SUMO-binding motif (SBM) that can interact non-covalently with SUMO has helped understand SUMO-mediated protein interactions. The trafficking protein RanGAP1 is SUMOylated and associated with the nuclear pore complex protein RanBP2 via the SIM motif of RanBP2 (Song et al., 2004). There are several instances where SUMO has been shown to regulate protein stability, targeting modified proteins to the proteasomal degradation machinery (Ghioni et al., 2005; Gresko et al., 2005; Klenk et al., 2006). A particular case is the ubiquitination of SUMOylated proteins where a



dedicated ubiquitin E3 ligase recognizes poly-SUMO chains, targeting them for ubiquitination and subsequent proteasomal degradation (Uzunova et al., 2007). These proteins, designated as STUbLs (SUMO-targeted ubiquitin ligases), represent a specialization and co-evolution of the SUMO and ubiquitin pathways. Key examples are the poly-ubiquitination and subsequent degradation of the SUMOylated Promyelocytic leukemia (PML) nuclear body by the STUbLs RNF4 (Tatham et al., 2008) and Arkadia/Rnf111 (Erker et al., 2013).

One puzzling aspect of SUMOylation is that only a small proportion (<5%) of the total protein in the cell is modified by SUMO at equilibrium. The rapid conjugation-deconjugation cycles by SUMO-specific proteases bring about this transient state of SUMOylated species. Based on this low proportion, SUMO-conjugation resistant (SCR) variants of the protein should not substantially affect function as around 95% of the protein is in its original 'non-SUMOylated' state. However, in most cases, an SCR mutation strongly affects function. This indicates that SUMO-conjugation may be a rate-limiting step for a crucial functional transition. The transition may be related to the folding of the protein, movement between compartments, and association/disassociation, all because of a transient SUMO conjugation/deconjugation step. In the absence of de-SUMOylation, the protein would stall in a non-functional state, reducing the population of the functional state over time and thus affecting function (Celen & Sahin, 2020; Hay, 2005; Puntambekar et al., 2016).

SUMO seems to be required to adapt to cellular stresses, as evidenced by an increase in global SUMO conjugates in response to several abiotic stresses. This global change, termed the SUMO stress response (SSR), involves an increase in SUMO conjugated substrates and is thought to play a pro-survival role (Kurepa *et al.* 2003; Zhou *et al.* 2004; Jiang *et al.* 2012; Enserink 2015). Higher molecular weight SUMO2/3 conjugates increased when cells were exposed to detrimental conditions like heat shock, oxidative stress, osmotic stress, etc. The levels of free SUMO rapidly plummet, and SUMOylated proteins increasingly exist as functional clusters. Large-scale mass spectrometric results have corroborated this initial study, providing insight into protein-specific and site-specific modifications (Tammsalu *et al.* 2014; Hendriks *et al.* 2015a; b, 2017, 2018; Hendriks and Vertegaal 2016b; Lamoliatte *et al.* 2017; McManus *et al.* 2018). Heat shock and proteasomal inhibition increased global SUMOylation events by around 50%, with proteins displaying conjugation at

multiple sites (Hendriks *et al.* 2018). However, different stresses tended to elicit SUMOylation of certain common proteins at different sites (Hendriks *et al.* 2017). The studies highlighted a possible role for context-specific site-SUMOylation converging at common stress effectors to provide a cyto-protective function.

#### **1.4 SUMO in host defense**

Interest in the roles of SUMO conjugation in regulating the immune response originates from the finding that I $\kappa$ B, the inhibitor of NF- $\kappa$ B, is SUMO conjugated (Desterro *et al.*, 1998). This reversible modification reduced the degradation and attenuation of NF- $\kappa$ B signaling. Following this study, the Courey laboratory (Bhaskar *et al.* 2002) showed that *Drosophila* NF- $\kappa$ B, Dorsal (DL) was SUMO-conjugated and that SUMOylation of DL attenuated the activation of DL target genes and thus the immune response. These seminal studies were followed by several studies on other substrate proteins and pathways that confirmed roles for SUMO conjugation and also members of the SUMO cycle in regulating the immune response (Pascual *et al.* 2005; Huang *et al.* 2005; Chiu *et al.* 2005a; Liu *et al.* 2007; Ozato *et al.* 2007; Garaude *et al.* 2008). Research in the last decade has further strengthened the belief that SUMO conjugation of proteins regulates the host immune response. An important landmark for the burgeoning role of SUMO conjugation in host defense was the discovery that pathogens could hijack the SUMO conjugation machinery of the host for increased pathogenicity. Initial studies showed regulation of host E1 activity during adenoviral infection (Boggio *et al.*, 2004; Colombo *et al.*, 2002), followed by similar studies using viruses such as Ebola (Chang *et al.*, 2009; Vidal *et al.*, 2019) and Influenza (Pal *et al.*, 2011). Bacterial pathogens could also regulate the SUMO cycle. Examples include *Listeria* (Ribet *et al.*, 2010), *Shigella* (Fritah *et al.*, 2014), and *Salmonella* (Verma *et al.*, 2015). The current era of SUMO proteomics, 2010 onwards, suggests that 10-30% of total proteins in the cell are SUMOylated and that SUMO conjugation is dynamic and context-dependent. A significant fraction of the SUMOylated proteins identified is part of protein networks that function in host defense. The number of studies that have attempted to identify SUMO targets modulated in the immune response is limited, as are studies showing mechanistic data for SUMO conjugation in immunity. Sloan and co-workers (Sloan *et al.*, 2015) list 877 targets for SUMO-2 infection with HSV-1; Our lab has listed 710 *Drosophila*

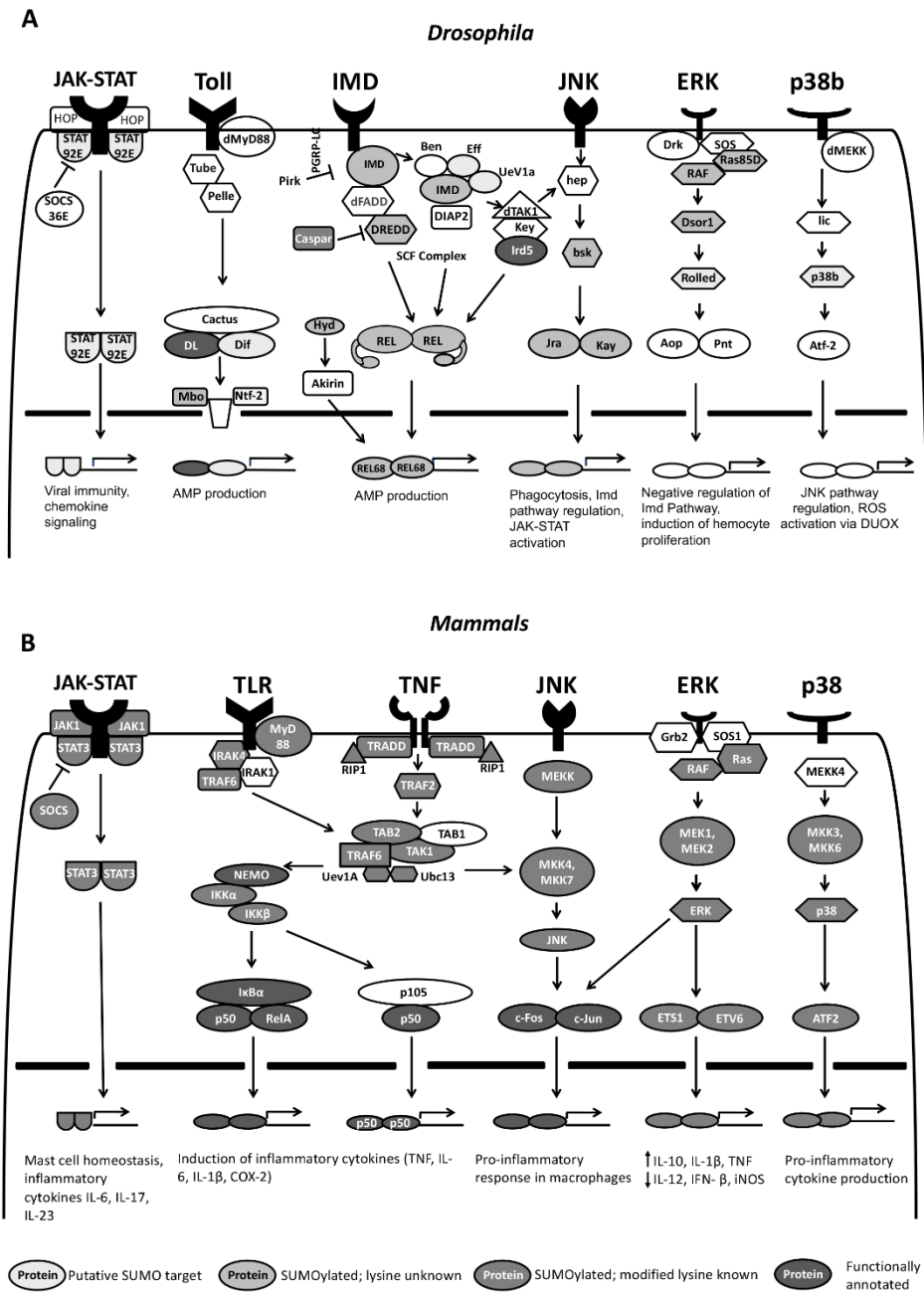


**Fig. 1.2. SUMO targets in immune signaling.** Schematic for proteins involved in immune cascades in *Drosophila* (A) and mammals (B). Six orthologous pathways are shown, namely the JAK-STAT, Toll/TLR, IMD/TNF, JNK, ERK, and p38. Descriptions of these immune regulatory pathways in *Drosophila* and their mammalian orthologs can be found in excellent reviews that have been published (Govind and Nehm 2004; Cherry and Silverman 2006; Lemaitre and Hoffmann 2007; Ferrandon *et al.* 2007; Ligoxygakis 2013; Buchon *et al.* 2014; Imler 2014). SUMO targets are marked by varying shades of grey. The darker the shade of grey, the higher the confidence for a role of that protein as a validated SUMOylated substrate, with known target lysine(s), involved in the immune response.

proteins enriched after LPS challenge in Schneider cells (Handu *et al.* 2015b), and Impens and co-workers identified 125 immune-specific SUMO targets for listeriolysin O (Impens *et al.*, 2014). A number of the SUMOylated proteins identified belong to immune signaling pathways. Fig. 1.2 summarizes the major immune signaling pathways in *Drosophila* (Fig. 1.2A) and mammals (Fig. 1.2B). Proteins that are SUMOylated are represented in grey, with darker shades indicating increased confidence for functional roles for SUMO conjugation for that substrate in immunity. Since actual mechanistic studies are limited, many of these proteins are only potential substrates and must be validated as genuine SUMO targets in the host immune response. Studies have indicated that a *bonafide* SUMO substrate has a greater chance of being SUMOylated in a specific context, albeit at a different lysine; hence proteomics studies give us additional confidence in these substrates (Hendriks *et al.* 2017). In *Drosophila*, Toll/NF- $\kappa$ B and IMD/NF- $\kappa$ B are the primary signaling pathways for the innate immune response.

The JAK-STAT, JNK, ERK, and p38 pathways play supporting roles in immune regulation, including roles in the cellular immune response. Orthologous signaling pathways exist in mammals, with signaling playing roles in innate and adaptive immunity (Fig. 1.2).

The larger number of SUMO targets in mammals (Fig. 1.2B), as emphasized by dark grey shades, are merely a reflection of the extensive proteomic experiments on mammalian cell lines – less than 10% substrates of these have been shown to modulate the immune response in either cell culture or animal experiments.

In the next few sections, I discuss in detail the modulation of the Toll/NF- $\kappa$ B and IMD/NF- $\kappa$ B pathways by SUMO. We also take a few substrates that have been validated *in-vivo* as SUMO targets as specific examples to bring out the roles for SUMO conjugation from a mechanistic standpoint and to compare and contrast the evolution of SUMO-related regulatory mechanisms from flies to mammals.

## **1.5 SUMOylation regulates Toll/TLR signaling**

In both flies and mammals, it is evident that SUMO conjugation modulates signaling in both the Toll (Bhaskar *et al.* 2002; Paddibhatla *et al.* 2010) and TLR signaling

(Aillet et al., 2012; Desterro et al., 1998) modules. Of the many proteins in the Toll/TLR cascades, in mammals, I $\kappa$ B appears to be a major SUMO target (Desterro et al., 1998) (Fig. 1.3). A holistic picture of I $\kappa$ B $\alpha$  regulation has emerged over the years. NF- $\kappa$ B is held in the cytoplasm by I $\kappa$ B $\alpha$  in an inactive state. At this stage, the SUMO-1-modified I $\kappa$ B $\alpha$  is resistant to ubiquitination (Desterro et al., 1998; Hay et al., 1999). Upon stimulation with a suitable ligand, a phosphorylation cascade is initiated. Phosphorylation of I $\kappa$ B $\alpha$ , aided by the I $\kappa$ B kinase (IKK) complex, is thought to recruit SUMO-2/3, possibly through a change in conformation (Aillet et al., 2012). Though the site of SUMO-2 conjugation remains identical to that of SUMO-1, I $\kappa$ B $\alpha$  now undergoes polyubiquitination, primed by polySUMO. These polySUMO-polyubiquitin hybrid chains target I $\kappa$ B $\alpha$  to the 26S proteasomal machinery, freeing NF- $\kappa$ B for nuclear translocation (Aillet et al., 2012) (Fig. 1.3).

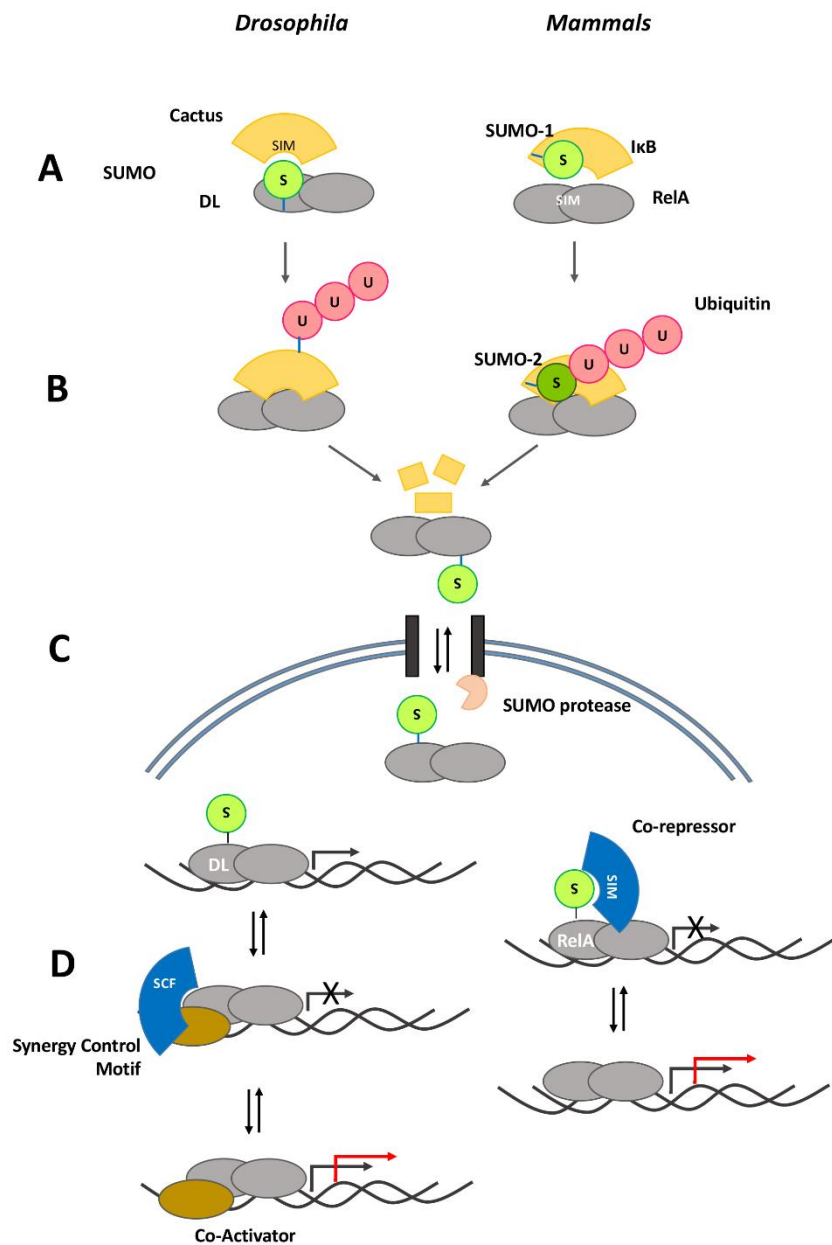


**Fig. 1.3. Mechanistic models for SUMO regulation of Toll/TLR signaling.** DL, SUMOylated at K382 appears to be a key SUMO substrate in the fly Toll pathway in contrast to IκB SUMOylation at K21 in humans. Possible models/mechanisms for regulation of Toll/TLR signaling include. SUMO:SIM interactions may play a major role in the evolutionary conserved DL:Cact and NF-κB:IκB complexes (A). The stability of the complex, and the release of DL/NF-κB after Cact/IκB degradation, in response to Toll/TLR signaling is a central feature of the mechanism. SUMO conjugation of DL in flies, and IκB in mammals, may define the binding dynamics or even enhance poly-ubiquitination and subsequent degradation in a context dependant manner.

B. Poly-ubiquitination of Cact/I $\kappa$ B is an essential step for release of DL/NF- $\kappa$ B for transcriptional activation and/or nuclear import. In mammals this step involves a complex exchange of SUMO1 with SUMO2 and subsequent poly-ubiquitination of SUMO2.

C. Import of DL into the nucleus may be dependent on a SUMO 'ticket' that is cleaved off during transit through the nuclear pore. In mammals, the NF- $\kappa$ B/I $\kappa$ B complex as a whole can enter the nucleus, allowing the possibility of SUMO-dependent nuclear import (or export). This model highlights the importance of SUMOylation as a rate-limiting step for nuclear trafficking and the small fraction of SUMOylated protein compared to the non-SUMOylated substrate that can exist and regulate the critical import/export step.

D. A SUMOylation/deSUMOylation cycle may regulate transcriptional activation of defense genes activated by DL/NF- $\kappa$ B. SCR-DL is a better transcriptional activator, suggesting that SUMO conjugation may restrain DL-mediated activation (Bhaskar *et al.* 2002). A synergy control motif with a SIM has been hypothesized to bind and regulate SUMOylated DL (Bhaskar *et al.* 2002). Mammalian data suggests that RelA is SUMOylated, and SUMO conjugation inhibits RelA transcriptional activity (Liu *et al.* 2012). Without RelA SUMOylation, the co-repressor may not be recruited efficiently.

In *Drosophila*, the broad outline of the signaling events is conserved, culminating in phosphorylation of Cact. Cact is then ubiquitinated and degraded, though the evidence for SUMOylation of the fly ortholog of I $\kappa$ B, Cact is indirect and not strong (Chiu *et al.* 2005a). Also, the fly expresses a single SUMO isoform resembling SUMO2/3, and cannot form SUMO chains since it lacks the critical lysine (Ureña *et al.*, 2015). Cact has a single non-consensus site predicted as a SUMO conjugation site (<http://www.jassa.fr/>: (Beauchair *et al.* 2015)), and researchers in the field have been unable to demonstrate that Cact is conjugated or regulated by SUMO. Hence the scenario for Cact regulation may differ significantly from mammalian I $\kappa$ B $\alpha$ . In mammals, SUMOylation of p100 (NF- $\kappa$ B2) is required for NF- $\kappa$ B inducing kinase (NIK) dependent phosphorylation and processing of inactive p100 (Vatsyayan *et al.*, 2008), while SUMO1 conjugation of RelB has been implicated in converting this NF- $\kappa$ B from an activator to a repressor (Leidner *et al.* 2014) (Fig. 1.3D).

A validated target for SUMO conjugation in Toll signaling in flies is DL at K382. DL acts redundantly with a related Rel-family protein, Dif, to mount an immune response. SUMO-conjugation resistant (SCR) DL<sup>K382R</sup> mutant showed a 5 to 10-fold increase in reporter gene activity compared to the wild-type protein (Bhaskar *et al.* 2002), indicating that SUMO conjugation decreased Toll signaling. However, the same manuscript had data suggesting that an increase in global SUMO conjugation

would lead to increased Toll signaling. Since an increased global SUMO conjugation would lead to a rise in SUMOylated DL, the data was inconsistent with the idea of non-SUMOylated DL, mimicked by DL<sup>K382R</sup> being a stronger transcriptional activator. To explain the conflicting data, the authors hypothesized that K382 was part of a crucial synergy control motif, facilitating interaction with a transcriptional attenuator, termed synergy control factor (SCF; Fig. 1.3D). A DL<sup>K382R</sup> mutation or SUMO-conjugation at the site would disrupt the interaction with the SCF and hence upregulate Toll signaling, explaining the greater target gene activation in these opposing scenarios (Bhaskar *et al.* 2002) (Fig. 1.3D).

The idea that SUMO conjugation primarily acts as a brake was consistent with experiments in the organism by the Govind lab, which found *Ubc9* to be a negative regulator of Toll signaling in the larval immune response (Huang *et al.* 2005; Chiu *et al.* 2005a). Reduction of *Ubc9* levels manifest as melanotic masses, caused by the over-proliferation of blood cells. The over-proliferation phenotype was found to be correlated with high levels of nuclear DL in hemocytes. Loss-of-function mutations of *DL* and *Dif* in a *Ubc9* mutant background suppressed this phenotype, suggesting a genetic interaction of the SUMO machinery with elements of the Toll pathway (Huang *et al.* 2005; Chiu *et al.* 2005a). The authors hypothesized that the physical interaction between *Ubc9* and Cactus (Cact), the fly I $\kappa$ B $\alpha$  ortholog, could be important for sequestering DL/Dif in the cytoplasm, which is lost in the *ubc9* mutant (Fig. 1.3). Another possibility is the SUMOylation of Cact or DL/Dif, preventing the aberrant activation of Cact or the untimely translocation DL/Dif. Further investigation demonstrated that *Ubc9* mutant larvae had reduced levels of Cact, re-iterating the significance of SUMO cycle components in regulating the Cact/DL/Dif complex (Paddibhatla *et al.* 2010). SUMOylation may also occlude the site for Cact ubiquitination, in agreement with mammalian studies on I $\kappa$ B $\alpha$  (Hay *et al.*, 1999). An alternate explanation is the change in DL/Dif stability and/or localization due to altered Cact stability, since the stability of Cact is intimately linked to DL binding (Kubota and Gay 1995) and mediated mainly via its ankyrin repeat domain (Kidd 1992). Cact also has three hydrophobic core regions- putative SIM motifs nestled in its ankyrin repeat domain (VDVV 243-246, ILLL 284-287, IDIL 375-378), (<http://www.jassa.fr/>; (Beauclair *et al.* 2015)) which could also facilitate interaction with SUMOylated DL/Dif, aiding in their cytoplasmic sequestration (Fig 3A). Fig. 1.3



lists the possible existing models that could explain the regulation of Toll/TLR signaling at different levels. At the level of the DL: Cactus or NF- $\kappa$ B: I $\kappa$ B complex, SUMO interactions with SIM may help stabilize (or destabilize) the complex. SUMO may also be important in nuclear import/export with Ulp1 being localized, in *Drosophila*, to the nuclear side of the nuclear pore complex (Smith *et al.* 2004a). At the level of transcriptional activation, as discussed, for both mammals and flies, the data strongly suggests that non-SUMOylated DL/ NF- $\kappa$ B is a stronger transcriptional activator. In flies, this is explained by the loss of binding to an SCF. At the same time, in mammals, the SUMOylated species is postulated to recruit co-repressors to dampen or stop transcriptional activation.

### **1.6 SUMOylation regulates TNF/ IMD signaling**

Immune signaling is a hub of PTM cross-talk. SUMOylation and ubiquitination further fine-tune the fundamental backbone of a phosphorylation-dependent relay of the stimulus. The role of the classical K48-linked ubiquitin-proteasome system and K63-linked-ubiquitin-signaling systems have been investigated in depth. A few instances of SUMO and ubiquitin cross-talk are presented here, focusing on the IMD/ TNF signaling pathways. In mammals, the binding of a ligand to the TNF (tumor necrosis factor) receptor initiates downstream events, culminating in NF- $\kappa$ B activation. Genotoxic stress also triggers this pathway, deciding the apoptotic fate of the cell. When cells are subjected to DNA-damaging agents, the first step is the recruitment of the adaptor protein RIP1 (receptor-interacting protein 1) to the cytoplasmic tail of the TNF receptor (Hayden & Ghosh, 2014). RIP1 undergoes K63-linked polyubiquitination, an essential step in enlisting TAK1 (Transforming growth factor beta-activated kinase 1) and IKK complex proteins through the adaptor NEMO (NF- $\kappa$ B essential modulator) (Fig. 1.4) (Devin *et al.*, 2000; Lee *et al.*, 2004). Interestingly, it was observed that SUMO modification of RIP1 preceded this ubiquitination step (Y. Yang *et al.*, 2011). Lysine to arginine mutations of RIP1 at residues 105, 140, 305, and 565 abolished SUMO conjugation. This four lysine to arginine (4KR) mutant failed to undergo ubiquitination, ceasing to activate NF- $\kappa$ B, since the IKK complex remained inactive (Y. Yang *et al.*, 2011). Hence, timely action of SUMO dictates further events of ubiquitination and complex formation in this case. Though the cellular inhibitor of apoptosis protein-1 (cIAP) family of proteins has been implicated

in the ubiquitination of RIP1 (Hayden & Ghosh, 2014), whether their recruitment is contingent upon SUMOylation of RIP1 remains unknown.

In *Drosophila*, the orthologous IMD pathway recognizes gram-negative bacterial cues, deploying Relish (Rel) to produce AMPs (Chen et al., 2017; Ganesan et al., 2011; C.-H. Kim et al., 2014; Kleino & Silverman, 2014). The death domain of IMD bears a striking resemblance to that of RIP1. After processing by the caspase DREDD, IMD is ubiquitinated, by *Drosophila* inhibitor of apoptosis-2 (dIAP-2), much like RIP1 (Kleino & Silverman, 2014; Paquette et al., 2010). Whether this step is evolutionarily conserved with mammals and requires SUMOylation awaits further study.

SUMO also forms an integral part of signaling at the nodal IKK complex. Comprised of IKK $\alpha$ , IKK $\beta$ , and NEMO in mammals, the fly counterpart has two components, immune response-deficient 5 (IRD5/IKK $\beta$ ) and Kenny (Key/IKK $\gamma$ ) (Fig. 1.4). NEMO is also SUMOylated at K277/309 (T. T. Huang et al., 2003). Genotoxic stress, ethanol, or hydrogen peroxide are sufficient to move cytoplasmic NEMO to the nucleus, where it is SUMO modified (Angela M. Mabb et al., 2006). This facilitates retention in the nucleus and initiation of further signaling events. A cycle of deSUMOylation ensues, leading to phosphorylation and subsequent ubiquitination at the same lysine. NEMO is exported from the nucleus, which associates with the IKK complex and activates the NF- $\kappa$ B cascade (Angela M. Mabb et al., 2006). In this manner, the sequential modification of NEMO by SUMOylation, phosphorylation, and ubiquitination is necessary for altered localization of NEMO and NF- $\kappa$ B activation.

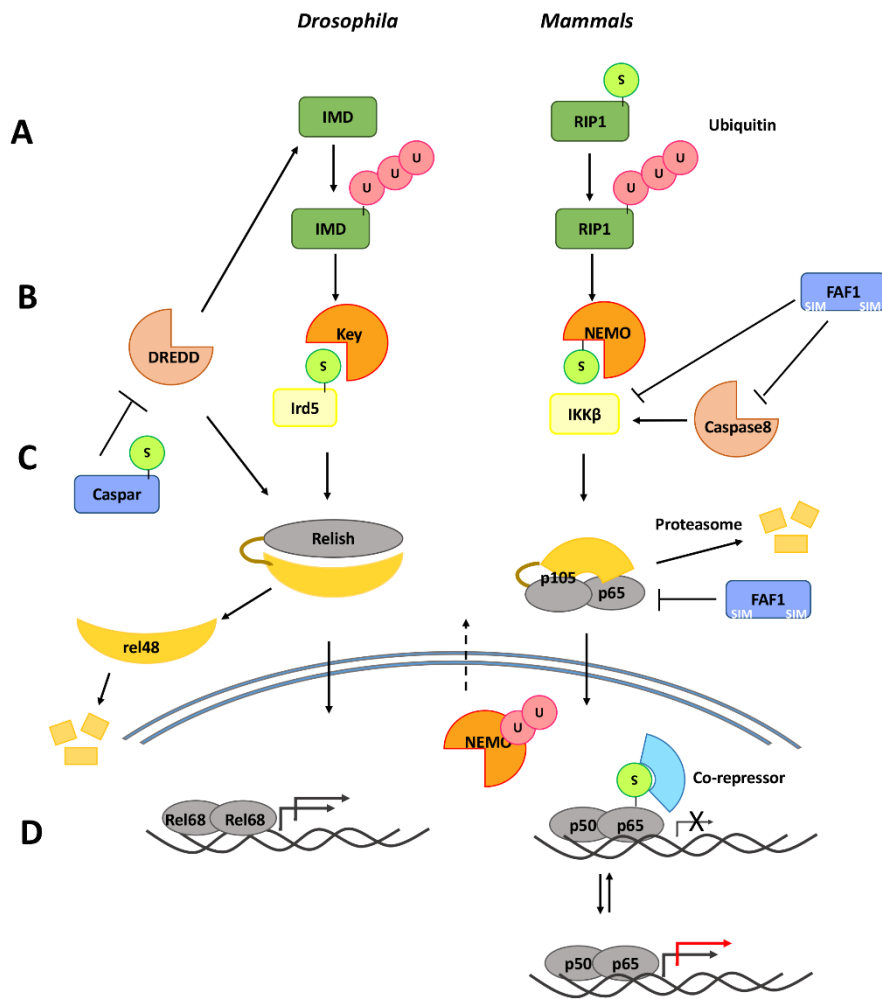


**Fig. 1.4. Mechanistic models for SUMO Regulation of IMD/TNF signaling.** Group SUMOylation and subsequent protein interactions may play crucial roles in stabilizing complexes in the IMD/TNF signaling pathway upon an immune challenge. Possible models/mechanisms include,

A. Ubiquitination of the adaptors IMD/RIP1 appears to be required for signaling to the IKK complex. The ubiquitination may be dependent on SUMOylation of the adaptor. This mechanism has been demonstrated in mammals but not flies.

B. The IKK complex, Key:IRD5 in flies and IKK $\alpha$ :NEMO:IKK $\beta$  may represent another instance of the evolutionary conservation of a functional complex via a SUMO:SIM interaction. SUMO conjugation of IRD5 at 152 may facilitate transduction of signal in the IKK complex, by modulation of its interaction with Kenny, while SUMO modification of NEMO facilitates nuclear import and subsequent ubiquitination, which appears necessary for nuclear export.

C. In *Drosophila*, SUMOylated Casp may impinge on the DREDD-dependent cleavage of Relish (Kim *et al.* 2006), which in turn affects Rel nuclear import and subsequent transcription

of defense genes. Interestingly, the mammalian Casp ortholog, FAF1, is also a negative regulator of NF- $\kappa$ B (Park *et al.* 2004, 2007). Its ability to regulate NF- $\kappa$ B signaling appears to depend on its physical interactions with the IKK complex as also p65/p50. FAF1 contains consensus sites for SUMOylation, but is not a validated target.

D. There is some evidence for Relish being a direct target of SUMO conjugation (Pirone *et al.* 2017), but whether this holds true in the immune context needs to be ascertained. Similarly, neither p100 or p105, the Ankyrin domain containing counterparts of Relish in mammals have been shown to be SUMO conjugated upon an immune challenge. The cleaved fragments however can form heterodimers with RelA(p65) or RelB, both SUMO substrates and thus influence transcription.

To gain more insight into the *Drosophila* IMD pathway, Fukuyama and colleagues used a proteomics approach to generate an interactome of 369 proteins in S2 cells challenged by *E. coli* (Fukuyama *et al.*, 2013). In addition to validating previous findings that IMD-FADD-DREDD and IRD5-Key exist as complexes, analysis of the IKK complex revealed interaction of IRD5 (IKK $\beta$ ) and KEY (IKK $\gamma$ ) with SUMO pathway components, hinting at possible SUMO-mediated protein interactions. Furthermore, IRD5 was SUMOylated at K152, and a K152A mutant displayed reduced induction of the AMP *Attacin A* transcripts *in vivo* (Fukuyama *et al.*, 2013). This contrasts with the mammalian IKK complex, where IKK $\gamma$  (NEMO) is SUMOylated. Similar to the I $\kappa$ B $\alpha$ /NF- $\kappa$ B complex, the interaction is evolutionarily conserved and might serve an analogous purpose, though the SUMOylated entities differ. Coupled with the study demonstrating an enrichment of SUMOylated proteins upon LPS challenge in S2 cells (Handu *et al.*, 2015a), a new paradigm of protein interactions mediated by group SUMOylation in managing the *Drosophila* immune response is emerging.

Dampening the immune response after successful resolution of infection and preventing the unrestrained activation of immune effectors in the absence of threats is another facet of signaling (F. Wang & Xia, 2018). Some of these negative regulators are a target of SUMO modification as well. The *Drosophila* Fas-associated factor 1 (FAF1) ortholog Caspar (Casp) was found to be SUMOylated in two independent studies (Handu *et al.* 2015b; Pirone *et al.* 2017). Casp is required to prevent the untimely processing of Relish via the caspase DREDD (Kim *et al.* 2006). Animals that lack Casp constitutively express the AMP *dipthericin* and are resistant to bacterial infection (Kim *et al.* 2006). Generating a SUMO-conjugation resistant Casp

mutant will help deduce the function of SUMO in an immune context. The mammalian ortholog FAF1 also negatively regulates NF- $\kappa$ B by binding to the IKK complex (Park *et al.* 2007) and caspase-8 (Ryu *et al.*, 2003), preventing its activation. Furthermore, FAF1 interacts with RelA, preventing its nuclear localization (Fig. 1.4) (Park *et al.* 2004). Though SUMOylation of FAF1 has not been studied in the immune context, two bonafide SIM motifs are documented in FAF1. However, they do not seem to impinge on NF- $\kappa$ B activation (Wang *et al.* 2019), as evidenced by mutational studies in cells. Whether this holds true in an intact organism like the fly in the context of immunity can only be demonstrated unequivocally in a genome-edited mutant for the SUMO/SIM sites.

The study of PTMs has proved challenging due to the low stoichiometry of the modified protein compared to the total protein. In the case of SUMO, three rate limiting steps have held back the progress of studies. First is our lack of ability to accurately predict SUMO conjugation sites on substrate proteins. Comparisons of sites predicted with current state-of-the-art programs with actual sites discovered using proteomics suggest that <50% of sites can be predicted based on 'canonical' SUMO motifs. The remaining must be discovered by experimental methods and may be context-dependent. The second hurdle is the identification of SUMOylation sites by mass spectrometry. The mammalian SUMO1 has a trypsin cleavage site close to the C-terminal -GG and thus leaves a short tail. Since the total conjugated 'T-junction' fragment is small and its mass can be measured accurately by mass spectrometers, efficient identification of the SUMOylation site is possible. In contrast, the mammalian SUMO2/3 and the fly SUMO ortholog leave behind a large mass remnant after protein digestion, hampering accurate site identification. One way around this problem has been to introduce tagged, cleavable forms of SUMO2/3 (Hendriks & Vertegaal, 2016a), but these raise additional concerns. SUMOylation of a fraction of targets could be due to the overexpression and introduction of the tagged SUMO. This means that a fair amount of time and effort must be expended in identifying target lysines by mutagenesis screens and then validating these as genuine SUMO sites. Recently, researchers have focussed on studying native SUMO modifications in endogenous tissues by utilizing a modified set of proteases that leave behind a digested fragment amenable to mass-spectrometric site-identification (Hendriks *et al.* 2018). The compatibility of this proteomics pipeline with

*Drosophila* SUMO is a promising indicator of possible SUMO site identifications in the near future.

The third challenge for a SUMO researcher is to create mutant versions of the proteins resistant to SUMO conjugation. This is especially tedious and time-consuming when working with whole organisms rather than cell lines. The recent advent of genome editing methods, namely TALEN, ZnF and CRISPR-Cas9 (Gupta et al., 2019; Harrison & Hart, 2018), has revolutionized our ability to make targeted Lys to Arg mutations directly at the genomic locus. CRISPR-Cas9 has significantly upgraded the versatile genome-engineering toolbox in *Drosophila*. Targeted editing in flies, especially at the level of changing a single amino acid, has been a challenging task. In the past, point mutations were routinely generated by large chemical mutagenesis screens at random sites, and modifications of interest were subsequently identified, enriched, and stabilized (Bökel, 2008; St Johnston, 2002). The second routine method to study mutants was first to generate null flies for the target locus and rescue the null by expression of either wild-type or mutant allele, usually by inserting the transgene at a site distant from the target locus (Brand and Perrimon 1993; Venken *et al.* 2006). In recent years, the utility of the CRISPR-Cas9 toolbox to edit the genomic locus directly and efficiently has revolutionized fly biology. After the initial demonstration of CRISPR-Cas9 genome editing in mammalian cells (Doudna & Charpentier, 2014; Hsu et al., 2014; Jinek et al., 2013; Mali et al., 2013; L. Yang et al., 2014), fly biologists developed equivalent methodologies to engineer the fly (Bassett *et al.* 2013; Gratz *et al.* 2013; Kondo and Ueda 2013). Today, a fly biologist can routinely generate site-directed mutations, such as replacing a target lysine with an arginine, creating a SUMO resistant site, using the CRISPR-Cas9 toolbox in the fly.

In the absence of comprehensive studies demonstrating physiological roles for SUMO in NF- $\kappa$ B signaling, we hoped to elucidate the function of SUMO for two NF- $\kappa$ B substrates. Dorsal (DL) and Caspar (Casp) are a part of the Toll and IMD pathways, respectively. Using the CRISPR-Cas9 gene-editing toolbox, we explored the functional relevance of SUMO-conjugation.

## 1.7 Aim of the study

To understand the physiological consequences of SUMO-conjugation of Dorsal and Caspar in *Drosophila*.

### Specific Aims

- Does SUMOylation of DL regulate Toll/NF- $\kappa$ B signaling?
  - Generate DL<sup>SCR</sup> mutants using CRISPR/Cas9 genome editing.
  - Evaluate roles in development.
  - Evaluate roles in host defense.
- Does SUMOylation of Caspar regulate IMD/NF- $\kappa$ B signaling?
  - Generate Caspar<sup>SCR</sup> mutants using CRISPR/Cas9 genome editing.
  - Evaluate roles in host defense.

**Notes/ Contributions:** Parts of this chapter have been published as a review article, 'Hegde, S., Soory, A., Kaduskar, B., & Ratnaparkhi, G. S. (2020). SUMO conjugation regulates immune signalling. *Fly*, 14(1-4), 62-79.'

## 1.8 References

1. Adorasio, S., Fierabracci, A., Muscari, I., Liberati, A. M., Ayroldi, E., Migliorati, G., Thuy, T. T., Riccardi, C., & Delfino, D. V. (2017). SUMO proteins: Guardians of immune system. *Journal of Autoimmunity*, *84*, 21–28.  
<https://doi.org/10.1016/j.jaut.2017.09.001>
2. Aillet, F., Lopitz-Otsoa, F., Egaña, I., Hjerpe, R., Fraser, P., Hay, R. T., Rodriguez, M. S., & Lang, V. (2012). Heterologous SUMO-2/3-Ubiquitin Chains Optimize IκBα Degradation and NF-κB Activity. *PLOS ONE*, *7*(12), e51672.
3. Bassett, A. R., Tibbit, C., Ponting, C. P., & Liu, J.-L. (2013). Highly Efficient Targeted Mutagenesis of *Drosophila* with the CRISPR/Cas9 System. *Cell Reports*, *4*(1), 220–228. <https://doi.org/10.1016/j.celrep.2013.06.020>
4. Beauclair, G., Bridier-Nahmias, A., Zagury, J.-F., Saïb, A., & Zamborlini, A. (2015). JASSA: a comprehensive tool for prediction of SUMOylation sites and SIMs. *Bioinformatics*, *31*(21), 3483–3491.  
<https://doi.org/10.1093/bioinformatics/btv403>
5. Bhaskar, V., Smith, M., & Courey, A. J. (2002). Conjugation of Smt3 to dorsal may potentiate the *Drosophila* immune response. *Molecular and Cellular Biology*, *22*(2), 492–504. <https://doi.org/10.1128/MCB.22.2.492-504.2002>
6. Boggio, R., Colombo, R., Hay, R. T., Draetta, G. F., & Chiocca, S. (2004). A Mechanism for Inhibiting the SUMO Pathway. *Molecular Cell*, *16*(4), 549–561.  
<https://doi.org/10.1016/j.molcel.2004.11.007>
7. Bökel, C. (2008). EMS Screens. In C. Dahmann (Ed.), *Drosophila. Methods in Molecular Biology* (pp. 119–138). Humana Press. [https://doi.org/10.1007/978-1-59745-583-1\\_7](https://doi.org/10.1007/978-1-59745-583-1_7)
8. Bossis, G., Malnou, C. E., Farras, R., Andermarcher, E., Hipskind, R., Rodriguez, M., Schmidt, D., Muller, S., Jariel-Encontre, I., & Piechaczyk, M. (2005). Down-Regulation of c-Fos/c-Jun AP-1 Dimer Activity by Sumoylation. *Molecular and Cellular Biology*, *25*(16), 6964 LP – 6979.  
<https://doi.org/10.1128/MCB.25.16.6964-6979.2005>
9. Brand, A. H., & Perrimon, N. (1993). Targeted gene expression as a means of altering cell fates and generating dominant phenotypes. *Development*, *118*(2), 401–415. <https://www.ncbi.nlm.nih.gov/pubmed/8223268>
10. Buchon, N., Silverman, N., & Cherry, S. (2014). Immunity in *Drosophila melanogaster* — from microbial recognition to whole-organism physiology. *Nature*



- Reviews Immunology*, 14(12), 796–810. <https://doi.org/10.1038/nri3763>
11. Cappadocia, L., & Lima, C. D. (2018). Ubiquitin-like Protein Conjugation: Structures, Chemistry, and Mechanism. *Chemical Reviews*, 118(3), 889–918. <https://doi.org/10.1021/acs.chemrev.6b00737>
  12. Celen, A. B., & Sahin, U. (2020). Sumoylation on its 25th Anniversary: Mechanisms, Pathology and Emerging Concepts. *The FEBS Journal*, n/a(n/a). <https://doi.org/10.1111/febs.15319>
  13. Chang, T.-H., Kubota, T., Matsuoka, M., Jones, S., Bradfute, S. B., Bray, M., & Ozato, K. (2009). Ebola Zaire Virus Blocks Type I Interferon Production by Exploiting the Host SUMO Modification Machinery. *PLOS Pathogens*, 5(6), e1000493.
  14. Chen, L., Paquette, N., Mamoor, S., Rus, F., Nandy, A., Leszyk, J., Shaffer, S. A., & Silverman, N. (2017). Innate immune signaling in *Drosophila* is regulated by TGF $\beta$ -activated kinase (Tak1)-triggered ubiquitin editing. *Journal of Biological Chemistry*. <https://doi.org/10.1074/jbc.M117.788158>
  15. Cherry, S., & Silverman, N. (2006). Host-pathogen interactions in *drosophila*: new tricks from an old friend. *Nature Immunology*, 7(9), 911–917. <https://doi.org/10.1038/ni1388>
  16. Chiu, H., Ring, B. C., Sorrentino, R. P., Kalamarz, M., Garza, D., & Govind, S. (2005). dUbc9 negatively regulates the Toll-NF- $\kappa$ B pathways in larval hematopoiesis and drosomycin activation in *Drosophila*. *Developmental Biology*, 288(1), 60–72. <https://doi.org/10.1016/J.YDBIO.2005.08.008>
  17. Chymkowitch, P., Le May, N., Charneau, P., Compe, E., & Egly, J.-M. (2011). The phosphorylation of the androgen receptor by TFIID directs the ubiquitin/proteasome process. *The EMBO Journal*, 30(3), 468–479. <https://doi.org/10.1038/emboj.2010.337>
  18. Citra, S., & Chiocca, S. (2013). Sumo paralogs: redundancy and divergencies. *Frontiers in Bioscience - Scholar*, 5, 544–553. <https://doi.org/10.2741/s388>
  19. Colombo, R., Boggio, R., Seiser, C., Draetta, G. F., & Chiocca, S. (2002). The adenovirus protein Gam1 interferes with sumoylation of histone deacetylase 1. *EMBO Reports*, 3(11), 1062–1068. <https://doi.org/10.1093/embo-reports/kvf213>
  20. Desterro, J. M., Rodriguez, M. S., & Hay, R. T. (1998). SUMO-1 modification of I $\kappa$ B $\alpha$  inhibits NF- $\kappa$ B activation. *Molecular Cell*, 2(2), 233–239. [https://doi.org/10.1016/S1097-2765\(00\)80133-1](https://doi.org/10.1016/S1097-2765(00)80133-1)

21. Devin, A., Cook, A., Lin, Y., Rodriguez, Y., Kelliher, M., & Liu, Z.-G. (2000). The Distinct Roles of TRAF2 and RIP in IKK Activation by TNF-R1: TRAF2 Recruits IKK to TNF-R1 while RIP Mediates IKK Activation. *Immunity*, *12*(4), 419–429. [https://doi.org/10.1016/S1074-7613\(00\)80194-6](https://doi.org/10.1016/S1074-7613(00)80194-6)
22. Domingues, P., Golebiowski, F., Tatham, M. H., Lopes, A. M., Taggart, A., Hay, R. T., & Hale, B. G. (2015). Global Reprogramming of Host SUMOylation during Influenza Virus Infection. *Cell Reports*, *13*(7), 1467–1480. <https://doi.org/10.1016/j.celrep.2015.10.001>
23. Doudna, J. A., & Charpentier, E. (2014). The new frontier of genome engineering with CRISPR-Cas9. *Science*, *346*(6213).
24. Eifler, K., & Vertegaal, A. C. O. (2015). Mapping the SUMOylated landscape. *The FEBS Journal*, *282*(19), 3669–3680. <https://doi.org/10.1111/febs.13378>
25. Enserink, J. M. (2015). Sumo and the cellular stress response. *Cell Division*, *10*, 4. <https://doi.org/10.1186/s13008-015-0010-1>
26. Erker, Y., Neyret-Kahn, H., Seeler, J. S., Dejean, A., Atfi, A., & Levy, L. (2013). Arkadia, a Novel SUMO-Targeted Ubiquitin Ligase Involved in PML Degradation. *Molecular and Cellular Biology*, *33*(11), 2163 LP – 2177. <https://doi.org/10.1128/MCB.01019-12>
27. Everett, R. D., Boutell, C., & Hale, B. G. (2013). Interplay between viruses and host sumoylation pathways. *Nature Reviews Microbiology*, *11*(6), 400–411. <https://doi.org/10.1038/nrmicro3015>
28. Ferrandon, D., Imler, J.-L., Hetru, C., & Hoffmann, J. A. (2007). The Drosophila systemic immune response: sensing and signalling during bacterial and fungal infections. *Nature Reviews. Immunology*, *7*(11), 862–874. <https://doi.org/10.1038/nri2194>
29. Fritah, S., Lhocine, N., Golebiowski, F., Mounier, J., Andrieux, A., Jouvion, G., Hay, R. T., Sansonetti, P., & Dejean, A. (2014). Sumoylation controls host anti-bacterial response to the gut invasive pathogen *Shigella flexneri*. *EMBO Reports*, *15*(9), 965–972. <https://doi.org/10.15252/embr.201338386>
30. Fukuyama, H., Verdier, Y., Guan, Y., Makino-Okamura, C., Shilova, V., Liu, X., Maksoud, E., Matsubayashi, J., Haddad, I., Spirohn, K., Ono, K., Hetru, C., Rossier, J., Ideker, T., Boutros, M., Vinh, J., & Hoffmann, J. A. (2013). Landscape of protein–protein interactions in Drosophila immune deficiency signaling during bacterial challenge. *Proceedings of the National Academy of Sciences of the*

*United States of America*, 110(26), 10717–10722.

<https://doi.org/10.1073/pnas.1304380110>

31. Ganesan, S., Aggarwal, K., Paquette, N., & Silverman, N. (2011). NF- $\kappa$ B/Rel proteins and the humoral immune responses of *Drosophila melanogaster*. *Current Topics in Microbiology and Immunology*, 349, 25–60.  
[https://doi.org/10.1007/82\\_2010\\_107](https://doi.org/10.1007/82_2010_107)
32. Garaude, J., Farrás, R., Bossis, G., Charni, S., Piechaczyk, M., Hipskind, R. A., & Villalba, M. (2008). SUMOylation Regulates the Transcriptional Activity of JunB in T Lymphocytes. *The Journal of Immunology*, 180(9), 5983 LP – 5990.  
<https://doi.org/10.4049/jimmunol.180.9.5983>
33. Garcia, B. A. (2019). *Post-translational Modifications That Modulate Enzyme Activity*. Academic Press.
34. Geiss-Friedlander, R., & Melchior, F. (2007). Concepts in sumoylation: a decade on. *Nature Reviews Molecular Cell Biology*, 8(12), 947–956.  
<https://doi.org/10.1038/nrm2293>
35. Ghioni, P., D'Alessandra, Y., Mansueto, G., Jaffray, E., Hay, R. T., La Mantia, G., & Guerrini, L. (2005). The protein stability and transcriptional activity of p63alpha are regulated by SUMO-1 conjugation. *Cell Cycle*, 4(1), 183–190.  
<https://doi.org/10.4161/cc.4.1.1359>
36. Golebiowski, F., Matic, I., Tatham, M. H., Cole, C., Yin, Y., Nakamura, A., Cox, J., Barton, G. J., Mann, M., & Hay, R. T. (2009). System-wide changes to SUMO modifications in response to heat shock. *Science Signaling*, 2(72), ra24.  
<https://doi.org/10.1126/scisignal.2000282>
37. Govind, S., & Nehm, R. H. (2004). Innate Immunity in Fruit Flies: A Textbook Example of Genomic Recycling. *PLOS Biology*, 2(8), e276.
38. Gratz, S. J., Cummings, A. M., Nguyen, J. N., Hamm, D. C., Donohue, L. K., Harrison, M. M., Wildonger, J., & O'Connor-Giles, K. M. (2013). Genome engineering of *Drosophila* with the CRISPR RNA-guided Cas9 nuclease. *Genetics*, 194(4), 1029–1035. <https://doi.org/10.1534/genetics.113.152710>
39. Gresko, E., Möller, A., Roscic, A., & Schmitz, M. L. (2005). Covalent modification of human homeodomain interacting protein kinase 2 by SUMO-1 at lysine 25 affects its stability. *Biochemical and Biophysical Research Communications*, 329(4), 1293–1299. <https://doi.org/10.1016/j.bbrc.2005.02.113>
40. Gupta, D., Bhattacharjee, O., Mandal, D., Sen, M. K., Dey, D., Dasgupta, A.,

- Kazi, T. A., Gupta, R., Sinharoy, S., Acharya, K., Chattopadhyay, D., Ravichandiran, V., Roy, S., & Ghosh, D. (2019). CRISPR-Cas9 system: A new-fangled dawn in gene editing. *Life Sciences*, 232, 116636.  
<https://doi.org/10.1016/j.lfs.2019.116636>
41. Handu, M., Kaduskar, B., Ravindranathan, R., Soory, A., Giri, R., Elango, V. B., Gowda, H., & Ratnaparkhi, G. S. (2015a). SUMO Enriched Proteome for *Drosophila* Innate Immune Response. *G3 (Bethesda, Md.)*, 91(0).  
<https://doi.org/10.1534/g3.115.020958>
42. Handu, M., Kaduskar, B., Ravindranathan, R., Soory, A., Giri, R., Elango, V. B., Gowda, H., & Ratnaparkhi, G. S. (2015b). SUMO-Enriched Proteome for *Drosophila* Innate Immune Response. *G3*, 5(10), 2137–2154.  
<https://doi.org/10.1534/g3.115.020958>
43. Harding, J. J., & Crabbe, M. J. C. (1991). *Post-translational Modifications of Proteins*.
44. Harrison, P. T., & Hart, S. (2018). A beginner's guide to gene editing. *Experimental Physiology*, 103(4), 439–448. <https://doi.org/10.1113/EP086047>
45. Hay, R. T. (2005). SUMO: a history of modification. *Molecular Cell*, 18(1), 1–12.  
<https://doi.org/10.1016/j.molcel.2005.03.012>
46. Hay, R. T. (2013). Decoding the SUMO signal. *Biochemical Society Transactions*, 41(2), 463–473. <https://doi.org/10.1042/BST20130015>
47. Hay, R. T., Vuillard, L., Desterro, J. M. P., & Rodriguez, M. S. (1999). Control of NF- $\kappa$ B transcriptional activation by signal induced proteolysis of I $\kappa$ B $\alpha$ . *Philosophical Transactions of the Royal Society B: Biological Sciences*, 354(1389), 1601–1609. <https://doi.org/10.1098/rstb.1999.0504>
48. Hayden, M. S., & Ghosh, S. (2014). Regulation of NF- $\kappa$ B by TNF family cytokines. *Seminars in Immunology*, 26(3), 253–266.  
<https://doi.org/10.1016/j.smim.2014.05.004>
49. Hendriks, I. A., D'Souza, R. C., Chang, J.-G., Mann, M., & Vertegaal, A. C. O. (2015). System-wide identification of wild-type SUMO-2 conjugation sites. *Nature Communications*, 6(1), 7289. <https://doi.org/10.1038/ncomms8289>
50. Hendriks, I. A., Lyon, D., Su, D., Skotte, N. H., Daniel, J. A., Jensen, L. J., & Nielsen, M. L. (2018). Site-specific characterization of endogenous SUMOylation across species and organs. *Nature Communications*, 9(1), 2456.  
<https://doi.org/10.1038/s41467-018-04957-4>

51. Hendriks, I. A., Lyon, D., Young, C., Jensen, L. J., Vertegaal, A. C. O., & Nielsen, M. L. (2017). Site-specific mapping of the human SUMO proteome reveals co-modification with phosphorylation. *Nature Structural & Molecular Biology*, *24*(3), 325–336. <https://www.nature.com/articles/nsmb.3366>
52. Hendriks, I. A., Treffers, L. W., Verlaan-de Vries, M., Olsen, J. V., & Vertegaal, A. C. O. (2015). SUMO-2 Orchestrates Chromatin Modifiers in Response to DNA Damage. *Cell Reports*, *10*(10), 1778–1791. <https://doi.org/10.1016/j.celrep.2015.02.033>
53. Hendriks, I. A., & Vertegaal, A. C. O. (2016a). A high-yield double-purification proteomics strategy for the identification of SUMO sites. *Nature Protocols*, *11*(9), 1630–1649. <https://doi.org/10.1038/nprot.2016.082>
54. Hendriks, I. A., & Vertegaal, A. C. O. (2016b). A comprehensive compilation of SUMO proteomics. *Nature Reviews. Molecular Cell Biology*, *17*(9), 581–595. <https://doi.org/10.1038/nrm.2016.81>
55. Hong, Y., Rogers, R., Matunis, M. J., Mayhew, C. N., Goodson, M., Park-Sarge, O. K., & Sarge, K. D. (2001). Regulation of Heat Shock Transcription Factor 1 by Stress-induced SUMO-1 Modification. *Journal of Biological Chemistry*, *276*(43), 40263–40267. <https://doi.org/10.1074/jbc.M104714200>
56. Hsu, P. D., Lander, E. S., & Zhang, F. (2014). Development and applications of CRISPR-Cas9 for genome engineering. *Cell*, *157*(6), 1262–1278. <https://doi.org/10.1016/j.cell.2014.05.010>
57. Huang, L., Ohsako, S., & Tanda, S. (2005). The lesswright mutation activates Rel-related proteins, leading to overproduction of larval hemocytes in *Drosophila melanogaster*. *Developmental Biology*, *280*(2), 407–420. <https://doi.org/10.1016/j.ydbio.2005.02.006>
58. Huang, T. T., Wuerzberger-Davis, S. M., Wu, Z.-H., & Miyamoto, S. (2003). Sequential Modification of NEMO/IKK $\gamma$  by SUMO-1 and Ubiquitin Mediates NF- $\kappa$ B Activation by Genotoxic Stress. *Cell*, *115*(5), 565–576. [https://doi.org/10.1016/S0092-8674\(03\)00895-X](https://doi.org/10.1016/S0092-8674(03)00895-X)
59. Imler, J.-L. (2014). Overview of *Drosophila* immunity: A historical perspective. *Developmental & Comparative Immunology*, *42*(1), 3–15. <https://doi.org/10.1016/j.dci.2013.08.018>
60. Impens, F., Radoshevich, L., Cossart, P., & Ribet, D. (2014). Mapping of SUMO sites and analysis of SUMOylation changes induced by external stimuli.

- Proceedings of the National Academy of Sciences of the United States of America*, 111(34), 12432–12437. <https://doi.org/10.1073/pnas.1413825111>
61. Jiang, Z., Fan, Q., Zhang, Z., Zou, Y., Cai, R., Wang, Q., Zuo, Y., & Cheng, J. (2012). SENP1 deficiency promotes ER stress-induced apoptosis by increasing XBP1 SUMOylation. *Cell Cycle*, 11(6), 1118–1122. <https://doi.org/10.4161/cc.11.6.19529>
62. Jinek, M., East, A., Cheng, A., Lin, S., Ma, E., & Doudna, J. (2013). RNA-programmed genome editing in human cells. *ELife*, 2, e00471. <https://doi.org/10.7554/eLife.00471>
63. Johnson, E. S., Schwienhorst, I., Dohmen, R. J., & Blobel, G. (1997). The ubiquitin-like protein Smt3p is activated for conjugation to other proteins by an Aos1p/Uba2p heterodimer. *The EMBO Journal*, 16(18), 5509–5519. <https://doi.org/10.1093/emboj/16.18.5509>
64. Kidd, S. (1992). Characterization of the *Drosophila cactus* locus and analysis of interactions between cactus and dorsal proteins. *Cell*, 71(4), 623–635. [https://doi.org/10.1016/0092-8674\(92\)90596-5](https://doi.org/10.1016/0092-8674(92)90596-5)
65. Kim, C.-H., Paik, D., Rus, F., & Silverman, N. (2014). The Caspase-8 Homolog Dredd Cleaves Imd and Relish but Is Not Inhibited by p35. *Journal of Biological Chemistry*, 289(29), 20092–20101. <https://doi.org/10.1074/jbc.M113.544841>
66. Kim, M., Lee, J. H., Lee, S. Y., Kim, E., & Chung, J. (2006). Caspar, a suppressor of antibacterial immunity in *Drosophila*. *Proceedings of the National Academy of Sciences of the United States of America*, 103(44), 16358–16363. <https://doi.org/10.1073/pnas.0603238103>
67. Kleino, A., & Silverman, N. (2014). The *Drosophila* IMD pathway in the activation of the humoral immune response. *Developmental & Comparative Immunology*, 42(1), 25–35. <https://doi.org/10.1016/j.dci.2013.05.014>
68. Klenk, C., Humrich, J., Quitterer, U., & Lohse, M. J. (2006). SUMO-1 Controls the Protein Stability and the Biological Function of Phosducin. *Journal of Biological Chemistry*, 281(13), 8357–8364. <https://doi.org/10.1074/jbc.M513703200>
69. Kondo, S., & Ueda, R. (2013). Highly improved gene targeting by germline-specific Cas9 expression in *Drosophila*. *Genetics*, 195(3), 715–721. <https://doi.org/10.1534/genetics.113.156737>
70. Kubota, K., & Gay, N. J. (1995). The dorsal protein enhances the biosynthesis and stability of the *Drosophila* IκB homologue cactus. *Nucleic Acids Research*,

- 23(16), 3111–3118. <https://doi.org/10.1093/nar/23.16.3111>
71. Kunz, K., Piller, T., & Müller, S. (2018). SUMO-specific proteases and isopeptidases of the SENP family at a glance. *Journal of Cell Science*, 131(6). <https://doi.org/10.1242/jcs.211904>
72. Kurepa, J., Walker, J. M., Smalle, J., Gosink, M. M., Davis, S. J., Durham, T. L., Sung, D.-Y., & Vierstra, R. D. (2003). The Small Ubiquitin-like Modifier (SUMO) Protein Modification System in Arabidopsis : ACCUMULATION OF SUMO1 AND -2 CONJUGATES IS INCREASED BY STRESS. *Journal of Biological Chemistry*, 278(9), 6862–6872. <https://doi.org/10.1074/jbc.M209694200>
73. Lamoliatte, F., McManus, F. P., Maarifi, G., Chelbi-Alix, M. K., & Thibault, P. (2017). Uncovering the SUMOylation and ubiquitylation crosstalk in human cells using sequential peptide immunopurification. *Nature Communications*, 8(1), 14109. <https://doi.org/10.1038/ncomms14109>
74. Lee, T. H., Shank, J., Cusson, N., & Kelliher, M. A. (2004). The Kinase Activity of Rip1 Is Not Required for Tumor Necrosis Factor- $\alpha$ -induced I $\kappa$ B Kinase or p38 MAP Kinase Activation or for the Ubiquitination of Rip1 by Traf2. *Journal of Biological Chemistry*, 279(32), 33185–33191.
75. Leidner, J., Voogdt, C., Niedenthal, R., Möller, P., Marienfeld, U., & Marienfeld, R. B. (2014). SUMOylation attenuates the transcriptional activity of the NF- $\kappa$ B subunit RelB. *Journal of Cellular Biochemistry*, 115(8), 1430–1440. <https://doi.org/10.1002/jcb.24794>
76. Lemaitre, B., & Hoffmann, J. (2007). The Host Defense of *Drosophila melanogaster*. *Annual Review of Immunology*, 25(1), 697–743. <https://doi.org/10.1146/annurev.immunol.25.022106.141615>
77. Liang, Y.-C., Lee, C.-C., Yao, Y.-L., Lai, C.-C., Schmitz, M. L., & Yang, W.-M. (2016). SUMO5, a Novel Poly-SUMO Isoform, Regulates PML Nuclear Bodies. *Scientific Reports*, 6(1), 26509. <https://doi.org/10.1038/srep26509>
78. Ligoxygakis, P. (2013). *Chapter Two - Genetics of Immune Recognition and Response in Drosophila host defense* (T. Friedmann, J. C. Dunlap, & S. F. B. T.-. A. in G. Goodwin, Eds.; Vol. 83, pp. 71–97). Academic Press. <https://doi.org/10.1016/B978-0-12-407675-4.00002-X>
79. Liu, B., Yang, Y., Chernishof, V., Loo, R. R. O., Jang, H., Tahk, S., Yang, R., Mink, S., Shultz, D., Bellone, C. J., Loo, J. A., & Shuai, K. (2007). Proinflammatory Stimuli Induce IKK $\alpha$ -Mediated Phosphorylation of PIAS1 to

- Restrict Inflammation and Immunity. *Cell*, 129(5), 903–914.  
<https://doi.org/10.1016/j.cell.2007.03.056>
80. Liu, Y., Bridges, R., Wortham, A., & Kulesz-Martin, M. (2012). NF- $\kappa$ B repression by PIAS3 mediated RelA SUMOylation. *PloS One*, 7(5), e37636.  
<https://doi.org/10.1371/journal.pone.0037636>
81. Mabb, A. M., & Miyamoto, S. (2007). SUMO and NF- $\kappa$ B ties. *Cellular and Molecular Life Sciences*, 64(15), 1979–1996. <https://doi.org/10.1007/s00018-007-7005-2>
82. Mabb, Angela M., Wuerzberger-Davis, S. M., & Miyamoto, S. (2006). PIASy mediates NEMO sumoylation and NF- $\kappa$ B activation in response to genotoxic stress. *Nature Cell Biology*, 8(9), 986–993. <https://doi.org/10.1038/ncb1458>
83. Mali, P., Yang, L., Esvelt, K. M., Aach, J., Guell, M., DiCarlo, J. E., Norville, J. E., & Church, G. M. (2013). RNA-Guided Human Genome Engineering via Cas9. *Science*, 339(6121), 823 LP – 826. <https://doi.org/10.1126/science.1232033>
84. Matunis, M. J., Coutavas, E., & Blobel, G. (1996). A novel ubiquitin-like modification modulates the partitioning of the Ran-GTPase-activating protein RanGAP1 between the cytosol and the nuclear pore complex. *Journal of Cell Biology*, 135(6), 1457–1470. <https://doi.org/10.1083/jcb.135.6.1457>
85. McManus, F. P., Bourdeau, V., Acevedo, M., Lopes-Paciencia, S., Mignacca, L., Lamoliatte, F., Rojas Pino, J. W., Ferbeyre, G., & Thibault, P. (2018). Quantitative SUMO proteomics reveals the modulation of several PML nuclear body associated proteins and an anti-senescence function of UBC9. *Scientific Reports*, 8(1), 1–15. <https://doi.org/10.1038/s41598-018-25150-z>
86. Melchior, F. (2000). SUMO—Nonclassical Ubiquitin. *Annual Review of Cell and Developmental Biology*, 16(1), 591–626.  
<https://doi.org/10.1146/annurev.cellbio.16.1.591>
87. Meluh, P. B., & Koshland, D. (1995). Evidence that the MIF2 gene of *Saccharomyces cerevisiae* encodes a centromere protein with homology to the mammalian centromere protein CENP-C. *Molecular Biology of the Cell*, 6(7), 793–807. <https://doi.org/10.1091/mbc.6.7.793>
88. Miles, W. O., Jaffray, E., Campbell, S. G., Takeda, S., Bayston, L. J., Basu, S. P., Li, M., Raftery, L. A., Ashe, M. P., Hay, R. T., & Ashe, H. L. (2008). Medea SUMOylation restricts the signaling range of the Dpp morphogen in the *Drosophila* embryo. *Genes & Development*, 22(18), 2578–2590.



<https://doi.org/10.1101/gad.494808>

89. Mukhopadhyay, D., & Dasso, M. (2017). The Role of SUMO in Mitosis. In *Advances in Experimental Medicine and Biology* (Vol. 963, pp. 171–184). <https://doi.org/10.1007/978-3-319-50044-7>
90. Müller, S., Berger, M., Lehembre, F., & Seeler, J. S. (2000). c-Jun and p53 activity is modulated by SUMO-1 modification. *Journal of Biological Chemistry*. [https://www.jbc.org/article/S0021-9258\(19\)80689-0/abstract](https://www.jbc.org/article/S0021-9258(19)80689-0/abstract)
91. Nayak, A., & Müller, S. (2014). SUMO-specific proteases/isopeptidases: SENPs and beyond. *Genome Biology*, 15(7), 422. <https://doi.org/10.1186/s13059-014-0422-2>
92. Ozato, K., Tailor, P., & Kubota, T. (2007). The Interferon Regulatory Factor Family in Host Defense: Mechanism of Action. *Journal of Biological Chemistry*, 282(28), 20065–20069.
93. Paddibhatla, I., Lee, M. J., Kalamarz, M. E., Ferrarese, R., & Govind, S. (2010). Role for sumoylation in systemic inflammation and immune homeostasis in *Drosophila* larvae. *PLoS Pathogens*, 6(12), e1001234. <https://doi.org/10.1371/journal.ppat.1001234>
94. Pal, S., Santos, A., Rosas, J. M., Ortiz-Guzman, J., & Rosas-Acosta, G. (2011). Influenza A virus interacts extensively with the cellular SUMOylation system during infection. *Virus Research*, 158(1), 12–27. <https://doi.org/10.1016/j.virusres.2011.02.017>
95. Paquette, N., Broemer, M., Aggarwal, K., Chen, L., Husson, M., Ertürk-Hasdemir, D., Reichhart, J.-M., Meier, P., & Silverman, N. (2010). Caspase-Mediated Cleavage, IAP Binding, and Ubiquitination: Linking Three Mechanisms Crucial for *Drosophila* NF- $\kappa$ B Signaling. *Molecular Cell*, 37(2), 172–182. <https://doi.org/10.1016/j.molcel.2009.12.036>
96. Park, M. Y., Jang, H. D., Lee, S. Y., Lee, K. J., & Kim, E. (2004). Fas-associated factor-1 inhibits nuclear factor- $\kappa$ B (NF- $\kappa$ B) activity by interfering with nuclear translocation of the RelA (p65) subunit of NF- $\kappa$ B. *The Journal of Biological Chemistry*. [https://www.jbc.org/article/S0021-9258\(18\)52618-1/abstract](https://www.jbc.org/article/S0021-9258(18)52618-1/abstract)
97. Park, Moon, Lee, Choi, & Chung. (2007). FAF1 suppresses I $\kappa$ B kinase (IKK) activation by disrupting the IKK complex assembly. *Bollettino Della Societa Italiana Di Biologia Sperimentale*. [https://www.jbc.org/article/S0021-9258\(20\)58651-1/abstract](https://www.jbc.org/article/S0021-9258(20)58651-1/abstract)

98. Pascual, G., Fong, A. L., Ogawa, S., Gamliel, A., Li, A. C., Perissi, V., Rose, D. W., Willson, T. M., Rosenfeld, M. G., & Glass, C. K. (2005). A SUMOylation-dependent pathway mediates transrepression of inflammatory response genes by PPAR- $\gamma$ . *Nature*, *437*(7059), 759–763. <https://doi.org/10.1038/nature03988>
99. Pirone, L., Xolalpa, W., Sigurðsson, J. O., Ramirez, J., Pérez, C., González, M., de Sabando, A. R., Elortza, F., Rodriguez, M. S., Mayor, U., Olsen, J. V., Barrio, R., & Sutherland, J. D. (2017). A comprehensive platform for the analysis of ubiquitin-like protein modifications using in vivo biotinylation. *Scientific Reports*, *7*, 40756. <https://doi.org/10.1038/srep40756>
100. Puntambekar, S. S., Nyayanit, D., Saxena, P., & Gadgil, C. J. (2016). Identification of Unintuitive Features of Sumoylation through Mathematical Modeling. *The Journal of Biological Chemistry*, *291*(18), 9458–9468. <https://doi.org/10.1074/jbc.M115.676122>
101. Reverter, D., & Lima, C. D. (2005). Insights into E3 ligase activity revealed by a SUMO–RanGAP1–Ubc9–Nup358 complex. *Nature*, *435*(7042), 687–692. <https://doi.org/10.1038/nature03588>
102. Ribet, D., Hamon, M., Gouin, E., Nahori, M.-A., Impens, F., Neyret-Kahn, H., Gevaert, K., Vandekerckhove, J., Dejean, A., & Cossart, P. (2010). *Listeria monocytogenes* impairs SUMOylation for efficient infection. *Nature*, *464*(7292), 1192–1195. <https://doi.org/10.1038/nature08963>
103. Ryu, S.-W., Lee, S.-J., Park, M.-Y., Jun, J.-I., Jung, Y.-K., & Kim, E. (2003). Fas-associated Factor 1, FAF1, Is a Member of Fas Death-inducing Signaling Complex. *Journal of Biological Chemistry*, *278*(26), 24003–24010. <https://doi.org/10.1074/jbc.M302200200>
104. Saitoh, H., Pu, R. T., & Dasso, M. (1997). SUMO-1: wrestling with a new ubiquitin-related modifier. *Trends in Biochemical Sciences*, *22*(10), 374–376. [https://doi.org/10.1016/S0968-0004\(97\)01102-X](https://doi.org/10.1016/S0968-0004(97)01102-X)
105. Seufert, W., Futcher, B., & Jentsch, S. (1995). *Role of a ubiquitin-conjugating enzyme in degradation of S- and M-phase cyclins.*
106. Sloan, E., Tatham, M. H., Gros Lambert, M., Glass, M., Orr, A., Hay, R. T., & Everett, R. D. (2015). Analysis of the SUMO2 Proteome during HSV-1 Infection. *PLOS Pathogens*, *11*(7), e1005059.
107. Smith, M., Bhaskar, V., Fernandez, J., & Courey, A. J. (2004). *Drosophila* Ulp1, a Nuclear Pore-associated SUMO Protease, Prevents Accumulation of

- Cytoplasmic SUMO Conjugates. *Journal of Biological Chemistry*, 279(42), 43805–43814. <https://doi.org/10.1074/jbc.M404942200>
108. Song, J., Durrin, L. K., Wilkinson, T. A., Krontiris, T. G., & Chen, Y. (2004). Identification of a SUMO-binding motif that recognizes SUMO-modified proteins. *Proceedings of the National Academy of Sciences of the United States of America*, 101(40), 14373 LP – 14378. <https://doi.org/10.1073/pnas.0403498101>
109. Srikanth, C. V., & Verma, S. (2017). Sumoylation as an Integral Mechanism in Bacterial Infection and Disease Progression. In V. G. Wilson (Ed.), *SUMO Regulation of Cellular Processes*. Springer, Cham. [https://doi.org/10.1007/978-3-319-50044-7\\_22](https://doi.org/10.1007/978-3-319-50044-7_22)
110. St Johnston, D. (2002). The art and design of genetic screens: *Drosophila melanogaster*. *Nature Reviews Genetics*, 3(3), 176–188. <https://doi.org/10.1038/nrg751>
111. Steinacher, R., & Schär, P. (2005). Functionality of Human Thymine DNA Glycosylase Requires SUMO-Regulated Changes in Protein Conformation. *Current Biology*, 15(7), 616–623. <https://doi.org/10.1016/j.cub.2005.02.054>
112. Talamillo, A., Sánchez, J., & Barrio, R. (2008). Functional analysis of the SUMOylation pathway in *Drosophila*. *Biochemical Society Transactions*, 36(5), 868–873. <https://doi.org/10.1042/BST0360868>
113. Tammsalu, T., Matic, I., Jaffray, E. G., Ibrahim, A. F. M., Tatham, M. H., & Hay, R. T. (2014). Proteome-Wide Identification of SUMO2 Modification Sites. *Science Signaling*, 7(323), rs2 LP-rs2. <https://doi.org/10.1126/scisignal.2005146>
114. Tatham, M. H., Geoffroy, M.-C., Shen, L., Plechanovova, A., Hattersley, N., Jaffray, E. G., Palvimo, J. J., & Hay, R. T. (2008). RNF4 is a poly-SUMO-specific E3 ubiquitin ligase required for arsenic-induced PML degradation. *Nature Cell Biology*, 10(5), 538–546. <https://doi.org/10.1038/ncb1716>
115. Tempé, D., Vives, E., Brockly, F., Brooks, H., De Rossi, S., Piechaczyk, M., & Bossis, G. (2014). SUMOylation of the inducible (c-Fos:c-Jun)/AP-1 transcription complex occurs on target promoters to limit transcriptional activation. *Oncogene*, 33(7), 921–927. <https://doi.org/10.1038/onc.2013.4>
116. Ureña, E., Pirone, L., Chafino, S., Pérez, C., Sutherland, J. D., Lang, V., Rodriguez, M. S., Lopitz-Otsoa, F., Blanco, F. J., Barrio, R., & Martín, D. (2015). Evolution of SUMO Function and Chain Formation in Insects. *Molecular Biology and Evolution*, 33(2), 568–584. <https://doi.org/10.1093/molbev/msv242>

117. Uzunova, K., Götttsche, K., Miteva, M., Weisshaar, S. R., Glanemann, C., Schnellhardt, M., Niessen, M., Scheel, H., Hofmann, K., Johnson, E. S., Praefcke, G. J. K., & Dohmen, R. J. (2007). Ubiquitin-dependent Proteolytic Control of SUMO Conjugates. *Journal of Biological Chemistry*, *282*(47), 34167–34175. <https://doi.org/10.1074/jbc.M706505200>
118. van der Veen, A. G., & Ploegh, H. L. (2012). Ubiquitin-Like Proteins. *Annual Review of Biochemistry*, *81*(1), 323–357. <https://doi.org/10.1146/annurev-biochem-093010-153308>
119. Vatsyayan, J., Qing, G., Xiao, G., & Hu, J. (2008). SUMO1 modification of NF- $\kappa$ B2/p100 is essential for stimuli-induced p100 phosphorylation and processing. *EMBO Reports*, *9*(9), 885—890. <https://doi.org/10.1038/embor.2008.122>
120. Venken, K. J. T., He, Y., Hoskins, R. A., & Bellen, H. J. (2006). P[acman]: A BAC Transgenic Platform for Targeted Insertion of Large DNA Fragments in *D. melanogaster*. *Science*, *314*(5806), 1747 LP – 1751. <https://doi.org/10.1126/science.1134426>
121. Verma, S., Mohapatra, G., Ahmad, S. M., Rana, S., Jain, S., Khalsa, J. K., & Srikanth, C. V. (2015). Salmonella Engages Host MicroRNAs To Modulate SUMOylation: a New Arsenal for Intracellular Survival. *Molecular and Cellular Biology*, *35*(17), 2932 LP – 2946. <https://doi.org/10.1128/MCB.00397-15>
122. Vidal, S., El Motiam, A., Seoane, R., Preitakaite, V., Bouzaher, Y. H., Gómez-Medina, S., San Martín, C., Rodríguez, D., Rejas, M. T., Baz-Martínez, M., Barrio, R., Sutherland, J. D., Rodríguez, M. S., Muñoz-Fontela, C., & Rivas, C. (2019). Regulation of the Ebola Virus VP24 Protein by SUMO. *Journal of Virology*, *94*(1), e01687-19. <https://doi.org/10.1128/JVI.01687-19>
123. Vierstra, R. D. (2012). The Expanding Universe of Ubiquitin and Ubiquitin-Like Modifiers. *Plant Physiology*, *160*(1), 2 LP – 14. <https://doi.org/10.1104/pp.112.200667>
124. Voet, D., Voet, J. G., & Pratt, C. W. (2006). *Fundamentals of Biochemistry: Life at the Molecular Level, 5th Edition*. Wiley.
125. Walsh, C. T., Garneau-Tsodikova, S., & Gatto, G. J., Jr. (2005). Protein Posttranslational Modifications: The Chemistry of Proteome Diversifications. *Angewandte Chemie International Edition*, *44*(45), 7342–7372. <https://doi.org/10.1002/anie.200501023>

126. Wang, C.-H., Hung, P.-W., Chiang, C.-W., Lombès, M., Chen, C.-H., Lee, K.-H., Lo, Y.-C., Wu, M.-H., Chang, W.-C., & Lin, D.-Y. (2019). Identification of two independent SUMO-interacting motifs in Fas-associated factor 1 (FAF1): Implications for mineralocorticoid receptor (MR)-mediated transcriptional regulation. *Biochimica et Biophysica Acta (BBA) - Molecular Cell Research*, 1866(8), 1282–1297. <https://doi.org/10.1016/j.bbamcr.2019.03.014>
127. Wang, F., & Xia, Q. (2018). Back to homeostasis: Negative regulation of NF- $\kappa$ B immune signaling in insects. *Developmental & Comparative Immunology*, 87, 216–223. <https://doi.org/10.1016/j.dci.2018.06.007>
128. Wilson, V. G. (2017). Introduction to Sumoylation. In *SUMO Regulation of Cellular Processes* (pp. 1–12). <https://doi.org/10.1007/978-3-319-50044-7>
129. Yang, L., Mali, P., Kim-Kiselak, C., & Church, G. (2014). CRISPR-Cas-Mediated Targeted Genome Editing in Human Cells. In F. Storici (Ed.), *Gene Correction* (pp. 245–267). Humana Press, Totowa, NJ. [https://doi.org/10.1007/978-1-62703-761-7\\_16](https://doi.org/10.1007/978-1-62703-761-7_16)
130. Yang, Y., Xia, F., Hermance, N., Mabb, A., Simonson, S., Morrissey, S., Gandhi, P., Munson, M., Miyamoto, S., & Kelliher, M. A. (2011). A Cytosolic ATM/NEMO/RIP1 Complex Recruits TAK1 To Mediate the NF- $\kappa$ B and p38 Mitogen-Activated Protein Kinase (MAPK)/MAPK-Activated Protein 2 Responses to DNA Damage. *Molecular and Cellular Biology*, 31(14), 2774 LP – 2786. <https://doi.org/10.1128/MCB.01139-10>
131. Zhou, W., Ryan, J. J., & Zhou, H. (2004). Global Analyses of Sumoylated Proteins in *Saccharomyces cerevisiae*: INDUCTION OF PROTEIN SUMOYLATION BY CELLULAR STRESSES. *Journal of Biological Chemistry*, 279(31), 32262–32268. <https://doi.org/10.1074/jbc.M404173200>

## Chapter 2: SUMOylation of Dorsal attenuates Toll/NF- $\kappa$ B signaling; a developmental perspective

### 2.1 Abstract

In *Drosophila*, Toll/NF- $\kappa$ B signaling plays critical roles in animal development and host defense. The activation, intensity, and kinetics of Toll signaling are regulated by post-translational modifications such as phosphorylation, SUMOylation, or ubiquitination that target multiple proteins in the Toll/NF- $\kappa$ B cascade.

Here, we have generated a CRISPR-Cas9 edited Dorsal (DL) variant that is SUMO conjugation resistant (SCR) and explored roles for SUMO-conjugation of DL in early development. Intriguingly, embryos laid by *dl*<sup>SCR</sup> mothers overcome *dl* haploinsufficiency and complete the developmental program. This ability appears to be a result of higher transcriptional activation by DL<sup>SCR</sup>. In contrast, SUMOylation dampens DL transcriptional activation, ultimately conferring robustness to the dorso-ventral program. Our findings define SUMO conjugation as an important regulator of the Toll signaling cascade in early embryonic development. Our results broadly suggest that SUMO attenuates DL at the level of transcriptional activation.

### **Keywords**

*Drosophila*, Haploinsufficiency, SUMO, transcription

## 2.2 Introduction

Toll-like receptor (TLR) signaling is a highly conserved, ancient response to combat pathogenic attacks in multicellular eukaryotes (Kopp and Ghosh 1995; Medzhitov *et al.* 1997; Zhang and Ghosh 2001; Janeway and Medzhitov 2002). In *Drosophila*, in addition to its role in regulating the host response to infection, the Toll/Dorsal pathway has been co-opted to orchestrate early development, laying down the foundations for the dorso-ventral (DV) body plan (reviewed by (Steward and Govind 1993; Morisato and Anderson 1995; Belvin and Anderson 1996; Rusch and Levine 1996; Stathopoulos and Levine 2002; Valanne *et al.* 2011)). The chief effector in DV development, the NF- $\kappa$ B transcription factor Dorsal (DL) is held inactive in the cytoplasm by the I $\kappa$ B ortholog Cactus (Cact) (Steward 1987; Roth *et al.* 1989, 1991; Rushlow *et al.* 1989; Geisler *et al.* 1992; Govind *et al.* 1993; Whalen and Steward 1993). The asymmetric binding of the ligand Spaetzle (Spz) to the Toll receptor sets in motion a kinase cascade, leading to the formation of a DV gradient of DL (Steward *et al.* 1988; Roth *et al.* 1989; Bergmann *et al.* 1996) in the syncytial blastoderm, where DL activates 50-70 target genes to specify the presumptive germ layers of the fly (Kosman *et al.* 1991, 1992; Ip *et al.* 1992; Araujo and Bier 2000).

DL is a SUMO target based on experiments conducted in *Drosophila* S2 cells (Bhaskar *et al.* 2000, 2002). Studies in larvae have also emphasized the interplay of SUMO and the Toll pathway in modulating host defense. Mutations in the SUMO E2 ligase Ubc9, encoded by *lesswright* (*lwr*) in *Drosophila*, lead to the over-proliferation of hemocytes. Introducing mutations in the *dl* and *Dif* loci in a *lwr* mutant background restores the wild-type blood cell population, providing evidence for the intersection of Toll signaling with the SUMO conjugation machinery (Huang *et al.* 2005; Chiu *et al.* 2005b). In the embryo, mass spectrometric studies suggest that DL is SUMO conjugated (Nie *et al.* 2009). However, roles for DL SUMOylation in the animal have not been studied.

Here, we sought to delineate the function of SUMO conjugation of DL in *Drosophila* embryonic development (this chapter) and immunity (Chapter 3). In our study, we employ a CRISPR-Cas9-based strategy, which allows precise editing of the DL locus, replacing the 382<sup>nd</sup> lysine, the site for SUMOylation, with a charge-preserving arginine. This *dl*<sup>K382R</sup> animal is then subsequently evaluated for its effect on early

development and host-defense (discussed in Chapter 3), both of which represent critical spatiotemporal domains for Toll/DL signaling. Our studies uncover roles for SUMO conjugation of DL in supporting the robustness of embryonic DV patterning. DL SUMO conjugation negatively regulates Toll signaling by specifically attenuating DL mediated transcriptional activation.

## 2.3 Results

### 2.3.1 Generation of a genome-edited *dl*<sup>K382R</sup> mutant.

In recent years, the advent of CRISPR-Cas9 genome editing technology has allowed the generation of point mutations in a straightforward and site-directed manner (Bassett *et al.* 2014; Gratz *et al.* 2014; Bier *et al.* 2018). DL is SUMOylated (Bhaskar *et al.* 2000; Smith *et al.* 2004b) and has a single, well-characterized, and validated SUMO conjugation site at K382 (Fig. 2.1A) (Bhaskar *et al.* 2002; Anjum *et al.* 2013), supported by SUMO prediction algorithms (Ren *et al.* 2009; Zhao *et al.* 2014; Beauclair *et al.* 2015) as a direct consensus SC-SUMO site. Further, mass spectrometry experiments indicate that DL is SUMOylated in S2 cells (Pirone *et al.* 2017) and in the early embryo (Nie *et al.* 2009). Proteome-wide acetylation studies (Weinert *et al.* 2011) and *Drosophila* PTM databases (Hu *et al.* 2019) do not suggest DL to be acetylated or methylated. Therefore, the DL<sup>K382R</sup> mutation exclusively abolishes SUMO conjugation, generating a SUMO-conjugation-resistant (SCR) variant of DL and is therefore an ideal target for a CRISPR-based mutagenesis experiment. We employed the following genome editing protocol (Fig. 2.1A, B; Materials and Methods) to generate the *dl*<sup>K382R</sup> mutation (Fig. 2.1C, D). A single guide RNA (sgRNA) targeting the *dl* locus, with no predicted off-target cleavage sites was cloned into the pBFv-U6.2 plasmid. A 100 bp-long ssODN (Fig. 2.1A) harboring the K382R mutation was supplied as the repair template and co-injected along with the sgRNA plasmid in embryos expressing Cas9 in the *vasa* domain. The 450 flies (F0) that emerged from the injected embryos were crossed to a second chromosome *w*; *Tft/CyO* balancer (Fig. 2.1B). Three animals from each vial, for each of the 400 lines,



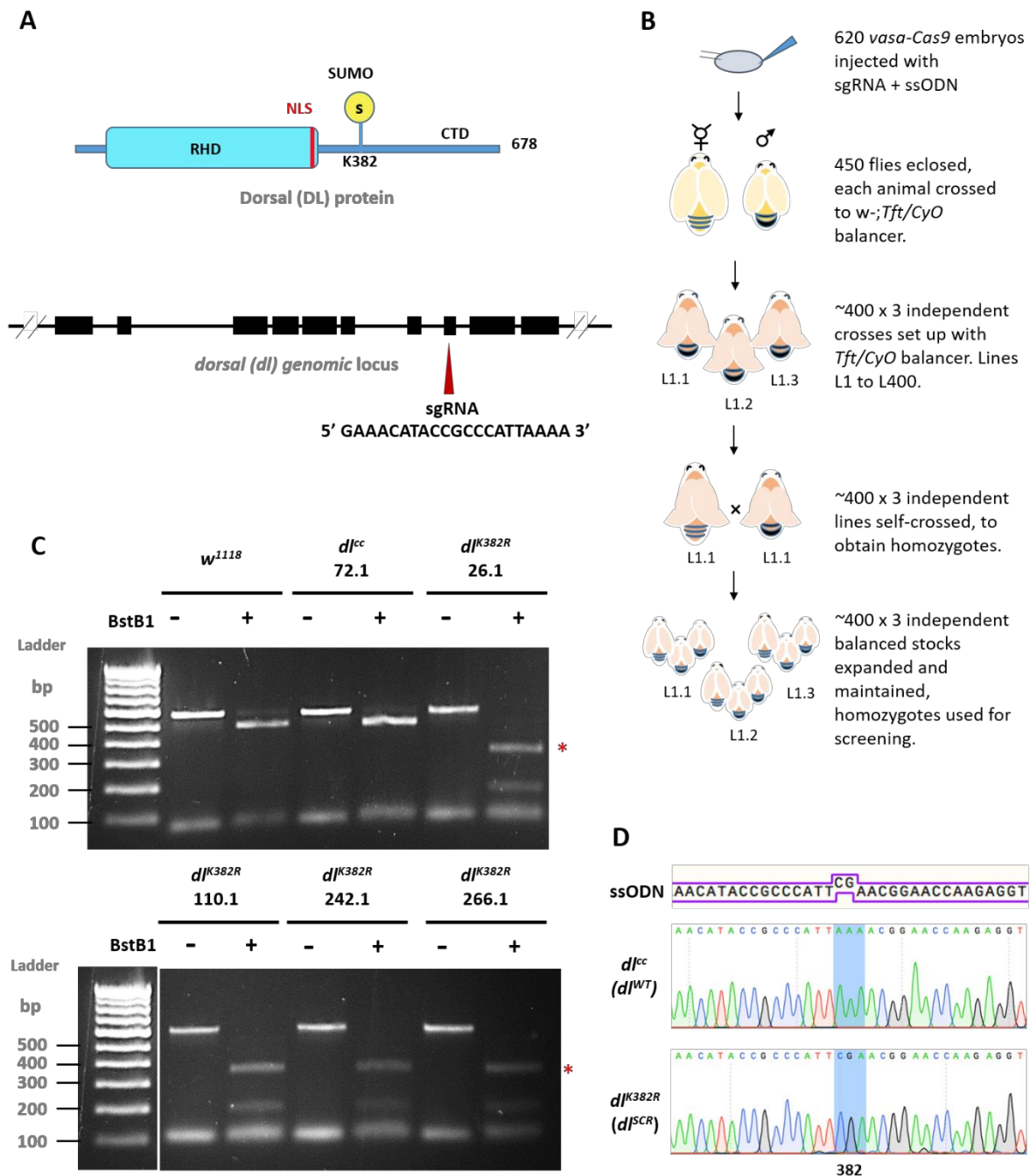


**Fig. 2.1. Creating the *dl<sup>K382R</sup>* mutant using the CRISPR-Cas9 system.** A schematic of the DL protein (in blue) and gene locus (in black) is presented in panel (A). DL is SUMOylated at K382, part of the consensus motif IKTE. A 20 bp sgRNA was designed to create a double strand break in the vicinity of *dl<sup>K382</sup>*, in exon 8. The detailed crossing scheme for the generation of the *dl<sup>K382R</sup>* allele after injection of the gRNA plasmid and ssODN is outlined in (B). Homozygous flies obtained were screened by genomic PCR and digestion with the BstB1 enzyme, which recognizes the engineered site of mutation, TTCGAA (C). Four independent lines – 26.1, 110.1, 242.1 and 266.1 showed a distinct digest of the PCR product (indicated by red asterisks), while line 72.1 served as a control. (D) The presence of the mutation was confirmed through sequencing (codon CGA highlighted in blue).

were crossed again to *w<sup>1118</sup>;Tft/CyO*, to generate stable, putative, *dI<sup>K382R</sup>/CyO* lines. Of these, 200 homozygous, putative transformants were screened for insertion of the ssODN by PCR amplification of the genomic locus followed by restriction digestion by BstBI (Fig. 2.1C). The screening strategy incorporated a BstBI site in the ssODN, validating the successful incorporation of the mutation in the genome. Based on restriction digestion patterns, ~2% of lines (4 out of 200), harbored the mutation and we validated these (26.1, 110.1, 242.1, 266.1) by sequencing (Fig. 2.1C). Representative sequencing data is shown in Fig. 2.1D. A few lines containing wild-type sequences were also retained and one of these (72.1) was defined as a ‘CRISPR-control’, *dI<sup>WT</sup>*, at par with the wild-type animal. The *dI<sup>K382R</sup>* genome-edited lines were also used in a trans-allelic combination (e.g 26.1/110.1) to negate off-target effects. Here onwards, *dI<sup>K382R</sup>* is referred to as *dI<sup>SCR</sup>*, a line where DL is resistant to SUMO conjugation. All *dI<sup>K382R</sup>* and *dI<sup>WT</sup>* lines were homozygous viable with comparable *dI* transcript levels (Fig. 2.2) across developmental stages.

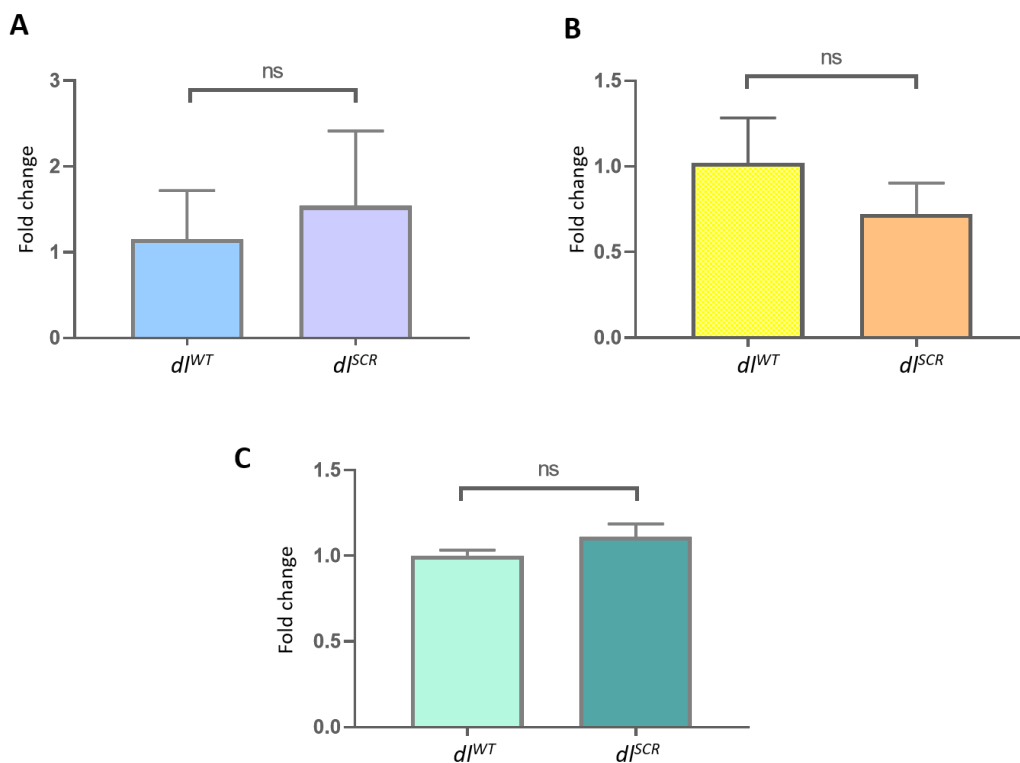


**Fig. 2.2. *dI* transcripts express at similar levels in *dI<sup>WT</sup>* and *dI<sup>SCR</sup>*.** *dI* transcript levels assayed by qRT-PCR across different stages of the fly life cycle- embryo (A), larva (B) and adult (D) for the genotypes *dI<sup>WT</sup>* and *dI<sup>SCR</sup>*. N=3, Unpaired t-test, (ns)  $P > 0.05$ .

### 2.3.2 Early development proceeds normally in *dl<sup>SCR</sup>* embryos

*dl* is deposited maternally and DL functions as a master regulator in specifying the dorso-ventral (DV) axis (Santamaria and Nüsslein-Volhard 1983; Anderson and Nüsslein-Volhard 1984; Roth *et al.* 1989; Steward and Govind 1993; Morisato and Anderson 1995; Rusch and Levine 1996). Using mass-spectrometry, DL is also among the ~140 maternal proteins identified as substrates for SUMO conjugation in the 0-3 hour embryo (Nie *et al.* 2009). In eggs laid by homozygous *dl<sup>SCR</sup>* mothers, antibody staining indicates that the DL gradient (Lieberman *et al.* 2009; Reeves *et al.* 2012; Trisnadi *et al.* 2013), which could be influenced by SUMO conjugation, appears to be normal (Fig. 2.3A). A quantitative comparison in embryonic cross-sections (Fig. 2.3B-D) confirmed equivalent gradients for DL<sup>WT</sup> and DL<sup>SCR</sup>. The equivalence of gradients is further supported by the observation that there are no discernible differences in embryonic viability (Fig. 2.3F). Additionally, the cuticular pattern, a sensitive readout for aberrations in both maternal and zygotic stages (Fig. 2.3E) is normal for both genotypes. These observations suggest that lack of SUMO conjugation of DL does not significantly change the DV program. Transcript levels, measured by real-time PCR of *dl* and its primary ventral targets *twist* (*twi*) and *snail* (*sna*) were similar to controls, while *zerknüllt* (*zen*) levels were ~2 fold higher in *dl<sup>SCR</sup>* mutants (Fig. 2.3G). Taken together, these results suggest that DL SUMOylation is either dispensable or that the effect of the *dl<sup>SCR</sup>* mutation is compensated for by unknown mechanisms in the developing embryo.

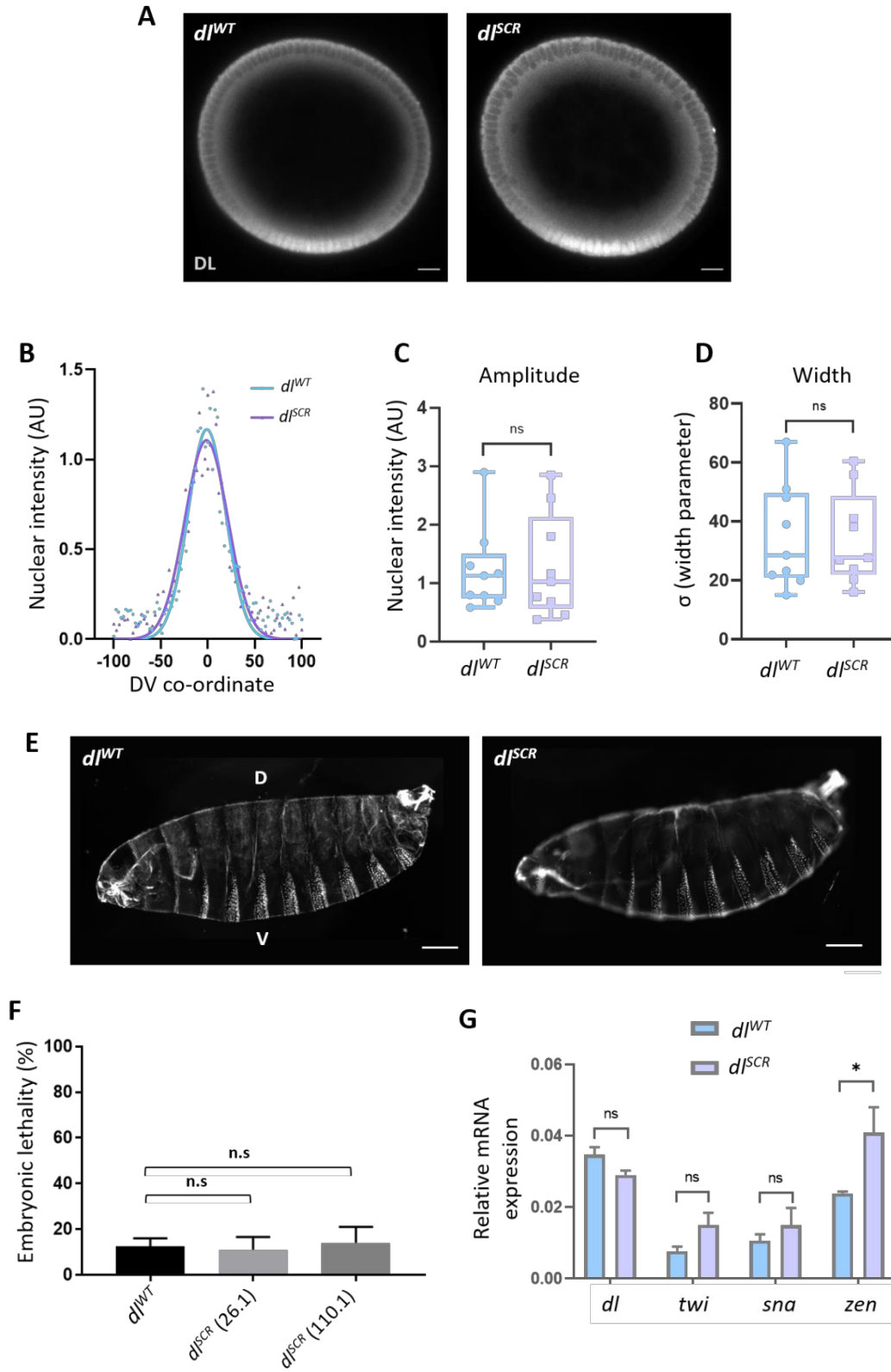


**Fig. 2.3. SUMO conjugation is dispensable for embryonic development.** Transverse sections of cellular blastoderm embryos stained for DL (A). Localization in the nuclei was observed in embryos oriented dorsal-side up and ventral-side at the bottom. (B) shows

representative intensity profiles of  $dI^{WT}$  and  $dI^{SCR}$  embryos, fitted to a Gaussian, with the gradient centered at the ventral midline. The amplitude (C) and width (D) of the gradient are plotted for each embryo.  $n=9$ , student's t-test, (ns)  $P > 0.05$ . Cuticle preparations (E) indicate regular arrangement of denticle bands. The percentage of unhatched embryos is plotted as embryonic lethality for control and two of the mutant lines, 26.1 and 110.1 (F). Genotype of mated mothers is listed on the X-axis.  $N=3$ , ordinary one-way ANOVA, (ns)  $P > 0.05$ . (G) represents qRT-PCR analysis of  $dI$  transcripts and DL target genes *twi*, *sna* and *zen* for embryos from mated females of the genotypes  $dI^{WT}$  and  $dI^{SCR}$ .  $N=3$ , Two-way ANOVA, (ns)  $P > 0.05$ , (\*)  $P < 0.05$ .

### 2.3.3 Haploinsufficiency of $dI$ is rescued in $dI^{SCR}$ embryos

Since SUMO is essential to adapt to a multitude of cellular stresses, we reasoned that a requirement for SUMOylation of DL would only be apparent under conditions of stress (Tempé *et al.* 2008). A well-known allelic combination that disrupts the DV developmental program is  $dI$  haploinsufficiency at 29 °C (Nüsslein-Volhard 1979; Nüsslein-Volhard *et al.* 1980; Simpson 1983). Unlike at 25 °C, where ~95% of embryos hatch into larvae (Fig. 2.4A), at 29 °C, ~50% of embryos laid by  $dI^{WT}/Df$  or  $dI^{WT}/dI^1$  females fail to hatch (Fig. 2.4B; Fig. 2.5B). The J4 allele, a deletion spanning *dI*, *dif*, and an uncharacterized transcriptional unit C2 (Meng *et al.* 1999) was used as a deficiency allele (*Df*), while  $dI^1$  is a null allele. Surprisingly, the embryonic lethality of  $dI^{SCR}/Df$  (Fig. 2.4B) or  $dI^{SCR}/dI^1$  (Fig. 2.5B) was significantly lower, at 15% in comparison to the 55% lethality of  $dI^{WT}/Df$  embryos. This result was consistent across two of the  $dI^{SCR}$  lines tested, 26.1 and 110.1. At 25 °C, the embryonic lethality for both  $dI^{SCR}/dI^1$  and  $dI^{WT}/dI^1$  were comparable (Fig. 2.4A), indicating that a reduction of  $dI$  gene dosage at 25 °C is sufficiently well-tolerated, unlike at 29 °C. To determine if the lethality due to haploinsufficiency was the consequence of an underlying deficit in DL-mediated patterning, we turned our attention to the cuticles of first instar larvae (Fig. 2.4, C1). Cuticles with wild-type pattern were designated as Class 1, those with mild head defects as Class 2 and those with a severe phenotype, reminiscent of dorsalized, D3 embryos as Class 3. 50% of  $dI^{WT}/Df$  embryos, in contrast to 87% of  $dI^{SCR}/Df$  embryos appear as Class 1 (Fig. 2.4, C2-C3; Fig. 2.4D), concurrent with the percentage of embryos that hatch. 47% of  $dI^{WT}/Df$  embryos showed Class 2 phenotypes, that were drastically reduced in  $dI^{SCR}/Df$ , to 11%. A small fraction of embryos (~3% of  $dI^{WT}/Df$  and ~2% of  $dI^{SCR}/Df$ ) showed a more severe Class 3

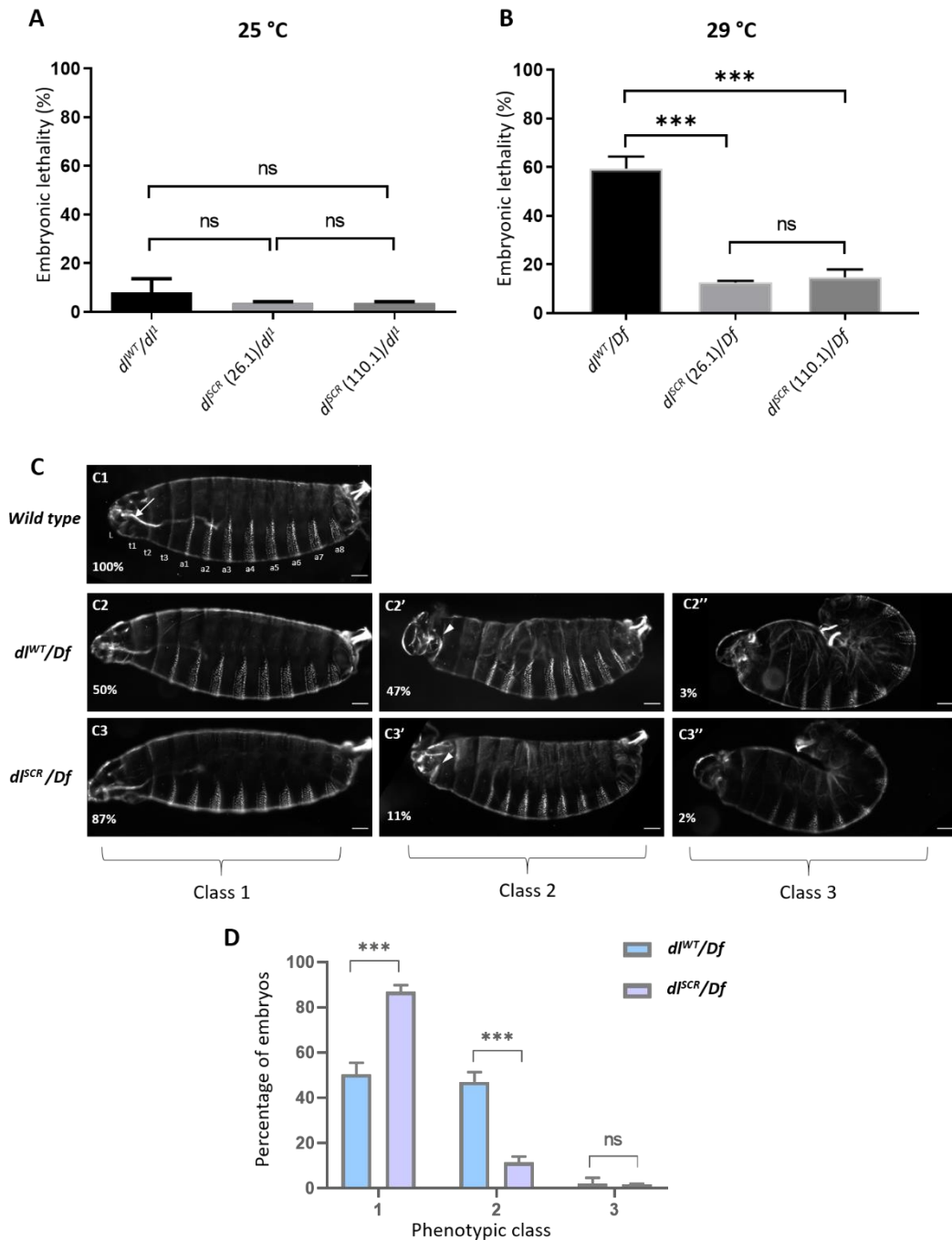


**Fig. 2.4.  $dl^{SCR}$  is haplo-sufficient.** Progeny of mothers of the indicated genotype, with one functional copy of DL, were scored for viability, 48 hours after egg lay, at 25 °C (A) and 29 °C (B). N=3, mean  $\pm$  SEM, Ordinary one-way ANOVA, (ns)  $P > 0.05$ , (\*\*\*)  $P < 0.001$ . Cuticle preparations of progeny of the maternal genotypes  $dl^{WT}/Df$  and  $dl^{SCR}/Df$ , visualized under a dark-field microscope yielded three major ranges of phenotypes, classified as class 1 (intact head region/ mouth hook; ventral denticle bands and filzkörper normal), class 2 (defective head structure; denticle bands and filzkörper intact) and class 3 (twisted embryos; defective head structures and filzkörper) (C). Cuticles are oriented dorsal-side up and anterior-side on the left. >100 embryos were scored in each replicate, and the percentage of each

phenotypic class is plotted for  $dI^{WT}/Df$  and  $dI^{SCR}/Df$  (D). N=3, mean  $\pm$  SEM, Two-way ANOVA, (ns)  $P > 0.05$ , (\*\*\*)  $P < 0.001$ .

phenotype (Fig. 2.4, C2''-C3''). The rescue of embryonic lethality appeared to be a direct result of Class 2 embryos transitioning to normal, Class 1 embryos in the presence of the  $dI^{SCR}$  allele. Our findings demonstrate that the  $dI^{SCR}$  allele alleviates temperature-dependent haploinsufficiency, rescuing developmental patterning.

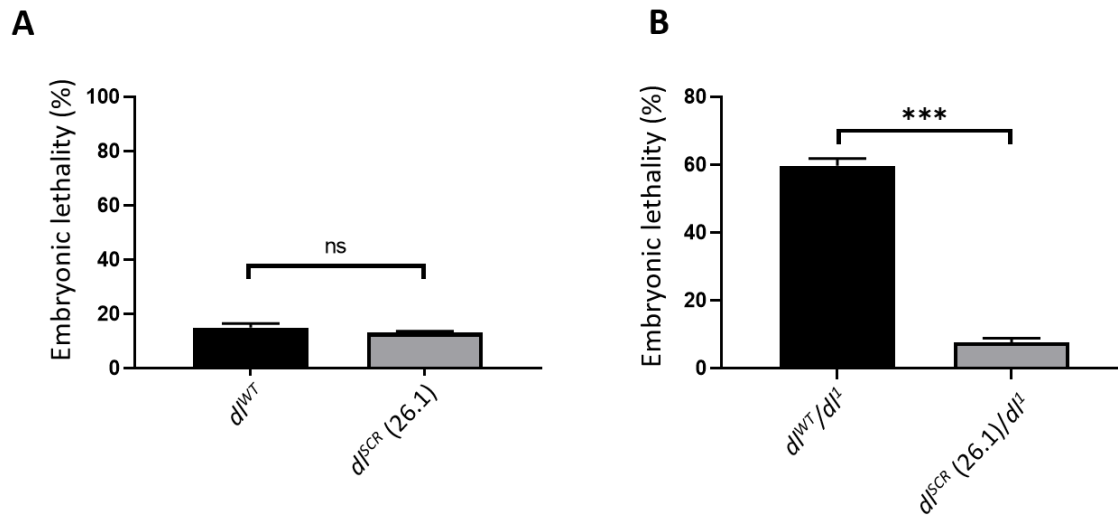


**Fig. 2.5. Haplo-sufficiency of the  $dI^{SCR}$  allele.** Embryonic lethality is plotted for the indicated genotypes, at 29 °C. N=3, mean  $\pm$  SEM, Unpaired t-test, (ns)  $P > 0.05$ , (\*\*\*)  $P < 0.001$ . Embryonic hatching suggests viability.

### 2.3.4 DL<sup>SCR</sup> supports the developmental program under haploinsufficient conditions.

The nuclear DL gradient was similar between  $dI^{WT}/Df$  and  $dI^{SCR}/Df$  in both sagittal (Fig. 2.6A) and transverse cross sections (Fig. 2.7A). As compared to WT controls, a single copy of the  $dI$  allele ( $dI^{WT}/Df$  or  $dI^{SCR}/Df$ ) in mothers led to shallow and broad gradients (Fig. 2.7B) in embryos, consistent with earlier studies (Lieberman *et al.* 2009; Reeves *et al.* 2012; Ambrosi *et al.* 2014; Carrell *et al.* 2017; Al Asafen *et al.* 2020), though the differences are statistically insignificant. The  $dI^{WT}/Df$  or  $dI^{SCR}/Df$  gradients were also similar to each other (Fig. 2.7B-D). On the ventral and lateral sides of the embryo, nuclear DL activates 50-70 genes, e.g. *twi*, *sna*, *rhomboid* (*rho*), *brinker* (*brk*), *short gastrulation* (*sog*), while a smaller number, such as *decapentaplegic* (*dpp*) and *zen* are transcriptionally repressed. *twi* is one of the earliest targets of DL to be activated in the ventral region in the wild-type embryo

(Fig. 2.6, B1) (Jiang *et al.* 1991; Kosman *et al.* 1992). *In-situ* hybridization indicated that a large fraction (~40%) of embryos laid by  $d^{WT}/Df$  mothers deviate from normal *twi* patterning (Fig. 2.6, B2), and we observed a drastic reduction or complete disruption of *twi* expression in the regions that intersect with the presumptive cephalic furrow, in stage 5 embryos (Fig. 2.6, B1'-B2''), when compared to wild-type embryos (Fig. 2.6, B1-B2). We refer to this region (arrow), as the DL 'weak activation region' or 'WAR'. The lack of *twi* activation is not transient and persists even at later stages of germ band extension (Fig. 2.6, B3' vs B3). We observed similar defects in embryos derived from  $d^{SCR}/Df$  females (Fig. 2.6, B1'', B2'', and B3''), but their numbers were dramatically reduced in comparison to  $d^{WT}/Df$  (Fig. 2.6F). The DL gradient in  $d^{WT}/Df$  and  $d^{SCR}/Df$  embryos (Fig. 2.6A, insets) is uninterrupted in the WAR in all embryos, pointing to a local failure of DL mediated activation rather than reduced or lack of expression of DL, in the WAR region.

DL and *Tw* work synergistically to activate *sna* which is critical for mesoderm specification. Haploinsufficiency of *d* also manifests as a severe loss or absence of *sna* at the WAR, closely mirroring the defects in *twi* expression in  $d^{WT}/Df$  and  $d^{SCR}/Df$  embryos (Fig. 2.6, C1- C2''). While ~30% of  $d^{WT}/Df$  embryos appear defective in *sna* expression, only ~15% of  $d^{SCR}/Df$  embryos display *sna* abnormalities (Fig. 2.6C1-2, C1'-2', C1''-2'' and Fig. 2.6G). In ~10-15% of  $d^{WT}/Df$  and  $d^{SCR}/Df$  embryos (Fig. 2.6, D1', D''; Fig. 2.6G), the *sog* gradient is expanded in the WAR, allowing the two lateral *sog* stripes to fuse ventrally (Fig. 2.6, D1' and D1''). The expansion of *sog* in the ventral domain is a direct consequence of the weaker expression of *sna/Sna* in the WAR. *zen*, repressed in the ventral and lateral regions by DL and expressed only at the dorsal-side of the embryo remained unperturbed in the haploinsufficient embryos of both  $d^{WT}$  and  $d^{SCR}$  (Fig. 2.6, E1- E1''). This was in stark contrast to the failure of DL-mediated activation, suggesting that DL-mediated repression was not influenced by the SUMOylation status of DL, even under haploinsufficient conditions.

Thus, the  $d^{SCR}$  allele rescues the failure of activation in the WAR for a large fraction of haploinsufficient embryos. The data described in this section argues for a role for SUMO conjugation of DL in regulating activation of DL target genes, especially *twi* and *sna*, in the WAR. SUMO conjugation-competent embryos (wild-type) have a high



failure rate for activation of *twi* and *sna* in the WAR under haploinsufficient conditions when compared to DL<sup>SCR</sup>. The *in-situ* data presented in this section is

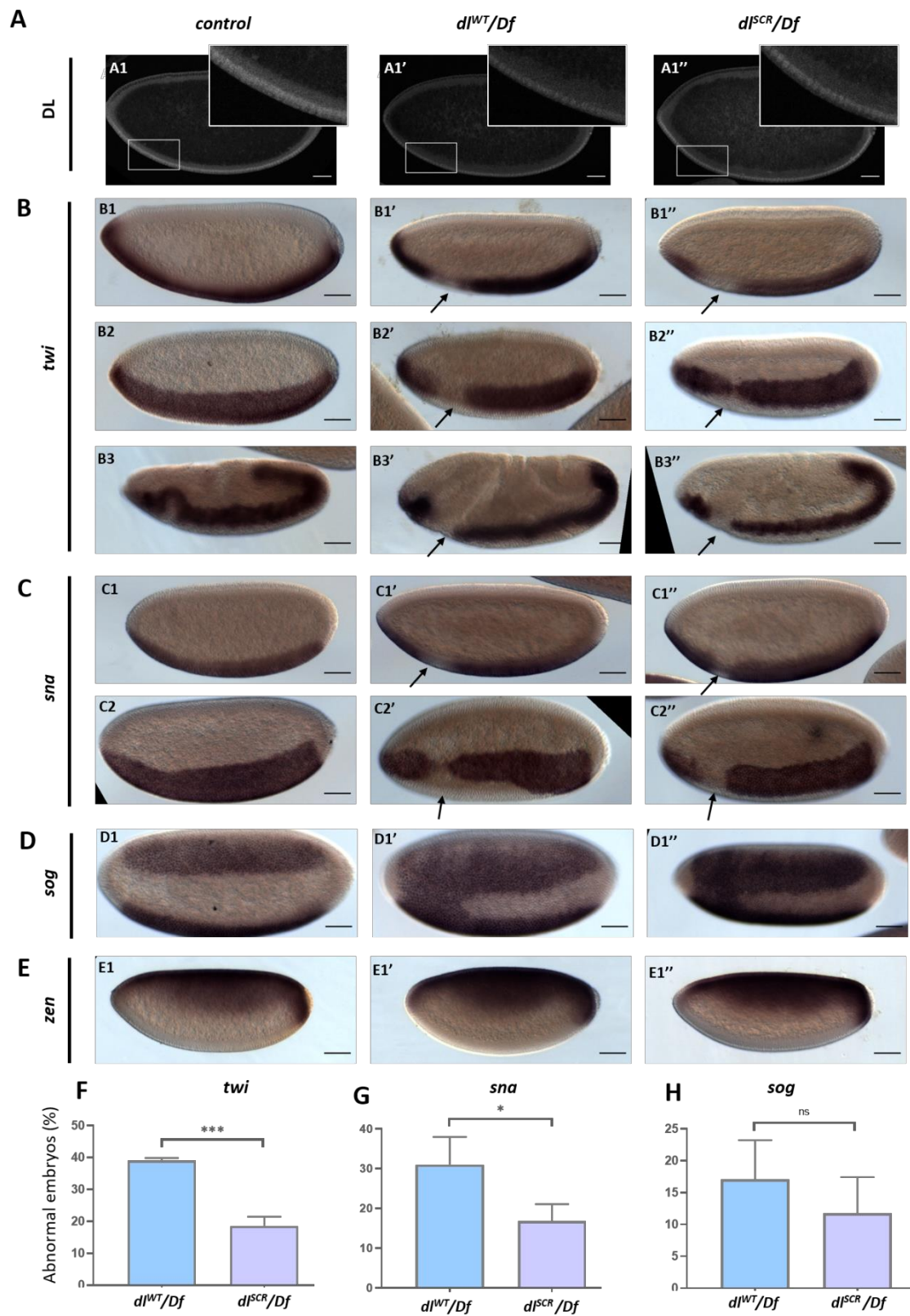


**Fig. 2.6. DL activity is altered in the SUMO-deficient mutant.** The DL gradient was visualized with a DL antibody in *control*, *dI<sup>WT</sup>/Df* and *dI<sup>SCR</sup>/Df* embryos (A). Insets represent a zoomed-in view of the presumptive cephalic furrow in the ventral region. In situ hybridization images of stage 5 embryos probed with digoxigenin-AP-labeled antisense RNA probes against *twi* (B), *sna* (C), *sog* (D), and *zen* (E) are shown (B3–B3" are stage 7 embryos, an exception). Embryos are oriented with the anterior side to the left and ventral side down (B1–B1"; B3–B3"; C1–C1"; E1–E1"), or tilted toward the reader (B2–B2"; C2–C2"; D1–D1"), for *control* (B1–E1), *dI<sup>WT</sup>/Df* (B1'–E1'), and *dI<sup>SCR</sup>/Df* (B1"–E1"). Arrows indicate a narrowing or an absence of the *twi* (a) and *sna* (b) pattern at the region of the presumptive cephalic furrow. D1'–D1") A fusion of the *sog* gradient near the ventral cephalic region. Embryos showing a deviation from the normal pattern (narrowing/absence/fusion) for *twi*, *sna*, and *sog* were plotted as a percentage of total stained embryos, for the *control*, *dI<sup>WT</sup>/Df*, and *dI<sup>SCR</sup>/Df* (f–h). Approximately 50 embryos were scored in each technical replicate, across 3 technical replicates. Data represented as mean  $\pm$  SEM, unpaired *t*-test, (ns)  $P > 0.05$ , (\*\*\*)  $P < 0.001$ , (\*)  $P < 0.05$ .

excellent for discerning spatio-temporal changes in the expression of DL target genes. What is yet unanswered is the effect of DL<sup>SCR</sup> on the levels of transcripts of DL targets, especially in conditions of haploinsufficiency. For this, we turned to quantitative mRNA measurements using RNA sequencing, described in the next section.

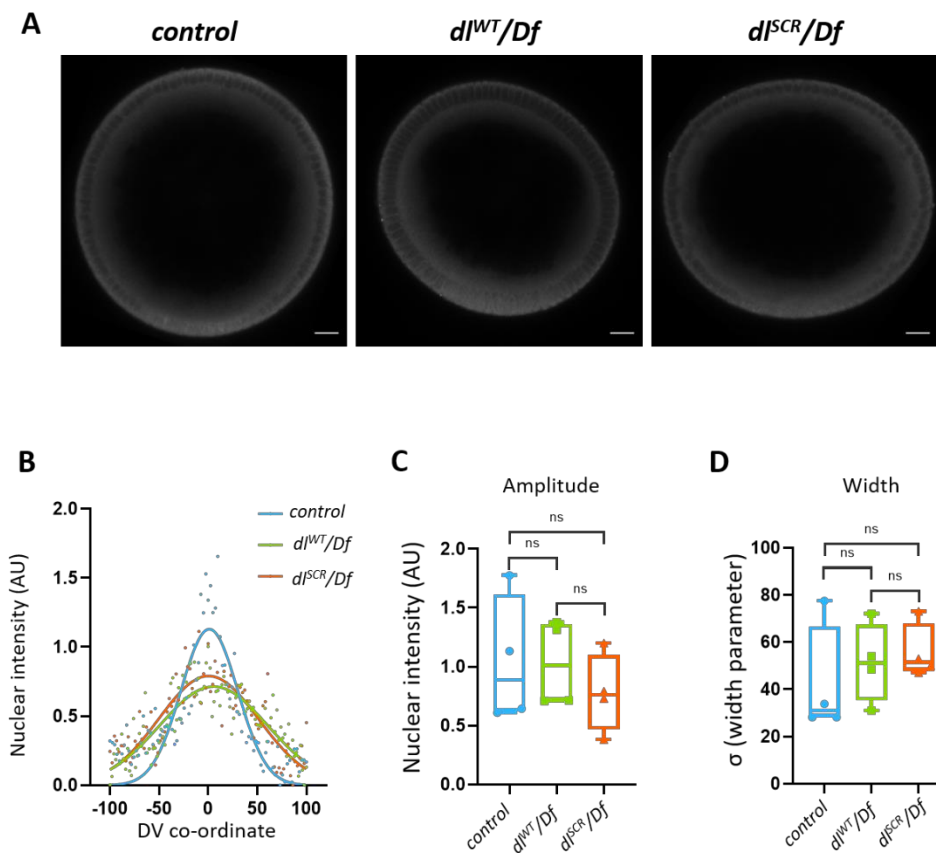


**Fig. 2.7. The DL gradient visualized with a DL antibody in control,  $dI^{WT}/Df$ , and  $dI^{SCR}/Df$  embryos.** (A) Transverse sections of nc 14 embryos of the specified genotypes. (B) shows representative intensity profiles of control,  $dI^{WT}/Df$  and  $dI^{SCR}/Df$  embryos, fitted to a Gaussian. The amplitude (C) and width (D) of the gradient centered at the ventral midline is plotted. n = 4, ordinary one-way ANOVA, (ns)  $P > 0.05$ .

### **2.3.5 $DL^{SCR}$ is a stronger transcriptional activator than $DL^{WT}$ under conditions of haploinsufficiency**

To obtain a global picture of the transcriptional activity of  $DL^{SCR}$ , we conducted a quantitative 3' RNA sequencing experiment on embryos laid by  $dI^{WT}$  and  $dI^{SCR}$  mothers, as well as embryos derived from  $dI^{WT}/Df$  and  $dI^{SCR}/Df$  mothers. The experiment was conducted at 29 °C for embryos aged 0-2 hours after egg lay, to capture possible quantitative differences in activation of DL target genes on account of maternal DL. Details of the methodology can be found in Materials and Methods. Overall, across the four genotypes ( $dI^{WT}$ ,  $dI^{SCR}$ ,  $dI^{WT}/Df$  and  $dI^{SCR}/Df$ , Fig. 2.8A) studied, 194 genes are differentially expressed ( $-0.58 > \log_2 \text{Fold change} > 0.58$ , at  $FDR < 0.1$ ), visualized as a heat map (Fig. 2.9A). A gene ontology analysis confirmed significant enrichment of genes encoding proteins involved in DNA-binding and embryonic developmental processes (Fig. 2.9B). Of these, we focused on genes that are bona-fide DL targets (n = 163, Fig. 2.8B), collated from studies on DV mutants using microarray chips, ChIP-chip analysis and bioinformatics studies (Markstein *et al.* 2002; Stathopoulos *et al.* 2002; Zeitlinger *et al.* 2007). Of the 194 differentially expressed genes (DEGs) in our 3' RNA sequencing experiment, 19 are known DL

targets (Fig 2.8B), and we generated a heat map to visualize the differences in gene expression across the four genotypes (Fig. 2.8C).

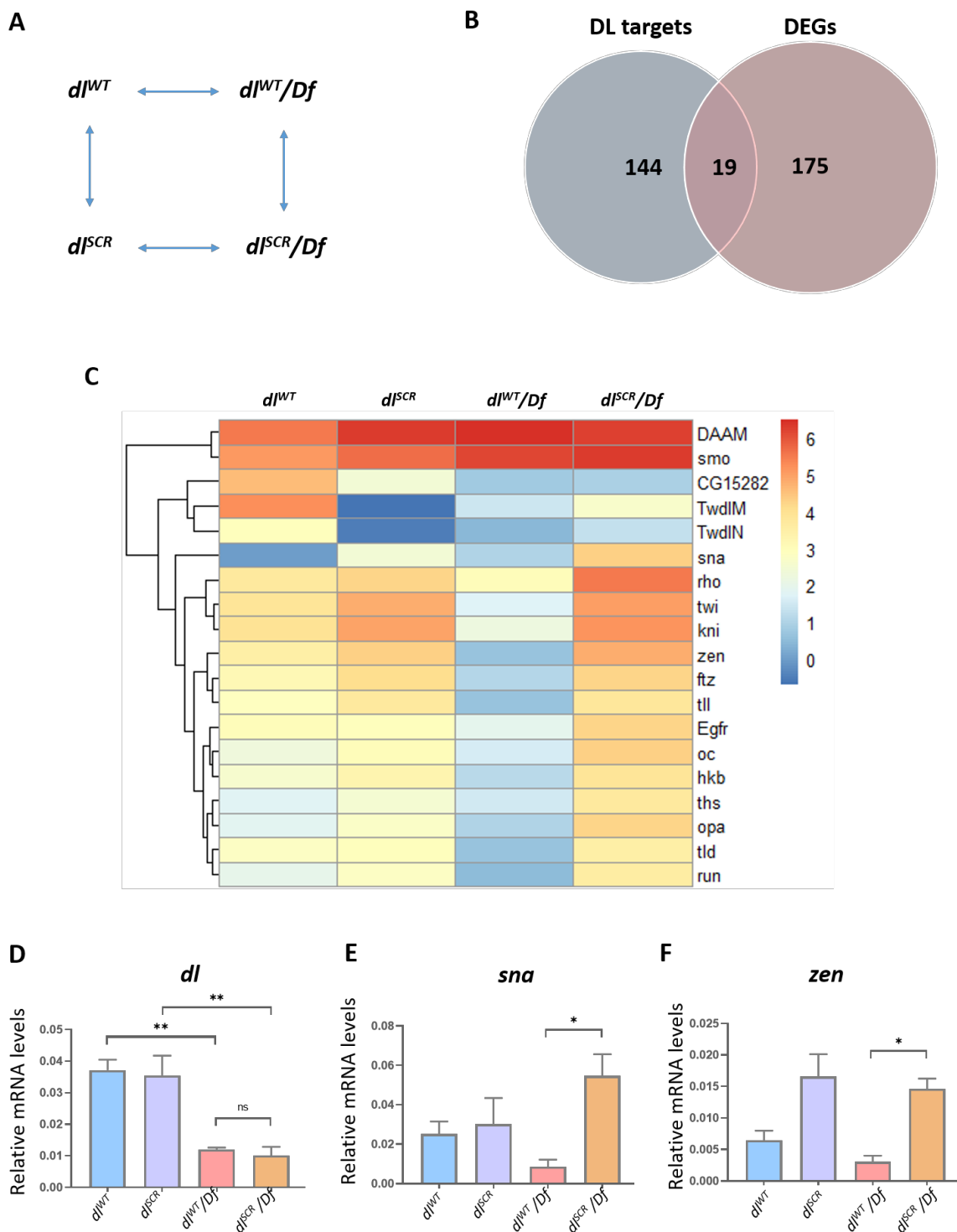


**Fig. 2.8. DL<sup>SCR</sup> displays higher transcriptional activity.** Maternal genotypes of the embryos used for the 3' RNA-seq analysis and their pairwise comparison to obtain differentially expressed genes (DEGs) is presented in (A). Genes that were identified as direct targets of DL from published literature and DEGs across all the conditions are represented as a Venn diagram in (B). The subset of DEGs with known binding sites for DL

are represented as a heatmap, for  $dl^{WT}$ ,  $dl^{SCR}$ ,  $dl^{WT}/Df$ , and  $dl^{SCR}/Df$  embryos at 29 °C, in (C). LogCPM values are plotted. (D), (E) and (F) denote relative mRNA expression levels of *dl*, *sna*, and *zen* transcripts respectively, measured by qRT-PCR analysis, for 0-2 hour embryos laid by mothers of the indicated genotypes at 29 °C. N=3, mean  $\pm$  SEM, Ordinary one-way ANOVA, (ns)  $P > 0.05$ , (\*\*)  $P < 0.01$ , (\*)  $P < 0.05$

As expected, analysis of the transcript levels (represented as log<sub>CPM</sub> values) clearly indicates that genes like *twi*, *knirps* (*kni*), *zen*, *fushi tarazu* (*ftz*), *tailless* (*tll*), and *tolloid* (*tld*) show lowered transcripts in  $dl^{WT}/Df$  compared to  $dl^{WT}$ . A reduction in the dose of *dl* in haploinsufficient embryos leads to reduced transcriptional activation of DL target genes (Fig. 2.8C). Exceptions include *Dishevelled Associated Activator of Morphogenesis* (*DAAM*) and *smoothened* (*smo*), whose transcript levels go up significantly, with decreased *dl* levels. When compared to  $dl^{WT}$ ,  $dl^{SCR}$  did not display statistically significant differences for *twi*, *kni*, *zen*, *ftz*, and *tll*, nor did we observe significant differences between  $dl^{SCR}/Df$  and  $dl^{SCR}$  (Fig. 2.8C). Intriguingly, 14 DL target genes are significantly upregulated in  $dl^{SCR}/Df$  compared to  $dl^{WT}/Df$  (Fig 2.8C; Fig. 2.9C) suggesting that for DL<sup>SCR</sup>, the lowered dose of DL in the haploinsufficient embryos is compensated for by higher transcriptional activation of critical DL target genes. These genes include DV patterning targets such as *twi*, *sna*, *zen* and *rho*, and antero-posterior (AP) target genes such as *kni* and *huckebein* (*hkb*) (Fig. 2.9C). The *dl*, *sna* and *zen* transcript levels were further independently assessed in a qRT-PCR experiment (Fig. 2.8 D-F). *dl* transcripts themselves are comparable across  $dl^{WT}/Df$  and  $dl^{SCR}/Df$ , downregulated by ~50% compared to the control (Fig. 2.8D), indicating that *dl* mRNA levels are not affected in  $dl^{SCR}$ . *sna* and *zen*, however show 6–8-fold higher transcript levels (Fig. 2.8E, 2.8F) in  $dl^{SCR}/Df$ , in agreement with our 3' mRNA sequencing data (Fig. 2.8C). *zen* is a target for DL-mediated repression, but in the absence of expansion of the *zen* expression domain, the transcript data suggests that a transcriptional activator responsible for switching on *zen* may be indirectly influenced by DL.

The greater rate of hatching and survival of  $dl^{SCR}/Df$  compared to  $dl^{WT}/Df$  is possibly a function of increased, compensatory transcription of DL targets and the previously described rescue of activation in the WAR. SUMOylation of DL thus plays a global role in decreasing transcription of DL targets in general and in addition, has an important role in the WAR for activation of *twi/sna*. The higher activation of DL target

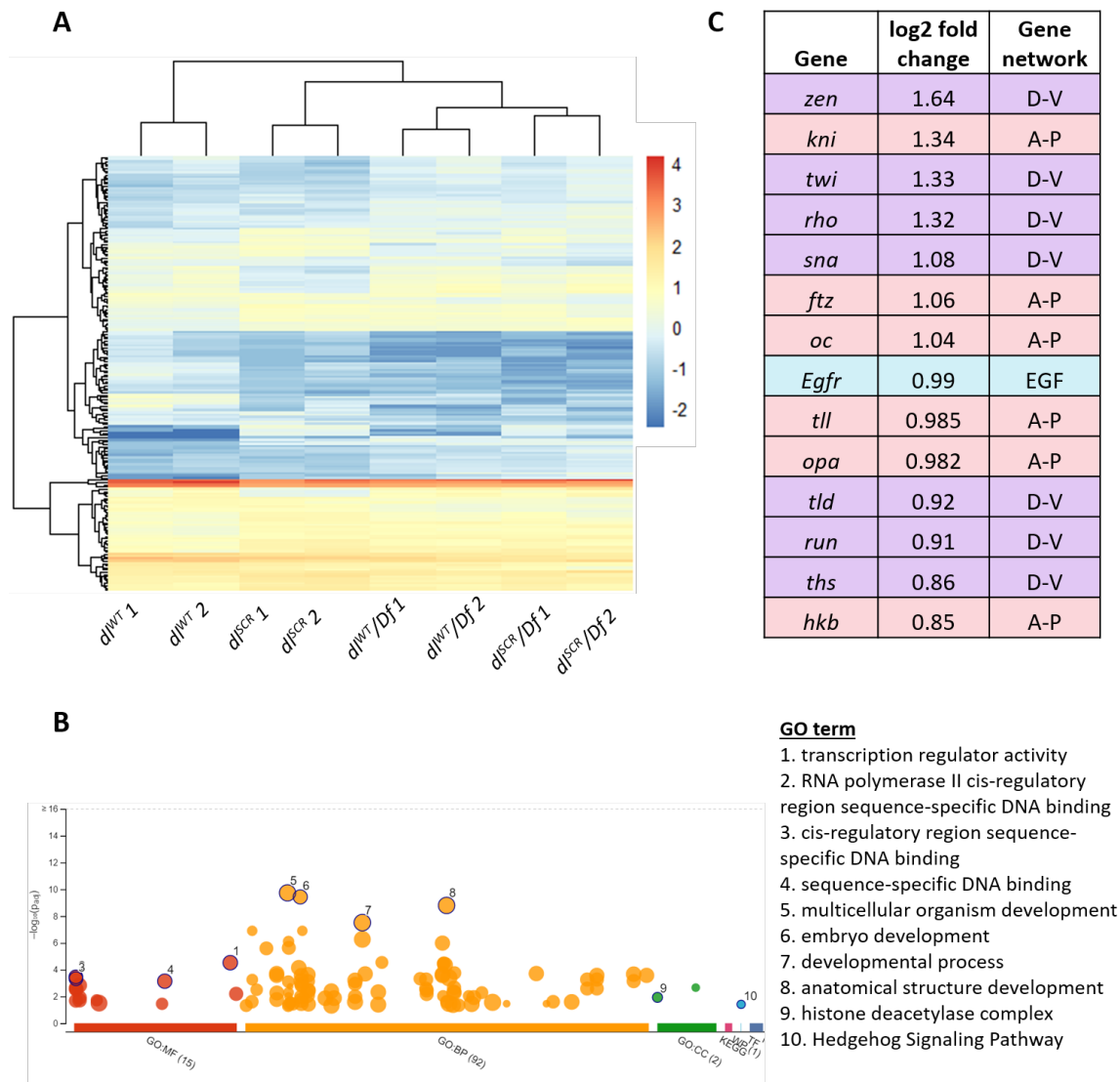


**Fig. 2.9. Quantitative changes in the transcriptome of embryos laid by  $dl^{SCR}$  mothers** (A) Heat map of differentially expressed genes across  $dl^{WT}$ ,  $dl^{SCR}$ ,  $dl^{WT}/Df$ ,  $dl^{SCR}/Df$  are represented, in duplicates. Scaled, LogCPM values are plotted. (B) denotes significantly enriched gene ontology (GO) terms, for genes in (A), categorized by molecular function (MF), biological process (BP), cellular component (CC) and pathway (KEGG). A subset of differentially regulated genes compared across  $dl^{WT}/Df$  and  $dl^{SCR}/Df$  with known binding sites for DL is listed in (C), along with the corresponding log2 fold-change values. The genes are broadly classified according to the gene regulatory network they are a part of in the early embryo: D-V (Dorso-ventral patterning; in purple), A-P (Antero-posterior patterning; in pink) and the EGF signaling pathway (in blue).

genes in  $dl^{SCR}/Df$  leads us to hypothesize (see Discussion) that SUMO conjugation of DL may be part of a negative feedback loop to curtail transcription of DL targets.

## 2.4 Discussion

Comprehensive proteomic studies across species have led to the identification of SUMOylated proteins (Wykoff and O'Shea 2005; Handu *et al.* 2015b; Hendriks and Vertegaal 2016b; Pirone *et al.* 2017; Hendriks *et al.* 2018). One class of proteins studied in detail is transcription factors (TFs) (Verger *et al.* 2003), with ~50% being SUMOylated in humans (Hendriks *et al.* 2017). Upon SUMOylation, changes in the transcriptional output of TFs can be brought about by alterations in DNA-binding, eviction from the chromatin, or a re-shaping of their protein-interaction landscape (Ouyang and Gill 2009; Raman *et al.* 2013; Wotton *et al.* 2017; Rosonina *et al.* 2017; Rosonina 2019). Amongst the well-studied TFs is the NF- $\kappa$ B family (Kracklauer and Schmidt 2003; Mabb and Miyamoto 2007). SUMOylation of NF- $\kappa$ B was first demonstrated in *Drosophila*, for DL (Bhaskar *et al.* 2000). In mammals, RelA undergoes SUMOylation after TNF $\alpha$  stimulation, aided by the E3 ligase PIAS3. The authors also observe, interestingly, that only the DNA-bound form of RelA is SUMO-modified (Liu *et al.* 2012) and acts as a repressor. RelB, another NF- $\kappa$ B family transcription factor, is also negatively regulated by SUMOylation, though its DNA binding remains unchanged (Leidner *et al.* 2014).

In *Drosophila*, the Toll/NF- $\kappa$ B cascade has been best studied in two diverse contexts, in DV patterning, and in the immune response. In early development, where perturbations to the DL gradient could derail DV patterning, we do not see any effect of lack of SUMOylation on DL activity. Increase in the transcriptional activity of DL<sup>SCR</sup> in the embryo becomes apparent only in conditions of haploinsufficiency (*d<sup>SCR</sup>/Df*), where DL target genes are, surprisingly, activated at wild-type levels. This enhanced transcriptional activation with reduced DL dosage leads us to suggest that SUMO conjugation may be linked to a negative-feedback loop (Fig. 9C), where transcription of DL-target genes is sensed by a hypothetical sensor, that triggers SUMOylation of DL by Ubc9. In our model, DL<sup>S</sup>, when bound to the promoter, would block activation by DL<sup>U</sup>, and attenuate DL signaling. The sensor would ideally sense transcripts of DL target genes, as shown for miRNAs (Li *et al.* 2021). Under conditions of haploinsufficiency (*d<sup>WT</sup>/Df*) at 29 °C, DL<sup>U</sup> activates target genes, with DL<sup>S</sup> dampening the response, leading to lowered levels of transcripts. In the case of *d<sup>SCR</sup>/Df*, the circuit (Fig. 9C) is broken, with Ubc9 unable to SUMOylate DL<sup>SCR</sup>. Here, DL-

mediated activation cannot be dampened, leading to higher levels of target transcripts.

An interesting feature of haploinsufficiency in the embryo is the WAR. This phenomenon goes beyond a generic lowering of *twi* activation, and is possibly related to the modulation of a physical interactor of DL (Fig. S8). Candidates include Daughterless (Da), Achaete-scute complex (AS-C), Nejire(Nej)/CREB binding protein(CBP) and TBP-associated factors (TAFs). Embryos laid by *nej<sup>3</sup>/+;dl<sup>1</sup>/+* mothers showed weaker *twi* expression and a lack of expression in the WAR (Akimaru *et al.* 1997). Similar effects were seen in eggs laid by *dl<sup>1</sup>/+;TAF<sub>II</sub>110/+* or *dl<sup>1</sup>/+;TAF<sub>II</sub>60/+* mothers (Zhou *et al.* 1998) as also *dl<sup>8</sup>/+;da<sup>11B31</sup>/+* mothers (González-Crespo and Levine 1993). We hypothesize that DL forms complexes with these proteins to activate *twi* and this complex formation is critical in the WAR (Fig. 9D). DL<sup>U</sup> is efficient at interacting with one (or all) of these proteins whereas DL<sup>S</sup> destabilizes the activation complex (Fig. 9D). Hence, in the *dl<sup>SCR</sup>* animal, the absence of DL<sup>S</sup> leads to a robust activation of *twi* in the WAR, suppressing the lethality under conditions of haploinsufficiency.

Does our data suggest any role for DL in DV patterning under ambient conditions with normal DL concentrations? Since the developing embryo would face temperature fluctuations, DL<sup>S</sup> could fine-tune transcription rates and influence the robustness of the DL activity gradient. SUMO conjugation of DL would thus be a mechanism for developmental canalization, as hypothesized by Conrad Waddington (Waddington 1959). High transcriptional activation by DL<sup>U</sup>, which could disturb DV patterning, would be dampened by DL<sup>S</sup>, allowing the embryo to maintain graded DL-activity and complete the DV program successfully. In poikilotherms such as *Drosophila*, SUMO conjugation of DL would be a useful mechanism to buffer transcriptional activity against environmental perturbations and stochastic fluctuations, late in the cascade, specifically at the level of transcriptional activation.

## 2.5 Materials and Methods

### *Fly husbandry and stocks*



Flies were raised on standard cornmeal agar at 25 °C unless stated otherwise. For the *dl* deficiency experiments, flies were crossed and maintained at 29 °C. The following fly stocks were procured from the Bloomington *Drosophila* Stock Centre: *dl*<sup>1</sup>/*CyO* (3236), *dl*<sup>4</sup>/*CyO* (7096), and *vasa-Cas9* (51323). The *dl* deficiency allele *w*-, *y*; *J4/CyO* containing a precise deletion of the *dl* and *dif* loci, was a kind gift from the Govind laboratory, City University of New York (CUNY), NY.

#### *Generation of transgenic CRISPR lines*

The Fly CRISPR Optimal Target Finder was used to design the gRNA with zero predicted off-target effects. The gRNA sequence 5' GAAACATACCGCCCATTA AAA 3' was incorporated into the forward primer sequence GAAACATACCGCCCATTA AAAAGTTTTAGAGCTAGAAATAGC. A reverse primer of the following sequence was used: GAAGTATTGAGGAAAACATA. The gRNA was cloned into the pBFv-U6.2 vector as described previously (Kondo and Ueda 2013), using the primers listed above. The 100-mer ssODN sequence is as follows:  
TTTAACTAGGTTTTTTTTTTGTAGTTTTAGTGTATAAACTCACCTCTTGGTTCCG  
TTCGAATGGGCGGTATGTTTTGTGTATTCCAGCAATTCATGTTA

A total of 620 *vasa-Cas9* embryos were co-injected with the gRNA and ssODN, at the C-CAMP facility, NCBS. 450 F0 adults that emerged were crossed with *Tft/CyO* balancer flies individually. Three emergent flies from each cross were balanced further, with the *Tft/CyO* balancer, and maintained as separate lines. Homozygous flies from these founder lines were screened for the presence of the mutation by PCR followed by restriction digestion. For the isolation of genomic DNA, flies were placed in 0.2mL tubes individually and lysed in 50µL of squishing buffer (10mM Tris-HCl pH 8, 1mM EDTA, 25mM NaCl, and 0.2 mg/mL Proteinase K). After incubation at 37 °C for 30 minutes, Proteinase K was inactivated by heating at 85 °C. 1µL of the genomic DNA was used in a 10 µL PCR reaction. The following primers were used for the PCR: F: CAGTTCTGAGTAAGTCTTTATCGGAGTTCA; R: CCAAAGGGTTGTGGCGAGGTAT. The PCR product was digested with the restriction enzyme BstBI and resolved on a 1.2% agarose gel. Four transformants were obtained after screening 200 lines.

#### *Cuticle preparation*

Embryos were collected for three hours and aged for 22 hours at 25 °C or 29 °C, depending on the nature of the experiment. They were dechorionated in a 4% sodium hypochlorite solution for 2 minutes. Dechorionated embryos were washed thoroughly under running tap water and transferred to a scintillation vial containing 1:1 methanol: heptane. The vial was shaken vigorously for a few minutes, and devitellinized embryos in the lower methanol phase were transferred to a new vial with fresh methanol. Embryos were transferred onto a slide, mounted in 85% lactic acid, and incubated overnight at 55 °C on a slide warmer. Cuticles were imaged on a Zeiss Axio Imager Z1 microscope, using dark field illumination, with a 10X objective.

*Embryo staining:* 0-3 hour embryos were dechorionated in 4% sodium hypochlorite for 2 minutes. Embryos were rinsed and fixed in a 1:1 solution of 4% formaldehyde in 1X Phosphate-buffered saline (PBS): heptane for 20 minutes. The aqueous phase containing formaldehyde was removed, and embryos were devitellinized by adding an equal volume of ice-cold methanol followed by vigorous shaking. Devitellinized embryos were washed thrice in methanol. Embryos were re-hydrated and permeabilized by giving six 15-minute washes in 1X PBS containing 0.3% Triton X-100 (0.3% PBS-T). After blocking with 2% Bovine serum albumin (BSA) in 0.3% PBS-T, embryos were incubated overnight at 4 °C with the primary antibody. Following four 15-minute washes with 0.3% PBS-T, embryos were incubated with the secondary antibody for an hour at room temperature. Embryos were washed thrice in 0.3% PBS-T, and DAPI was added in the penultimate wash. Embryos were mounted in SlowFade Gold mountant (Invitrogen) and imaged on a Leica Sp8 confocal microscope under a 20X oil-immersion objective. To obtain transverse cross sections, embryos were sectioned with a razor as previously described (Liberman *et al.* 2009; Reeves *et al.* 2012; Trisnadi *et al.* 2013) and mounted in 70% glycerol. Embryos were imaged on a Leica Sp8 confocal microscope with a 40X oil-immersion objective. The following antibodies were used: Mouse anti-Dorsal, 1:1000 (DSHB 7A4-c) and goat anti-mouse Alexa568 secondary antibody, 1:1000 (Invitrogen).

#### *Image analysis of fixed embryos*

Images of transverse sections were analyzed as described in (Trisnadi *et al.* 2013), with minor modifications. Briefly, the StarDist plugin in ImageJ was used to obtain

nuclear masks of the DAPI channel with distinct numerical labels. For each nucleus identified, corresponding DL fluorescence intensity values were obtained. Normalized values of DL nuclear intensities were calculated as a ratio of DL intensity to that of the nuclear channel. The DL gradient was fit to a Gaussian, using GraphPad Prism8, to obtain the amplitude and width parameters. The amplitude is the height of the curve's peak, while  $\sigma$  is the measure of one standard deviation, determining the width of the distribution.

### *RNA in-situ hybridization*

Embryos were collected and aged at 29 °C. Anti-sense digoxigenin-labelled RNA probes for *twi*, *sna*, *sog*, and *zen* were used and hybridization was carried out as previously described (Tautz and Pfeifle 1989). Anti-Digoxigenin-Alkaline phosphatase antibody (Merck) was used at a concentration of 1:2000 and NBT/BCIP (Merck) was used as the color-development substrate for AP. Images were acquired on a Zeiss Axio Imager Z1 microscope, using DIC optics, with a 10X objective.

### *Quantitative PCR*

RNA was extracted from appropriately staged embryos using the RNeasy Plus Universal mini kit (Qiagen) according to the manufacturer's instructions. 1  $\mu$ g of total RNA was used to generate cDNA using the High-Capacity cDNA Reverse Transcription kit (Thermo Fisher Scientific). The qPCR reaction was performed on a qTOWER<sup>3</sup> real-time thermal cycler (Analytik Jena) with KAPA SYBR FAST master mix (Sigma-Aldrich). Gene expression was monitored using gene-specific primers. Transcript levels were calculated using the comparative Ct method to obtain fold change values. Relative mRNA levels were calculated using the delta Ct values. Rp49 was used as a reference gene. The following primer pairs were used (Forward primer, F and reverse primer, R):

*rp49* F: GACGCTTCAAGGGACAGTATC, *rp49* R: AAACGCGGTTCTGCATGAG;

*dl* F: ATCCGTGTGGATCCGTTTAA, *dl* R: AATCGCACCGAATTCAGATC;

*twi* F: AAGTCCCTGCAGCAGATCAT, *twi* R: CGGCACAGGAAGTCAATGTA;

*sna* F: CGGAACCGAAACGTGACTAT, *sna* R: CCTTTCCGGTGTTTTTGAAA;

*zen* F: TACTATCCAGTTCACCAGGCTAA, *zen* R: TCTGATTGTAGTTGGGAGGCA;

### *Quantitative RNA sequencing and analysis*

Cages containing flies of the appropriate genotype were set up with sugar-agar plates. Plates were changed twice after 1 hour intervals and the third collection was used for the experiment. Embryos were collected at 29 °C for two hours. RNA was isolated from two biological replicates for each sample using the RNeasy Plus Universal mini kit (Qiagen). RNA concentration was determined using a NanoDrop instrument, and 500ng of RNA was used to generate the cDNA library with the QuantSeq 3'mRNA-Seq Library Prep Kit FWD for Illumina (Lexogen), according to the manufacturer's instructions. The library size and quality were determined on a Bioanalyzer with a high sensitivity chip (Agilent) and concentration assessed using a Qubit fluorometer, with a dsDNA High Sensitivity assay kit (Thermo Fisher Scientific). The equimolar, pooled library was sequenced on an Illumina NextSeq 550 system, generating 75 bp single-end reads. The sequencing files obtained were uploaded onto BlueBee's genomics analysis platform (<https://lexogen.bluebee.com/quantseq/>). Reads were trimmed in BlueBee using bbduk (v35.92). Reads were aligned, counted, and mapped using BlueBee's STAR-aligner (v2.5.2a), HTSeq-count (v0.6.0), and RSEQC (v2.6.4), respectively. A DESeq2 application within BlueBee (Lexogen Quantseq DE 1.2) was used to obtain normalized gene counts and identify differentially expressed genes based on a false discovery rate (FDR) cut-off *P*-adjusted value <0.1. Downstream analysis was performed on EdgeR. Raw count data was transformed using the logCPM function to obtain values for the heatmap, generated using pheatmap in RStudio. GO enrichment analysis was performed using gProfiler (<https://biit.cs.ut.ee/gprofiler/gost>).

**Notes/ Contributions:** Parts of this chapter have been published as a research article, 'Hegde, S., Sreejan, A., Gadgil, C. J., & Ratnaparkhi, G. S. (2022). SUMOylation of Dorsal attenuates Toll/NF-κB signaling. *Genetics*, 221(3), iyac081.'

## **2.6 References**

1. Akimaru H., D. X. Hou, and S. Ishii, 1997 *Drosophila* CBP is required for dorsal-dependent twist gene expression. *Nat. Genet.* 17: 211–214.  
<https://doi.org/10.1038/ng1097-211>
2. Al Asafen H., P. U. Bandodkar, S. Carrell-Noel, A. E. Schloop, J. Friedman, *et al.*, 2020 Robustness of the Dorsal morphogen gradient with respect to morphogen dosage. *PLoS Comput. Biol.* 16: e1007750.  
<https://doi.org/10.1371/journal.pcbi.1007750>
3. Ambrosi P., J. S. Chahda, H. R. Koslen, H. J. Chiel, and C. M. Mizutani, 2014 Modeling of the dorsal gradient across species reveals interaction between embryo morphology and Toll signaling pathway during evolution. *PLoS Comput. Biol.* 10: e1003807. <https://doi.org/10.1371/journal.pcbi.1003807>
4. Anderson K. V., and C. Nüsslein-Volhard, 1984 Information for the dorsal–ventral pattern of the *Drosophila* embryo is stored as maternal mRNA. *Nature* 311: 223–227. <https://doi.org/10.1038/311223a0>
5. Anjum S. G., W. Xu, N. Nikkholgh, S. Basu, Y. Nie, *et al.*, 2013 Regulation of Toll signaling and inflammation by  $\beta$ -arrestin and the SUMO protease Ulp1. *Genetics* 195: 1307–1317. <https://doi.org/10.1534/genetics.113.157859>
6. Araujo H., and E. Bier, 2000 *sog* and *dpp* exert opposing maternal functions to modify toll signaling and pattern the dorsoventral axis of the *Drosophila* embryo. *Development* 127: 3631–3644.
7. Bassett A. R., C. Tibbit, C. P. Ponting, and J.-L. Liu, 2014 Highly Efficient Targeted Mutagenesis of *Drosophila* with the CRISPR/Cas9 System. *Cell Rep.* 6: 1178–1179. <https://doi.org/10.1016/j.celrep.2014.03.017>
8. Beauclair G., A. Bridier-Nahmias, J.-F. Zagury, A. Saïb, and A. Zamborlini, 2015 JASSA: a comprehensive tool for prediction of SUMOylation sites and SIMs. *Bioinformatics* 31: 3483–3491. <https://doi.org/10.1093/bioinformatics/btv403>
9. Belvin M. P., and K. V. Anderson, 1996 A conserved signaling pathway: the *Drosophila* toll-dorsal pathway. *Annu. Rev. Cell Dev. Biol.* 12: 393–416.  
<https://doi.org/10.1146/annurev.cellbio.12.1.393>
10. Bergmann A., D. Stein, R. Geisler, S. Hagenmaier, B. Schmid, *et al.*, 1996 A gradient of cytoplasmic Cactus degradation establishes the nuclear localization gradient of the dorsal morphogen in *Drosophila*. *Mech. Dev.* 60: 109–123.  
[https://doi.org/10.1016/S0925-4773\(96\)00607-7](https://doi.org/10.1016/S0925-4773(96)00607-7)

11. Bhaskar V., S. A. Valentine, and A. J. Courey, 2000 A functional interaction between dorsal and components of the Smt3 conjugation machinery. *J. Biol. Chem.* 275: 4033–4040. <https://doi.org/10.1074/jbc.275.6.4033>
12. Bhaskar V., M. Smith, and A. J. Courey, 2002 Conjugation of Smt3 to dorsal may potentiate the *Drosophila* immune response. *Mol. Cell. Biol.* 22: 492–504. <https://doi.org/10.1128/MCB.22.2.492-504.2002>
13. Bier E., M. M. Harrison, K. M. O'Connor-Giles, and J. Wildonger, 2018 Advances in Engineering the Fly Genome with the CRISPR-Cas System. *Genetics* 208: 1–18. <https://doi.org/10.1534/genetics.117.11113>
14. Carrell S. N., M. D. O'Connell, T. Jacobsen, A. E. Pomeroy, S. M. Hayes, *et al.*, 2017 A facilitated diffusion mechanism establishes the *Drosophila* Dorsal gradient. *Development* 144: 4450–4461. <https://doi.org/10.1242/dev.155549>
15. Chiu H., B. C. Ring, R. P. Sorrentino, M. Kalamarz, D. Garza, *et al.*, 2005 dUbc9 negatively regulates the Toll-NF- $\kappa$ B pathways in larval hematopoiesis and drosomycin activation in *Drosophila*. *Dev. Biol.* 288: 60–72. <https://doi.org/10.1016/j.ydbio.2005.08.008>
16. Geisler R., A. Bergmann, Y. Hiromi, and C. Nüsslein-Volhard, 1992 cactus, a gene involved in dorsoventral pattern formation of *Drosophila*, is related to the I $\kappa$ B gene family of vertebrates. *Cell* 71: 613–621. [https://doi.org/10.1016/0092-8674\(92\)90595-4](https://doi.org/10.1016/0092-8674(92)90595-4)
17. González-Crespo S., and M. Levine, 1993 Interactions between dorsal and helix-loop-helix proteins initiate the differentiation of the embryonic mesoderm and neuroectoderm in *Drosophila*. *Genes Dev.* 7: 1703–1713. <https://doi.org/10.1101/gad.7.9.1703>
18. Govind S., L. Brennan, and R. Steward, 1993 Homeostatic balance between dorsal and cactus proteins in the *Drosophila* embryo. *Development* 117: 135–148.
19. Gratz S. J., F. P. Ukken, C. D. Rubinstein, G. Thiede, L. K. Donohue, *et al.*, 2014 Highly specific and efficient CRISPR/Cas9-catalyzed homology-directed repair in *Drosophila*. *Genetics* 196: 961–971. <https://doi.org/10.1534/genetics.113.160713>
20. Handu M., B. Kaduskar, R. Ravindranathan, A. Soory, R. Giri, *et al.*, 2015 SUMO-Enriched Proteome for *Drosophila* Innate Immune Response. *G3* 5: 2137–2154. <https://doi.org/10.1534/g3.115.020958>

21. Hendriks I. A., and A. C. O. Vertegaal, 2016 A comprehensive compilation of SUMO proteomics. *Nat. Rev. Mol. Cell Biol.* 17: 581–595.  
<https://doi.org/10.1038/nrm.2016.81>
22. Hendriks I. A., D. Lyon, C. Young, L. J. Jensen, A. C. O. Vertegaal, *et al.*, 2017 Site-specific mapping of the human SUMO proteome reveals co-modification with phosphorylation. *Nat. Struct. Mol. Biol.* 24: 325–336.
23. Hendriks I. A., D. Lyon, D. Su, N. H. Skotte, J. A. Daniel, *et al.*, 2018 Site-specific characterization of endogenous SUMOylation across species and organs. *Nat. Commun.* 9: 2456. <https://doi.org/10.1038/s41467-018-04957-4>
24. Hu Y., R. Sopko, V. Chung, M. Foos, R. A. Studer, *et al.*, 2019 iProteinDB: An Integrative Database of Drosophila Post-translational Modifications. *G3: Genes, Genomes, Genetics* 9: 1–11. <https://doi.org/10.1534/g3.118.200637>
25. Huang L., S. Ohsako, and S. Tanda, 2005 The lesswright mutation activates Rel-related proteins, leading to overproduction of larval hemocytes in *Drosophila melanogaster*. *Dev. Biol.* 280: 407–420.  
<https://doi.org/10.1016/j.ydbio.2005.02.006>
26. Ip Y. T., R. E. Park, D. Kosman, E. Bier, and M. Levine, 1992 The dorsal gradient morphogen regulates stripes of rhomboid expression in the presumptive neuroectoderm of the *Drosophila* embryo. *Genes Dev.* 6: 1728–1739.  
<https://doi.org/10.1101/gad.6.9.1728>
27. Janeway C. A. Jr, and R. Medzhitov, 2002 Innate immune recognition. *Annu. Rev. Immunol.* 20: 197–216.  
<https://doi.org/10.1146/annurev.immunol.20.083001.084359>
28. Jiang J., D. Kosman, Y. T. Ip, and M. Levine, 1991 The dorsal morphogen gradient regulates the mesoderm determinant twist in early *Drosophila* embryos. *Genes Dev.* 5: 1881–1891. <https://doi.org/10.1101/gad.5.10.1881>
29. Kondo S., and R. Ueda, 2013 Highly improved gene targeting by germline-specific Cas9 expression in *Drosophila*. *Genetics* 195: 715–721.  
<https://doi.org/10.1534/genetics.113.156737>
30. Kopp E. B., and S. Ghosh, 1995 NF- $\kappa$ B and Rel proteins in innate immunity. *Adv. Immunol.* 58.
31. Kosman D., Y. T. Ip, M. Levine, and K. Arora, 1991 Establishment of the mesoderm-neuroectoderm boundary in the *Drosophila* embryo. *Science* 254: 118–122. <https://doi.org/10.1126/science.1925551>

32. Kosman D., K. Yazdanbakhsh, and M. Levine, 1992 dorsal-twist interactions establish snail expression in the presumptive mesoderm of the *Drosophila* embryo. *Genes* .
33. Kracklauer M. P., and C. Schmidt, 2003 At the crossroads of SUMO and NF- $\kappa$ B. *Mol. Cancer* 2: 39. <https://doi.org/10.1186/1476-4598-2-39>
34. Leidner J., C. Voogdt, R. Niedenthal, P. Möller, U. Marienfeld, *et al.*, 2014 SUMOylation attenuates the transcriptional activity of the NF- $\kappa$ B subunit RelB. *J. Cell. Biochem.* 115: 1430–1440. <https://doi.org/10.1002/jcb.24794>
35. Li R., X. Yao, H. Zhou, P. Jin, and F. Ma, 2021 The *Drosophila* miR-959–962 Cluster Members Repress Toll Signaling to Regulate Antibacterial Defense during Bacterial Infection. *Int. J. Mol. Sci.* 22: 886. <https://doi.org/10.3390/ijms22020886>
36. Liberman L. M., G. T. Reeves, and A. Stathopoulos, 2009 Quantitative imaging of the Dorsal nuclear gradient reveals limitations to threshold-dependent patterning in *Drosophila*. *Proc. Natl. Acad. Sci. U. S. A.* 106: 22317–22322. <https://doi.org/10.1073/pnas.0906227106>
37. Liu Y., R. Bridges, A. Wortham, and M. Kulesz-Martin, 2012 NF- $\kappa$ B repression by PIAS3 mediated RelA SUMOylation. *PLoS One* 7: e37636. <https://doi.org/10.1371/journal.pone.0037636>
38. Mabb A. M., and S. Miyamoto, 2007 SUMO and NF- $\kappa$ B ties. *Cell. Mol. Life Sci.* 64: 1979–1996. <https://doi.org/10.1007/s00018-007-7005-2>
39. Markstein M., P. Markstein, V. Markstein, and M. S. Levine, 2002 Genome-wide analysis of clustered Dorsal binding sites identifies putative target genes in the *Drosophila* embryo. *Proc. Natl. Acad. Sci. U. S. A.* 99: 763–768. <https://doi.org/10.1073/pnas.012591199>
40. Medzhitov R., P. Preston-Hurlburt, and C. A. Janeway Jr, 1997 A human homologue of the *Drosophila* Toll protein signals activation of adaptive immunity. *Nature* 388: 394–397. <https://doi.org/10.1038/41131>
41. Meng X., B. S. Khanuja, and Y. T. Ip, 1999 Toll receptor-mediated *Drosophila* immune response requires Dif, an NF- $\kappa$ B factor. *Genes Dev.* 13: 792–797. <https://doi.org/10.1101/gad.13.7.792>
42. Morisato D., and K. V. Anderson, 1995 Signaling pathways that establish the dorsal-ventral pattern of the *Drosophila* embryo. *Annu. Rev. Genet.* 29: 371–399. <https://doi.org/10.1146/annurev.ge.29.120195.002103>



43. Nie M., Y. Xie, J. A. Loo, and A. J. Courey, 2009 Genetic and proteomic evidence for roles of *Drosophila* SUMO in cell cycle control, Ras signaling, and early pattern formation. *PLoS One* 4: e5905.  
<https://doi.org/10.1371/journal.pone.0005905>
44. Nüsslein-Volhard C., 1979 Maternal effect mutations that alter the spatial coordinates of the embryo of *Drosophila melanogaster*. *Determinants of spatial organization* 28.
45. Nüsslein-Volhard C., M. Lohs-Schardin, K. Sander, and C. Cremer, 1980 A dorso-ventral shift of embryonic primordia in a new maternal-effect mutant of *Drosophila*. *Nature* 283: 474–476. <https://doi.org/10.1038/283474a0>
46. Ouyang J., and G. Gill, 2009 SUMO engages multiple corepressors to regulate chromatin structure and transcription. *Epigenetics* 4: 440–444.  
<https://doi.org/10.4161/epi.4.7.9807>
47. Pirone L., W. Xolalpa, J. O. Sigurðsson, J. Ramirez, C. Pérez, *et al.*, 2017 A comprehensive platform for the analysis of ubiquitin-like protein modifications using in vivo biotinylation. *Sci. Rep.* 7: 40756. <https://doi.org/10.1038/srep40756>
48. Raman N., A. Nayak, and S. Muller, 2013 The SUMO system: a master organizer of nuclear protein assemblies. *Chromosoma* 122: 475–485.  
<https://doi.org/10.1007/s00412-013-0429-6>
49. Reeves G. T., N. Trisnadi, T. V. Truong, M. Nahmad, S. Katz, *et al.*, 2012 Dorsal-ventral gene expression in the *Drosophila* embryo reflects the dynamics and precision of the dorsal nuclear gradient. *Dev. Cell* 22: 544–557.  
<https://doi.org/10.1016/j.devcel.2011.12.007>
50. Ren J., X. Gao, C. Jin, M. Zhu, X. Wang, *et al.*, 2009 Systematic study of protein sumoylation: Development of a site-specific predictor of SUMOsp 2.0. *Proteomics* 9: 3409–3412. <https://doi.org/10.1002/pmic.200800646>
51. Rosonina E., A. Akhter, Y. Dou, J. Babu, and V. S. Sri Theivakadadcham, 2017 Regulation of transcription factors by sumoylation. *Transcription* 8: 220–231.  
<https://doi.org/10.1080/21541264.2017.1311829>
52. Rosonina E., 2019 A conserved role for transcription factor sumoylation in binding-site selection. *Curr. Genet.* 65: 1307–1312.  
<https://doi.org/10.1007/s00294-019-00992-w>
53. Roth S., D. Stein, and C. Nüsslein-Volhard, 1989 A gradient of nuclear localization of the dorsal protein determines dorsoventral pattern in the

- Drosophila* embryo. *Cell* 59: 1189–1202. [https://doi.org/10.1016/0092-8674\(89\)90774-5](https://doi.org/10.1016/0092-8674(89)90774-5)
54. Roth S., Y. Hiromi, D. Godt, and C. Nüsslein-Volhard, 1991 cactus, a maternal gene required for proper formation of the dorsoventral morphogen gradient in *Drosophila* embryos. *Development* 112: 371–388.
55. Rusch J., and M. Levine, 1996 Threshold responses to the dorsal regulatory gradient and the subdivision of primary tissue territories in the *Drosophila* embryo. *Curr. Opin. Genet. Dev.* 6: 416–423. [https://doi.org/10.1016/s0959-437x\(96\)80062-1](https://doi.org/10.1016/s0959-437x(96)80062-1)
56. Rushlow C. A., K. Han, J. L. Manley, and M. Levine, 1989 The graded distribution of the dorsal morphogen is initiated by selective nuclear transport in *Drosophila*. *Cell* 59: 1165–1177. [https://doi.org/10.1016/0092-8674\(89\)90772-1](https://doi.org/10.1016/0092-8674(89)90772-1)
57. Santamaria P., and C. Nüsslein-Volhard, 1983 Partial rescue of dorsal , a maternal effect mutation affecting the dorso-ventral pattern of the *Drosophila* embryo, by the injection of wild-type cytoplasm. *EMBO J.* 2: 1695–1699. <https://doi.org/10.1002/j.1460-2075.1983.tb01644.x>
58. Simpson P., 1983 Maternal-Zygotic Gene Interactions during Formation of the Dorsoventral Pattern in *Drosophila* Embryos. *Genetics* 105: 615–632.
59. Smith M., V. Bhaskar, J. Fernandez, and A. J. Courey, 2004 *Drosophila* Ulp1, a Nuclear Pore-associated SUMO Protease, Prevents Accumulation of Cytoplasmic SUMO Conjugates \*. *J. Biol. Chem.* 279: 43805–43814. <https://doi.org/10.1074/jbc.M404942200>
60. Stathopoulos A., and M. Levine, 2002 Dorsal gradient networks in the *Drosophila* embryo. *Dev. Biol.* 246: 57–67. <https://doi.org/10.1006/dbio.2002.0652>
61. Stathopoulos A., M. Van Drenth, A. Erives, M. Markstein, and M. Levine, 2002 Whole-genome analysis of dorsal-ventral patterning in the *Drosophila* embryo. *Cell* 111: 687–701. [https://doi.org/10.1016/s0092-8674\(02\)01087-5](https://doi.org/10.1016/s0092-8674(02)01087-5)
62. Steward R., 1987 Dorsal, an embryonic polarity gene in *Drosophila*, is homologous to the vertebrate proto-oncogene, c-rel. *Science* 238: 692–694. <https://doi.org/10.1126/science.3118464>
63. Steward R., S. B. Zusman, L. H. Huang, and P. Schedl, 1988 The dorsal protein is distributed in a gradient in early *Drosophila* embryos. *Cell* 55: 487–495. [https://doi.org/10.1016/0092-8674\(88\)90035-9](https://doi.org/10.1016/0092-8674(88)90035-9)

64. Steward R., and S. Govind, 1993 Dorsal-ventral polarity in the *Drosophila* embryo. *Curr. Opin. Genet. Dev.* 3: 556–561. [https://doi.org/10.1016/0959-437x\(93\)90090-c](https://doi.org/10.1016/0959-437x(93)90090-c)
65. Tautz D., and C. Pfeifle, 1989 A non-radioactive in situ hybridization method for the localization of specific RNAs in *Drosophila* embryos reveals translational control of the segmentation gene hunchback. *Chromosoma* 98: 81–85. <https://doi.org/10.1007/BF00291041>
66. Tempé D., M. Piechaczyk, and G. Bossis, 2008 SUMO under stress. *Biochem. Soc. Trans.* 36: 874–878. <https://doi.org/10.1042/BST0360874>
67. Trisnadi N., A. Altinok, A. Stathopoulos, and G. T. Reeves, 2013 Image analysis and empirical modeling of gene and protein expression. *Methods* 62: 68–78. <https://doi.org/10.1016/j.ymeth.2012.09.016>
68. Valanne S., J. H. Wang, and M. Rämet, 2011 The *Drosophila* toll signaling pathway. *The Journal of Immunology*.
69. Verger A., J. Perdomo, and M. Crossley, 2003 Modification with SUMO. A role in transcriptional regulation. *EMBO Rep.* 4: 137–142. <https://doi.org/10.1038/sj.embor.embor738>
70. Waddington C. H., 1959 Canalization of Development and Genetic Assimilation of Acquired Characters. *Nature* 183: 1654–1655. <https://doi.org/10.1038/1831654a0>
71. Weinert B. T., S. A. Wagner, H. Horn, P. Henriksen, W. R. Liu, *et al.*, 2011 Proteome-wide mapping of the *Drosophila* acetylome demonstrates a high degree of conservation of lysine acetylation. *Sci. Signal.* 4: ra48. <https://doi.org/10.1126/scisignal.2001902>
72. Whalen A. M., and R. Steward, 1993 Dissociation of the dorsal-cactus complex and phosphorylation of the dorsal protein correlate with the nuclear localization of dorsal. *J. Cell Biol.* 123: 523–534. <https://doi.org/10.1083/jcb.123.3.523>
73. Wotton D., L. F. Pemberton, and J. Merrill-Schools, 2017 SUMO and Chromatin Remodeling. *Adv. Exp. Med. Biol.* 963: 35–50. [https://doi.org/10.1007/978-3-319-50044-7\\_3](https://doi.org/10.1007/978-3-319-50044-7_3)
74. Wykoff D. D., and E. K. O'Shea, 2005 Identification of Sumoylated Proteins by Systematic Immunoprecipitation of the Budding Yeast Proteome \*. *Mol. Cell. Proteomics* 4: 73–83. <https://doi.org/10.1074/mcp.M400166-MCP200>

75. Zeitlinger J., R. P. Zinzen, A. Stark, and M. Kellis, 2007 Whole-genome ChIP–chip analysis of Dorsal, Twist, and Snail suggests integration of diverse patterning processes in the *Drosophila* embryo. *Genes* .
76. Zhang G., and S. Ghosh, 2001 Toll-like receptor–mediated NF- $\kappa$ B activation: a phylogenetically conserved paradigm in innate immunity. *J. Clin. Invest.* 107: 13–19. <https://doi.org/10.1172/JCI11837>
77. Zhao Q., Y. Xie, Y. Zheng, S. Jiang, W. Liu, *et al.*, 2014 GPS-SUMO: a tool for the prediction of sumoylation sites and SUMO-interaction motifs. *Nucleic Acids Res.* 42: W325-30. <https://doi.org/10.1093/nar/gku383>
78. Zhou J., J. Zwicker, P. Szymanski, M. Levine, and R. Tjian, 1998 TAFII mutations disrupt Dorsal activation in the *Drosophila* embryo. *Proc. Natl. Acad. Sci. U. S. A.* 95: 13483–13488. <https://doi.org/10.1073/pnas.95.23.13483>

## Chapter 3: SUMOylation of Dorsal attenuates Toll/NF- $\kappa$ B signaling; an immune perspective

### 3.1 Abstract

Previously, we have explored roles for SUMO-conjugation of DL in regulating early development in *Drosophila*. Using the genome-edited *DL<sup>SCR</sup>* allele, we show that the larval innate immune response is affected in the absence of DL SUMOylation. Assaying blood cells and antimicrobial peptides, we find that SUMOylation of DL is critical for both cellular and humoral immunity. SUMOylation of DL also influences the level of Cact, a transcriptional target and an interacting partner, in infected larvae. A mathematical model that evaluates the contribution of the small fraction of SUMOylated DL (1-5%) suggests that it acts to block transcriptional activation, which is driven primarily by DL that is not SUMO conjugated. In agreement with the embryonic data, we reinforce the idea that SUMOylation of DL is essential to restrain transcriptional activation.

### **Key words**

Larval immunity, fat body, transcription, nuclear translocation

## 3.2 Introduction

The Toll signaling arm is also deployed later in the *Drosophila* life-cycle to ward off fungal and Gram-positive bacterial insults, triggering the humoral immune response (Lemaitre *et al.* 1996; Rutschmann *et al.* 2002; Ferrandon *et al.* 2007). Here, DL acts in concert with DL-related Immunity Factor (Dif) to aid in host defense (Lemaitre *et al.* 1995; Anderson 2000). Toll/NF- $\kappa$ B signaling is subject to regulation by post-translational modifiers (PTMs), like SUMO (discussed in Chapter 1) (Karin and Ben-Neriah 2000; Zhou *et al.* 2005).

Studies in *Drosophila* larvae have also emphasized the interplay of SUMO and the Toll pathway in modulating host defense. Mutations in the SUMO E2 ligase Ubc9, encoded by *lesswright (lwr)* in *Drosophila*, lead to the over-proliferation of hemocytes. Introducing mutations in the *dl* and *Dif* loci in a *lwr* mutant background restores the wild-type blood cell population, providing evidence for the intersection of Toll signaling with the SUMO conjugation machinery (Huang *et al.* 2005; Chiu *et al.* 2005b).

In this chapter, I discuss the roles for SUMO in modulating DL function in the larval immune response. We find that DL SUMOylation has roles in both the cellular and humoral response in the larvae. In both the developmental and immune context, a common mechanism that emerges is the role of DL SUMO conjugation in negatively regulating Toll signaling by specifically attenuating DL mediated transcriptional activation.

## 3.3 Results

### 3.3.1 SUMO restrains DL activity in the larval immune response

Earlier, Bhaskar *et al.*, 2002, found that DL<sup>SCR</sup> is a better transcriptional activator, assessed by luciferase reporter activity on artificial promoter clusters in S2 cells. Since S2 cells are hematopoietic in origin, we reasoned that SUMO conjugation of DL may also influence the immune response in animals. The *dl*<sup>SCR</sup> line allows us to conduct similar experiments in the larvae, with twin advantages over S2 cells of working in the animal and the absence of confounding wild-type DL in the background. Septic injury by Gram-positive bacteria (or fungal infections) leads to

the upregulation of *dl* transcripts and translocation of DL to the nucleus in the larval fat body, a major effector site of the humoral response (Reichhart *et al.* 1993; Lemaitre *et al.* 1995; Manfrulli *et al.* 1999). Similar behavior was seen for Dif (Ip *et al.* 1993; Meng *et al.* 1999; Govind 1999; Hoffmann 2003). Gain-of-function mutants in Toll/ NF- $\kappa$ B signaling display an over-proliferation of hemocytes (Qiu *et al.* 1998; Matova and Anderson 2006). Studies have also implicated Dif and DL as effectors causing melanotic tumors when constitutively nuclear (Huang *et al.* 2005; Chiu *et al.* 2005b). We reasoned that if DL activity was indeed affected in *dl<sup>SCR</sup>*, it might influence blood cell numbers, but the number of circulating plasmatocytes remained unchanged in *dl<sup>SCR</sup>* mutants (Fig. 3.1A), in uninfected conditions. We also looked at crystal cells (Fig 3.1, B1), a platelet-like population of cells important for melanization and wound healing (Vlisidou and Wood 2015), visualizing the activation of the melanization cascade in response to heating/boiling of larvae (Rizki and Rizki 1959; Lanot *et al.* 2001). To our surprise, *dl<sup>SCR</sup>* larvae showed a marked increase in crystal cell numbers (Fig. 3.1, B2; Fig. 3.1C) in comparison to the wild-type (Fig. 3.1, B1; Fig. 3.1C). Also striking was the near absence of crystal cells in *dl<sup>1</sup>/dl<sup>1</sup>* animals (Fig. 3.1, B4; Fig. 3.1C), defined in literature as a null allele (Isoda *et al.* 1992), which we find is *dl<sup>S317N</sup>* (Fig. 3.2). A severe reduction in crystal cell number is also evident when another null allele of *dl*, *dl<sup>4</sup>* is used in a trans-allelic combination with *dl<sup>1</sup>* (Fig. 3.1, B5; Fig. 3.1C). Crystal cell numbers were intermediate when only one functional allele of *dl* was present (Fig. 3.1, B3; Fig. 3.1C). A similar dose-dependent response of crystal cell number is observed when *dl<sup>SCR</sup>* is compared with *dl<sup>1</sup>/dl<sup>SCR</sup>* or *dl<sup>4</sup>/dl<sup>SCR</sup>* larvae (Fig. 3.3). DL may regulate phenoloxidase activity (Bettencourt *et al.* 2004) or determine crystal cell fate, which is known to be specified by interactions between Serpent, Lozenge and U-shaped (Banerjee *et al.* 2019). Though evidence for DL/Srp co-operativity in determining hematopoietic cell-fate is lacking, we do see a direct correlation between melanized cells and levels of DL activity, with *dl<sup>null</sup>* animals lacking melanization and *dl<sup>SCR</sup>*, our presumptive transcriptionally active allele (*dl<sup>SCR</sup>*) showing the highest levels.

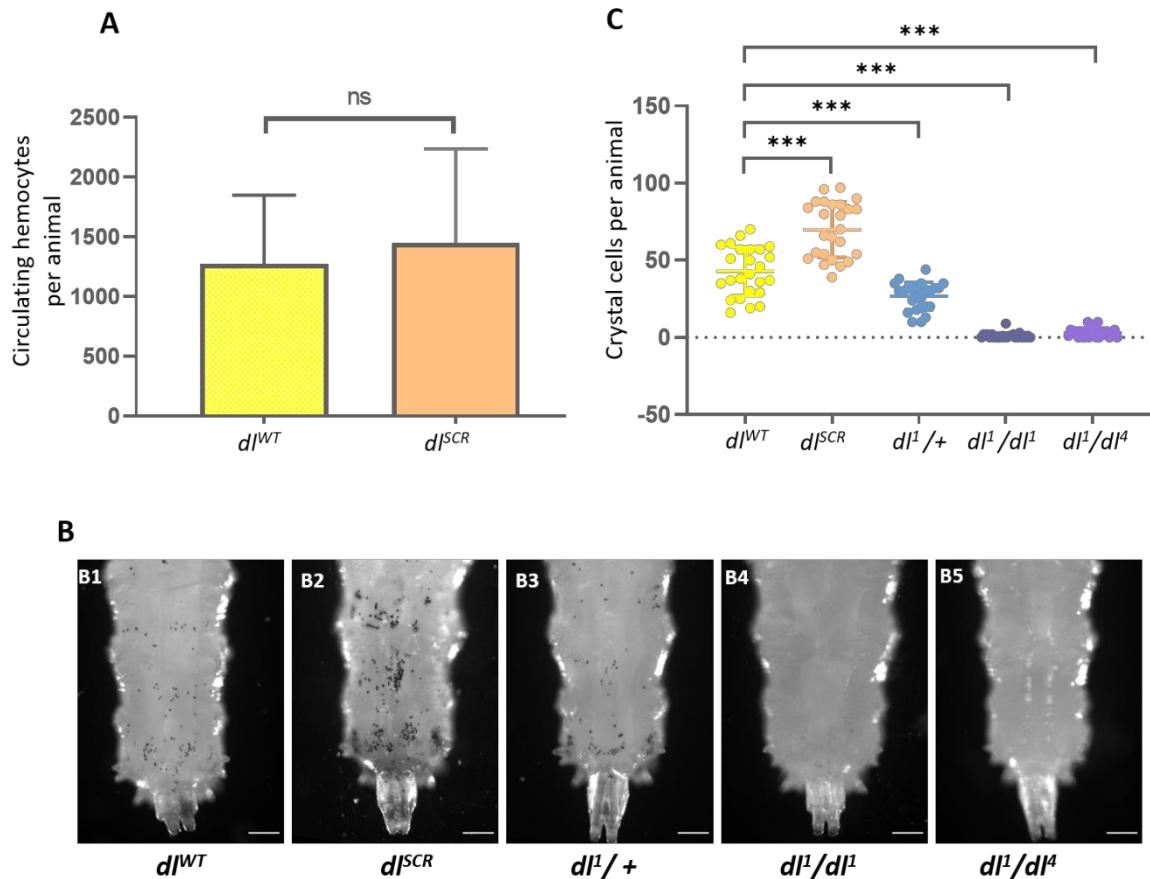


**Fig. 3.1. DL<sup>SCR</sup> is a robust immune effector in the larva.** Total circulating hemocytes for *dI<sup>WT</sup>* and *dI<sup>SCR</sup>* are plotted as a bar graph in (A). N=3, Mean ± SEM, Unpaired t-test, (ns)  $P > 0.05$ . Crystal cells in the third-instar larva were observed under a bright-field microscope, for the genotypes indicated in (B). The last three posterior segments were imaged with the dorsal side facing the viewer. The number of crystal cells in the posterior segments were counted per animal for each genotype, and are represented in (C). N=3, Mean ± SEM, ordinary one-way ANOVA, (\*\*\*)  $P < 0.0001$ .



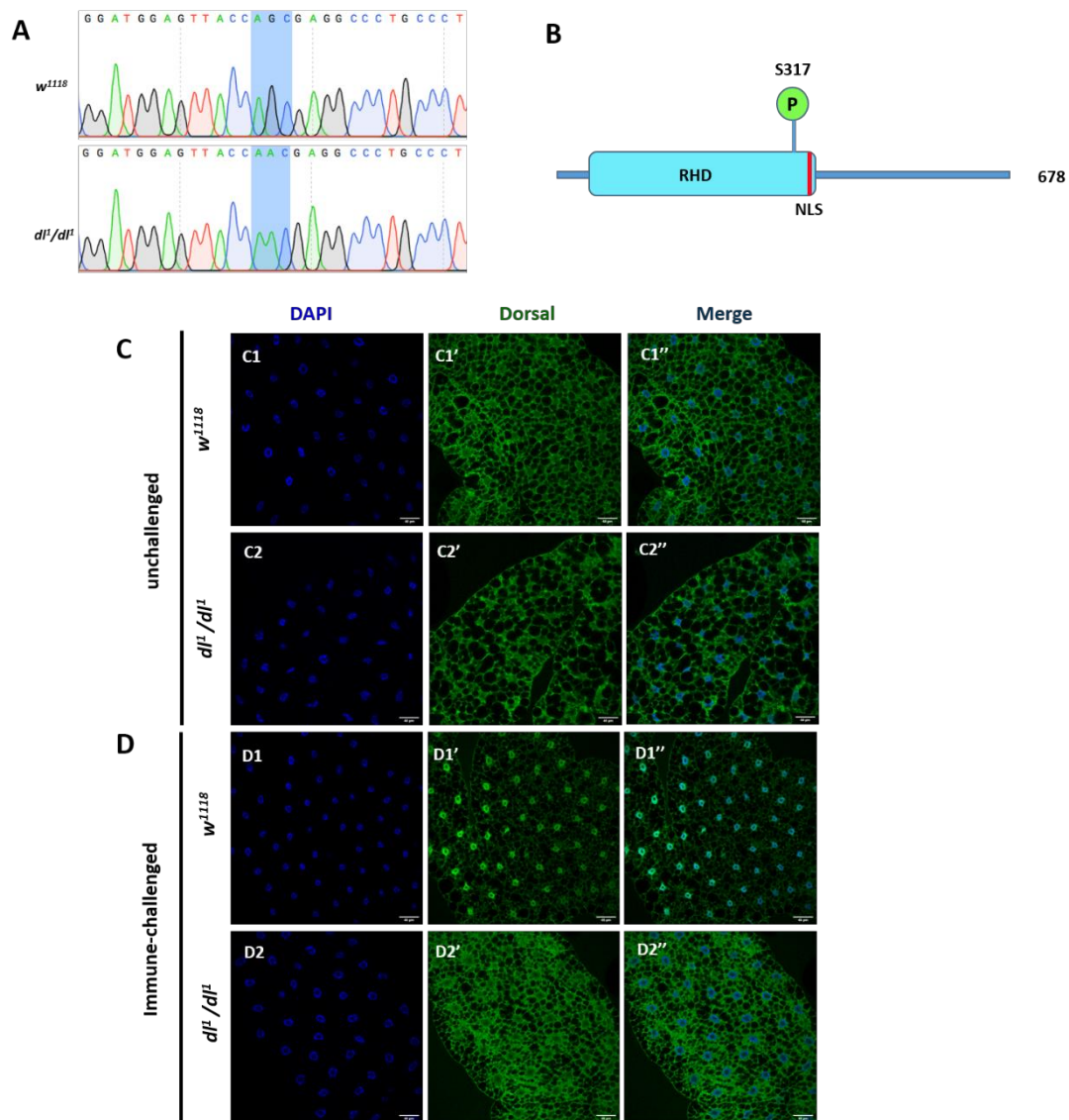


**Fig. 3.2. *dl<sup>1</sup>* is a S317N mutant and is resistant to Toll signaling.** The CDS of *dl<sup>1</sup>/dl<sup>1</sup>* was sequenced and found to harbour a mutation in a critical S317 residue in the rel-homology domain, subject to a phospho-modification (A). The presence of the S317N mutation is highlighted in blue, in (B), along with a reference sequence for *w<sup>1118</sup>*. In the unchallenged condition, immunostaining with a DL antibody reveals a pre-dominantly cytoplasmic distribution of DL in *dl<sup>1</sup>/dl<sup>1</sup>* and *w<sup>1118</sup>* (C'-C'') in the fat body. Septic injury with *S. saprophyticus* triggers the nuclear migration of DL in the wild-type animal (D1-D1''), while DL1 is retained in the cytoplasm (D2-D2''). Nuclei are marked with DAPI. N = 3, n = 5.

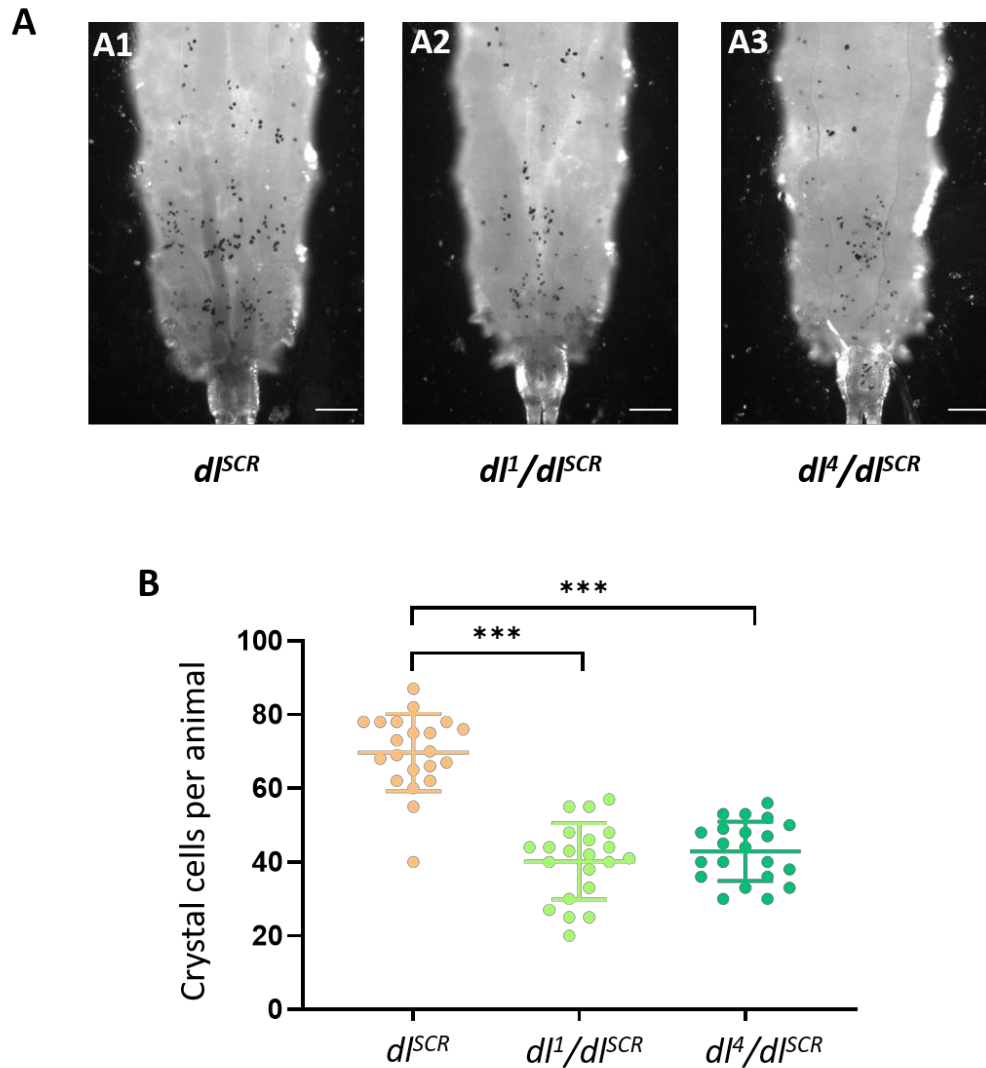


**Fig. 3.3. Crystal cells in  $dl^{SCR}$ ,  $dl^1/dl^{SCR}$ , and  $dl^4/dl^{SCR}$  larvae.** Crystal cells in the third-instar larva were observed under a bright-field microscope, for the genotypes indicated in (A). The last three posterior segments were imaged with the dorsal side facing the viewer. The number of crystal cells in the posterior segments were counted and are plotted in (B).  $n=20$ , Mean  $\pm$  SEM, ordinary one-way ANOVA, (\*\*\*)  $P < 0.0001$ .

We also monitored the temporal expression of AMPs upon septic injury in  $dl^{WT}$  and  $dl^{SCR}$ , to gauge the humoral response. Third instar larvae were infected with the Gram-positive bacteria *Staphylococcus saprophyticus* and the induction of Toll-specific AMPs *drosomycin* (*drs*) and *metchnikowin* (*mtk*) was analyzed using qRT-PCR at 2 hours and 4 hours post-infection.  $DL^{SCR}$  induced AMPs to a two-fold higher level, in comparison to  $DL^{WT}$  (Fig. 3.4A, B). The effect was more prominent at 4

hours post-infection, with both *drs* and *mtk* showing significantly higher expression (Fig. 3.4A, B). These above results agree with our thesis that DL<sup>SCR</sup> is a stronger transcriptional activator, and are also in agreement with S2 cell data published previously (Bhaskar *et al.* 2002).

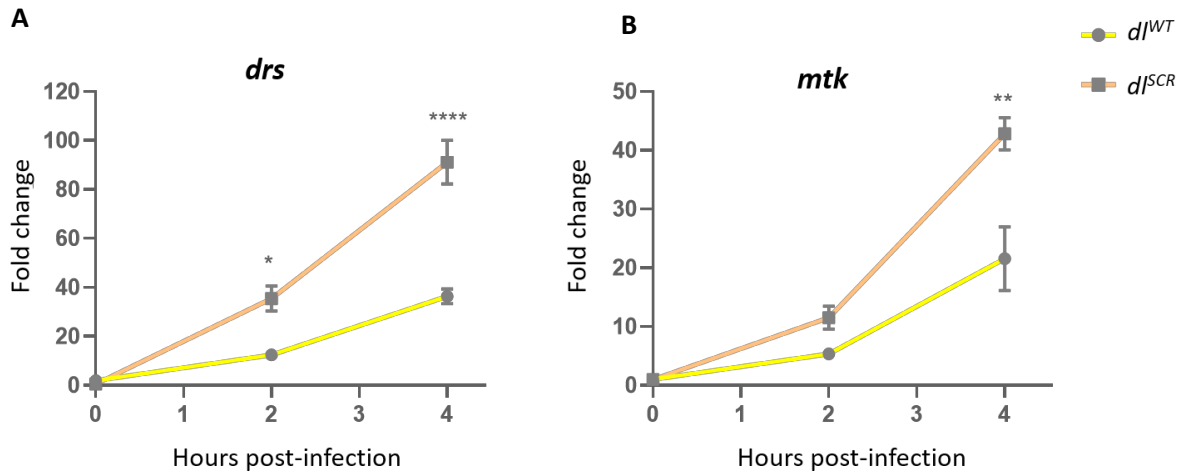


**Fig. 3.4. AMPs are upregulated in *dl<sup>SCR</sup>* animals.** Transcript levels of Toll-responsive AMPs – *drs* and *mtk* (A, B) analysed by qRT-PCR are plotted for the control and *dl<sup>SCR</sup>*. Data was collected at 0, 2, and 4 hours after septic injury with the gram positive pathogen *S. saprophyticus*, in third instar larvae. N = 3, Mean ± SEM, Two-way ANOVA, (\*)  $P < 0.05$ , (\*\*)  $P < 0.01$ , (\*\*\*\*)  $P < 0.0001$ . Data is representative of at least 8 larvae per replicate, across three independent biological replicates.

### 3.3.2 Dynamics of nuclear import of DL<sup>SCR</sup> in the larval fat body

In the context of the embryo, DL import appeared to be normal in the SCR allele, with no evidence that supported a change in the DL DV gradient. The primary difference between the DL<sup>WT</sup> and DL<sup>SCR</sup> was seen in haploinsufficient conditions, where the overall DL-mediated activation was weaker (Chapter 2) due to low concentrations of DL in the nucleus. In addition to global lowering of transcripts of DL target genes, a complete loss of activation of *twi* was seen in a specific spatiotemporal region, the WAR. In *dl<sup>SCR</sup>* embryos, the absence of DL SUMOylation appeared to suppress the weakened transcriptional activation. This is in line with the higher transcriptional activation seen in S2 cells and also in the larval fat body for DL<sup>SCR</sup>. Further, we measured the extent of nuclear import in the fat body of larvae. DL<sup>SCR</sup> is retained in the cytoplasm in un-infected larvae, similar to the wild-type (Fig

3.5, A1''-A2''). Intensity-based quantitation of the nuclear to cytoplasmic ratio (N/C) is also comparable (Fig. 3.5B), indicating that DL's SUMOylation is dispensable in retention of the DL/Cact complex in the cytoplasm, in the absence of active Toll signaling.

We next monitored the status of DL in the fat body, 60 minutes after an immune challenge with the Gram-positive pathogen *Staphylococcus saprophyticus*. DL<sup>SCR</sup> is competent in its ability to enter the nucleus (Fig. 3.5, C2''), at par with the wild-type. Paradoxically, the normalized N/C ratio for DL appears to be lower than wild-type, in the *dl<sup>SCR</sup>* mutants (Fig. 3.5D), indicating that relative to wild-type, more DL is retained in the cytoplasm or that less DL is imported to the nucleus. The images (Fig. 3.5C) suggest that the former is true, with a larger fraction of DL<sup>SCR</sup> apparently retained in the cytoplasm compared to DL animals. The retention of DL<sup>SCR</sup> in the cytoplasm can be due to many reasons. There could be (i) an increased affinity of DL<sup>SCR</sup> for Cact (ii) decreased rate of nuclear import or an increased rate of nuclear export or (iii) an increase in Cact concentration in the cytoplasm, which would, in turn, stabilize and retain DL.

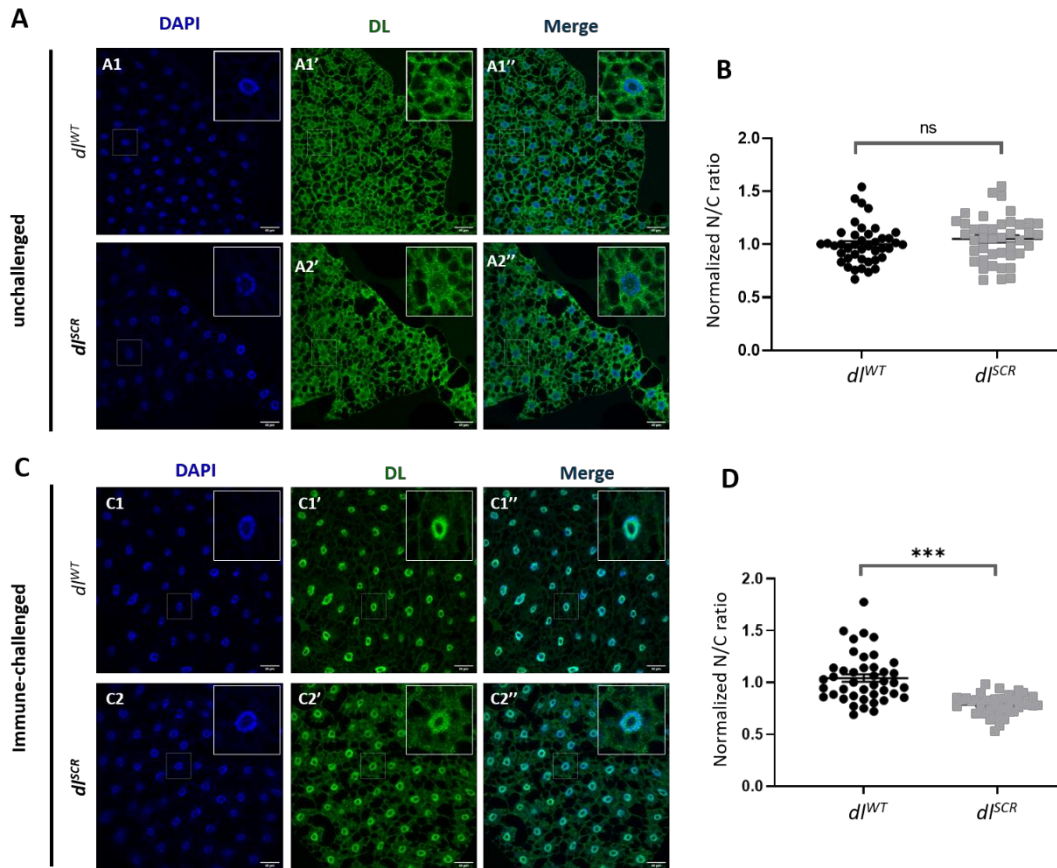


**Fig. 3.5. DL<sup>SCR</sup> is responsive to Toll signaling in the larval fat body.** DL is visualized via antibody staining (green), in the uninfected state (A) and infected state (C). Nuclei are labelled with DAPI (blue). Insets represent a zoomed-in view of individual cells. Merged images A1'' and A2'' indicate uniform distribution in fat body cells. DL levels in the cytoplasm and nucleus were quantified and plotted as a nuclear/cytoplasmic (N/C) ratio for the control and mutant (B). The N/C ratio was calculated for >40 cells in at least 5 fat bodies, across three independent replicates. Individual values are represented on a scatter plot, bar denotes mean  $\pm$  SEM, statistical significance inferred by unpaired t-test, (ns)  $P > 0.05$ , (\*\*\*)  $P < 0.001$ . DL predominantly partitions to the nucleus 60 minutes after infection with *S. saprophyticus*, evident in merged images C1'' and C2''. N/C ratio was quantified and plotted for *dl*<sup>SCR</sup> and *dl*<sup>WT</sup> (D), as in (B).

Western blots suggest that both DL<sup>WT</sup> and DL<sup>SCR</sup> are expressed at similar levels in the fat body, both in unchallenged and *S. saprophyticus*-challenged larvae (Fig. 3.6A), potentially ruling out the K382 residue as a site for ubiquitination that specifically affects DL stability. Intriguingly, Cact levels were found to be higher in infected conditions in *dl*<sup>SCR</sup> animals (Fig. 3.6D). The *cact* promoter/enhancer region has binding sites for DL, allowing DL to positively regulate Cact levels (Nicolas *et al.* 1998; Paddibhatla *et al.* 2010). Though there are multiple possibilities, we

hypothesize that the DL<sup>SCR</sup> allele, being more active, leads to increased transcription of *cact*. Excess Cact in the cytoplasm, in turn, leads to efficient retention of DL.

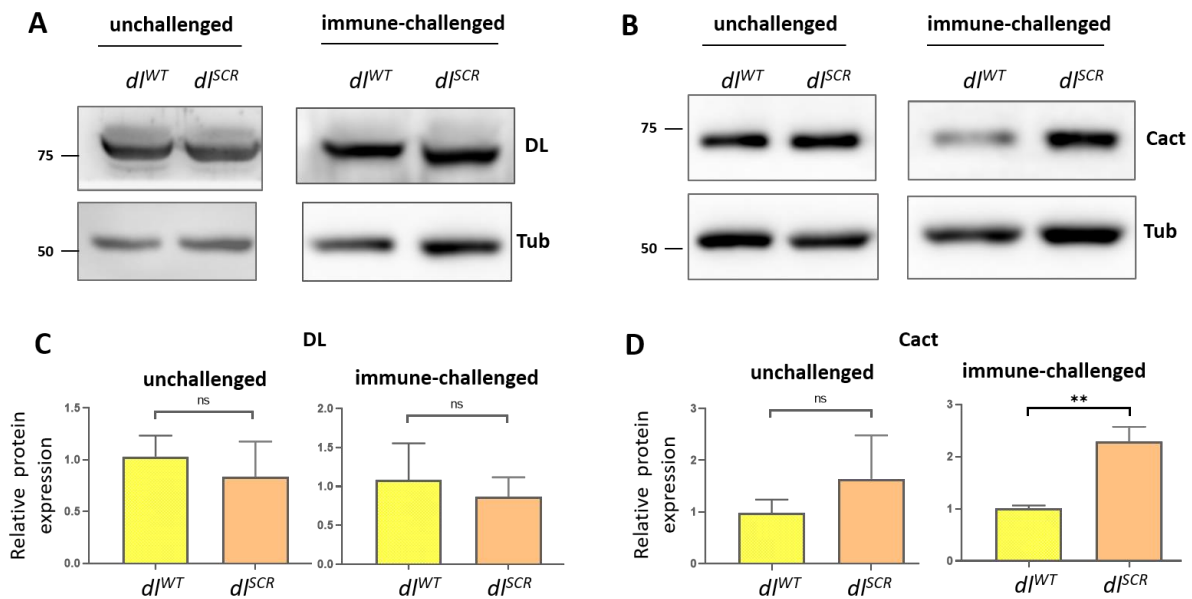


**Fig. 3.6. Cact levels are elevated in *dI*<sup>SCR</sup> animals.** Protein levels of DL and Cact in the unchallenged and immune-challenged fat body were determined by a western blot, shown in (E) and (F) respectively. Protein levels were normalized to the loading control (tubulin) and quantified, represented as relative expression levels below the respective blots for *dI*<sup>WT</sup> (yellow bar) and *dI*<sup>SCR</sup> (orange bar) (G and H). N=3, bar chart represents mean  $\pm$  SEM, statistical significance calculated by unpaired t-test, (ns)  $P > 0.05$ , (\*\*\*)  $P < 0.001$ .

### 3.3.3 A mathematical model to investigate the activity of SUMOylated DL

Experimental data from S2 cells, the embryo and larvae, all suggest that UnSUMOylated DL (DL<sup>U</sup>) is a stronger transcriptional activator with SUMOylation of DL being a mechanism to attenuate DL mediated activation. Since SUMOylated DL (DL<sup>S</sup>) levels are in the range 1-5% of total DL (Bhaskar *et al.* 2000; Smith *et al.* 2004b), as estimated by the ratio of SUMOylated/unSUMOylated species on western blots, it is difficult to examine the activity of DL<sup>S</sup> experimentally. We have attempted to gain additional insight into roles for the DL<sup>S</sup> species by generating a mathematical model and numerically evaluating the effect of DL SUMOylation. This work was carried out in collaboration with Ashley Sreejan and Chetan Gadgil at NCL, Pune.

In order to computationally explore potential causes for the observed increase in reporter expression in *dI*<sup>SCR</sup> compared to *dI*<sup>WT</sup>, we have incorporated processes involved in DL signaling, such as reversible dimerization, Cact-binding, nuclear partitioning, and binding/activity at promoter sites, in our mathematical model (Fig.



3.7A). The rates and therefore the equilibrium constants of the reactions defined in our model may be different for  $DL^S$  and  $DL^U$ . The rate of reporter expression (Fig 3.7A), which is equivalent to measuring DL-mediated transcription, is assumed to depend on the fraction of dimers bound to the promoter site, with a specific rate depending on whether the dimers exist as  $DL^S$  or  $DL^U$  homodimers. In our model, we

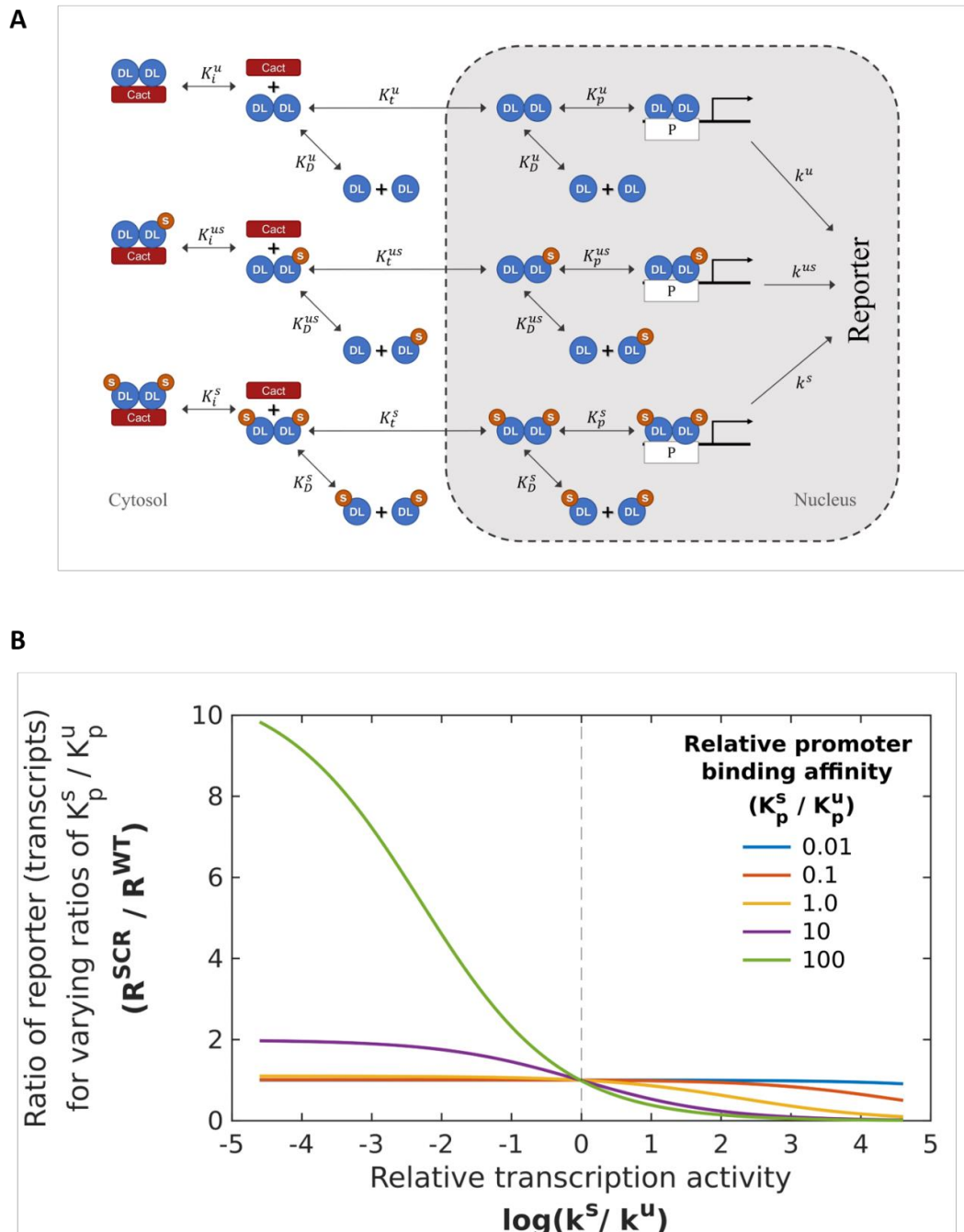


**Fig. 3.7. Mathematical model to understand roles for SUMOylated DL.** SUMO conjugated DL ( $DL^S$ ) in the cell is  $<5\%$  of total DL, with unSUMOylated DL ( $DL^U$ ) constituting the larger fraction ( $95\%$ );  $DL=DL^U + DL^S$ . We utilize a mathematical model (A) to understand conditions/parameters where a small fraction of  $DL^S$ , fixed at  $5\%$ , can influence Toll

signaling. The cytosolic and nuclear species are denoted as  $DL_C$  and  $DL_N$  respectively.  $P$  represents the binding site for  $DL^S$  and  $DL$  in the nucleus.  $K_i$ ,  $K_t$  and  $K_p$  denote the equilibrium constants for  $DL:Cact$  association, transport of  $DL$  into the nucleus, and binding of nuclear  $DL$  to the promoter  $P$ , respectively. (B). Simulating the effect of SUMOylation of  $DL$  on transcription of  $DL$  target genes. The reporter expression levels for the  $DL^{SCR}$  is greater than the corresponding WT level when the specific transcription rate is lower ( $k^S/k^U < 1$ ) for  $DL^S$  relative to  $DL^U$ . Tighter binding to promoter ( $K_p^S/K_p^U > 1$ ) enhances this effect.

assume that the reactions are in a (pseudo) steady state, *i.e.* we assume that there is no change in total  $DL$  and total  $Cact$  levels due to expression or degradation.

With a steady state assumption, information on equilibrium constants, and not the individual reaction rate constants is required for every reversible process. These parameters were approximated from reported values for the same or similar proteins from mammalian (Tay *et al.* 2010) and insect (Kanodia *et al.* 2009; Carrell *et al.* 2017; Ramsey *et al.* 2019; Al Asafen *et al.* 2020) systems. These parameters were used for reactions involving  $DL^U$ , and values for the SUMOylated  $DL$  reactions were varied a hundred-fold relative to the starting value. A mass balance on each component resulted in 18 algebraic equations and four conservation equations that were simplified and numerically solved (Methods). For a given set of parameters, the steady state reporter expression is calculated for WT and SCR conditions (*i.e.* 5% SUMOylated and 0% SUMOylated  $DL$  respectively).

The ratio ( $R^{SCR}/R^{WT}$ ) of the steady state reporter expression for  $dI^{SCR}$  and  $dI^{WT}$  thus calculated is represented on the y-axis of Fig 3.7B. A value of one indicates that the reporter expression is unchanged in the  $dI^{SCR}$  and  $dI^{WT}$ , and values greater than one indicate that the reporter expression is greater in the SCR mutant, as is observed experimentally. Hence, we seek to computationally identify conditions that lead to a value greater than one for the relative reporter expression. To this end, we repeat the calculations of relative expression ratio for multiple values of the equilibrium constant corresponding to the SUMOylated species for one process (such as specific transcriptional activity  $k^S$ ), while keeping the equilibrium values constant for the corresponding process with  $DL^U$  (such as  $k^U$ ). This is represented in the x-axis of Fig 3.7B. Here, the specific activity ( $k^S$ ) corresponding to bound  $DL^S$  is varied over two orders of magnitude relative to  $k^U$ . For each value of  $k^S/k^U$  from 0.01 to 100 (x-axis value from -4.6 to 4.6 corresponding to  $\ln(.01)$  and  $\ln(100)$  respectively), the



reporter expression ratio is calculated and plotted on the y-axis. This calculation of relative reporter expression as a function of specific activity is repeated at five different promoter binding affinity values ( $K_p^S$ ) for dimers containing DL<sup>S</sup> (colored lines plotted in Fig. 3.7B corresponding to values of  $K_p^S/K_p^U$  from 0.01 to 100). The parameters for the other processes involving DL<sup>S</sup> are assumed to be the same as the parameters for the corresponding processes with DL<sup>U</sup>. We observe that when SUMOylation does not affect the specific activity ( $x = 0$  on the graph in Fig. 3.7B, i.e.  $k^u = k^s$ ,  $\ln(k^s/k^u) = 0$ ), the relative reporter expression ( $R^{SCR}/R^{WT}$ ) remains almost constant at one, irrespective of the change in binding affinity by multiple orders of magnitude. Only when  $k^s < k^u$ , i.e.  $\ln(k^s/k^u) < 0$ , does the relative reporter expression become greater than one. Note that this increase is seen only when there is a substantial enhancement in the promoter-binding ability of dimers containing DL<sup>S</sup> (i.e.,  $K_p^S/K_p^U \geq 10$ ). Further calculations show that while decrease in transcriptional activity of promoter-bound dimers containing DL<sup>S</sup> compared to the activity of bound DL<sup>U</sup> homodimers ( $k^s < k^u$ ) is necessary, another factor that enhances the fraction of bound SUMOylated DL dimers, such as greater binding ability (Fig. 3.7B) or greater extent of partitioning to the nucleus or lesser sequestration by Cact, is required for a substantial increase in the reporter expression for SCR mutants. Simulating combinations of changes due to SUMOylation in other processes, keeping the transcriptional/reporter activity of bound DL<sup>S</sup> and DL<sup>U</sup> unchanged (i.e.,  $k^u=k^s$ ), does not change the relative expression ratio substantially (Fig. S7, left-side, all panels). These results indicate that increased expression in  $dI^{SCR}$  mutants is likely to be associated with ( $k^s < k^u$ ), or a reduced activity of bound DL<sup>S</sup>. This may also explain the ability of DL<sup>SCR</sup> in the embryo to rescue the effect of  $dI$  haploinsufficiency. Lower total DL due to the loss of an allele may lead to lower activation, which increases to near-WT levels when SUMOylation is abrogated.

### 3.4 Discussion

In response to infection (Fig. 3.8B),  $dI^{SCR}$  larvae exhibit an increase in the transcription of Toll-specific AMPs and show a higher number of crystal cells.  $dI^{SCR}$  animals show 2-4 fold higher transcripts of *drs* and *mtk*, under infective conditions and a 2-fold increase in crystal cells, in the absence of infection. Again, as suggested earlier (Fig. 3.8C), SUMOylation of DL may be a mechanism to attenuate

DL-mediated activation. Here, the GATA-family transcription factor Serpent (Srp) may be an essential player. DL, Dif, and Relish are known to synergize with Srp (Petersen *et al.* 1999; Senger *et al.* 2004) in the larvae, and SUMOylation of DL may weaken or break these interactions. Srp and the RUNX-factor Lozenge (Lz) are critical for specifying crystal cell fate in embryonic and larval stages (Fossett *et al.* 2003).

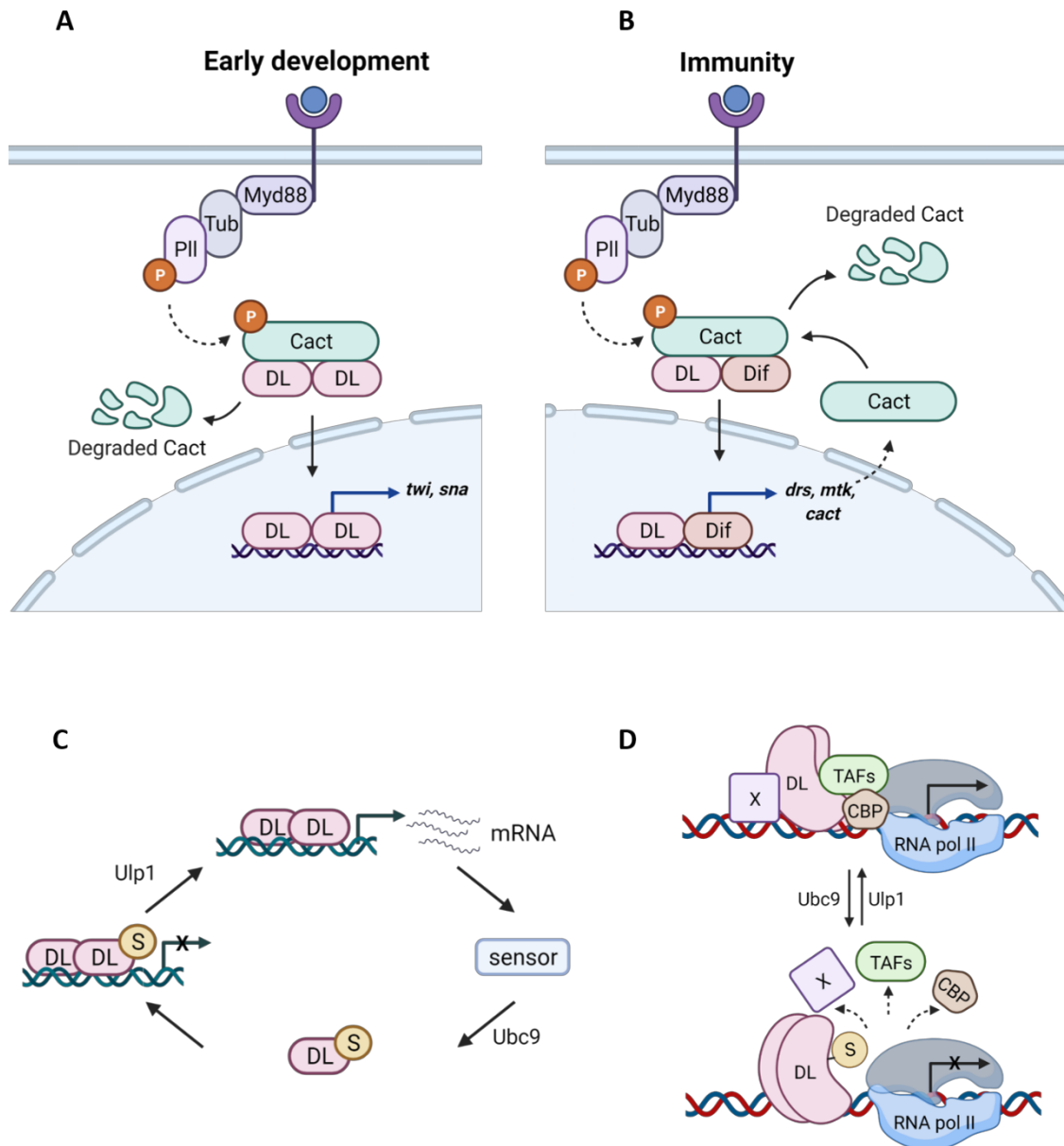


**Fig. 3.8. DL SUMOylation attenuates Toll signaling.** A probable model for dampening of the Toll signal upon DL SUMOylation. When Toll signaling is initiated, DL migrates to the

nucleus, and activates target genes, in both the developmental and immune context (A and B respectively). Once optimum levels of target transcripts are reached, or under conditions of stress, SUMOylation of DL is triggered, through as yet unknown mechanisms, curtailing excessive transcription (C). Transcriptional activity of DL may be regulated via conserved interactions with CBP and/or TAFs in association with with a protein X, most likely GATA-factor Srp in immunity or bHLH proteins like daughterless/achaete-scute, in early development (D). SUMOylation of DL may perturb these interactions, attenuating transcription.

Our observation that *dl<sup>null</sup>* animals have few or no melanized crystal cells while *dl<sup>SCR</sup>* larvae have increased crystal cells may point to a hitherto unknown function of DL carried out in assistance with Srp/Lz. Further, in the larval fat body, nuclear partitioning of DL is affected in *dl<sup>SCR</sup>* animals in response to septic injury. Cact is more stable in the cytoplasm of *dl<sup>SCR</sup>* animals, and this would lead to retention of DL. Nevertheless, transcript levels of DL target genes are higher, leading us to hypothesize that *dl<sup>SCR</sup>* animals have higher *Cact* levels, and higher *Cact* levels could explain the enhanced retention of DL in the cytoplasm. However, the possibility of increased binding affinity of DL<sup>U</sup> for Cact cannot be ruled out.

Our work further highlights the intricate fine-tuning that regulates signaling cascades. Toll signaling is modulated at multiple levels (Anderson, 2000). Extracellular feedback exerted by serine hydrolase cascades serves as an initial checkpoint for receptor activation. Cact and WntD (Ganguly *et al.* 2005; Gordon *et al.* 2005) act as intracellular, cytoplasmic gatekeepers of DL activation. An additional phosphorylation step is necessary for the nuclear import of DL (Drier *et al.* 1999). Once in the nucleus, DL can interact with partner activators and co-repressors to calibrate the transcriptional output. Our data suggests an additional layer of control, within the nucleus, with SUMO conjugation as a means of keeping DL in check, downstream of its nuclear import. The SUMO conjugation machinery resides in the nucleus and this is the most probable site for SUMO-conjugation/deconjugation of DL. The SUMO conjugase Ubc9 is a physical interactor of DL (Fig. 3.8D) and presumed to be placed proximal to the site of transcription (Bhaskar *et al.* 2000). The SUMO deconjugase Ulp1 may also be similarly localized (Anjum *et al.* 2013).

Interestingly, a previous study indicated that SUMO-conjugated DL showed an increased activation of target genes compared to wild-type DL, though considerably lower than DL<sup>K382R</sup> (Bhaskar *et al.* 2002). The authors suggest that the presence of a

synergy consensus (SC) motif at K382 recognized by a putative SC factor (SCF) that is recruited to DL<sup>WT</sup> attenuates transcription. Both SUMOylation and the K382R mutation in DL are thought to abolish the interaction with the SCF, leading to higher transcriptional activation. In contrast, our data suggests that the fraction of DL<sup>S</sup> in the WT animal acts as an impediment to transcription, while DL<sup>SCR</sup> or DL<sup>U</sup> are better transcriptional activators. A caveat of the previous study is the overexpression of Ubc9 being used as a proxy for increased DL SUMOylation. The overexpression of Ubc9 could influence the SUMOylation status of various other proteins, including DL interactors, indirectly affecting the transcriptional output of DL. The CRISPR-edited DL<sup>K382R</sup> in our study allows us to unequivocally assign the phenotypic effects observed to a loss of Dorsal SUMOylation.

Since a very small proportion of total DL is SUMO conjugated, SUMOylation/deSUMOylation may be a dynamic process that defines the occupancy of 'active' DL for transcription. Though we have assumed a value of 5% for the calculation in Fig. 3.7B, these results are qualitatively unchanged if lower (1%) or higher (10%) SUMOylated DL is assumed, or if Cact levels are changed by two orders of magnitude to simulate the change due to Toll signaling. Since we calculate expression relative to WT, the results depend to a lesser extent on the absolute values of the parameters, which are taken from previous studies. In this simplified model, the assumption of steady state disallows the possibility of simulating the time-dependent response to a change in stimulus. Therefore, the calculated values should be regarded as qualitative trends. Nevertheless, the simulation results suggest the necessary (though not sufficient) step among all those considered, and indicates that SUMOylation is likely to be associated with a lower transcriptional ability. Since DL<sup>U</sup> seems to be a better transcriptional activator, SUMOylation of DL may be a general mechanism to reduce occupancy of DL<sup>U</sup> at the promoter regions. Our mathematical model suggests that DL<sup>S</sup> dimers bind to the promoter and block access to the more transcriptionally efficient DL<sup>U</sup> dimers, thus attenuating transcription. Additionally, DL<sup>S</sup> may be deficient or less efficient in its ability to interact with the core transcriptional machinery or with partner basic helix-loop-helix proteins. DL<sup>S</sup> is, in all probability, a non-functional variant of DL. Alternatively, though not directly supported by our data, is the possibility that DL<sup>S</sup>, when bound to DNA can recruit a repressor and subsequently lead to deacetylation of the chromatin that

is resistant to transcription. SUMO-mediated attenuation of DL activity thus adds another layer to the complex regulation of Toll/NF- $\kappa$ B signaling.

**3.5 Notes/ Contributions:** The mathematical modeling and simulations were performed by Ashley Sreejan and Chetan Gadgil, NCL, Pune. Parts of this chapter have been published as a research article, 'Hegde, S., Sreejan, A., Gadgil, C. J., & Ratnaparkhi, G. S. (2022). SUMOylation of Dorsal attenuates Toll/NF- $\kappa$ B signaling. *Genetics*, 221(3), iyac081.'

### 3.6 Materials and Methods

#### *Fly husbandry and stocks*

Flies were raised on standard cornmeal agar at 25 °C unless stated otherwise. The following fly stocks were procured from the Bloomington *Drosophila* Stock Centre: *dl<sup>1</sup>/CyO* (3236), and *dl<sup>4</sup>/CyO* (7096).

#### *Western blots and their analysis*

Fat bodies (8-10 per sample) were dissected in ice-cold PBS and crushed in lysis buffer (2% SDS, 60 mM Tris-Cl pH 6.8, and 1X PIC). Samples were cleared by centrifuging at 21,000g for 30 minutes. Total protein was estimated by BCA assay (Pierce) and samples were boiled in 1X Laemmli buffer. Equal amounts of protein (30-40  $\mu$ g/sample) were resolved on a 10% polyacrylamide gel and transferred onto a PVDF membrane (Immobilon-E, Merck). The membrane was blocked with 5% milk in TBS containing 0.1% Tween20 (TBS-T) for an hour followed by incubation with the primary antibody diluted in 5% milk in TBS-T. Following three washes with TBS-T, the membrane was incubated with the secondary antibody diluted in 5% milk in TBS-T for an hour, at room temperature. The membrane was washed thrice with 0.1% TBS-T, incubated with Immobilon Western Chemiluminescent HRP substrate (Merck), and visualized on a LAS4000 Fuji imaging system. The following antibodies were used: Rabbit anti-Dorsal, 1:5000 (kind gift from the Courey laboratory); Mouse anti-Cactus, 1:100 (DSHB 3H12); Mouse anti- $\alpha$ -Tubulin, 1:10000 (T6074, Sigma-Aldrich); Goat anti-rabbit HRP and Goat anti-mouse HRP secondary antibodies, each at 1:10000 (Jackson ImmunoResearch).

### *Microbial infection*

*Staphylococcus saprophyticus* (ATCC 15305) was used for the septic injury experiments. For larval infection, the bacteria were grown overnight, concentrated by centrifugation, and the pellet washed with PBS. Larvae were placed on a cold agar plate and infected at the posterior region with a fine insect pin dipped in the concentrated culture, as described previously (Kenmoku *et al.* 2017). Infected larvae were transferred to a fresh sugar-agar plate, at 25 °C and processed at the appropriate time points.

### *Fat body staining*

Fat bodies from wandering third instar larvae were dissected in ice-cold PBS and fixed in 4% formaldehyde in PBS, for 20 minutes. The tissue was permeabilized by washing thrice in 0.1% PBS-T followed by blocking in 2% Bovine serum albumin (BSA) in 0.1% PBS-T. The tissue was incubated overnight with the primary antibody diluted in 2% BSA in 0.1% PBS-T, at 4 °C. Following three 15-minute washes with 0.1% PBS-T, secondary antibody diluted in 2% BSA in 0.1% PBS-T was added and incubated for an hour at RT. After three 15-minute washes with 0.1% PBS-T, with DAPI being added in the second wash, the tissue was mounted in SlowFade Gold mountant (Invitrogen) and imaged on a Leica Sp8 confocal microscope under a 20X oil-immersion objective. The antibodies used were: Mouse anti-Dorsal, 1:1000 (DSHB 7A4-c) and goat anti-mouse Alexa488 secondary antibody, 1:1000 (Invitrogen). Mean pixel intensity for DL staining in the cytoplasm and the nucleus was quantified using ImageJ software. The cytoplasmic intensity was averaged across three circular ROIs per cell and the same ROI was used to calculate the nuclear intensity. 5-7 cells per fat body were analyzed for at least 7-9 fat bodies across three biological replicates.

### *Quantitative PCR*

RNA was extracted from whole larvae (n = 10 /sample) using the RNeasy Plus Universal mini kit (Qiagen) according to the manufacturer's instructions. 1 µg of total RNA was used to generate cDNA using the High-Capacity cDNA Reverse Transcription kit (Thermo Fisher Scientific). The qPCR reaction was performed on a

qTOWER<sup>3</sup> real-time thermal cycler (Analytik Jena) with KAPA SYBR FAST master mix (Sigma-Aldrich). Gene expression was monitored using gene-specific primers. Transcript levels were calculated using the comparative Ct method to obtain fold change values. Relative mRNA levels were calculated using the delta Ct values. Rp49 was used as a reference gene. The following primer pairs were used (Forward primer, F and reverse primer, R):

*rp49* F: GACGCTTCAAGGGACAGTATC, *rp49* R: AAACGCGGTTCTGCATGAG;

*mtk* F: GCTACATCAGTGCTGGCAGA, *mtk* R: TTAGGATTGAAGGGCGACGG;

*drs* F: CTGTCCGGAAGATACAAGGG, *drs* R: TCGCACCAGCACTTCAGACT

#### *Blood cell preparation and counting*

Third instar larvae were cleaned with copious amounts of water and a brush, and placed individually in a drop of 20  $\mu$ L ice-cold PBS (5 per replicate) on a clean glass slide. Larvae were carefully ripped open in PBS using watchmaker's forceps, without damaging the internal organs. The carcass was discarded, and 10  $\mu$ L of the PBS solution containing blood cells was transferred to a Neubauer hemocytometer chamber (Hausser Scientific). Plasmatocytes were counted on a Zeiss Axio Vert.A1 microscope at 40X magnification using phase-contrast optics. To visualize crystal cells, wandering third instar larvae (8 per replicate) were heated at 60 °C in a water bath for 10 minutes. Images were acquired on a Zeiss Axio Vert.A1 microscope at 10X magnification. Crystal cells in three terminal segments were counted and plotted.

*Statistical Analysis:* All experiments were performed in three biological replicates, unless stated otherwise. Data is presented as mean  $\pm$  SEM. Statistical analysis was performed using GraphPad Prism8.

#### *Mathematical modeling and simulation*

Mathematical models for DL (or NF- $\kappa$ B) signaling (Schloop *et al.* 2020) have earlier been used to study the intracellular signaling kinetics of this pathway. Our objective was to simulate the effect of SUMOylation, and compare the response (reporter expression) of DL<sup>WT</sup> and DL<sup>SCR</sup>. To this end, we developed a simplified model (Fig.

3.7A) as described below. DL can exist either as monomers, homo-dimers of unSUMOylated DL ( $DL^U:DL^U$ ) or SUMOylated DL ( $DL^S:DL^S$ ) or as a  $DL^U:DL^S$  heterodimer. The rates and therefore the equilibrium constant of the dimerization reactions may be different for  $DL^U$  and  $DL^S$  monomers. The equilibrium constants for these reactions are denoted by  $K_D^u$ ,  $K_D^s$ , and  $K_D^{us}$  with superscripts indicating the nature of the monomers. Single  $u$  and  $s$  are used to denote the homodimer forms. Other processes included in the model are the dimers binding to Cact (equilibrium constants  $K_i^u$ ,  $K_i^s$  or  $K_i^{us}$  depending on the dimer), dimers partitioning to the nucleus (with partition coefficients  $K_t^u$ ,  $K_t^s$ ,  $K_t^{us}$  for the three dimer types), dimers in the nucleus binding to the promoter site P (with equilibrium constants  $K_p^u$ ,  $K_p^s$ ,  $K_p^{us}$ ) and reporter expression at rates  $k^u$ ,  $k^s$ ,  $k^{us}$  corresponding to the dimer bound to the promoters.

These parameters were estimated from reported values for the same proteins (SI-2), with values for mammalian systems used whenever necessary. We assume that the equilibrium constants for reactions involving  $DL^S$  homodimers and heterodimers are the same, but may be different from the equilibrium constant for the corresponding reaction where the  $DL^U$  homodimer is a reactant or product. Thus  $K_p^u \neq K_p^{us} = K_p^s$ ,  $k^u \neq k^{us} = k^s$  and so on. Parameters for the unSUMOylated DL reactions were based on previous reports (SI-2), and values for the SUMOylated DL reactions were explored in hundred-fold range relative to this value.

The change in the concentration of individual forms of DL (*i.e.* nuclear and cytoplasmic dimers, cactus-bound and promoter-bound), Cact, and the promoter is given by the difference in the rate at which other forms convert to that particular one, and the rate at which it is converted to another form. Assuming mass action kinetics for all reactions, this mass balance on individual forms can be mathematically expressed as a set of coupled differential equations. For instance, the rate of change of  $DL^U$  in the cytoplasm is the difference in the rates at which it is formed due to dimer dissociation and the rates at which it is converted to dimers. Using the steady state assumption, the net rate is set to zero. Similar balances are written for other forms. Four equations represented conservation of total  $DL^U$ ,  $DL^S$ , Cact and promoter sites. These equations can be simplified by substitution, leading to an expression for  $DL^U$  homodimer in terms of the equilibrium constants and



concentrations of  $DL^U$  monomer, nuclear homodimer and bound Cact. After many such successive substitutions, we get two equations for two unknown concentrations, which can be numerically solved numerically using the `fsolve` function in MATLAB 2020b. Since this is a (pseudo) steady state model, it is unable to simulate dynamic changes in the concentrations. In particular, the concentrations of promoter sites bound to  $DL^U$  homodimers and dimers containing  $DL^S$ , and the reporter expression levels, can be calculated. For WT, it is assumed that total DL comprises 5%  $DL^S$  and 95%  $DL^U$ . This assumed percentage is varied and results recalculated to check dependence of qualitative results on this assumption. In the SCR mutants,  $DL^S$  is absent. Total  $DL^S$  is set to zero, and the steady state reporter expression is calculated keeping all other parameters and total concentrations unchanged. The ratio ( $R^{SCR}/R^{WT}$ ) of the steady state reporter expression for SCR and WT is represented on the y-axis of Fig. 3.7B.

### 3.7 References

1. Al Asafen H., P. U. Bandodkar, S. Carrell-Noel, A. E. Schloop, J. Friedman, *et al.*, 2020 Robustness of the Dorsal morphogen gradient with respect to morphogen dosage. *PLoS Comput. Biol.* 16: e1007750. <https://doi.org/10.1371/journal.pcbi.1007750>
2. Anderson K. V., 2000 Toll signaling pathways in the innate immune response. *Curr. Opin. Immunol.* 12: 13–19. [https://doi.org/10.1016/s0952-7915\(99\)00045-x](https://doi.org/10.1016/s0952-7915(99)00045-x)
3. Anjum S. G., W. Xu, N. Nikkholgh, S. Basu, Y. Nie, *et al.*, 2013 Regulation of Toll signaling and inflammation by  $\beta$ -arrestin and the SUMO protease Ulp1. *Genetics* 195: 1307–1317. <https://doi.org/10.1534/genetics.113.157859>
4. Banerjee U., J. R. Girard, L. M. Goins, and C. M. Sprattford, 2019 *Drosophila* as a Genetic Model for Hematopoiesis. *Genetics* 211: 367–417. <https://doi.org/10.1534/genetics.118.300223>
5. Bettencourt R., H. Asha, C. Dearolf, and Y. T. Ip, 2004 Hemolymph-dependent and -independent responses in *Drosophila* immune tissue. *J. Cell. Biochem.* 92: 849–863. <https://doi.org/10.1002/jcb.20123>
6. Bhaskar V., S. A. Valentine, and A. J. Courey, 2000 A functional interaction between dorsal and components of the Smt3 conjugation machinery. *J. Biol. Chem.* 275: 4033–4040. <https://doi.org/10.1074/jbc.275.6.4033>

7. Bhaskar V., M. Smith, and A. J. Courey, 2002 Conjugation of Smt3 to dorsal may potentiate the *Drosophila* immune response. *Mol. Cell. Biol.* 22: 492–504.  
<https://doi.org/10.1128/MCB.22.2.492-504.2002>
8. Carrell S. N., M. D. O'Connell, T. Jacobsen, A. E. Pomeroy, S. M. Hayes, *et al.*, 2017 A facilitated diffusion mechanism establishes the *Drosophila* Dorsal gradient. *Development* 144: 4450–4461. <https://doi.org/10.1242/dev.155549>
9. Chiu H., B. C. Ring, R. P. Sorrentino, M. Kalamarz, D. Garza, *et al.*, 2005 dUbc9 negatively regulates the Toll-NF- $\kappa$ B pathways in larval hematopoiesis and drosomycin activation in *Drosophila*. *Dev. Biol.* 288: 60–72.  
<https://doi.org/10.1016/j.ydbio.2005.08.008>
10. Drier E. A., L. H. Huang, and R. Steward, 1999 Nuclear import of the *Drosophila* Rel protein Dorsal is regulated by phosphorylation. *Genes Dev.* 13: 556–568.  
<https://doi.org/10.1101/gad.13.5.556>
11. Ferrandon D., J.-L. Imler, C. Hetru, and J. A. Hoffmann, 2007 The *Drosophila* systemic immune response: sensing and signalling during bacterial and fungal infections. *Nat. Rev. Immunol.* 7: 862–874. <https://doi.org/10.1038/nri2194>
12. Fossett N., K. Hyman, K. Gajewski, S. H. Orkin, and R. A. Schulz, 2003 Combinatorial interactions of Serpent, Lozenge, and U-shaped regulate crystal cell lineage commitment during *Drosophila* hematopoiesis. *Proc. Natl. Acad. Sci. U. S. A.* 100: 11451–11456. <https://doi.org/10.1073/pnas.1635050100>
13. Ganguly A., J. Jiang, and Y. T. Ip, 2005 *Drosophila* WntD is a target and an inhibitor of the Dorsal/Twist/Snail network in the gastrulating embryo. *Development* 132: 3419–3429. <https://doi.org/10.1242/dev.01903>
14. Gordon M. D., M. S. Dionne, D. S. Schneider, and R. Nusse, 2005 WntD is a feedback inhibitor of Dorsal/NF- $\kappa$ B in *Drosophila* development and immunity. *Nature* 437: 746–749. <https://doi.org/10.1038/nature04073>
15. Govind S., 1999 Control of development and immunity by rel transcription factors in *Drosophila*. *Oncogene* 18: 6875–6887. <https://doi.org/10.1038/sj.onc.1203223>
16. Hoffmann J. A., 2003 The immune response of *Drosophila*. *Nature* 426: 33–38.  
<https://doi.org/10.1038/nature02021>
17. Huang L., S. Ohsako, and S. Tanda, 2005 The lesswright mutation activates Rel-related proteins, leading to overproduction of larval hemocytes in *Drosophila melanogaster*. *Dev. Biol.* 280: 407–420.  
<https://doi.org/10.1016/j.ydbio.2005.02.006>

18. Ip Y. T., M. Reach, Y. Engstrom, L. Kadalayil, H. Cai, *et al.*, 1993 Dif, a dorsal-related gene that mediates an immune response in *Drosophila*. *Cell* 75: 753–763. [https://doi.org/10.1016/0092-8674\(93\)90495-c](https://doi.org/10.1016/0092-8674(93)90495-c)
19. Isoda K., S. Roth, and C. Nüsslein-Volhard, 1992 The functional domains of the *Drosophila* morphogen dorsal: evidence from the analysis of mutants. *Genes Dev.* 6: 619–630. <https://doi.org/10.1101/gad.6.4.619>
20. Kanodia J. S., R. Rikhy, Y. Kim, V. K. Lund, R. DeLotto, *et al.*, 2009 Dynamics of the Dorsal morphogen gradient. *Proc. Natl. Acad. Sci. U. S. A.* 106: 21707–21712. <https://doi.org/10.1073/pnas.0912395106>
21. Karin M., and Y. Ben-Neriah, 2000 Phosphorylation meets ubiquitination: the control of NF- $\kappa$ B activity. *Annu. Rev. Immunol.* 18: 621–663. <https://doi.org/10.1146/annurev.immunol.18.1.621>
22. Kenmoku H., A. Hori, T. Kuraishi, and S. Kurata, 2017 A novel mode of induction of the humoral innate immune response in *Drosophila* larvae. *Dis. Model. Mech.* 10: 271–281. <https://doi.org/10.1242/dmm.027102>
23. Lanot R., D. Zachary, F. Holder, and M. Meister, 2001 Postembryonic hematopoiesis in *Drosophila*. *Dev. Biol.* 230: 243–257. <https://doi.org/10.1006/dbio.2000.0123>
24. Lemaitre B., M. Meister, S. Govind, P. Georgel, R. Steward, *et al.*, 1995 Functional analysis and regulation of nuclear import of dorsal during the immune response in *Drosophila*. *EMBO J.* 14: 536–545.
25. Lemaitre B., E. Nicolas, L. Michaut, J. M. Reichhart, and J. A. Hoffmann, 1996 The dorsoventral regulatory gene cassette *spätzle/Toll/cactus* controls the potent antifungal response in *Drosophila* adults. *Cell* 86: 973–983. [https://doi.org/10.1016/s0092-8674\(00\)80172-5](https://doi.org/10.1016/s0092-8674(00)80172-5)
26. Manfrulli P., J. M. Reichhart, R. Steward, J. A. Hoffmann, and B. Lemaitre, 1999 A mosaic analysis in *Drosophila* fat body cells of the control of antimicrobial peptide genes by the Rel proteins Dorsal and DIF. *EMBO J.* 18: 3380–3391. <https://doi.org/10.1093/emboj/18.12.3380>
27. Matova N., and K. V. Anderson, 2006 Rel/NF- $\kappa$ B double mutants reveal that cellular immunity is central to *Drosophila* host defense. *Proceedings of the National*.

28. Meng X., B. S. Khanuja, and Y. T. Ip, 1999 Toll receptor-mediated *Drosophila* immune response requires Dif, an NF-kappaB factor. *Genes Dev.* 13: 792–797. <https://doi.org/10.1101/gad.13.7.792>
29. Nicolas E., J. M. Reichhart, J. A. Hoffmann, and B. Lemaitre, 1998 In vivo regulation of the IκB homologue cactus during the immune response of *Drosophila*. *J. Biol. Chem.* 273: 10463–10469.
30. Paddibhatla I., M. J. Lee, M. E. Kalamarz, R. Ferrarese, and S. Govind, 2010 Role for sumoylation in systemic inflammation and immune homeostasis in *Drosophila* larvae. *PLoS Pathog.* 6: e1001234. <https://doi.org/10.1371/journal.ppat.1001234>
31. Petersen U. M., L. Kadalayil, K. P. Rehorn, D. K. Hoshizaki, R. Reuter, *et al.*, 1999 Serpent regulates *Drosophila* immunity genes in the larval fat body through an essential GATA motif. *EMBO J.* 18: 4013–4022. <https://doi.org/10.1093/emboj/18.14.4013>
32. Qiu P., P. C. Pan, and S. Govind, 1998 A role for the *Drosophila* Toll/Cactus pathway in larval hematopoiesis. *Development* 125: 1909–1920.
33. Ramsey K. M., W. Chen, J. D. Marion, S. Bergqvist, and E. A. Komives, 2019 Exclusivity and compensation in NFκB dimer distributions and IκB inhibition. *Biochemistry* 58: 2555–2563. <https://doi.org/10.1021/acs.biochem.9b00008>
34. Reichhart J. M., P. Georgel, M. Meister, B. Lemaitre, C. Kappler, *et al.*, 1993 Expression and nuclear translocation of the rel/NF-kappa B-related morphogen dorsal during the immune response of *Drosophila*. *C. R. Acad. Sci. III* 316: 1218–1224.
35. Rizki M. T., and R. M. Rizki, 1959 Functional significance of the crystal cells in the larva of *Drosophila melanogaster*. *J. Biophys. Biochem. Cytol.* 5: 235–240. <https://doi.org/10.1083/jcb.5.2.235>
36. Rutschmann S., A. Kilinc, and D. Ferrandon, 2002 Cutting edge: the toll pathway is required for resistance to gram-positive bacterial infections in *Drosophila*. *J. Immunol.* 168: 1542–1546. <https://doi.org/10.4049/jimmunol.168.4.1542>
37. Schloop A. E., P. U. Bandodkar, and G. T. Reeves, 2020 Formation, interpretation, and regulation of the *Drosophila* Dorsal/NF-κB gradient. *Curr. Top. Dev. Biol.* 137: 143–191. <https://doi.org/10.1016/bs.ctdb.2019.11.007>

38. Senger K., G. W. Armstrong, W. J. Rowell, J. M. Kwan, M. Markstein, *et al.*, 2004 Immunity Regulatory DNAs Share Common Organizational Features in *Drosophila*. *Mol. Cell* 13: 19–32. [https://doi.org/10.1016/S1097-2765\(03\)00500-8](https://doi.org/10.1016/S1097-2765(03)00500-8)
39. Smith M., V. Bhaskar, J. Fernandez, and A. J. Courey, 2004 *Drosophila* Ulp1, a Nuclear Pore-associated SUMO Protease, Prevents Accumulation of Cytoplasmic SUMO Conjugates \*. *J. Biol. Chem.* 279: 43805–43814. <https://doi.org/10.1074/jbc.M404942200>
40. Tay S., J. J. Hughey, T. K. Lee, T. Lipniacki, S. R. Quake, *et al.*, 2010 Single-cell NF-kappaB dynamics reveal digital activation and analogue information processing. *Nature* 466: 267–271. <https://doi.org/10.1038/nature09145>
41. Vlisidou I., and W. Wood, 2015 *Drosophila* blood cells and their role in immune responses. *FEBS J.* 282: 1368–1382. <https://doi.org/10.1111/febs.13235>
42. Zhou R., N. Silverman, M. Hong, D. S. Liao, Y. Chung, *et al.*, 2005 The role of ubiquitination in *Drosophila* innate immunity. *J. Biol. Chem.* 280: 34048–34055. <https://doi.org/10.1074/jbc.M506655200>

## Chapter 4: SUMOylation of Caspar, a negative regulator of IMD

### 4.1 Abstract

The *Drosophila* immune system possesses checks and balances to rein in and resolve immune activation under resting conditions and after removal of the aggravating stimulus. The intracellular protein Caspar (Casp) is a negative regulator of the innate immune IMD pathway responsive to Gram-negative bacterial insults. Casp, an ortholog of human Fas-associated factor 1, is post-translationally modified by Small Ubiquitin-related Modifier (SUMO) at lysine 551, with unknown consequences. In this study, we aimed to identify the physiological context and relevance of Casp SUMOylation in *Drosophila*. Using a combination of native and denaturing affinity purification, we sought to demonstrate the SUMOylation of Casp under immune and heat stress conditions. We also employed a CRISPR-Cas9 genome-edited *Casp*<sup>K551R</sup> line to study putative immune phenotypes in the fly in the absence of Casp SUMOylation. Though we do not observe drastic changes in the response of *Casp*<sup>K551R</sup> flies to an immune challenge, we find that they display lifespan defects. Taken together, SUMOylation of Casp may play a role in maintaining an optimal immune response under steady-state conditions.

### **Keywords**

Immunity, Inflammation, Immunoprecipitation, protein-protein interaction

## 4.2 Introduction

Negative regulation of NF- $\kappa$ B-dependant immunity has gained attention in recent years due to its implications on runaway inflammation, aging, and neurodegeneration (Arora & Ligoxygakis, 2020; DeVeale et al., 2004; Giunta et al., 2008; Gomez et al., 2005; Kounatidis et al., 2017; Libert et al., 2006). The *Drosophila* IMD pathway has proved to be an effective model for understanding the genetic basis for immune suppression (Aggarwal & Silverman, 2008; Myllymäki et al., 2014). Several negative regulators prevent constitutive activation in addition to attenuating the IMD signal. Similar to multiple layers of regulation of the Toll pathway (Discussed in Chapters 2 and 3), the first step of regulation of the IMD pathway involves dampening the activating signal, by degradation of the peptidoglycan (Bischoff et al., 2006; Charroux et al., 2018; Mengin-Lecreux & Lemaitre, 2005). Additionally, the peptidoglycan receptors on the surface can be degraded or form non-functional dimers to diminish the immune response (Basbous et al., 2011; Paredes et al., 2011; Persson et al., 2007; Zaidman-Rémy et al., 2006). PIRK is an intracellular negative regulator, preventing the association of the PGRP-LC receptor with IMD and depleting the available pool of receptors at the plasma membrane (Kleino et al., 2008).

A vast majority of IMD pathway components are regulated via their ubiquitination status. For instance, IMD accumulation is kept in check by active degradation of polyubiquitinated IMD through the *Drosophila* ubiquitin-specific protease 36 (dUSP36) protein (Thevenon et al., 2009). Another deubiquitinase, Trabid, downregulates IMD signaling by interacting with dTAK1 (Fernando et al., 2014). Finally, the ultimate effector of IMD, Relish (Rel) is a subject of extensive regulation. Held inactive in the cytoplasm by the protease Dredd, Rel is also regulated by the ubiquitin-proteasome system. *SkpA* encodes a component of the Skp1/Cullin/F-box protein (SCF)-E3 ubiquitin ligase and modulates the steady-state levels of full-length and processed Rel by influencing their ubiquitination (Khush et al., 2002). Additionally, the enzyme transglutaminase suppressed Rel activity by facilitating cross-linking and inactivation of cleaved Rel in the *Drosophila* gut (Shibata et al., 2013). Recently, SUMOylation of Relish has also been implicated in IMD regulation. The interaction of histone H2Av variant with the E3 enzyme Suppressor of variegation 2-10 (Su(var)2-10) promoted the SUMOylation of Rel. In the absence of

H2Av, immune dysfunction ensues, hyper-activating Rel-68 (Tang et al., 2021). Therefore, H2Av reins in Rel activity via SUMOylation.

Caspar (Casp) is also one such intracellular negative regulator discovered in a genetic screen to identify suppressors of antibacterial immunity (Kim *et al.* 2006). Flies mutant for *Casp* were identified due to their high rates of melanization, an innate immune response that encapsulates pathogens in the gut and fat body. Interestingly, these *Casp* mutants were resistant to Gram-negative bacterial infections due to elevated expression of the antimicrobial peptide (AMP) dipterin; consequently, infected flies survived longer than their wild-type counterparts. Strikingly, *Casp* overexpression inhibited the nuclear localization of Rel in response to infection in the fat body. An excess of *Casp* led to the cytoplasmic retention of Rel in its uncleaved, inactive form due to inhibition of the protease Dredd (Kim *et al.* 2006).

Sequence analysis of *Casp* indicates a high degree of similarity to the mammalian Fas-associated factor 1 (FAF1) protein (Kim *et al.* 2006) (Fig. 4.1). FAF1 is evolutionarily conserved and was initially discovered as an interactor of Fas, a proapoptotic member of the tumor necrosis factor receptor family (Chu et al., 1995).

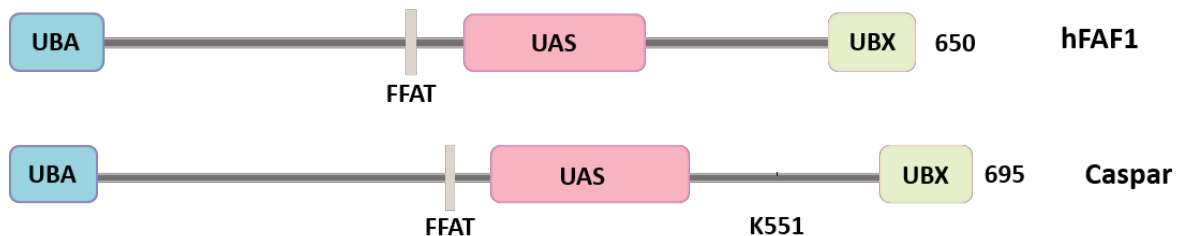


**Fig. 4.1. Casp is a FAF1 ortholog.** The conserved proteins domains of human FAF1 (hFAF1) and Caspar are represented.

FAF1 also interacts with the death-inducing signaling complex (DISC) components like the Fas-associated death domain (FADD) and Caspase-8 proteins (S.-W. Ryu et al., 2003). These interactions are mediated by the death effector domains (DED) in FADD and Caspase-8 and the DED-interacting domain (DEDID) in FAF1 (Fig. 4.2) (S.-W. Ryu et al., 2003). Overexpression and loss-of-function experiments indicated that FAF1 plays a crucial role in promoting cell death via transduction of the apoptotic signal (De Zio et al., 2008; S. W. Ryu & Kim, 2001).



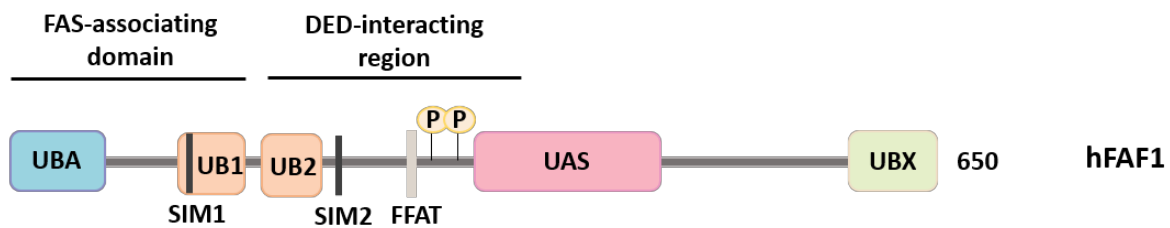


**Fig. 4.2. FAF1 domains and modifications modulate function.** FAF1 domains mediating protein interactions are depicted, in addition to phosphorylation sites.

FAF1's myriad cellular functions can be attributed to its multiple protein-interaction domains. A significant role of FAF1 is its participation in ubiquitin-related processes (Song *et al.* 2005). FAF1 harbors two Ubiquitin-like (UB) domains, a Ubiquitin-associated (UBA) domain, and a Ubiquitin-like regulatory X (UBX) domain (Fig. 4.2). The N-terminal UBA domain recruits polyubiquitinated proteins, leading to their accumulation (J. Song *et al.*, 2009) (Fig. 4.3). The C-terminal UBX domain interacts with the molecular chaperone, valosin-containing protein (VCP/p97) bound to the Npl4-Ufd1 heterodimeric complex (Ewens *et al.*, 2014; Kloppsteck *et al.*, 2012; Schuberth & Buchberger, 2008) (Fig. 4.3). FAF1 complexed with VCP-Npl4-Ufd1 and polyubiquitinated proteins is known to assist in endoplasmic reticulum-associated degradation (ERAD) (Lee *et al.*, 2013). A UAS domain, a domain of unknown function interacts with long-chain fatty acids. This interaction promotes the polymerization of FAF1 (H. Kim *et al.*, 2013).

FAF1 uses a two-pronged approach to modulate cell survival via NF- $\kappa$ B signaling. On the one hand, FAF1 can directly interact with the NF- $\kappa$ B subunit RelA/p65, inhibiting its nuclear translocation upon induction of tumor necrosis factor-alpha (TNF- $\alpha$ ) (Park *et al.* 2004). Subsequently, RelA transcriptional targets are downregulated. The second strategy involves inhibition of the I $\kappa$ B kinase complex (IKK), downregulating NF- $\kappa$ B activity (Park *et al.* 2007).

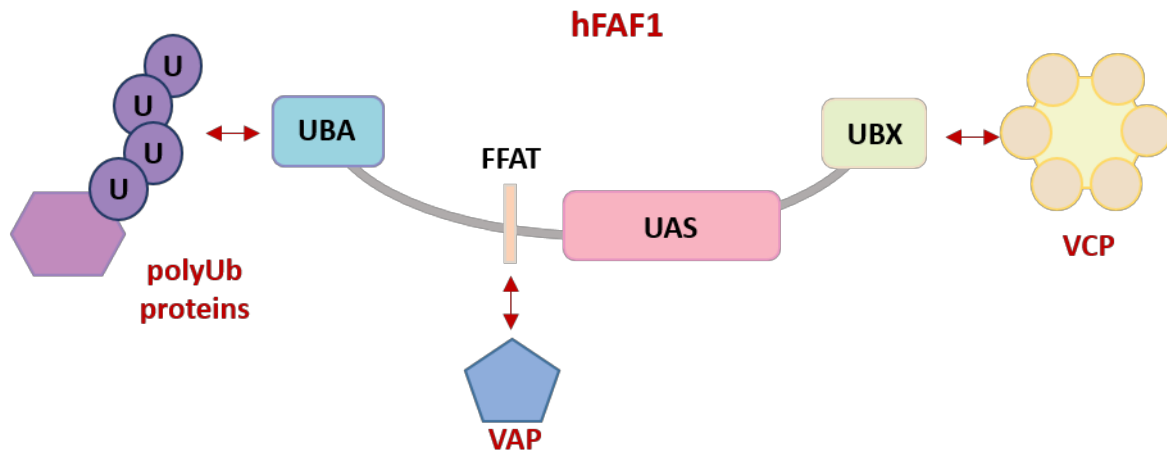


**Fig. 4.3. FAF1 interacts with polyubiquitinated proteins, VCP, and VAP.** The figure represents FAF1 domains and their major protein interactions.

Post-translational modifications also determine FAF1 function. FAF1 undergoes extensive phosphorylation on five residues (Y225, S270, S289, S291, and S320), impinging on cell cycle progression and apoptosis (Guerra et al., 2001; Jang et al., 2008; Jensen et al., 2001; Olsen et al., 2003). FAF1 also possesses two independent SUMO-interacting motifs (SIMs) (Wang *et al.* 2019) (Fig. 4.2). A FAF1 mutant lacking SIM sites could not mediate interaction with SUMOylated mineralocorticoid-receptor (MR), causing de-repression of MR-mediated transcription (Wang *et al.* 2019). FAF1 also comprises an FFAT (two phenylalanines in an acidic tract)-like motif through which it interacts with the Vesicle-associated proteins (VAP) VAPA and VAPB (Baron et al., 2014; Neefjes & Cabukusta, 2021) (Fig. 4.3).

FAF1 functions as a scaffold protein to suppress Wnt/ $\beta$ -catenin signaling. It interacts with the  $\beta$ -transducin repeat-containing protein ( $\beta$ -TrCP), an E3 ubiquitin ligase, to degrade polyubiquitinated  $\beta$ -catenin (Zhang *et al.* 2012). Interestingly, recent studies have also demonstrated the secretion of FAF1 in exosomes via ER/Golgi-independent routes, providing new insights into FAF1-mediated cell-cell signaling and cell death (G. Park et al., 2020). Physiologically, FAF1 is downregulated in multiple cancers such as brain, lung, prostate, breast, colon, etc. (Menges et al., 2009). FAF1 is also involved in the pathogenesis of Parkinson's disease (PD). PD mouse models displayed elevated FAF1 levels in the substantia nigra; FAF1 overexpression in the midbrain of PD mice promoted the neurodegeneration of dopaminergic cells via PARP1. PD mice mutant for FAF1 showed a decreased loss

of dopaminergic cells, suggesting that FAF1 positively modulates PD (Betarbet et al., 2008; Sul et al., 2013).

Most of the data on FAF1 function has been obtained from cell line studies due to the availability of few *in vivo* genetic models. In contrast, *Drosophila* affords a genetically tractable *in vivo* model to understand the physiological functions of Casp and its post-translationally modified forms. The only known role of Casp to date is the negative regulation of the IMD immune response. A proteomics study conducted in the lab to identify differentially SUMOylated substrates in response to an immune challenge identified Casp as a bonafide target in S2 cells (Handu *et al.* 2015b). The SUMO prediction software JASSA identifies three SUMO consensus sites on Casp; K436 and K484 had a low predictive score, while K551 scored high (Fig 4.4A).

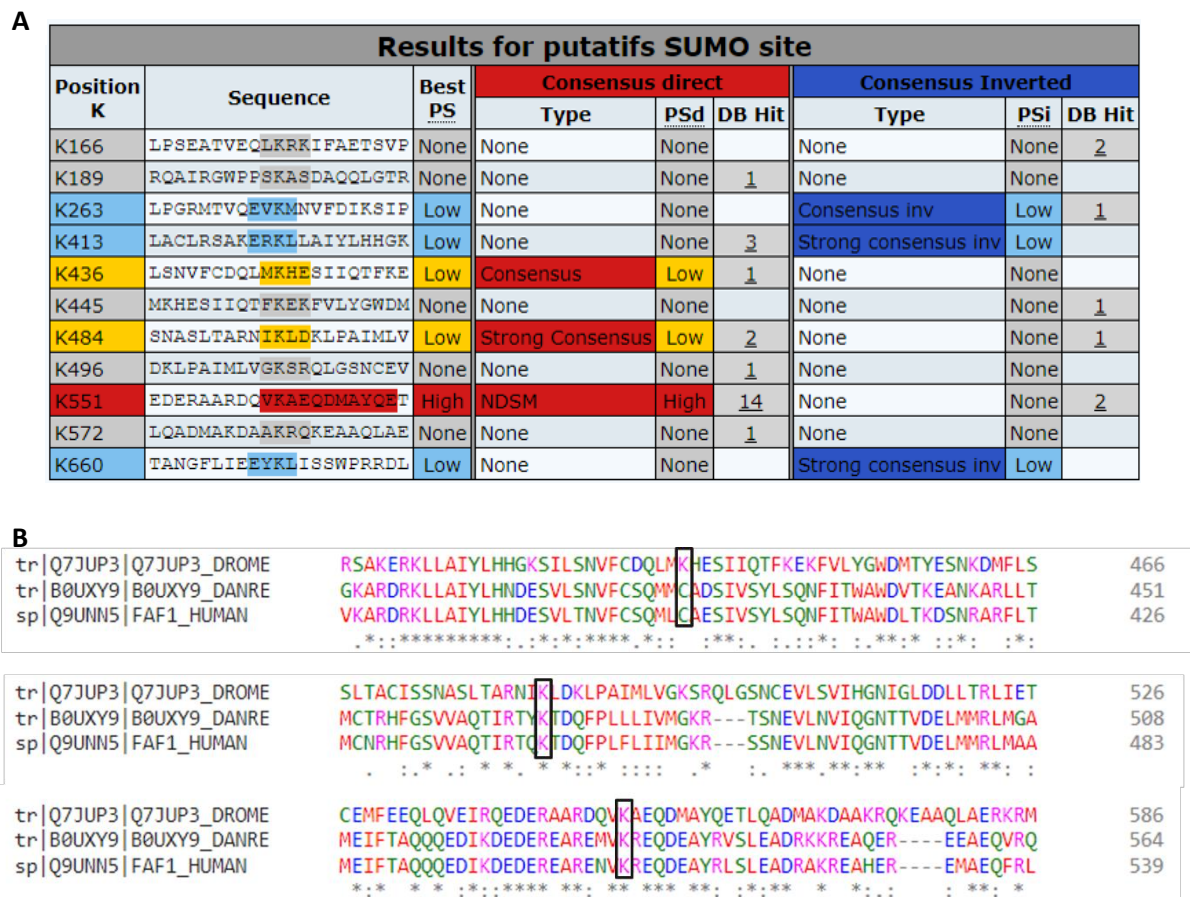


**Fig. 4.4. SUMO predictions for Casp.** SUMO site predictions for Casp and the associated confidence scores from JASSA are indicated in (A). Sequence alignment of *Drosophila*, zebrafish, and human FAF1 shows the conservation of lysines at the 484<sup>th</sup> and 551<sup>st</sup> position, while 436<sup>th</sup> was not (B). Clustal Omega was used for sequence alignment (Sievers et al., 2011). The predicted SUMO consensus sequences are highlighted.

Additionally, the K551 and K484 residues were conserved across *Drosophila*, zebrafish, and humans (Fig. 4.4B). An *in bacto* SUMOylation assay implicated K551 as the site of SUMOylation; a K551R mutant failed to show a higher molecular weight SUMOylated species. In contrast, a K436R mutant showed the presence of the intact SUMOylated Casp (Handu *et al.* 2015b).

This study sought to demonstrate Casp SUMOylation *in vivo* and determine physiological contexts for its altered SUMOylation status. Using a fly line mutant for the SUMO acceptor site (*Casp<sup>K551R</sup>*) generated using CRISPR/Cas9 gene-editing, we explored possible contributions of SUMO to Casp function in the immune response and lifespan of the fly.

### 4.3 Results

#### 4.3.1 Attempts to demonstrate SUMOylation of Casp *in vivo*

Casp SUMOylation was upregulated in S2 cells in response to an LPS challenge. Moreover, Casp was SUMOylated at K551 in an *in bacto* SUMOylation assay system (Handu *et al.* 2015b). To determine the physiological roles for SUMOylation of Casp, we attempted to identify conditions under which the status of SUMOylation might change *in vivo*. First, we confirmed the specificity of the immunoprecipitation (IP) by affinity purifying Casp using a Casp antibody (Tendulkar *et al.* 2022). In wild-type animals (*w<sup>1118</sup>*), a western blot with a Casp antibody after affinity purification indicates a solitary band corresponding to the molecular weight of Casp in the IP fraction (Fig. 4.5A). We also tested the IP in fly lines overexpressing a His-FLAG-tagged SUMO variant and Casp with a C-terminal FLAG-HA tag, driven by the *daughterless* (*Da*) promoter. These lines are referred to as *Da>HF-SUMO* and *UAS-Casp*, respectively, hereafter. Similar results were obtained, and Casp was enriched at the appropriate molecular weight (Fig. 4.5B).

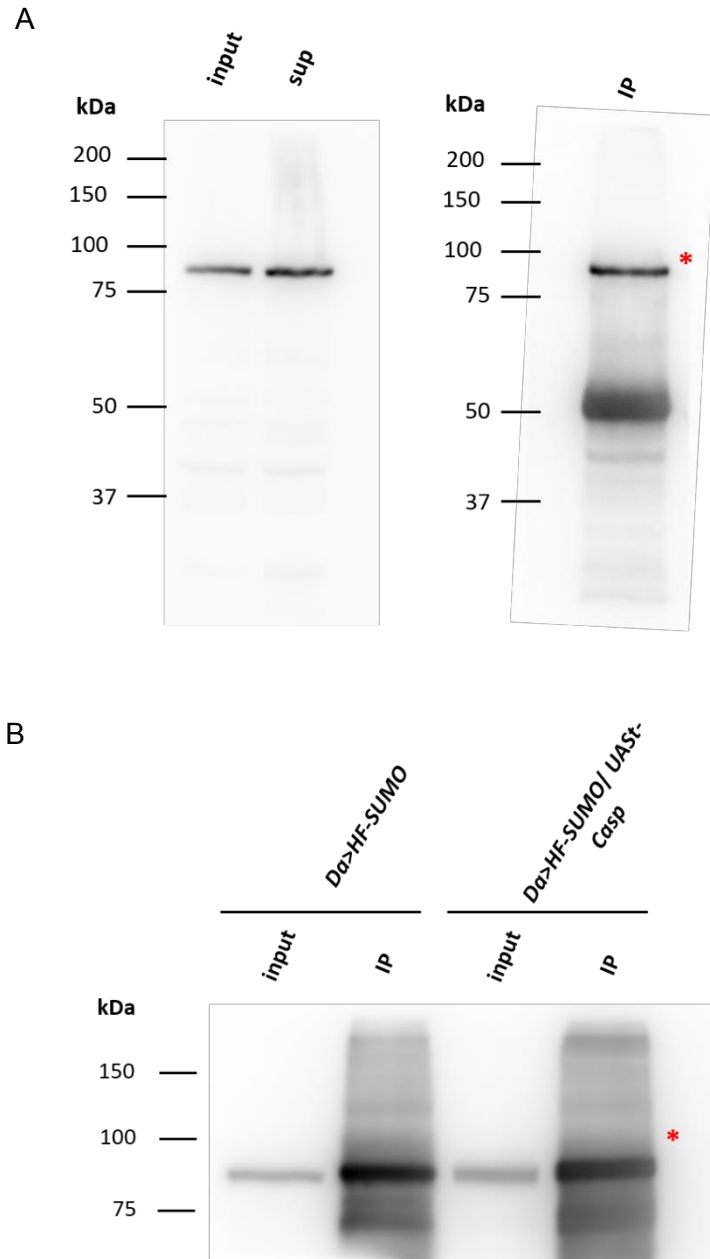
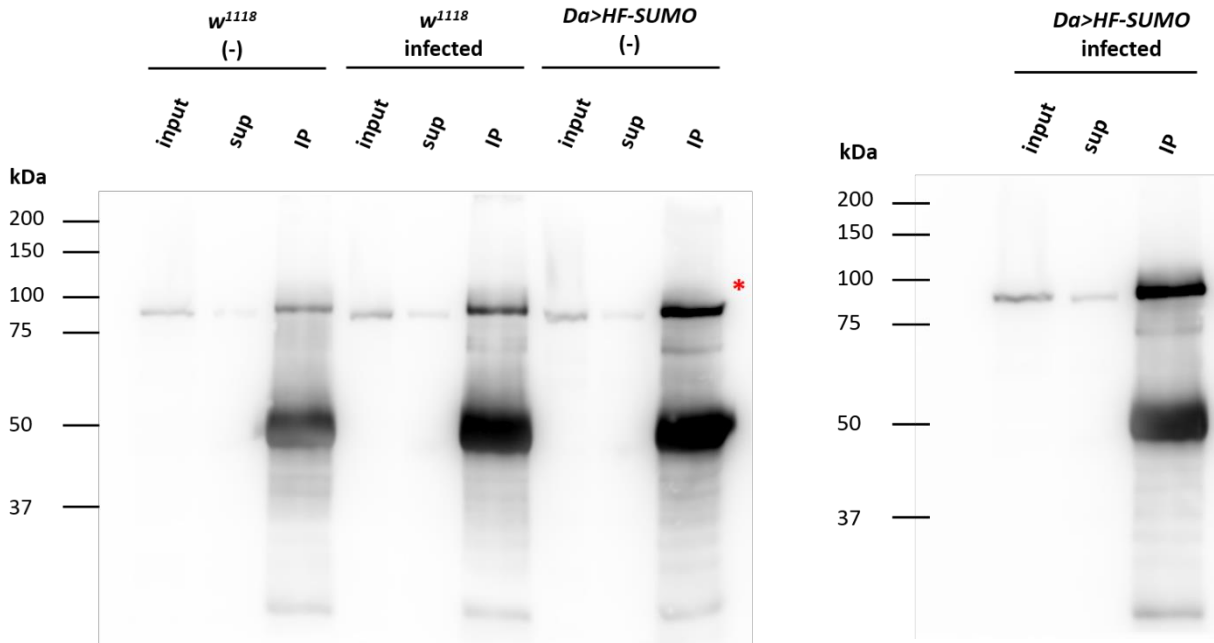


**Fig. 4.5. Immunoprecipitation of Casp with a Casp-specific antibody.** (A) depicts a western blot analysis of immunoprecipitated Casp from  $w^{1118}$  flies. The asterisk denotes the fraction of Casp enriched after the IP, eluted from the bound beads. The input consists of 5% of the total lysate, and the supernatant (sup) represents 5% of the unbound lysate after IP. A similar experiment was performed with the *Da>HF-SUMO* and the *Da>HF-SUMO/UAS-Casp* lines (B). The input and IP fractions contain Casp (asterisk).

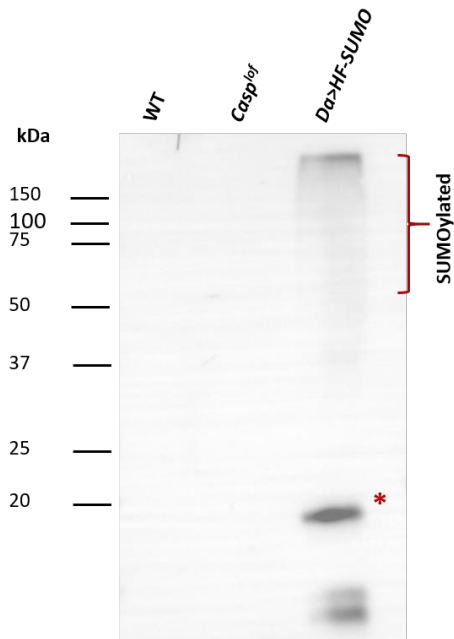
Since the only known role for Casp is in modulating the immune response via the IMD pathway (Kim *et al.* 2006), and SUMOylation was first identified in S2 cells derived from a macrophage-like cell lineage, we tested SUMOylation upon infection. Adult flies of the wild-type genotype ( $w^{1118}$ ) were infected with the Gram-negative bacteria *E. coli*. To increase the available pool of conjugatable SUMO, the transgenic fly line constitutively expressing *6XHis-FLAG-SUMO*, driven by the *daughterless* promoter (*Da>HF-SUMO*), was also used. After one hour of infection, flies were lysed, and the total protein was subjected to IP with the Casp antibody. However, no higher molecular weight bands corresponding to SUMOylated Casp could be detected in either treatment or genotype in the western blot (Fig. 4.6A, B).

Next, a Ni-NTA affinity approach was adopted to detect SUMOylated Casp under denaturing conditions. The single-step affinity purification would allow enrichment of SUMOylated proteins by virtue of the *6XHis* tag on SUMO. A subsequent western blot with the Casp antibody would enable the detection of SUMOylated Casp explicitly. Lysis under denaturing conditions also provides twin advantages of reducing the enrichment of non-specific proteins and eliminating confounding non-covalent SUMO-interactors, if any. Enrichment of SUMOylated proteins after Ni-NTA affinity purification was confirmed with a FLAG western blot. The proteins conjugated with the *6XHis-FLAG-SUMO* are visible as higher-molecular weight-migrating bands, while unconjugated, free *6XHis-FLAG-SUMO* can be detected at ~20 kDa (Fig. 4.6B) in the *Da>HF-SUMO* line. The wild-type and a null fly line for Casp (*Casp<sup>lof</sup>*) act as controls and show an absence of this characteristic banding pattern (Fig. 4.6B). *Da>HF-SUMO* flies infected with *E. coli* were lysed and the lysates were incubated with Ni-NTA agarose beads, followed by Casp detection on a western blot. This approach also did not reveal the presence of SUMOylated Casp, in either the control or the infected *Da>HF-SUMO* flies (Fig. 4.6C).

A



B



C

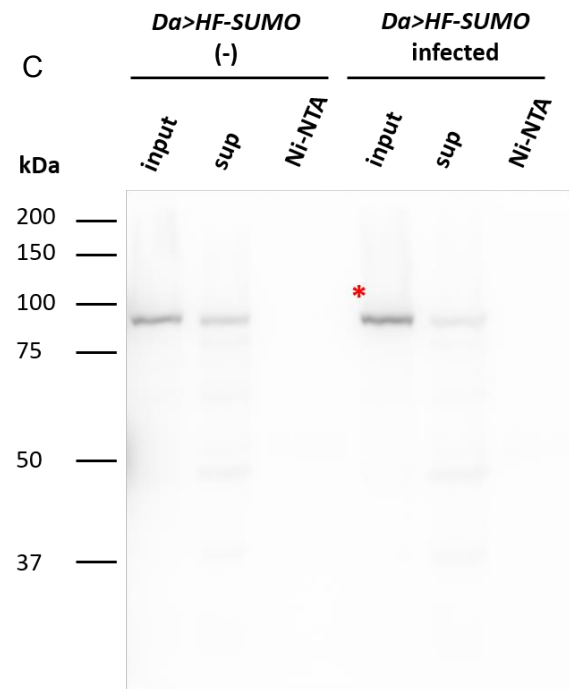


**Fig. 4.6. Evaluating SUMOylation of Casp under conditions of immune stress.** Western blot for Casp after immunoprecipitation with a Casp-specific antibody in uninfected and infected flies of the genotypes  $w^{1118}$  and  $Da>HF-SUMO$  (A). No higher-migrating bands, indicative of SUMOylated species, were observed. The asterisk denotes non-SUMOylated Casp. (B) shows a western blot with a FLAG antibody following Ni-NTA affinity purification. SUMOylated proteins are visible as higher molecular weight species exclusively in the  $Da>HF-SUMO$  line.  $w^{1118}$  and  $Casp^{lof}$  serve as negative controls. The asterisk denotes free, unconjugated His-FLAG-SUMO detected by the FLAG antibody. The  $Da>HF-SUMO$  fly line was used for further infection experiments, followed by Ni-NTA affinity purification and western blot (C). Casp is present in the input and sup fractions but absent in the Ni-NTA affinity purified fraction, suggesting an absence of SUMOylated Casp under infected conditions. The asterisk indicates the non-SUMOylated form of Casp.

We also tested the possibility of SUMOylation of Casp in response to heat shock, a well-known stressor affecting global SUMOylation levels. We did not observe SUMOylation of Casp upon Ni-NTA affinity purification and western blot analysis, in these conditions as well (Fig. 4.7). Therefore, we conclude that Casp does not undergo SUMOylation under the conditions tested, or that SUMOylation of Casp is below our detection limits.

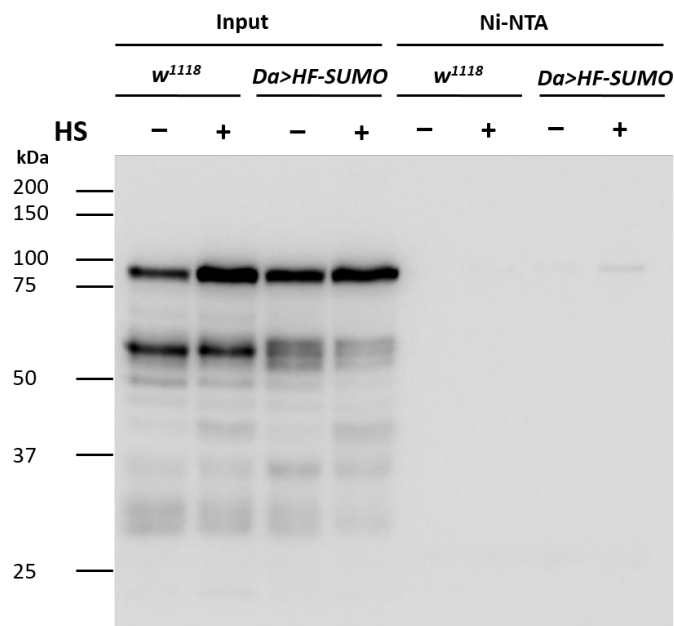


**Fig. 4.7. Attempt to detect SUMOylated Casp in response to heat stress.** Western blot of Casp, affinity purified by Ni-NTA agarose in flies subjected to heat shock. SUMOylated Casp failed to be detected in the Ni-NTA fraction.



### 4.3.2 Altered lifespan in *Casp*<sup>K551R</sup> mutants.

Though we were unable to detect SUMOylation of Casp under the conditions tested, we proceeded to test fly lines mutant for the lysine conjugated to SUMO (inferred from the *in bacto* SUMOylation assay) for phenotypic defects, if any. *Casp*<sup>K551R</sup> mutants were generated via CRISPR/Cas9 gene editing (Bhagyashree/Deepti) (Kaduskar et al., 2020). The presence of the mutation was confirmed by PCR amplification and restriction digestion of the mutated sequence, using the enzyme BssHII (Fig. 4.8). A distinct digestion pattern is observed in two *Casp*<sup>K551R</sup> CRISPR-edited lines tested: 7A and 17C, while the un-edited control line (*Casp*<sup>cc</sup>) showed the presence of an intact, uncut amplicon (Fig. 4.8).

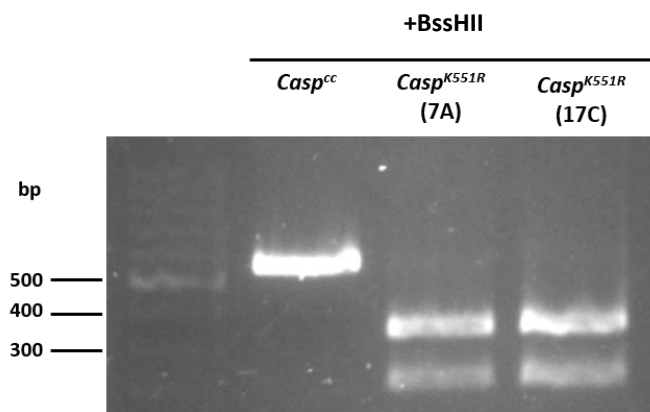


**Fig. 4.8. Confirming the presence of the K551R mutation in the CRISPR-Cas9 Casp gene-edited lines.** The genomic region harboring the mutation was amplified and the PCR product was used for restriction digestion with the BssHII enzyme recognizing the G/CGCGC sequence in *Casp*<sup>K551R</sup> flies. The agarose gel shows a digested product in the two mutant lines, 7A and 17C, while the control shows an intact PCR product.

To gauge broad defects, if any, the lifespan of the flies was assessed. A *Casp*<sup>lof</sup> allele, described in (Kaduskar et al., 2020) was used as a putative null allele for Casp. Survival of the *Casp*<sup>K551R</sup> lines was compared to *Casp*<sup>lof</sup> and the control. Interestingly, both *Casp*<sup>K551R</sup> and *Casp*<sup>lof</sup> homozygotes had significantly shorter lifespans than the control, for both males and females (Fig. 4.9). For males, the median lifespan was 48 days in *Casp*<sup>cc</sup> animals, while both the *Casp*<sup>K551R</sup> lines demonstrated a shorter median lifespan, at 31 and 41 days respectively. The *Casp*<sup>lof</sup>

animals also had a shorter median survival, at 41 days. A similar scenario was observed in females; *Casp*<sup>K551R</sup> lines had a median survival of 43 and 44.5 days. While 50% death was observed in females of *Casp*<sup>lof</sup> by day 53, >50% of *Casp*<sup>cc</sup> females were alive on day 53 (Fig. 4.9). Therefore, the K551 residue of Casp, a putative SUMO target in the fly, plays an essential role in regulating the *Drosophila* lifespan.

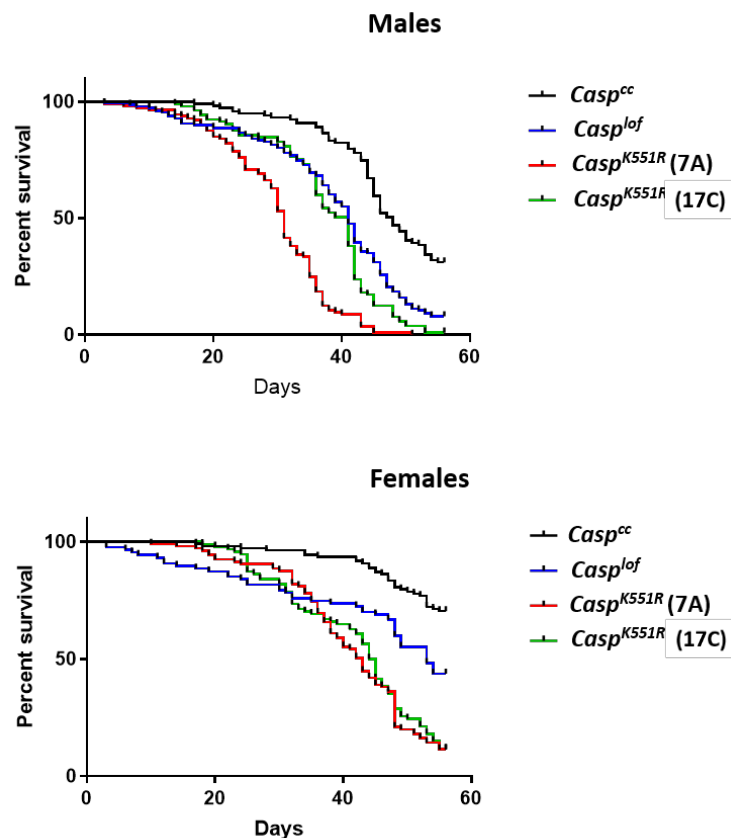


**Fig. 4.9. SUMO-conjugation-resistant Casp mutants exhibit altered lifespan.** Survival curves plotted for *Casp*<sup>cc</sup>, *Casp*<sup>lof</sup>, *Casp*<sup>K551R</sup> (7A), and *Casp*<sup>K551R</sup> (17C). Survival was monitored in males and females of the indicated genotypes.

#### 4.3.3 Bacterial clearance remains unchanged in *Casp*<sup>K551R</sup> mutants

Next, we tested whether the *Casp*<sup>K551R</sup> mutants had a differential ability to respond to infection. A quick readout of a robust immune response is the potential to eliminate bacteria efficiently. *Casp*<sup>K551R</sup>, *Casp*<sup>lof</sup>, and control flies were infected with the Gram-negative bacteria *E. coli*. After 6 hours, the number of colony forming units (CFUs) were monitored as a proxy for the bacterial load. *Casp*<sup>lof</sup> animals, lacking a negative regulator, mounted a robust immune response, clearing ~80% of the bacterial load by 6 hours, while the control flies had cleared ~50% (Fig. 4.10). In contrast, both the *Casp*<sup>K551R</sup> fly lines tested did not differ significantly from the control in their ability to

clear the bacterial infection. Therefore, we conclude that SUMOylation of Casp does not influence its function as a negative regulator in the immune response.

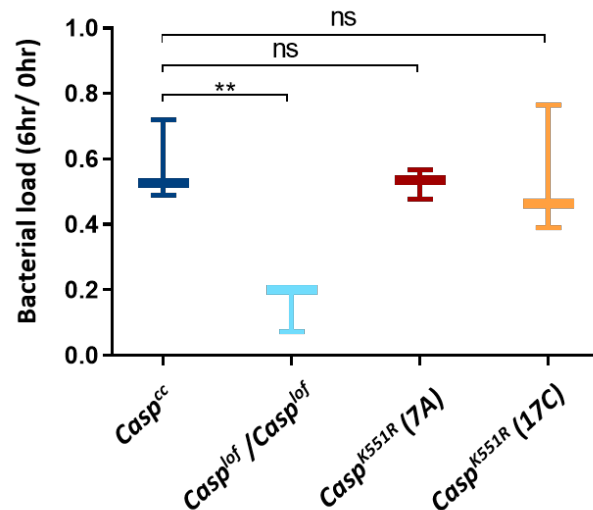


**Fig. 4.10. Bacterial clearance is comparable across control and SUMO-conjugation-resistant Casp mutants.** Bacterial load was plotted as a ratio of the bacteria after 6 hrs of infection, and the initial load for the genotypes indicated. N = 3, One-way ANOVA, (\*\*)  $P < 0.01$ .

#### 4.3.4 A possible maternal role for Casp?

Casp has a well-established role in the immune response. modENCODE RNAseq and proteomics data indicate that Casp is highly expressed in the 0-3 hour embryo (Fig. 4.11A) (Brown et al., 2014; Casas-Vila et al., 2017). A snapshot of Casp staining in a high-throughput RNA *in-situ* experiment indicates maternal, ubiquitous expression of Casp in the *Drosophila* embryo (Fig. 4.11B) (Weizmann et al., 2009). During the course of our investigation into Casp function, we stumbled upon an interesting observation. Significant embryonic lethality was observed in embryos derived from Casp<sup>lof</sup> mothers (Wagh, 2019). Since there is a lack of literature on the specific function of Casp in the early embryo, we followed up on these observations, described in detail in Chapter 5.

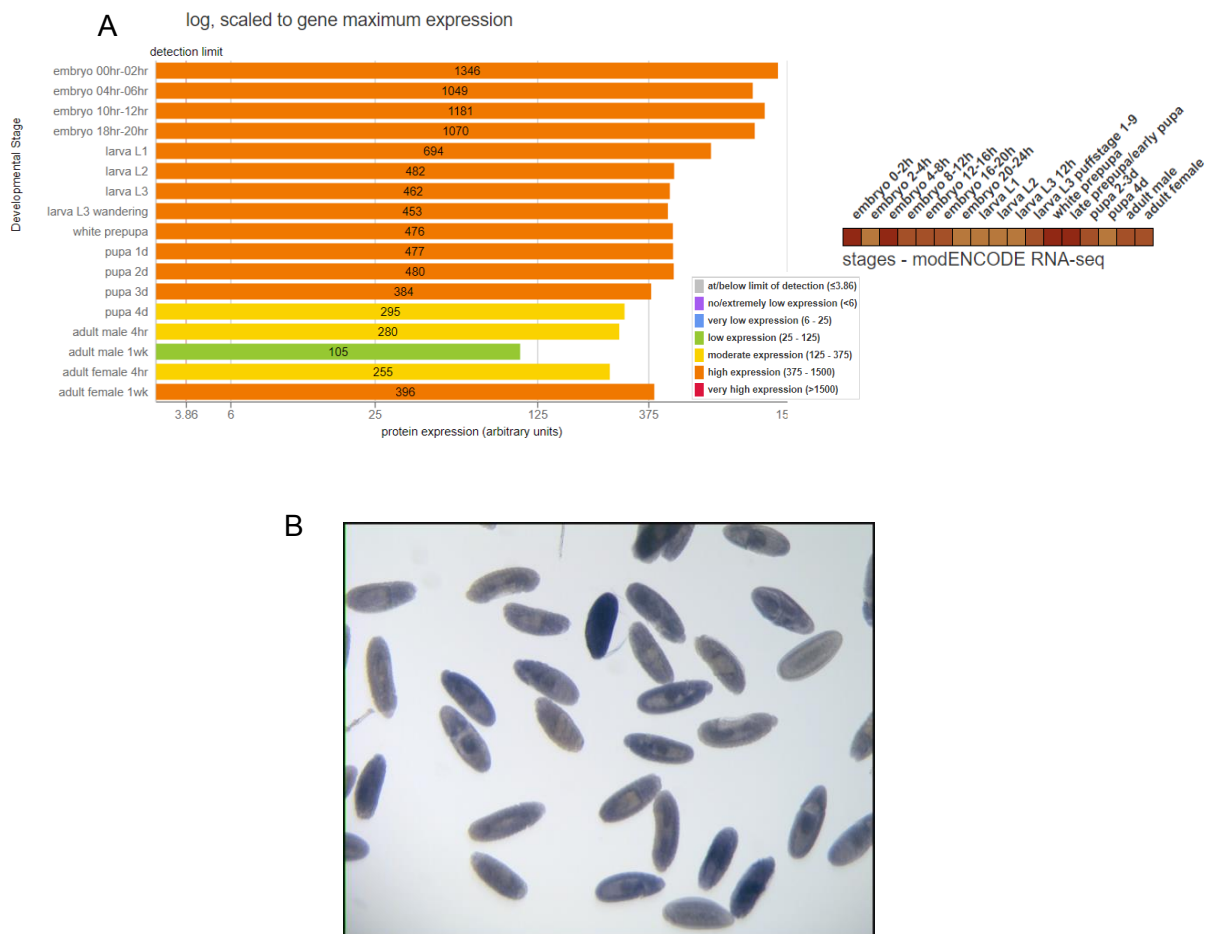


**Fig. 4.11. Casp is deposited maternally.** (A) represents protein and RNA expression data for Casp at various stages of development. Adapted from (Casas-Vila et al., 2017; Graveley et al., 2011) (B) shows RNA in situ hybridization of Casp in the embryo. Adapted from (Weizmann et al., 2009).

#### 4.4 Discussion

In this study, we have attempted to understand the significance of Casp SUMOylation. First, we tried to establish physiological paradigms for Casp SUMOylation by looking at bacterial infection and heat shock. However, we were unable to detect SUMOylation of Casp under these conditions. After that, we used a genome-edited, SUMO-conjugation resistant *Casp*<sup>K551R</sup> to study the putative immune phenotypes. Though bacterial clearance ability remained unaltered, the *Casp*<sup>K551R</sup> mutants exhibited diminished lifespan, confirming results of a previous study in the lab (Kaduskar et al., 2020).

SUMO is known to provide a cytoprotective response to stress; SUMOylation of Casp may be required under basal conditions to keep runaway inflammation in check. Inflammation is a contributor to premature aging, and absence of SUMOylation in the *Casp*<sup>K551R</sup> line could be affecting Casp's function in this regard. *Casp*<sup>K551R</sup> might be less effective as a negative regulator, enhancing Relish turnover, and accelerating AMP production. It remains to be seen whether SUMOylation of Casp affects its interaction with DREDD or members of the IMD pathway. Alternatively, SUMOylation of Casp could be affecting ubiquitin-related processes in the IMD pathway, leading to hyperactive Relish.

## 4.5 Materials and methods

### *Fly husbandry and stocks*

Flies were raised on standard cornmeal agar at 25 °C unless stated otherwise. *Casp*<sup>of</sup> (11373) was procured from the Bloomington *Drosophila* Stock Centre. The generation of the *Casp*<sup>K551R</sup> line has been described in (Kaduskar et al., 2020).

### *Survival Analysis*

Newly eclosed flies of the appropriate genotypes were collected over a span of two days and transferred to standard fly media. After two days, mated male and female flies were sorted and placed in separate vials, with around 20 flies per vial. Survival was recorded daily and flies were transferred to fresh media every 3 days. All experiments were carried out at 25 °C. Survival was monitored for ~100 flies in total.

### *Bacterial Infection and Clearance*

*Escherichia coli* encoding a plasmid for Ampicillin resistance was used for the septic injury experiments. Bacteria were grown overnight till an O.D of ~4 was reached. 5-7 day-old male flies were infected at the sternopleural plate of the thorax with an insulin needle dipped in the *E. coli* culture. Infected flies were transferred to fresh media vials for the duration of the experiment (6 hours). Groups of four flies were sterilized with 70% ethanol, transferred to a sterile 1.5 mL Eppendorf tube, and crushed with a sterile pestle after adding 200 µL of Luria-Bertani broth. The lysate was plated on to an Ampicillin-Agar plate and incubated overnight at 37 °C. Number of colony forming units (CFUs) were counted using ImageJ.

### *Immunoprecipitation and Western Blotting*

To detect SUMOylated Caspar, 5-7 day old adult flies were subjected to heat stress (37 °C for 3 hours) or bacterial infection (septic injury with *E. coli*, as described previously). 50 flies were lysed using a Dounce homogenizer in 500 µL of Radioimmunoprecipitation assay buffer (RIPA) supplemented with 20 mM N-ethylmaleimide (NEM) and 1X Protease inhibitor cocktail to inactivate SUMO isopeptidases and proteases respectively. The protocol for the Ni-NTA affinity purification is described in Appendix I. After incubation at 4° C for 30 minutes, the lysates were cleared by centrifuging at 21,000g for 30 minutes. 15 µL of lysate was used as input while the remaining lysate was pre-cleared with 10 µL of Protein A/G sepharose beads (GE). 1.5 µg of the primary antibody was bound to 20 µL of Protein A/G slurry by incubating at 4 °C for 4 hours. The pre-cleared lysate was added to antibody-bound beads and incubated overnight 4 °C. Beads were washed four times with RIPA and once with 1X PBS. The beads were re-constituted with 25 µL of 1X PBS and 5 µL of 5X Laemmli buffer.

The input and IP fraction were resolved on a 10% polyacrylamide gel and transferred onto a PVDF membrane (Immobilon-E, Merck). The membrane was blocked with 5% milk in TBS containing 0.1% Tween20 (TBS-T) for an hour followed by incubation with the primary antibody diluted in 5% milk in TBS-T. Following three washes with TBS-T, the membrane was incubated with the secondary antibody diluted in 5% milk in TBS-T for an hour, at room temperature. The membrane was washed thrice with 0.1% TBS-T, incubated with Immobilon Western Chemiluminescent HRP substrate (Merck), and visualized on a LAS4000 Fuji imaging system. The following antibodies were used: Rabbit anti-Caspar, (1: 10,000); Rabbit anti-FLAG, 1:5000 (DSHB 3H12); Goat anti-rabbit HRP secondary antibody at 1:10000 (Jackson ImmunoResearch).

**4.6 Contributions/Notes:** The *Casp*<sup>K551R</sup> line was generated as part of Bhagyashree Kaduskar's PhD thesis (Kaduskar, B. (2017). *Systemic regulation of Drosophila innate immune response* (Doctoral dissertation)). The data presented in this Chapter adds on to the earlier work.

## 4.7 References

1. Aggarwal, K., & Silverman, N. (2008). Positive and negative regulation of the *Drosophila* immune response. *BMB Reports*, *41*(4), 267–277.  
<https://doi.org/10.5483/bmbrep.2008.41.4.267>
2. Arora, S., & Ligoxygakis, P. (2020). Beyond Host Defense: Deregulation of *Drosophila* Immunity and Age-Dependent Neurodegeneration. *Frontiers in Immunology*, *11*, 1574. <https://doi.org/10.3389/fimmu.2020.01574>
3. Baron, Y., Pedrioli, P. G., Tyagi, K., Johnson, C., Wood, N. T., Fountaine, D., Wightman, M., & Alexandru, G. (2014). VAPB/ALS8 interacts with FFAT-like proteins including the p97 cofactor FAF1 and the ASNA1 ATPase. *BMC Biology*, *12*, 39. <https://doi.org/10.1186/1741-7007-12-39>
4. Basbous, N., Coste, F., Leone, P., Vincentelli, R., Royet, J., Kellenberger, C., & Roussel, A. (2011). The *Drosophila* peptidoglycan-recognition protein LF interacts with peptidoglycan-recognition protein LC to downregulate the Imd pathway. *EMBO Reports*, *12*(4), 327–333. <https://doi.org/10.1038/embor.2011.19>
5. Betarbet, R., Anderson, L. R., Gearing, M., Hodges, T. R., Fritz, J. J., Lah, J. J., & Levey, A. I. (2008). Fas-associated factor 1 and Parkinson's disease. *Neurobiology of Disease*, *31*(3), 309–315.  
<https://doi.org/10.1016/j.nbd.2008.05.006>
6. Bischoff, V., Vignal, C., Duvic, B., Boneca, I. G., Hoffmann, J. A., & Royet, J. (2006). Downregulation of the *Drosophila* immune response by peptidoglycan-recognition proteins SC1 and SC2. *PLoS Pathogens*, *2*(2), e14.  
<https://doi.org/10.1371/journal.ppat.0020014>
7. Brown, J. B., Boley, N., Eisman, R., May, G. E., Stoiber, M. H., Duff, M. O., Booth, B. W., Wen, J., Park, S., Suzuki, A. M., Wan, K. H., Yu, C., Zhang, D., Carlson, J. W., Cherbas, L., Eads, B. D., Miller, D., Mockaitis, K., Roberts, J., ... Celniker, S. E. (2014). Diversity and dynamics of the *Drosophila* transcriptome. *Nature*, *512*(7515), 393–399. <https://doi.org/10.1038/nature12962>
8. Casas-Vila, N., Bluhm, A., Sayols, S., Dinges, N., Dejung, M., Altenhein, T., Kappei, D., Altenhein, B., Roignant, J.-Y., & Butter, F. (2017). The developmental proteome of *Drosophila melanogaster*. *Genome Research*, *27*(7), 1273–1285.  
<https://doi.org/10.1101/gr.213694.116>
9. Charroux, B., Capo, F., Kurz, C. L., Peslier, S., Chaduli, D., Viallat-Lieutaud, A., & Royet, J. (2018). Cytosolic and Secreted Peptidoglycan-Degrading Enzymes in

Drosophila Respectively Control Local and Systemic Immune Responses to Microbiota. *Cell Host & Microbe*, 23(2), 215-228.e4.

<https://doi.org/10.1016/j.chom.2017.12.007>

10. Chu, K., Niu, X., & Williams, L. T. (1995). A Fas-associated protein factor, FAF1, potentiates Fas-mediated apoptosis. *Proceedings of the National Academy of Sciences of the United States of America*, 92(25), 11894–11898.  
<https://doi.org/10.1073/pnas.92.25.11894>
11. De Zio, D., Ferraro, E., D'Amelio, M., Simoni, V., Bordi, M., Soroldoni, D., Berghella, L., Meyer, B. I., & Cecconi, F. (2008). Faf1 is expressed during neurodevelopment and is involved in Apaf1-dependent caspase-3 activation in proneural cells. *Cellular and Molecular Life Sciences: CMLS*, 65(11), 1780–1790.  
<https://doi.org/10.1007/s00018-008-8075-5>
12. DeVeale, B., Brummel, T., & Seroude, L. (2004). Immunity and aging: the enemy within? *Aging Cell*, 3(4), 195–208. <https://doi.org/10.1111/j.1474-9728.2004.00106.x>
13. Ewens, C. A., Panico, S., Kloppsteck, P., McKeown, C., Ebong, I.-O., Robinson, C., Zhang, X., & Freemont, P. S. (2014). The p97-FAF1 protein complex reveals a common mode of p97 adaptor binding. *The Journal of Biological Chemistry*, 289(17), 12077–12084. <https://doi.org/10.1074/jbc.M114.559591>
14. Fernando, M. D. A., Kounatidis, I., & Ligoxygakis, P. (2014). Loss of Trabid, a new negative regulator of the drosophila immune-deficiency pathway at the level of TAK1, reduces life span. *PLoS Genetics*, 10(2), e1004117.  
<https://doi.org/10.1371/journal.pgen.1004117>
15. Giunta, B., Fernandez, F., Nikolic, W. V., Obregon, D., Rrapo, E., Town, T., & Tan, J. (2008). Inflammaging as a prodrome to Alzheimer's disease. *Journal of Neuroinflammation*, 5, 51. <https://doi.org/10.1186/1742-2094-5-51>
16. Gomez, C. R., Boehmer, E. D., & Kovacs, E. J. (2005). The aging innate immune system. *Current Opinion in Immunology*, 17(5), 457–462.  
<https://doi.org/10.1016/j.coi.2005.07.013>
17. Graveley, B. R., Brooks, A. N., Carlson, J. W., Duff, M. O., Landolin, J. M., Yang, L., Artieri, C. G., van Baren, M. J., Boley, N., Booth, B. W., Brown, J. B., Cherbas, L., Davis, C. A., Dobin, A., Li, R., Lin, W., Malone, J. H., Mattiuzzo, N. R., Miller, D., ... Celniker, S. E. (2011). The developmental transcriptome of *Drosophila melanogaster*. *Nature*, 471(7339), 473–479. <https://doi.org/10.1038/nature09715>



18. Guerra, B., Boldyreff, B., & Issinger, O. G. (2001). FAS-associated factor 1 interacts with protein kinase CK2 in vivo upon apoptosis induction. *International Journal of Oncology*, 19(6), 1117–1126. <https://doi.org/10.3892/ijo.19.6.1117>
19. Handu, M., Kaduskar, B., Ravindranathan, R., Soory, A., Giri, R., Elango, V. B., Gowda, H., & Ratnaparkhi, G. S. (2015). SUMO-Enriched Proteome for Drosophila Innate Immune Response. *G3*, 5(10), 2137–2154. <https://doi.org/10.1534/g3.115.020958>
20. Jang, M.-S., Sul, J.-W., Choi, B.-J., Lee, S.-J., Suh, J.-H., Kim, N.-S., Kim, W. H., Lim, D.-S., Lee, C.-W., & Kim, E. (2008). Negative feedback regulation of Aurora-A via phosphorylation of Fas-associated factor-1. *The Journal of Biological Chemistry*, 283(47), 32344–32351. <https://doi.org/10.1074/jbc.M804199200>
21. Jensen, H. H., Hjerrild, M., Guerra, B., Larsen, M. R., Højrup, P., & Boldyreff, B. (2001). Phosphorylation of the Fas associated factor FAF1 by protein kinase CK2 and identification of serines 289 and 291 as the in vitro phosphorylation sites. *The International Journal of Biochemistry & Cell Biology*, 33(6), 577–589. [https://doi.org/10.1016/s1357-2725\(01\)00039-5](https://doi.org/10.1016/s1357-2725(01)00039-5)
22. Kaduskar, B., Trivedi, D., & Ratnaparkhi, G. S. (2020). Caspar SUMOylation regulates Drosophila lifespan. *MicroPublication Biology*, 2020. <https://doi.org/10.17912/micropub.biology.000288>
23. Khush, R. S., Cornwell, W. D., Uram, J. N., & Lemaitre, B. (2002). A Ubiquitin-Proteasome Pathway Represses the Drosophila Immune Deficiency Signaling Cascade. *Current Biology: CB*, 12(20), 1728–1737. [https://doi.org/10.1016/S0960-9822\(02\)01214-9](https://doi.org/10.1016/S0960-9822(02)01214-9)
24. Kim, H., Zhang, H., Meng, D., Russell, G., Lee, J. N., & Ye, J. (2013). UAS domain of Ubx<sub>d8</sub> and FAF1 polymerizes upon interaction with long-chain unsaturated fatty acids. *Journal of Lipid Research*, 54(8), 2144–2152. <https://doi.org/10.1194/jlr.M037218>
25. Kim, M., Lee, J. H., Lee, S. Y., Kim, E., & Chung, J. (2006). Caspar, a suppressor of antibacterial immunity in Drosophila. *Proceedings of the National Academy of Sciences of the United States of America*, 103(44), 16358–16363. <https://doi.org/10.1073/pnas.0603238103>
26. Kleino, A., Myllymäki, H., Kallio, J., Vanha-aho, L.-M., Oksanen, K., Ulvila, J., Hultmark, D., Valanne, S., & Rämet, M. (2008). Pirk is a negative regulator of the

- Drosophila Imd pathway. *Journal of Immunology* , 180(8), 5413–5422.  
<https://doi.org/10.4049/jimmunol.180.8.5413>
27. Klopsteck, P., Ewens, C. A., Förster, A., Zhang, X., & Freemont, P. S. (2012). Regulation of p97 in the ubiquitin–proteasome system by the UBX protein-family. *Biochimica et Biophysica Acta (BBA) - Molecular Cell Research*, 1823(1), 125–129. <https://doi.org/10.1016/j.bbamcr.2011.09.006>
28. Kounatidis, I., Chtarbanova, S., Cao, Y., Hayne, M., Jayanth, D., Ganetzky, B., & Ligoxygakis, P. (2017). NF-κB Immunity in the Brain Determines Fly Lifespan in Healthy Aging and Age-Related Neurodegeneration. *Cell Reports*, 19(4), 836–848. <https://doi.org/10.1016/j.celrep.2017.04.007>
29. Lee, J.-J., Park, J. K., Jeong, J., Jeon, H., Yoon, J.-B., Kim, E. E., & Lee, K.-J. (2013). Complex of Fas-associated factor 1 (FAF1) with valosin-containing protein (VCP)-Npl4-Ufd1 and polyubiquitinated proteins promotes endoplasmic reticulum-associated degradation (ERAD). *The Journal of Biological Chemistry*, 288(10), 6998–7011. <https://doi.org/10.1074/jbc.M112.417576>
30. Libert, S., Chao, Y., Chu, X., & Pletcher, S. D. (2006). Trade-offs between longevity and pathogen resistance in *Drosophila melanogaster* are mediated by NFκB signaling. *Aging Cell*, 5(6), 533–543. <https://doi.org/10.1111/j.1474-9726.2006.00251.x>
31. Menges, C. W., Altomare, D. A., & Testa, J. R. (2009). FAS-associated factor 1 (FAF1): diverse functions and implications for oncogenesis. *Cell Cycle* , 8(16), 2528–2534. <https://doi.org/10.4161/cc.8.16.9280>
32. Mengin-Lecreulx, D., & Lemaitre, B. (2005). Structure and metabolism of peptidoglycan and molecular requirements allowing its detection by the *Drosophila* innate immune system. *Journal of Endotoxin Research*, 11(2), 105–111. <https://doi.org/10.1179/096805105X35233>
33. Myllymäki, H., Valanne, S., & Rämet, M. (2014). The *Drosophila* imd signaling pathway. *Journal of Immunology* , 192(8), 3455–3462.  
<https://doi.org/10.4049/jimmunol.1303309>
34. Neefjes, J., & Cabukusta, B. (2021). What the VAP: The Expanded VAP Family of Proteins Interacting With FFAT and FFAT-Related Motifs for Interorganellar Contact. *Contact*, 4, 25152564211012250.  
<https://doi.org/10.1177/25152564211012246>

35. Olsen, B. B., Jessen, V., Højrup, P., Issinger, O.-G., & Boldyreff, B. (2003). Protein kinase CK2 phosphorylates the Fas-associated factor FAF1 in vivo and influences its transport into the nucleus. *FEBS Letters*, *546*(2–3), 218–222. [https://doi.org/10.1016/s0014-5793\(03\)00575-1](https://doi.org/10.1016/s0014-5793(03)00575-1)
36. Paredes, J. C., Welchman, D. P., Poidevin, M., & Lemaitre, B. (2011). Negative regulation by amidase PGRPs shapes the *Drosophila* antibacterial response and protects the fly from innocuous infection. *Immunity*, *35*(5), 770–779. <https://doi.org/10.1016/j.immuni.2011.09.018>
37. Park, G., Kim, B.-S., & Kim, E. (2020). A novel function of FAF1, which induces dopaminergic neuronal death through cell-to-cell transmission. *Cell Communication and Signaling: CCS*, *18*(1), 133. <https://doi.org/10.1186/s12964-020-00632-8>
38. Park, M. Y., Jang, H. D., Lee, S. Y., Lee, K. J., & Kim, E. (2004). Fas-associated factor-1 inhibits nuclear factor- $\kappa$ B (NF- $\kappa$ B) activity by interfering with nuclear translocation of the RelA (p65) subunit of NF- $\kappa$ B. *The Journal of Biological Chemistry*. [https://www.jbc.org/article/S0021-9258\(18\)52618-1/abstract](https://www.jbc.org/article/S0021-9258(18)52618-1/abstract)
39. Park, Moon, Lee, Choi, & Chung. (2007). FAF1 suppresses I $\kappa$ B kinase (IKK) activation by disrupting the IKK complex assembly. *Bollettino Della Societa Italiana Di Biologia Sperimentale*. [https://www.jbc.org/article/S0021-9258\(20\)58651-1/abstract](https://www.jbc.org/article/S0021-9258(20)58651-1/abstract)
40. Persson, C., Oldenvi, S., & Steiner, H. (2007). Peptidoglycan recognition protein LF: a negative regulator of *Drosophila* immunity. *Insect Biochemistry and Molecular Biology*, *37*(12), 1309–1316. <https://doi.org/10.1016/j.ibmb.2007.08.003>
41. Ryu, S. W., & Kim, E. (2001). Apoptosis induced by human Fas-associated factor 1, hFAF1, requires its ubiquitin homologous domain, but not the Fas-binding domain. *Biochemical and Biophysical Research Communications*, *286*(5), 1027–1032. <https://doi.org/10.1006/bbrc.2001.5505>
42. Ryu, S.-W., Lee, S.-J., Park, M.-Y., Jun, J.-I., Jung, Y.-K., & Kim, E. (2003). Fas-associated Factor 1, FAF1, Is a Member of Fas Death-inducing Signaling Complex \*. *The Journal of Biological Chemistry*, *278*(26), 24003–24010. <https://doi.org/10.1074/jbc.M302200200>

43. Schubert, C., & Buchberger, A. (2008). UBX domain proteins: major regulators of the AAA ATPase Cdc48/p97. *Cellular and Molecular Life Sciences: CMLS*, 65(15), 2360–2371. <https://doi.org/10.1007/s00018-008-8072-8>
44. Shibata, T., Sekihara, S., Fujikawa, T., Miyaji, R., Maki, K., Ishihara, T., Koshiba, T., & Kawabata, S.-I. (2013). Transglutaminase-Catalyzed Protein-Protein Cross-Linking Suppresses the Activity of the NF- $\kappa$ B–Like Transcription Factor Relish. *Science Signaling*, 6(285), ra61–ra61. <https://doi.org/10.1126/scisignal.2003970>
45. Sievers, F., Wilm, A., Dineen, D., Gibson, T. J., Karplus, K., Li, W., Lopez, R., McWilliam, H., Remmert, M., Söding, J., Thompson, J. D., & Higgins, D. G. (2011). Fast, scalable generation of high-quality protein multiple sequence alignments using Clustal Omega. *Molecular Systems Biology*, 7(1), 539. <https://doi.org/10.1038/msb.2011.75>
46. Song, E. J., Yim, S.-H., Kim, E., Kim, N.-S., & Lee, K.-J. (2005). Human Fas-associated factor 1, interacting with ubiquitinated proteins and valosin-containing protein, is involved in the ubiquitin-proteasome pathway. *Molecular and Cellular Biology*, 25(6), 2511–2524. <https://doi.org/10.1128/MCB.25.6.2511-2524.2005>
47. Song, J., Park, J. K., Lee, J.-J., Choi, Y.-S., Ryu, K.-S., Kim, J.-H., Kim, E., Lee, K.-J., Jeon, Y.-H., & Kim, E. E. (2009). Structure and interaction of ubiquitin-associated domain of human Fas-associated factor 1. *Protein Science: A Publication of the Protein Society*, 18(11), 2265–2276. <https://doi.org/10.1002/pro.237>
48. Sul, J.-W., Park, M.-Y., Shin, J., Kim, Y.-R., Yoo, S.-E., Kong, Y.-Y., Kwon, K.-S., Lee, Y. H., & Kim, E. (2013). Accumulation of the parkin substrate, FAF1, plays a key role in the dopaminergic neurodegeneration. *Human Molecular Genetics*, 22(8), 1558–1573. <https://doi.org/10.1093/hmg/ddt006>
49. Tang, R., Huang, W., Guan, J., Liu, Q., Beerntsen, B. T., & Ling, E. (2021). Drosophila H2Av negatively regulates the activity of the IMD pathway via facilitating Relish SUMOylation. *PLoS Genetics*, 17(8), e1009718. <https://doi.org/10.1371/journal.pgen.1009718>
50. Tendulkar, Hegde, & Garg. (2022). Caspar, an adapter for VAPB and TER94, modulates the progression of ALS8 by regulating IMD/NF $\kappa$ B-mediated glial inflammation in a Drosophila model of human .... *Human Molecular Genetics*. <https://doi.org/10.1093/hmg/ddac076/6563110>

51. Thevenon, D., Engel, E., Avet-Rochex, A., Gottar, M., Bergeret, E., Tricoire, H., Benaud, C., Baudier, J., Taillebourg, E., & Fauvarque, M.-O. (2009). The *Drosophila* ubiquitin-specific protease dUSP36/Scny targets IMD to prevent constitutive immune signaling. *Cell Host & Microbe*, 6(4), 309–320. <https://doi.org/10.1016/j.chom.2009.09.007>
52. Wagh, N. (2019). *A Maternal role for Drosophila Casp/dFAF1*. <http://210.212.192.152:8080/xmlui/handle/123456789/2988>
53. Wang, C.-H., Hung, P.-W., Chiang, C.-W., Lombès, M., Chen, C.-H., Lee, K.-H., Lo, Y.-C., Wu, M.-H., Chang, W.-C., & Lin, D.-Y. (2019). Identification of two independent SUMO-interacting motifs in Fas-associated factor 1 (FAF1): Implications for mineralocorticoid receptor (MR)-mediated transcriptional regulation. *Biochimica et Biophysica Acta (BBA) - Molecular Cell Research*, 1866(8), 1282–1297. <https://doi.org/10.1016/j.bbamcr.2019.03.014>
54. Weiszmam, R., Hammonds, A. S., & Celniker, S. E. (2009). Determination of gene expression patterns using high-throughput RNA in situ hybridization to whole-mount *Drosophila* embryos. *Nature Protocols*, 4(5), 605–618. <https://doi.org/10.1038/nprot.2009.55>
55. Zaidman-Rémy, A., Hervé, M., Poidevin, M., Pili-Floury, S., Kim, M.-S., Blanot, D., Oh, B.-H., Ueda, R., Mengin-Lecreulx, D., & Lemaitre, B. (2006). The *Drosophila* amidase PGRP-LB modulates the immune response to bacterial infection. *Immunity*, 24(4), 463–473. <https://doi.org/10.1016/j.immuni.2006.02.012>
56. Zhang, L., Zhou, F., Li, Y., Drabsch, Y., Zhang, J., van Dam, H., & ten Dijke, P. (2012). Fas-associated factor 1 is a scaffold protein that promotes  $\beta$ -transducin repeat-containing protein ( $\beta$ -TrCP)-mediated  $\beta$ -catenin ubiquitination and degradation. *The Journal of Biological Chemistry*, 287(36), 30701–30710. <https://doi.org/10.1074/jbc.M112.353524>

## Chapter 5: Caspar is a maternal effect gene required for early development

### 5.1 Abstract

Early embryonic development in metazoans is dependent on the deposition of maternal gene factors. Casp, previously implicated in host defense as a negative regulator of the immune deficiency (IMD) pathway, is expressed ubiquitously in the early embryo. Here, we delve deeper into its function in the embryo and report that loss of *casp* derails the developmental program. Time-lapse imaging and immunohistochemistry indicate that development of ~50% *casp* loss-of function (lof) embryos stall before the onset of gastrulation. We show that Casp, like its mammalian counterpart Fas-associated factor 1 (FAF1), associates with Transient Endoplasmic Reticulum 94 (TER94), a AAA-ATPase involved in protein degradation and also the ER based VAMP-associated protein (*VAP/VAP33A*). Similar to *casp<sup>lof</sup>*, maternal knockdown of *ter94* also leads to a cessation of development before the onset of gastrulation. Intriguingly, both *casp* and *ter94* loss-of-function embryos display aberrations in the formation of primordial germ cells. We speculate that the developmental phenotypes seen on removal of *casp* function result from the derailment of the maternal to zygotic transition, a consequence of the abnormal degradation of maternal proteins.

### **Key words**

Embryo, maternal-to-zygotic transition, ubiquitin-proteasomal degradation, germ cells

## 5.2 Introduction

Embryonic development is a critical stage of an organism's life, dictating its well-being in adulthood. In *Drosophila*, the blueprint for the body axes is laid down in the oocyte, and embryogenesis resumes with the fertilization of the oocyte (Horner & Wolfner, 2008; Lynch & Roth, 2011; Riechmann & Ephrussi, 2001; Stein & Stevens, 2014; van Eeden & St Johnston, 1999). Maternal deposition of mRNA and proteins in the oocyte regulates early (0-3 h) development, after which the zygotic genome takes over the functions of transcription and translation, termed the maternal-to-zygotic transition, or MZT (Laver et al., 2015; Nüsslein-Volhard, 1991; St Johnston & Nüsslein-Volhard, 1992). The MZT is primarily considered a biphasic event; in the first phase, the maternal contribution is actively eliminated, paving the way to the second phase, where transcription of the zygotic genome begins (Hamm & Harrison, 2018; Li et al., 2014; Sysoev et al., 2016; Vastenhouw et al., 2019; Walser & Lipshitz, 2011).

A landmark mutagenesis screen by Volhard and Wieschaus, referred to as the Heidelberg screen, uncovered many maternal effect genes patterning the body axis, broadly divisible into the antero-posterior (AP), dorso-ventral (DV), and terminal gene regulatory networks (Jürgens et al., 1984; Nüsslein-Volhard et al., 1985, 1984; Nüsslein-Volhard & Wieschaus, 1980; E. Wieschaus et al., 1984; Eric Wieschaus & Nüsslein-Volhard, 2016). The larval cuticle patterning was employed as the readout for discerning defects. Dorsal (DL) (Steward 1987; Steward *et al.* 1988; Roth *et al.* 1989) and Bicoid (*bcd*) (Anne Ephrussi & St Johnston, 2004; Frohnhofer & Nüsslein-Volhard, 1986; Simpson-Brose et al., 1994) initiate the cascade of events that culminate in the assumption of cell identity in the ventral and anterior regions, respectively (Fig. 5.1). A distinct Ras/MAPK pathway is required to form the distal-most structures, constituting the terminal pathway (St Johnston & Nüsslein-Volhard, 1992). Therefore, the coordinated orchestration of these initial events leads to the proper execution of axis specification (Fig. 5.1).

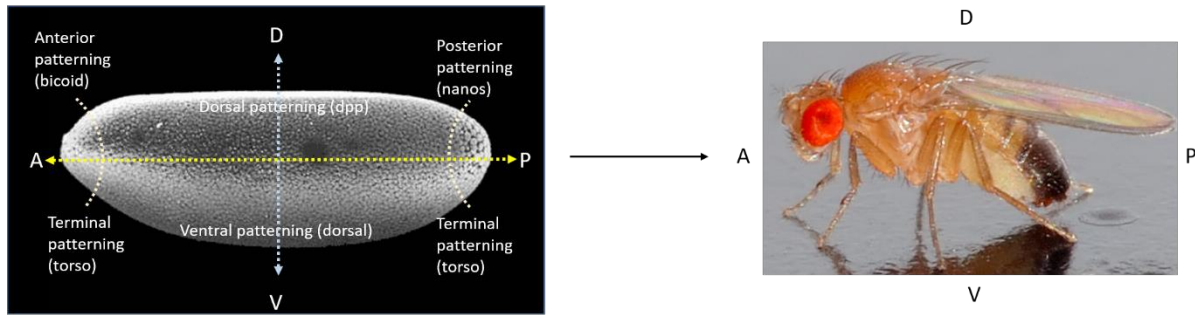


**Fig. 5.1. Patterning in the fly.** Cell fate is specified in the developing embryo primarily through the antero-posterior (AP), dorso-ventral (DV), and terminal patterning pathways, with critical players represented in parentheses. This leads to its distinct body plan, as an adult.

In this study, we explore the maternal roles for Caspar (Casp), the Fas-associated factor-1 (FAF1) ortholog. Intriguingly, Casp has not previously been identified as a maternal-affect gene in the Heidelberg screen. Nevertheless, *in vivo* studies in mice indicate that *faf1* is required for early embryogenesis. FAF1 was abundantly detected in mouse ovaries, testes, and pre-implantation stage embryos (Adham et al., 2008). siRNA-based depletion of FAF1 between the 1-cell to 8-cell stage led to a developmental arrest. Another study utilized a gene-trap system to disrupt the *faf1* locus. In these loss-of-function embryos, development proceeded till the 2-cell stage sustained by the contribution of maternal FAF1 (Peng et al., 2017). Further development was halted, corroborating the results of the previous study. Since FAF1 plays an essential role in the ubiquitin-proteasomal pathway, the authors speculate that the embryonic arrest could be mediated by a failure to degrade maternal proteins to facilitate the zygotic transition. Additional physiological functions known for Casp and FAF1 concerning their domains have been discussed in greater detail in Chapter 4.

Our study using a hypomorphic allele of *casp* in *Drosophila* shows that Casp is required maternally for embryonic development. Animals lacking Casp fail to progress to the gastrulation stage, and display a plethora of cell division defects. We also identify Transient endoplasmic Reticulum 94 (TER94), a AAA-ATPase and VAMP-associated protein 33kDa (VAP), an ER tethering protein, as interactors of Casp via mass spectrometry in the 0-3 h embryo. An association of Casp with germ plasm components also led us to investigate Casp's role germ cell formation. We observe that both Casp and TER94 play crucial roles in somatic cells and the future germline during embryogenesis.



## 5.3 Results

### 5.3.1 *casp<sup>lof</sup>* is a robust hypomorphic *casp* allele

We followed up on the embryonic lethality in *casp<sup>lof</sup>* alluded to in the previous chapter. The *casp<sup>c04227</sup>* allele was procured from the Bloomington *Drosophila* Stock Centre and is referred to as *casp<sup>lof</sup>* henceforth. The *casp<sup>lof</sup>* allele is reported to be an insertional mutant. It harbors a piggyBac insertion mapped to the 5' coding region (Fig. 5.2A). We first characterized embryonic lethality in this presumptive loss-of-function allele. The adults were homozygous viable, and the homozygous *casp<sup>lof</sup>* females were mated with wild-type males (*w<sup>1118</sup>*) to determine the maternal source of lethality, if any. We observed that ~40% of embryos failed to hatch. To negate off-target effects in the *casp<sup>lof</sup>* line and to pin down the specificity of the phenotype to the loss of Casp function, we used the *casp<sup>lof</sup>* line in a trans-heterozygous state with a chromosomal deficiency of *casp* (BL23691), hereafter referred to as *Df*. The *casp<sup>lof</sup>/Df* females mated with *w<sup>1118</sup>* males also demonstrated an embryonic lethality of >35% (Fig. 5.2B). 0-3 hour embryos derived from *casp<sup>lof</sup>/Df* mothers were also immunostained with the Casp antibody and visualized on a confocal fluorescence microscope. Casp in *w<sup>1118</sup>* was predominantly cytoplasmic and exhibited a ubiquitous distribution (Fig. 5.2C). Additionally, we characterized Casp protein levels in embryos laid by *casp<sup>lof</sup>/Df* mothers. Embryonic lysates probed with an antibody against full-length Casp showed a drastic reduction in Casp levels compared to *w<sup>1118</sup>* (Fig. 5.2D). The *casp<sup>lof</sup>/Df* embryos displayed a negligible Casp signal in contrast to *w<sup>1118</sup>*. Therefore, we validate the specificity of the antibody against Casp protein via western blot and immunostaining, while also confirming that *casp<sup>lof</sup>* is a bonafide hypomorphic, loss-of-function allele of *casp*. Moreover, the embryonic lethality experiments indicate that Casp is required maternally for embryonic development and hatching.

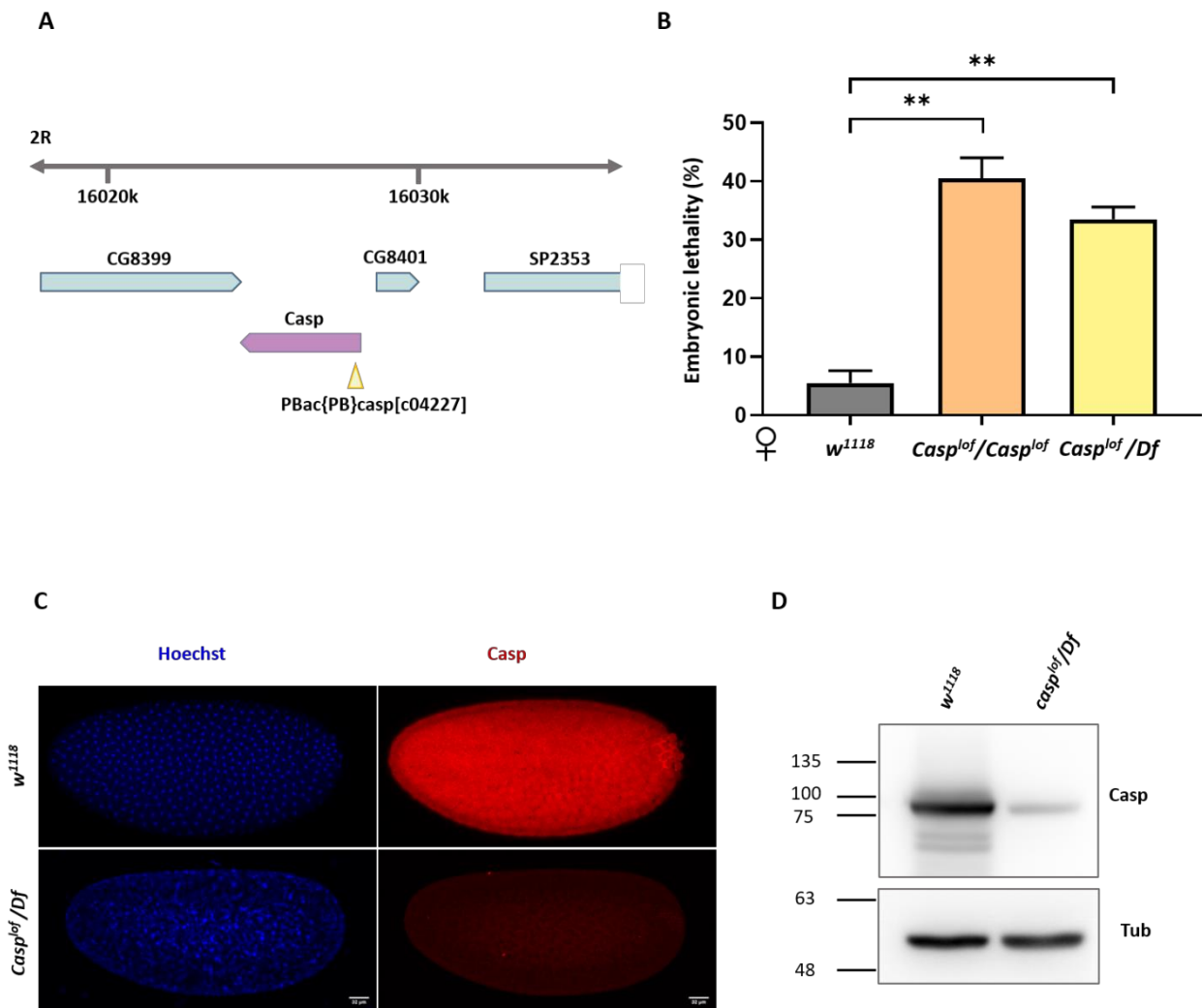


**Fig. 5.2.  $casp^{lof}$  is a hypomorphic Casp allele.** The chromosomal location of the Casp locus and the associated transposon insertion to generate the  $casp^{c04227}$  allele is depicted in (A). This allele is referred to as  $casp^{lof}$  hereafter. (B) represents embryonic lethality plotted as a bar graph. The X-axis lists the genotype of the mated mothers. N = 3, ordinary one-way ANOVA, (\*\*)  $P < 0.01$ . Immunofluorescence images of 0-3 h embryos derived from  $w^{1118}$  and  $casp^{lof}/Df$  stained with Hoechst and Casp is shown in (C). N = 3, n = 15. Casp protein levels were assessed in 0-3 embryos  $w^{1118}$  and  $casp^{lof}/Df$  animals via western blotting. Tubulin is used as a loading control. N = 3.

### 5.3.2 Casp function is required for early embryonic development

To further understand the basis of this lethality and identify developmental defects, we looked at the cuticle. 0-3 hour embryos were collected, aged for 22 hours, and their cuticles were visualized under a dark field microscope. While >60% of cuticles displayed a regular DV arrangement of cuticles, the rest did not deposit cuticles (visualized by the presence of the intact vitelline membrane) (data not shown). Therefore, we glean that loss of Casp leads to defects in early development or cuticle deposition.

To better understand the spatio-temporal dynamics of Casp in development and the precise stage of the death of *casp<sup>lof</sup>* animals, we performed time-lapse live imaging (Cavey & Lecuit, 2008). Bright-field imaging revealed that *casp<sup>lof</sup>* embryos did not proceed to gastrulation and showed a developmental arrest before stage 5 (Fig. 5.3). The embryos displayed irregular, uncoordinated morphogenetic movements with blebbing of the plasma membrane, impeding cephalic furrow formation, and germband elongation (Fig. 5.3). Moreover, immunostaining 0-3 h embryos with the nuclear dye Hoechst and phalloidin, which marks the cytoskeletal f-actin, indicates abnormalities (Fig. 5.4).

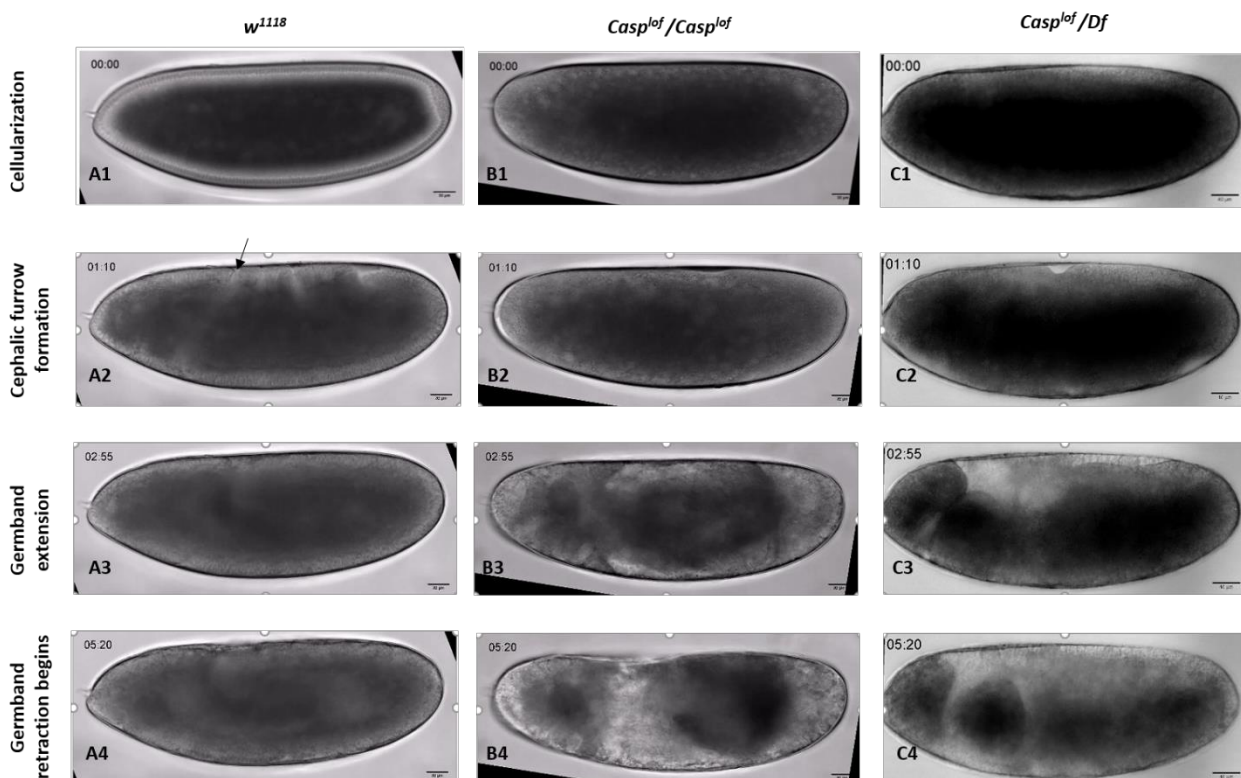


**Fig. 5.3. Casp assists in progression to gastrulation.** Out of 96 time-points imaged, four are shown for each genotype. Images were acquired from a single, constant plane unique to each embryo across 5-minute intervals. The developmental trajectory for  $w^{1118}$  can be followed from the cellularization stage to the beginning of germ band retraction for the time points indicated. Crucial developmental milestones are highlighted (A1-A4). The mutants did not exhibit characteristic stages of morphogenesis at comparable time points (B1-B4, C1-C4). n = 10.

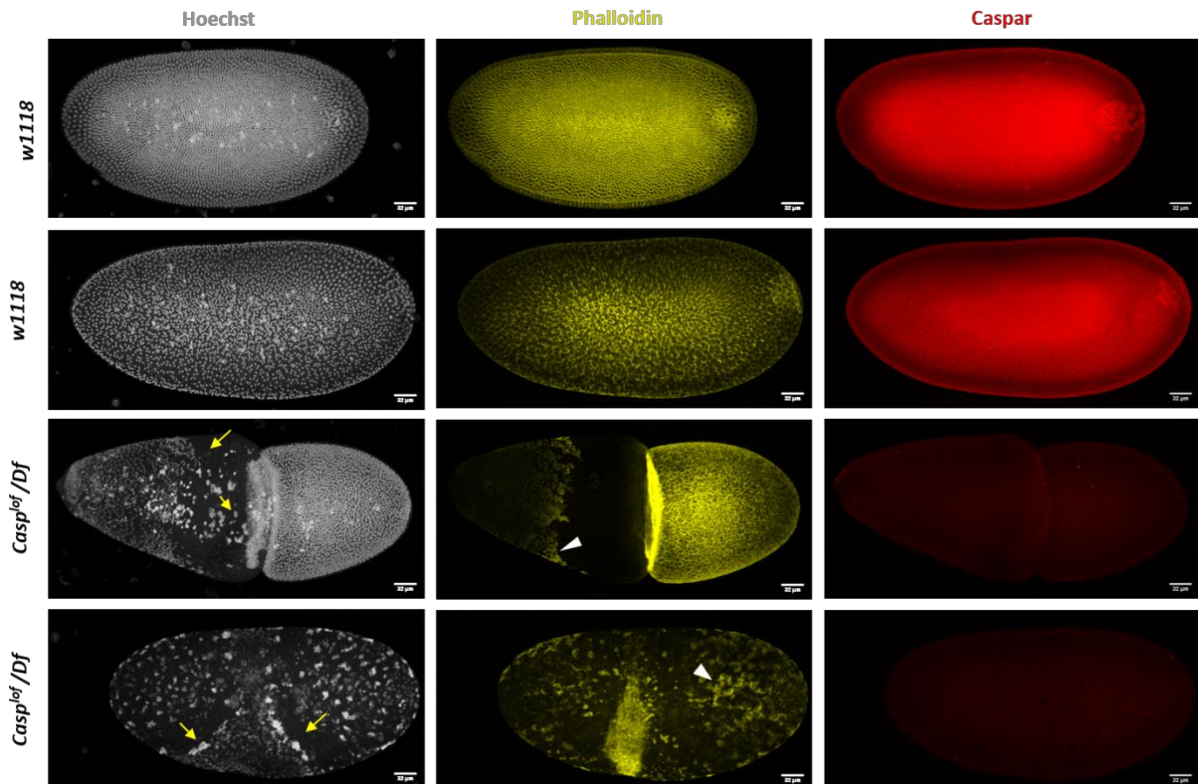


**Fig. 5.4.  $casp^{of}/Df$  embryos display nuclear division and cytoskeletal defects.** Representative images of 0-3 h  $w^{1118}$  and  $casp^{of}/Df$  embryos stained with Hoechst, phalloidin, and Caspar. Yellow arrows indicate disorganized nuclei, while white arrowheads show aggregates of f-actin, marked by phalloidin. n = 20

Therefore, we conclude that Casp plays an essential role in early embryonic development in *Drosophila*.

### 5.3.3 Casp interacts with TER94 and VAP in the early embryo

Casp is the *Drosophila* ortholog of mammalian FAF1. To understand its functional associations in the early embryo, we performed immunoprecipitation of Casp and identified interactors via mass spectrometry. Peptides from 122 proteins were recovered in the Casp IP but not the IgG IP and were considered significant interactors. The top 25 interactors are presented in Fig 5.5A. TER94 and VAP were the top interactors, reaffirming the conservation of Casp interactions with its mammalian counterpart, FAF1.

**A**

Protein	Peptide count
casp	73.5
TER94	18
Vap33	2.5
Tudor-SN	2.25
alphaTub85E	2
eIF4A	2
Npl4	2
SERCA	1.75
bel	1.75
CCT2	1.5
mRpS14	1.5
CCT6	1.5
Hacl	1.25
mAcon1	1.25
ATPsyngamma	1.25
mRpL27	1.25
alphaTub67C	1.25
eIF3b	1
ScsbetaA	1
26-29-p	1
lig	1
me31B	1
nocte	1
Ufd1-like	1

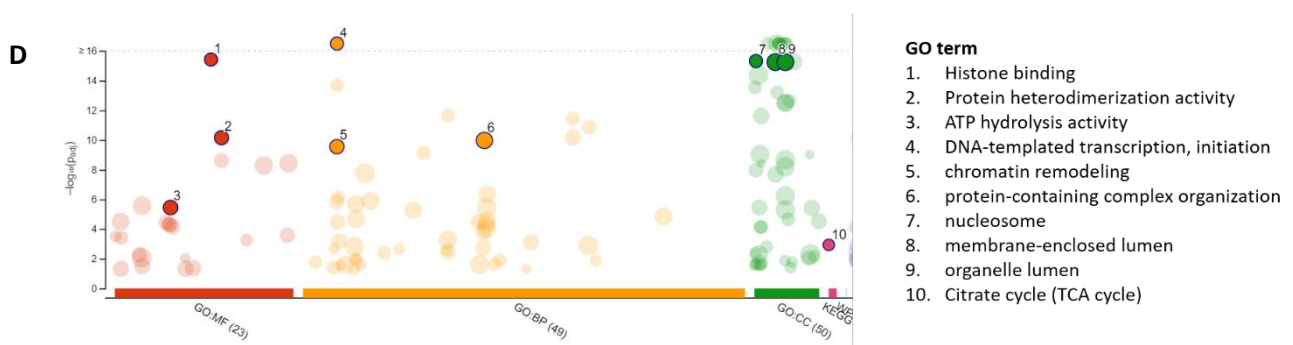
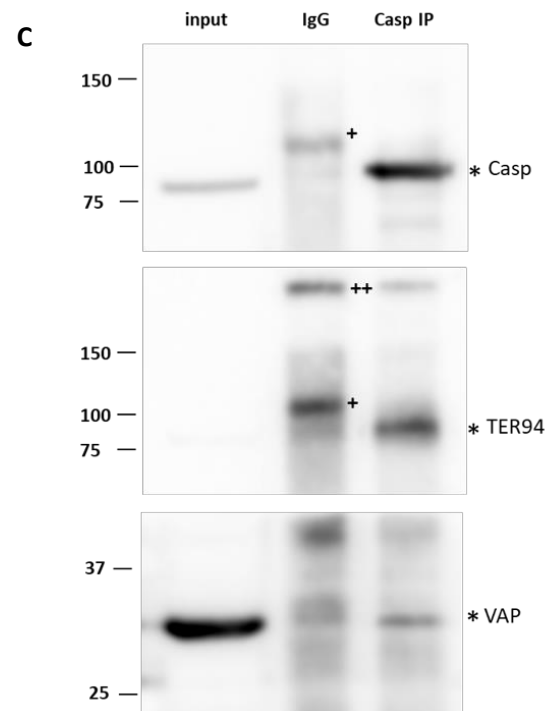
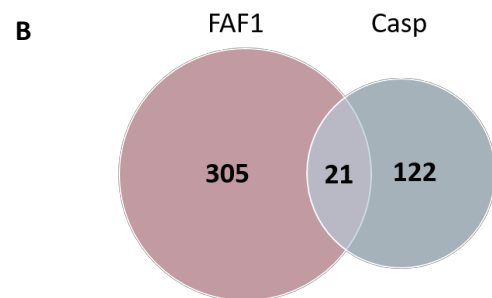


**Fig. 5.5. TER94 and VAP33 are major interactors of Casp.** (A) shows a list of the top 25 proteins enriched after a Casp IP followed by mass spectrometry, listed in the order of their peptide counts. The peptide counts are averaged from 4 biological replicates. The Venn diagram in (B) shows the number of interactors common to both FAF1 and Casp. A Casp IP and western blot for TER94 and VAP in S2 cells are shown in (C). (D) represents a gene ontology analysis of proteins enriched in the Casp IP and mass spectrometry.

FAF1 is known to interact with VCP, the mammalian TER94 ortholog, via its UBX domain, while the FFAT-like region mediates VAP interaction. Interestingly, mutations in both TER94 and VAP are known to cause neurodegenerative phenotypes.

A comparison of the Casp interactome with FAF1 interactors experimentally annotated and retrieved from the BioGRID database (Oughtred et al., 2021) indicates an overlap of 21 orthologous proteins (Fig. 5.5B). The interaction of TER94 and VAP with Casp was also re-affirmed in S2 cells via immunoprecipitation and western blotting (Fig. 5.5C). Since TER94 is known to interact with Npl4, p47, Ufd1-like, Prosalpha6, etc., it could be a crucial node arbitrating a handful of Casp interactions. A gene ontology (GO) analysis (Raudvere et al., 2019) indicates the enrichment of proteins involved in ATP hydrolysis, chromatin remodeling, TCA cycle, etc.

Taken together, the association of Casp with TER94 could be a major axis regulating its function. We explore the functions of TER94 in greater depth in the next section.

#### **5.3.4 TER94 is required maternally**

Mammalian VCP/p97 is an essential chaperone for proteostasis, modulating several ubiquitin-associated processes (Dai et al., 1998; Jentsch & Rumpf, 2007; H. Meyer et al., 2012; H. H. Meyer et al., 2000; Hemmo H. Meyer, 2005; Peters et al., 1990; Ye, 2006). Its *Drosophila* counterpart TER94 has been extensively studied in the context of neurodegeneration (Griciuc et al. 2010; Chang et al. 2011; Azuma et al. 2014; Kushimura et al. 2018; Tendulkar et al. 2022). Loss of TER94 was shown to ameliorate polyQ-induced eye degeneration. Moreover, the overexpression of TER94 promoted the apoptosis of neuronal cells (Higashiyama et al., 2002). The unavailability of TER94 germline clones and the VALIUM 20/22 maternal RNAi lines till recently had precluded the elucidation of TER94 function in the early embryo.

Nevertheless, the use of mutant *ter94* alleles has revealed a crucial role for TER94 in ER assembly in the egg chamber (Leon & McKearin, 1999). Mutations in TER94 also impaired the mRNA localization of *Oskar*, a germ cell determinant, during oogenesis (Ruden et al., 2000). The only study implicating TER94 in early embryogenesis comes from a genetic interaction study (Zeng et al., 2014). Perturbations in *Smurf/dpp*, components of BMP signaling, in a *ter94* mutant background led to decreased embryonic viability of the transheterozygotes compared to the single mutants. In these animals, the expression domain of the BMP target *race* was also severely reduced, consistent with the role of TER94 in regulating BMP signaling (Zeng et al., 2014).

Since TER94 was found to be an interactor of Casp, we wanted to check if TER94 exhibited maternal roles as well. We used a maternal GAL4 driver to deplete TER94 in the late stages of oogenesis and observed its effects in the early embryo. Egg-laying remained largely unaffected (data not shown), but viability was severely impaired in embryos derived from *Mat-GAL4/TER94i* mothers, with >95% of embryos failing to hatch (Fig. 5.6A). A western blot of embryonic lysates indicates a robust knockdown of TER94 (Fig. 5.6B). *Drosophila* embryogenesis progresses through a series of 13 precise, synchronous nuclear division cycles. A microscopy-based phenotypic analysis of embryos revealed that >70% of *Mat-GAL4/TER94i* embryos failed to progress to the syncytial blastoderm stage. The late-stage syncytial/ cellular blastoderm embryos were further assessed for cell cycle defects. Both *casp<sup>lof</sup>/Df* and *Mat-GAL4/TER94i* embryos displayed defects ranging from irregular nuclear distribution to perturbed f-actin localization, observed via DAPI and phalloidin staining, respectively (Fig. 5.6C). Therefore, Casp and TER94 perform essential functions in regulating the cell cycle.



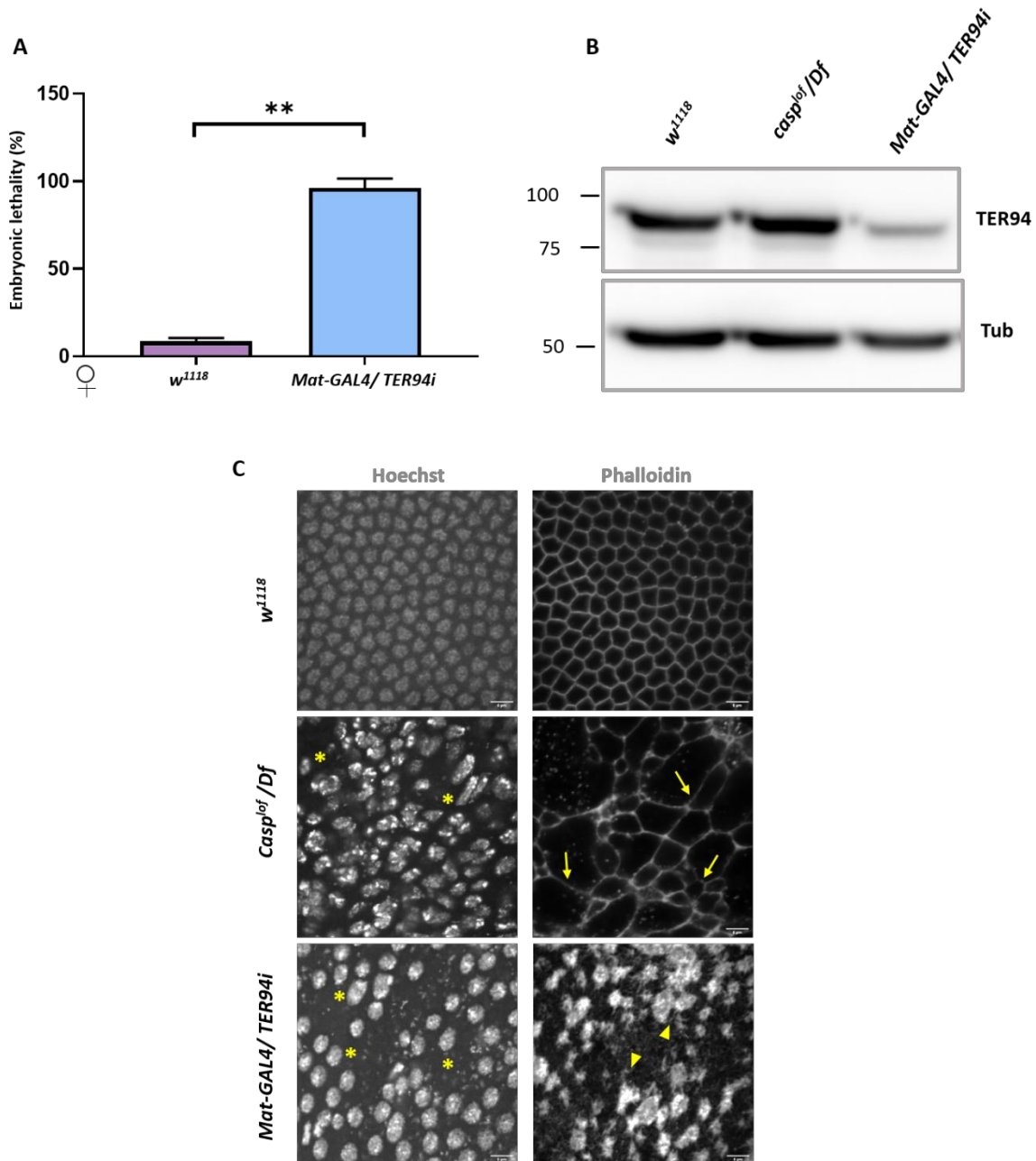


**Fig. 5.6. TER94 is required maternally.** Viability of embryos derived from *w<sup>1118</sup>* and *Mat-GAL4/TER94i* mothers is represented in the bar graph in (A). N = 3, ordinary one-way ANOVA, (\*\*\*)  $P < 0.001$ . (B) Western blot analysis indicates the knockdown efficiency of TER94 in the 0-3 h embryo. TER94 levels remain unaffected in *casp<sup>1of</sup>/Df* embryos. Tubulin acts as a loading control. N = 3. (C) depicts confocal images of zoomed-in sections of nuclear cycle 13/14 embryos of the indicated genotypes stained with Hoechst and phalloidin. The regular arrangement and density of peripheral nuclei is disrupted in the mutants, indicated by yellow asterisks. F-actin, marked with phalloidin, shows a regular, hexagonal arrangement in *w<sup>1118</sup>*, while disorganized (solid arrows) and aggregated f-actin (arrowheads) is observed in the mutants.



### 5.3.5 Caspar regulates primordial germ cell number

Intriguingly, a careful examination of the Casp interactome suggests that a subset of interactors constitutes the germplasm. These include eIF4A, me31B, and TER94, which form a part of the polar granules (Thomson et al., 2008).

Germ line-specific cells are demarcated early in the life of *Drosophila*, during embryogenesis (Donovan & de Miguel, 2003; Technau & Campos-Ortega, 1986). The specification of these cells is incumbent on the germplasm, a dedicated cytoplasm localized to the posterior of the embryo (Illmensee & Mahowald, 1974). The germplasm is supplemented with mitochondria and structures called polar granules, which are ribonucleoprotein complexes (A. P. Mahowald, 1968; Anthony P. Mahowald, 1962). A critical posterior determinant found at the polar granules is Oskar (Kim-Ha et al., 1991; Lehmann, 2016; Snee & Macdonald, 2004; Vanzo et al., 2007). Ectopic expression of Oskar at the anterior region of the embryo using the *bicoid* mRNA localization signal induces pole cell formation at the anterior, corroborating Oskar's role in pole cell determination (A. Ephrussi & Lehmann, 1992). *vasa* and *tudor* are two genes downstream of *Oskar* essential for the assembly of poleplasm (Arkov et al., 2006; Breitwieser et al., 1996; Jones & Macdonald, 2007).

Biochemical analysis of *vasa* (VAS) and Tudor (TUD) polar granule complexes identified eIF4A, me31B, and TER94, indicating an association with the translational machinery and endoplasmic reticulum (Thomson et al., 2008).

Caspar's association with these proteins could indicate a putative function in the poleplasm. Primordial germ cells (PGCs) undergo precocious cellularization and are set aside during the early stages of embryogenesis. Stage 5 embryos derived from wild-type (*w<sup>1118</sup>*) and *casp<sup>lof</sup>/Df* mothers were immunostained for the pole cell marker *vasa* and visualized under a confocal fluorescence microscope. While *w<sup>1118</sup>* embryos had an average of ~30 pole cells, *casp<sup>lof</sup>/Df* showed a drastic reduction to ~10 (Fig. 5.6A, B). Very few stage 5 embryos depleted of maternal TER94 (*Mat-GAL4/TER94<sup>i</sup>*) could be obtained, and pole cells could not be adequately quantified. The few nuclear cycle 11 embryos that were obtained also showed pole cell aberrations ranging from mislocalization to defects in cell size (Fig. 5.6C). Since TER94 is required for *Osk* mRNA localization in the oocyte, the embryonic defects could be an

extrapolation of the defective oocyte. That these defects could be a fallout of the pre-existing somatic division defects cannot also be ruled out.

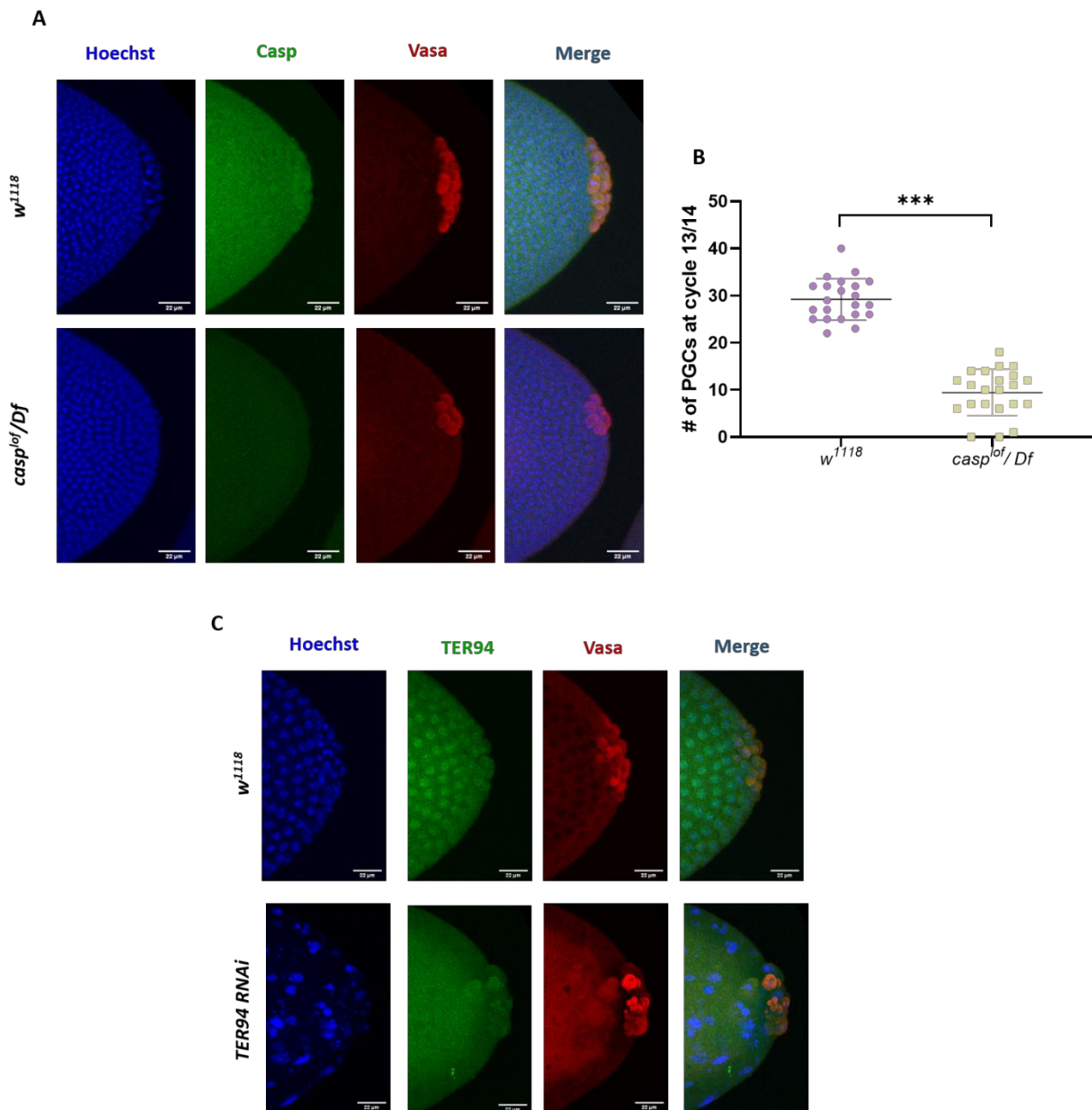


**Fig. 5.7. Casp influences PGC number.** Confocal microscopy images of nuclear cycle 13/14 embryos from *w<sup>1118</sup>* and *casp<sup>of</sup>/Df* immunostained with Casp and vasa antibodies is presented in (A). Hoechst marks the nuclei. The germ cells at the posterior marked by vasa were quantified and plotted as a bar graph (B).  $n = 20$ , Student's t-test, (\*\*\*)  $P < 0.001$ . (C) shows immunostaining of *w<sup>1118</sup>* and *Mat-GAL4/TER94i* embryos with antibodies against TER94 and vasa.  $n = 10$ .

### 5.3.6 Function of Casp domains

To dissect the function of Casp further, fly lines expressing domain deletions of Casp under the *pUASp* promoter were generated (Jyothish). The *pUASp-Casp<sup>ΔUBA</sup>*, *pUASp-Casp<sup>ΔUBX</sup>* and *pUASp-Casp<sup>ΔUAS</sup>* construct represent deletions of the UBA, UBX, and UAS domains, respectively. A full length coding sequence of Casp was also cloned and this *pUASp-Casp<sup>WT</sup>* line used as a control (Fig. 5.7A). The expression of these constructs was confirmed by a western blot in adult flies with *UAS-Casp<sup>domain deletion</sup>* driven by a ubiquitous *daughterless-GAL4* driver (Fig. 5.7B). To assess the domain-specific functions of Casp in isolation without the confounding effects of endogenous Casp, the fly lines were balanced with a *Casp<sup>lof</sup>* allele on the second chromosome. These balanced lines were crossed to a fly line with the maternal driver *Nanos-GAL4* (*Nos-GAL4* henceforth) on the third chromosome and an allele with a deficiency for *Casp* (*Df*). Embryos laid by mothers of the genotype *Casp<sup>lof</sup>/Df; Nos-GAL4/pUASp-Casp<sup>domain deletion</sup>* were used to determine maternal effects of the domain deletions. Preliminary lethality assays indicate that the rescue with *pUASp-Casp<sup>WT</sup>* restores the hatching to ~88% compared to *Casp<sup>lof</sup>/Df* alone, which is at ~70% (Fig. 5.7B); hence, the *nos-GAL4* driven *pUASp-Casp<sup>WT</sup>* allele is functional, and the null; rescue system is ideal for exploring the effects of the domain deletions. Rescuing *Casp<sup>lof</sup>/Df* with a *pUASp-Casp<sup>ΔUBX</sup>* or *pUASp-Casp<sup>ΔUAS</sup>* did not restore viability (Fig. 5.7C). *pUASp-Casp<sup>ΔUBA</sup>*, on the other hand, led to a rescue of hatching to ~80%. Therefore, these initial experiments hint at the importance of the UBX and the UAS domains in carrying out the maternal functions of Casp.

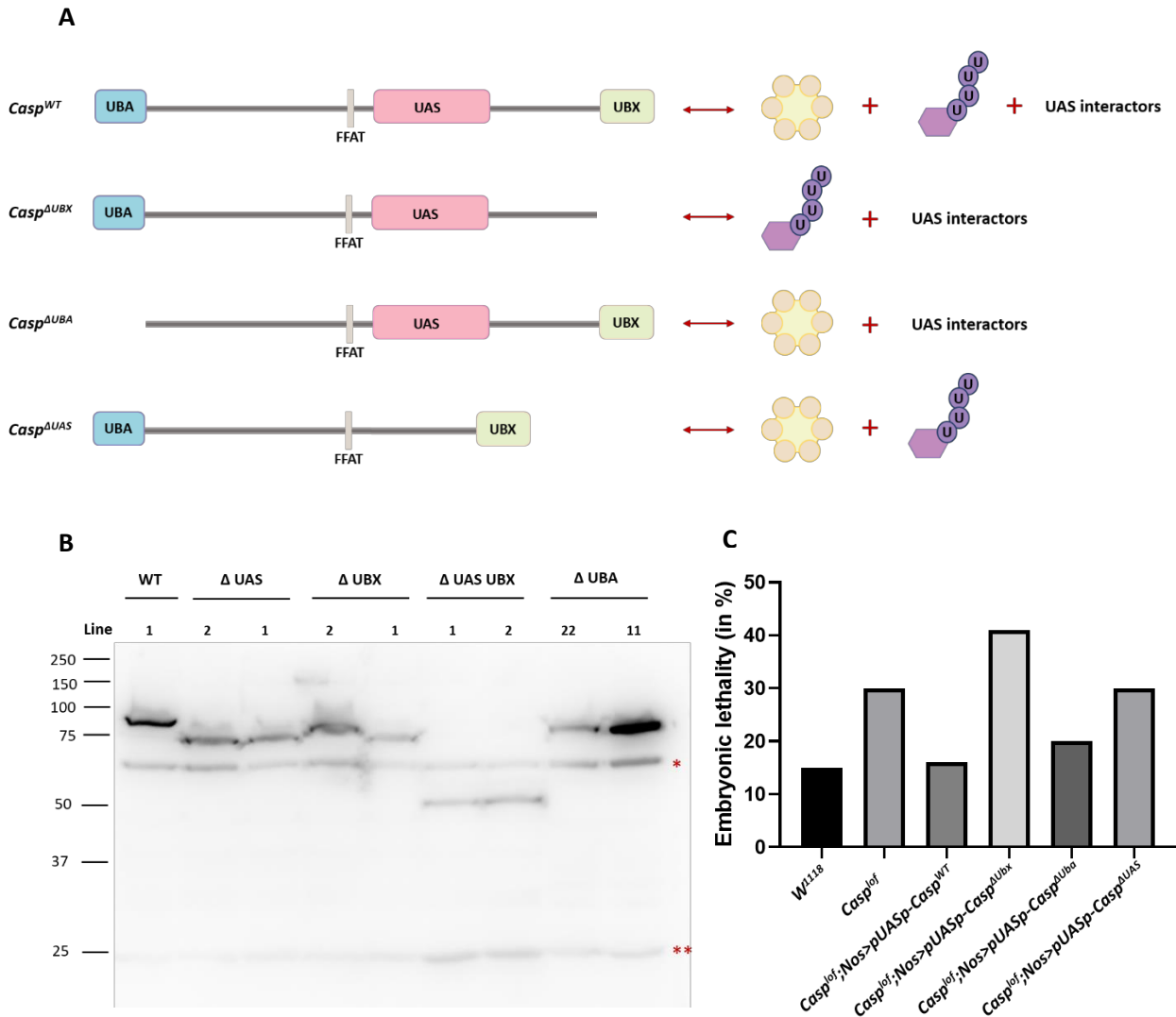


**Fig. 5.8. Casp domain deletions and their predicted interaction dynamics.** The putative proteins encoded and the interactions of domain deletion constructs of Casp are depicted in (A). (B) shows a western blot of the truncated Casp proteins, deficient in the domains indicated, probed with an HA antibody. WT serves as a control. Asterisks denote non-specific antibody binding. (C) shows embryonic lethality for the null; rescue with the domain deletions plotted as a bar graph. N = 1.

#### 5.4 Discussion

Previously, the role of Casp in *Drosophila* immunity was well characterized (Kim *et al.* 2006). However, developmental roles for Casp and functional associations were not well established.

Early embryonic development is a dynamic process in metazoans controlled by the deposition of maternal gene products (Schier, 2007). Here, we explored novel embryonic functions for the FAF1 ortholog Casp in *Drosophila*. We identify Casp as a maternal effect gene necessary for progression to gastrulation. We present proteomic data suggesting that TER94, an ER protein, is a major Casp interactor. Genetic evidence also indicates that TER94 and Casp regulate cell cycle processes in the early embryo. A subset of germplasm components was also observed to be a part of the interactome. Loss of function of Casp and TER94 led to aberrations in the primordial germ cells. Therefore, our data suggest that Casp and TER94 perform critical developmental functions in the *Drosophila* embryo.

In mammals, the FAF1-VCP interaction is mediated by the UBX domain. It is yet to be seen whether a similar interaction axis is conserved in *Drosophila*. A functional analysis of the domain deletion constructs would allow us to dissect the importance of the Casp-TER94 association further.

FAF1 participates in the ubiquitin proteasomal degradation via its N-terminal UBA domain (Song *et al.* 2005). Though the global ubiquitination profile remains unchanged (Fig. 5.8), Casp could be influencing the degradation dynamics of a specific set of proteins. Me31B, a Casp interactor in our IP-MS experiment, is an attractive candidate because it forms a critical component of both the germplasm and the maternal-to-zygotic transition. Me31B is an ATP-dependent RNA helicase associated with ribonucleoproteins (RNPs) in the germplasm and silences the translation of mRNAs like *Osk* (Nakamura *et al.*, 2001). Throughout embryogenesis, Me31B is also known to associate with maternal RNAs and repress translation. At the onset of zygotic genome activation, many RNA-binding proteins, including Me31B are eliminated, bringing about a change in the transcriptome (Cao *et al.*, 2020; Wang *et al.*, 2017). Data from recent studies support the involvement of the ubiquitin-proteasomal system, particularly the E3 CTLH ligase, in the active destruction of Me31B (Zavortink *et al.*, 2020). Therefore, the alteration in Casp levels in the *Casp<sup>lof</sup>* embryos could potentially affect the degradation of Me31B, disallowing MZT progression and causing lethality.

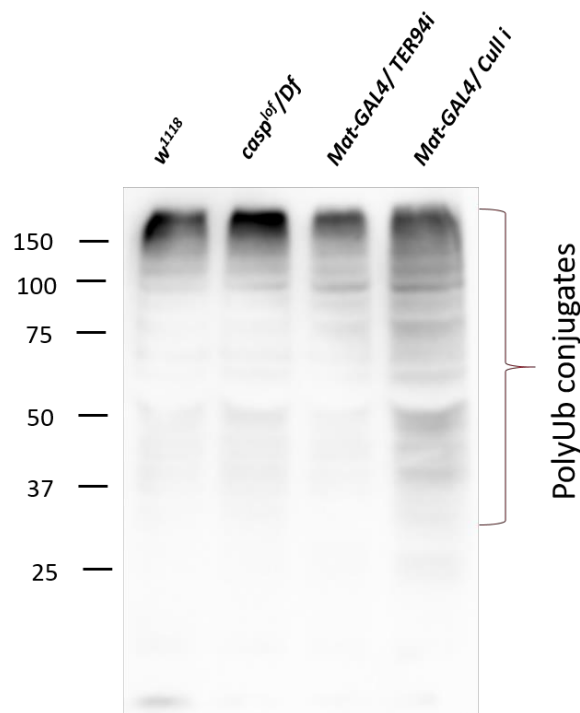


**Fig. 5.9. Global ubiquitination profile in *casp<sup>lof</sup>* and *ter94 i* embryos.** A western blot analysis of 0-3 h embryos for the genotypes indicated. PolyUbiquitin conjugates are detected as species migrating at a higher molecular weight. Maternal knockdown of Cullin1 (*Cull i*), a component of the SCF E3 ubiquitin ligase complex, is a positive control for ubiquitinated proteins. Equal protein was loaded. N = 2.

FAF1 interacts with  $\beta$ -catenin, a critical component of the Wnt/ $\beta$ -catenin pathway regulating bone formation (Zhang et al., 2011). FAF1 inhibits transcriptional targets of Wnt by promoting its polyubiquitination and subsequent degradation, mediated by its interaction with  $\beta$ -transducin repeat-containing protein ( $\beta$ -TrCP) (Zhang et al. 2011, 2012). Interestingly, our proteomic data implicates armadillo (arm), the *Drosophila*  $\beta$ -catenin ortholog, as an interactor of Casp. Arm is a co-activator of Wntless signaling, which regulates segmentation patterning in the embryo (Baker, 1988; Klingensmith & Nusse, 1994; Peifer et al., 1991). It also constitutes structural components of the adherens junction (Cox et al., 1996; Peifer, 1993, 1995). Loss of Casp could influence the degradation kinetics of arm, thereby disrupting homeostasis. Therefore, the developmental phenotypes observed could be a combination of multiple functions performed by Casp in the embryo. Due to the early lethality, patterning defects could not be studied in greater detail. Nonetheless, we

establish Casp and TER94 as essential modulators of early embryonic development in *Drosophila*.

## 5.5 Materials and methods

### *Fly husbandry and stocks*

Flies were raised on standard cornmeal agar at 25 °C unless stated otherwise. *Casp<sup>lof</sup>* (11373), *Casp Df* (BL23691), and *Cullin1 RNAi*, VALIUM22 (BL36601) were procured from the Bloomington *Drosophila* Stock Centre.

### *Embryonic lethality*

0-3 hr embryos were transferred to a new sugar-agar plate, and unhatched larvae were scored after 48 hours to determine viability.

### *Immunoprecipitation*

0–3-hour embryos were lysed in Co-IP Lysis Buffer (20mM Tris pH 8.0, 137mM NaCl, 1% IGEPAL, 2mM EDTA, 1X PIC) using a Dounce homogenizer, and centrifuged at 21,000 g for 30 minutes. 3 mg of total lysate was incubated with 5 µg of primary antibody (Rb anti-Caspar) and 5 µg of Normal Rabbit IgG overnight at 4 °C. Antigen-antibody complexes were captured using 50 µL of BioRad SureBeads Protein A (1614013) at 4 °C for 4 hours. Beads were washed six times with Co-IP Lysis Buffer and protein complexes eluted by boiling in 1X Laemmli Sample Buffer. Eluted proteins were resolved on a 10% polyacrylamide gel followed by western blotting or in-gel trypsin digestion, described in the following sections.

### *Western blot analysis*

0-3 hour embryos were lysed in RIPA buffer (50 mM Tris-Cl, 150 mM NaCl, 0.1% SDS, 0.01% Sodium azide, 0.5% sodium deoxycholate, 1 mM EDTA, 1% Triton X-100, 1X PIC) with a pellet pestle (Kontes). Lysates were cleared by centrifugation at 21,000 g at 4 °C for 30 minutes. Protein concentration was estimated using a BCA assay (Pierce) and 30-40 µg of total protein was loaded onto the gel after boiling in 1X Laemmli Sample Buffer. Proteins separated by 10% SDS-PAGE were transferred onto a PVDF membrane (Immobilon-E, Merck) and blocked in 5% milk in Tris-Buffer Saline (TBS) with 0.1% Tween 20 (TBS-T) for an hour. Blots were then incubated

overnight with primary antibody diluted in 5% milk in TBS-T, at 4 °C. Following three washes with TBS-T, blots were incubated with secondary antibodies diluted in 5% milk in TBS-T, for 1 hour at room temperature. Blots were washed thrice with TBS-T and visualized on a LAS4000 Fuji imaging system after incubating with Immobilon Western Chemiluminescent HRP substrate (Merck). The following antibodies were used: Rabbit anti-VAP, 1:10000 (Tendulkar *et al.* 2022), Mouse anti- $\alpha$ -Tubulin, 1:10000 (T6074, Sigma), Mouse anti-Ubiquitin, 1:1000 (P4D1, Santa Cruz Biotechnology), Mouse anti-HA, 1:5000 (H3663 HA-7, Sigma-Aldrich), Rabbit anti-Caspar, 1:10000 (Tendulkar *et al.* 2022), Goat anti-rabbit HRP and Goat anti-mouse HRP secondary antibodies, each at 1:10000 (Jackson ImmunoResearch).

#### *In-gel Trypsin Digestion and LC-MS/MS Analysis*

Before in-gel trypsin digestion of the Co-IP eluate, the antibody was crosslinked to the SureBeads using DMP (Sigma) according to the NEB crosslinking protocol to avoid elution of the antibody. After crosslinking 10 $\mu$ g Caspar antibody, Co-IP was performed as described above. In-gel trypsin digestion was carried out as previously described (SHEVCHENKO *et al.* 2006). Briefly, Coomassie-stained bands on the gel were excised and cut into 1 mm cubes. Gel pieces were transferred to a clean microcentrifuge tube and destained with buffer containing 50% acetonitrile in 50 mM Ammonium bicarbonate. Reduction and alkylation were carried out on the destained gel pieces by incubating with 10mM dithiothreitol (DTT) followed by incubating with 20mM iodoacetamide. Gel pieces were saturated with sequencing grade Trypsin (Promega) at a concentration of 10 ng/ $\mu$ L and incubated overnight at 37 °C. Peptides were extracted by sequential addition of 100  $\mu$ l of 0.4% Trifluoroacetic acid (TFA) in 10% ACN, 100  $\mu$ l of 0.4% TFA in 60% ACN and 100  $\mu$ l of ACN. The pooled extract was dried in a vacuum centrifuge and reconstituted with 50  $\mu$ l of 0.1% TFA. The peptides in TFA were purified using the StageTip protocol (RAPPSILBER *et al.* 2007). LC-MS/MS analysis was performed on the Sciex TripleTOF6600 mass spectrometer interfaced with an Eksigent nano-LC 425. Tryptic peptides (1  $\mu$ g) were loaded onto an Eksigent C18 trap (5  $\mu$ g capacity) and subsequently eluted with a linear acetonitrile gradient on an Eksigent C18 analytical column (15 cm  $\times$  75- $\mu$ m internal diameter). A typical LC run lasted 2 h post loading onto the trap at a constant flow rate of 300 nL/min with solvent A consisting of water + 0.1% formic acid and solvent B consisting of acetonitrile. The gradient schedule for the LC run was 5%



(vol/vol) B for 10 min, a linear gradient of B from 0% to 80% (vol/vol) over 80 min, 80% (vol/vol) B for 15 min and equilibration with 5% (vol/vol) B for 15 min. Data was acquired in an information-dependent acquisition (IDA) mode over a mass range of 300–2,000 m/z. Each full MS survey scan was followed by MS/MS of the 15 most intense peptides. Dynamic exclusion was enabled for all experiments (repeat count 1; exclusion duration 6 s). Peptides were identified and quantified using the SCIEX ProteinPilot software at a false discovery rate (FDR) of 1%. A RefSeq Drosophila protein database (release 6) was used for peptide identification. Proteins that were identified in two or more replicates were tabulated.

### *Fixation, immunostaining, and imaging of embryos*

0-3 hr embryos were collected in a sieve and dechorionated in 4% sodium hypochlorite for 90 seconds. After thorough washes with distilled water, embryos were fixed in a 1:1 heptane:4% PFA solution for 20 minutes. The PFA layer was removed, and embryos in heptane were re-constituted with an equal volume of methanol. Embryos were devitellinized by vigorous shaking in the 1:1 heptane:methanol mixture. The heptane layer and the interphase containing non-devitellinized embryos were carefully removed. Devitellinized embryos in the bottom methanol phase were washed twice with methanol and stored at -20 °C till they were ready to be immunostained. For phalloidin staining, embryos fixed in heptane: 4% PFA were hand de-vitellinized, after which the standard immunostaining procedure was followed. For immunostaining, embryos were rehydrated by washing thrice with 0.3% PBS-TritonX 100 (PBS-T) for 15 minutes each. Embryos were blocked in 2% BSA in 0.3% PBS-T for 1 hour at room temperature (RT). Embryos were incubated at 4 °C overnight with primary antibodies diluted in 2% BSA in 0.3% PBS-T at the appropriate dilutions. Following three 15-minute washes with 0.3% PBS-T, embryos were incubated in the appropriate secondary antibodies for 1 hour at room temperature. The following antibodies were used: Rabbit anti-Casp, 1:1000 (Tendulkar *et al.* 2022); Rat anti- $\alpha$ -vasa; 1:50 (DSHB); Rabbit anti-VCP, 1:200 (#2648, Cell Signaling Technology); Alexa Fluor 568 Phalloidin, 1:1000 (Invitrogen). The following antibodies were used: Mouse anti-Dorsal, 1:1000 (DSHB 7A4-c) and goat anti-mouse Alexa488/ goat anti-rabbit Alexa568/ goat anti-rat Alexa647 secondary antibodies, 1:1000 (Invitrogen). Embryos were washed thrice with 0.3% PBS-T, and DAPI/Hoechst (1:500) was added in the penultimate wash. Embryos

were mounted in 70% glycerol and observed under a Leica sp8 confocal microscope with a 20X objective.

### *Live imaging of embryos*

Embryos at the appropriate stage were washed and dechorionated as described previously. A 2-well Nunc™ Lab-Tek™ II Chamber Slide™ System (ThermoFisher Scientific) was affixed with a 3M Scotch double-sided tape, and dechorionated embryos with intact vitelline membranes were mounted on the tape under a dissecting microscope. Halocarbon oil 200 was used to cover the embryos to prevent dehydration during imaging. Time-lapse imaging of embryos was performed on an inverted LSM confocal system (Zeiss multiphoton 710) at 20X for ~8 hours. Embryo images were acquired at 5 min intervals.

## **5.6 References**

1. Adham, I. M., Khulan, J., Held, T., Schmidt, B., Meyer, B. I., Meinhardt, A., & Engel, W. (2008). Fas-associated factor (FAF1) is required for the early cleavage-stages of mouse embryo. *Molecular Human Reproduction*, *14*(4), 207–213. <https://doi.org/10.1093/molehr/gan009>
2. Arkov, A. L., Wang, J.-Y. S., Ramos, A., & Lehmann, R. (2006). The role of Tudor domains in germline development and polar granule architecture. *Development*, *133*(20), 4053–4062. <https://doi.org/10.1242/dev.02572>
3. Azuma, Y., Tokuda, T., Shimamura, M., Kyotani, A., Sasayama, H., Yoshida, T., Mizuta, I., Mizuno, T., Nakagawa, M., Fujikake, N., Ueyama, M., Nagai, Y., & Yamaguchi, M. (2014). Identification of ter94, *Drosophila* VCP, as a strong modulator of motor neuron degeneration induced by knockdown of Caz, *Drosophila* FUS. *Human Molecular Genetics*, *23*(13), 3467–3480. <https://doi.org/10.1093/hmg/ddu055>
4. Baker, N. E. (1988). Localization of transcripts from the wingless gene in whole *Drosophila* embryos. *Development*, *103*(2), 289–298. <https://doi.org/10.1242/dev.103.2.289>
5. Breitwieser, W., Markussen, F. H., Horstmann, H., & Ephrussi, A. (1996). Oskar protein interaction with Vasa represents an essential step in polar granule assembly. *Genes & Development*, *10*(17), 2179–2188. <https://doi.org/10.1101/gad.10.17.2179>

6. Cao, W. X., Kabelitz, S., Gupta, M., Yeung, E., Lin, S., Rammelt, C., Ihling, C., Pekovic, F., Low, T. C. H., Siddiqui, N. U., Cheng, M. H. K., Angers, S., Smibert, C. A., Wühr, M., Wahle, E., & Lipshitz, H. D. (2020). Precise Temporal Regulation of Post-transcriptional Repressors Is Required for an Orderly Drosophila Maternal-to-Zygotic Transition. *Cell Reports*, 31(12), 107783. <https://doi.org/10.1016/j.celrep.2020.107783>
7. Cavey, M., & Lecuit, T. (2008). Imaging cellular and molecular dynamics in live embryos using fluorescent proteins. *Methods in Molecular Biology*, 420, 219–238. [https://doi.org/10.1007/978-1-59745-583-1\\_13](https://doi.org/10.1007/978-1-59745-583-1_13)
8. Chang, Y.-C., Hung, W.-T., Chang, Y.-C., Chang, H. C., Wu, C.-L., Chiang, A.-S., Jackson, G. R., & Sang, T.-K. (2011). Pathogenic VCP/TER94 Alleles Are Dominant Actives and Contribute to Neurodegeneration by Altering Cellular ATP Level in a Drosophila IBMPFD Model. *PLoS Genetics*, 7(2), e1001288. <https://doi.org/10.1371/journal.pgen.1001288>
9. Cox, R. T., Kirkpatrick, C., & Peifer, M. (1996). Armadillo is required for adherens junction assembly, cell polarity, and morphogenesis during Drosophila embryogenesis. *The Journal of Cell Biology*, 134(1), 133–148. <https://doi.org/10.1083/jcb.134.1.133>
10. Dai, R. M., Chen, E., Longo, D. L., & Gorbea, C. M. (1998). Involvement of valosin-containing protein, an ATPase Co-purified with I $\kappa$ B $\alpha$  and 26 S proteasome, in ubiquitin-proteasome-mediated degradation of I $\kappa$ B $\alpha$ . *Journal of Biological*. [https://www.jbc.org/article/S0021-9258\(18\)93765-8/abstract](https://www.jbc.org/article/S0021-9258(18)93765-8/abstract)
11. Donovan, P. J., & de Miguel, M. P. (2003). Turning germ cells into stem cells. *Current Opinion in Genetics & Development*, 13(5), 463–471. <https://doi.org/10.1016/j.gde.2003.08.010>
12. Ephrussi, A., & Lehmann, R. (1992). Induction of germ cell formation by oskar. *Nature*, 358(6385), 387–392. <https://doi.org/10.1038/358387a0>
13. Ephrussi, Anne, & St Johnston, D. (2004). Seeing is believing: the bicoid morphogen gradient matures. *Cell*, 116(2), 143–152. [https://doi.org/10.1016/s0092-8674\(04\)00037-6](https://doi.org/10.1016/s0092-8674(04)00037-6)
14. Frohnhofer, H. G., & Nüsslein-Volhard, C. (1986). Organization of anterior pattern in the Drosophila embryo by the maternal gene bicoid. *Nature*, 324(6093), 120–125. <https://doi.org/10.1038/324120a0>

15. Griciuc, A., Aron, L., Roux, M. J., Klein, R., Giangrande, A., & Ueffing, M. (2010). Inactivation of VCP/ter94 suppresses retinal pathology caused by misfolded rhodopsin in *Drosophila*. *PLoS Genetics*, 6(8).  
<https://doi.org/10.1371/journal.pgen.1001075>
16. Hamm, D. C., & Harrison, M. M. (2018). Regulatory principles governing the maternal-to-zygotic transition: insights from *Drosophila melanogaster*. *Open Biology*, 8(12), 180183. <https://doi.org/10.1098/rsob.180183>
17. Higashiyama, H., Hirose, F., Yamaguchi, M., Inoue, Y. H., Fujikake, N., Matsukage, A., & Kakizuka, A. (2002). Identification of ter94, *Drosophila* VCP, as a modulator of polyglutamine-induced neurodegeneration. *Cell Death and Differentiation*, 9(3), 264–273. <https://doi.org/10.1038/sj.cdd.4400955>
18. Horner, V. L., & Wolfner, M. F. (2008). Transitioning from egg to embryo: triggers and mechanisms of egg activation. *Developmental Dynamics: An Official Publication of the American Association of Anatomists*, 237(3), 527–544.  
<https://doi.org/10.1002/dvdy.21454>
19. Illmensee, K., & Mahowald, A. P. (1974). Transplantation of posterior polar plasm in *Drosophila*. Induction of germ cells at the anterior pole of the egg. *Proceedings of the National Academy of Sciences of the United States of America*, 71(4), 1016–1020. <https://doi.org/10.1073/pnas.71.4.1016>
20. Jentsch, & Rumpf. (2007). Cdc48 (p97): a 'molecular gearbox' in the ubiquitin pathway? *Trends in Biochemical Sciences*.  
<https://www.sciencedirect.com/science/article/pii/S0968000406003227>
21. Jones, J. R., & Macdonald, P. M. (2007). Oskar controls morphology of polar granules and nuclear bodies in *Drosophila*. *Development*, 134(2), 233–236.  
<https://doi.org/10.1242/dev.02729>
22. Jürgens, G., Wieschaus, E., Nüsslein-Volhard, C., & Kluding, H. (1984). Mutations affecting the pattern of the larval cuticle in *Drosophila melanogaster*. *Wilhelm Roux's Archives of Developmental Biology*, 193(5), 283–295.  
<https://doi.org/10.1007/BF00848157>
23. Kim, M., Lee, J. H., Lee, S. Y., Kim, E., & Chung, J. (2006). Caspar, a suppressor of antibacterial immunity in *Drosophila*. *Proceedings of the National Academy of Sciences of the United States of America*, 103(44), 16358–16363.  
<https://doi.org/10.1073/pnas.0603238103>

24. Kim-Ha, J., Smith, J. L., & Macdonald, P. M. (1991). oskar mRNA is localized to the posterior pole of the *Drosophila* oocyte. *Cell*, *66*(1), 23–35.  
[https://doi.org/10.1016/0092-8674\(91\)90136-m](https://doi.org/10.1016/0092-8674(91)90136-m)
25. Klingensmith, J., & Nusse, R. (1994). Signaling by wingless in *Drosophila*. *Developmental Biology*, *166*(2), 396–414. <https://doi.org/10.1006/dbio.1994.1325>
26. Kushimura, Y., Tokuda, T., Azuma, Y., Yamamoto, I., Mizuta, I., Mizuno, T., Nakagawa, M., Ueyama, M., Nagai, Y., Yoshida, H., & Yamaguchi, M. (2018). Overexpression of *ter94*, *Drosophila* VCP, improves motor neuron degeneration induced by knockdown of TBPH, *Drosophila* TDP-43. *American Journal of Neurodegenerative Disease*, *7*(1), 11–31.  
<https://www.ncbi.nlm.nih.gov/pubmed/29531866>
27. Laver, J. D., Marsolais, A. J., Smibert, C. A., & Lipshitz, H. D. (2015). Regulation and Function of Maternal Gene Products During the Maternal-to-Zygotic Transition in *Drosophila*. *Current Topics in Developmental Biology*, *113*, 43–84.  
<https://doi.org/10.1016/bs.ctdb.2015.06.007>
28. Lehmann, R. (2016). Germ Plasm Biogenesis--An Oskar-Centric Perspective. *Current Topics in Developmental Biology*, *116*, 679–707.  
<https://doi.org/10.1016/bs.ctdb.2015.11.024>
29. Leon, A., & McKearin, D. (1999). Identification of TER94, an AAA ATPase Protein, as a Bam-dependent Component of the *Drosophila* Fusome. *Molecular Biology of the Cell*. <https://www.molbiolcell.org/doi/abs/10.1091/mbc.10.11.3825>
30. Li, X.-Y., Harrison, M. M., Villalta, J. E., Kaplan, T., & Eisen, M. B. (2014). Establishment of regions of genomic activity during the *Drosophila* maternal to zygotic transition. *ELife*, *3*. <https://doi.org/10.7554/eLife.03737>
31. Lynch, J. A., & Roth, S. (2011). The evolution of dorsal–ventral patterning mechanisms in insects. *Genes & Development*, *25*(2), 107–118.  
<https://doi.org/10.1101/gad.2010711>
32. Mahowald, A. P. (1968). Polar granules of *Drosophila*. II. Ultrastructural changes during early embryogenesis. *The Journal of Experimental Zoology*, *167*(2), 237–261. <https://doi.org/10.1002/jez.1401670211>
33. Mahowald, Anthony P. (1962). Fine structure of pole cells and polar granules in *Drosophila melanogaster*. *The Journal of Experimental Zoology*, *151*(3), 201–215. <https://doi.org/10.1002/jez.1401510302>

34. Meyer, H., Bug, M., & Bremer, S. (2012). Emerging functions of the VCP/p97 AAA-ATPase in the ubiquitin system. *Nature Cell Biology*.  
<https://www.nature.com/articles/ncb2407>
35. Meyer, H. H., Shorter, J. G., Seemann, J., & Pappin, D. (2000). A complex of mammalian ufd1 and npl4 links the AAA-ATPase, p97, to ubiquitin and nuclear transport pathways. *The EMBO Journal*.  
<https://www.embopress.org/doi/full/10.1093/emboj/19.10.2181>
36. Meyer, Hemmo H. (2005). Golgi reassembly after mitosis: the AAA family meets the ubiquitin family. *Biochimica et Biophysica Acta*, 1744(3), 481–492.  
<https://www.ncbi.nlm.nih.gov/pubmed/16038055>
37. Nakamura, A., Amikura, R., Hanyu, K., & Kobayashi, S. (2001). Me31B silences translation of oocyte-localizing RNAs through the formation of cytoplasmic RNP complex during *Drosophila* oogenesis. *Development*, 128(17), 3233–3242.  
<https://doi.org/10.1242/dev.128.17.3233>
38. Nüsslein-Volhard, C. (1991). Determination of the embryonic axes of *Drosophila*. *Development. Supplement*, 1, 1–10.  
<https://www.ncbi.nlm.nih.gov/pubmed/1742496>
39. Nüsslein-Volhard, C., Kluding, H., & Jürgens, G. (1985). Genes affecting the segmental subdivision of the *Drosophila* embryo. *Cold Spring Harbor Symposia on Quantitative Biology*, 50, 145–154.  
<https://doi.org/10.1101/sqb.1985.050.01.020>
40. Nüsslein-Volhard, C., & Wieschaus, E. (1980). Mutations affecting segment number and polarity in *Drosophila*. *Nature*, 287(5785), 795–801.  
<https://doi.org/10.1038/287795a0>
41. Nüsslein-Volhard, C., Wieschaus, E., & Kluding, H. (1984). Mutations affecting the pattern of the larval cuticle in *Drosophila melanogaster*. *Wilhelm Roux's Archives of Developmental Biology*, 193(5), 267–282.  
<https://doi.org/10.1007/BF00848156>
42. Oughtred, R., Rust, J., Chang, C., Breitkreutz, B.-J., Stark, C., Willems, A., Boucher, L., Leung, G., Kolas, N., Zhang, F., Dolma, S., Coulombe-Huntington, J., Chatr-Aryamontri, A., Dolinski, K., & Tyers, M. (2021). The BioGRID database: A comprehensive biomedical resource of curated protein, genetic, and chemical interactions. *Protein Science: A Publication of the Protein Society*, 30(1), 187–200. <https://doi.org/10.1002/pro.3978>

43. Peifer, M. (1993). The product of the *Drosophila* segment polarity gene *armadillo* is part of a multi-protein complex resembling the vertebrate adherens junction. *Journal of Cell Science*, *105* ( Pt 4), 993–1000.  
<https://doi.org/10.1242/jcs.105.4.993>
44. Peifer, M. (1995). Cell adhesion and signal transduction: the Armadillo connection. *Trends in Cell Biology*, *5*(6), 224–229. [https://doi.org/10.1016/s0962-8924\(00\)89015-7](https://doi.org/10.1016/s0962-8924(00)89015-7)
45. Peifer, M., Rauskolb, C., Williams, M., Riggleman, B., & Wieschaus, E. (1991). The segment polarity gene *armadillo* interacts with the wingless signaling pathway in both embryonic and adult pattern formation. *Development*, *111*(4), 1029–1043. <https://doi.org/10.1242/dev.111.4.1029>
46. Peng, H., Liu, H., Liu, F., Gao, Y., Chen, J., Huo, J., Han, J., Xiao, T., & Zhang, W. (2017). NLRP2 and FAF1 deficiency blocks early embryogenesis in the mouse. *Reproduction*, *154*(3), 245–251. <https://doi.org/10.1530/REP-16-0629>
47. Peters, J. M., Walsh, M. J., & Franke, W. W. (1990). An abundant and ubiquitous homo-oligomeric ring-shaped ATPase particle related to the putative vesicle fusion proteins Sec18p and NSF. *The EMBO Journal*, *9*(6), 1757–1767.  
<https://doi.org/10.1002/j.1460-2075.1990.tb08300.x>
48. Raudvere, U., Kolberg, L., Kuzmin, I., Arak, T., Adler, P., Peterson, H., & Vilo, J. (2019). g:Profiler: a web server for functional enrichment analysis and conversions of gene lists (2019 update). *Nucleic Acids Research*, *47*(W1), W191–W198. <https://doi.org/10.1093/nar/gkz369>
49. Riechmann, V., & Ephrussi, A. (2001). Axis formation during *Drosophila* oogenesis. *Current Opinion in Genetics & Development*, *11*(4), 374–383.  
[https://doi.org/10.1016/s0959-437x\(00\)00207-0](https://doi.org/10.1016/s0959-437x(00)00207-0)
50. Roth, S., Stein, D., & Nüsslein-Volhard, C. (1989). A gradient of nuclear localization of the dorsal protein determines dorsoventral pattern in the *Drosophila* embryo. *Cell*, *59*(6), 1189–1202. [https://doi.org/10.1016/0092-8674\(89\)90774-5](https://doi.org/10.1016/0092-8674(89)90774-5)
51. Ruden, D. M., Sollars, V., Wang, X., Mori, D., Alterman, M., & Lu, X. (2000). Membrane fusion proteins are required for oskar mRNA localization in the *Drosophila* egg chamber. *Developmental Biology*, *218*(2), 314–325.  
<https://doi.org/10.1006/dbio.1999.9583>


52. Schier, A. F. (2007). The maternal-zygotic transition: death and birth of RNAs. *Science*, 316(5823), 406–407. <https://doi.org/10.1126/science.1140693>
53. Simpson-Brose, M., Treisman, J., & Desplan, C. (1994). Synergy between the hunchback and bicoid morphogens is required for anterior patterning in *Drosophila*. *Cell*, 78(5), 855–865. [https://doi.org/10.1016/s0092-8674\(94\)90622-x](https://doi.org/10.1016/s0092-8674(94)90622-x)
54. Snee, M. J., & Macdonald, P. M. (2004). Live imaging of nuage and polar granules: evidence against a precursor-product relationship and a novel role for Oskar in stabilization of polar granule components. *Journal of Cell Science*, 117(Pt 10), 2109–2120. <https://doi.org/10.1242/jcs.01059>
55. Song, E. J., Yim, S.-H., Kim, E., Kim, N.-S., & Lee, K.-J. (2005). Human Fas-associated factor 1, interacting with ubiquitinated proteins and valosin-containing protein, is involved in the ubiquitin-proteasome pathway. *Molecular and Cellular Biology*, 25(6), 2511–2524. <https://doi.org/10.1128/MCB.25.6.2511-2524.2005>
56. St Johnston, D., & Nüsslein-Volhard, C. (1992). The origin of pattern and polarity in the *Drosophila* embryo. *Cell*, 68(2), 201–219. [https://doi.org/10.1016/0092-8674\(92\)90466-p](https://doi.org/10.1016/0092-8674(92)90466-p)
57. Stein, D. S., & Stevens, L. M. (2014). Maternal control of the *Drosophila* dorsal-ventral body axis. *Wiley Interdisciplinary Reviews. Developmental Biology*, 3(5), 301–330. <https://doi.org/10.1002/wdev.138>
58. Steward, R. (1987). Dorsal, an embryonic polarity gene in *Drosophila*, is homologous to the vertebrate proto-oncogene, c-rel. *Science*, 238(4827), 692–694. <https://doi.org/10.1126/science.3118464>
59. Steward, R., Zusman, S. B., Huang, L. H., & Schedl, P. (1988). The dorsal protein is distributed in a gradient in early *Drosophila* embryos. *Cell*, 55(3), 487–495. [https://doi.org/10.1016/0092-8674\(88\)90035-9](https://doi.org/10.1016/0092-8674(88)90035-9)
60. Sysoev, V. O., Fischer, B., Frese, C. K., Gupta, I., Krijgsveld, J., Hentze, M. W., Castello, A., & Ephrussi, A. (2016). Global changes of the RNA-bound proteome during the maternal-to-zygotic transition in *Drosophila*. *Nature Communications*, 7, 12128. <https://doi.org/10.1038/ncomms12128>
61. Technau, G. M., & Campos-Ortega, J. A. (1986). Lineage analysis of transplanted individual cells in embryos of *Drosophila melanogaster*. *Roux's Archives of Developmental Biology: The Official Organ of the EDBO*, 195(7), 445–454. <https://doi.org/10.1007/BF00375748>




62. Tendulkar, Hegde, & Garg. (2022). Caspar, an adapter for VAPB and TER94, modulates the progression of ALS8 by regulating IMD/NFκB-mediated glial inflammation in a Drosophila model of human .... *Human Molecular Genetics*. <https://doi.org/10.1093/hmg/ddac076/6563110>
63. Thomson, T., Liu, N., Arkov, A., Lehmann, R., & Lasko, P. (2008). Isolation of new polar granule components in Drosophila reveals P body and ER associated proteins. *Mechanisms of Development*, 125(9–10), 865–873. <https://doi.org/10.1016/j.mod.2008.06.005>
64. van Eeden, F., & St Johnston, D. (1999). The polarisation of the anterior-posterior and dorsal-ventral axes during Drosophila oogenesis. *Current Opinion in Genetics & Development*, 9(4), 396–404. [https://doi.org/10.1016/S0959-437X\(99\)80060-4](https://doi.org/10.1016/S0959-437X(99)80060-4)
65. Vanzo, N., Oprins, A., Xanthakis, D., & Ephrussi, A. (2007). Stimulation of endocytosis and actin dynamics by Oskar polarizes the Drosophila oocyte. *Developmental Cell*. <https://www.sciencedirect.com/science/article/pii/S1534580707001025>
66. Vastenhouw, N. L., Cao, W. X., & Lipshitz, H. D. (2019). The maternal-to-zygotic transition revisited. *Development*, 146(11). <https://doi.org/10.1242/dev.161471>
67. Walser, C. B., & Lipshitz, H. D. (2011). Transcript clearance during the maternal-to-zygotic transition. *Current Opinion in Genetics & Development*, 21(4), 431–443. <https://doi.org/10.1016/j.gde.2011.03.003>
68. Wang, M., Ly, M., Lugowski, A., Laver, J. D., Lipshitz, H. D., Smibert, C. A., & Rissland, O. S. (2017). ME31B globally represses maternal mRNAs by two distinct mechanisms during the Drosophila maternal-to-zygotic transition. *ELife*, 6. <https://doi.org/10.7554/eLife.27891>
69. Wieschaus, E., Nüsslein-Volhard, C., & Jürgens, G. (1984). Mutations affecting the pattern of the larval cuticle in Drosophila melanogaster. *Wilhelm Roux's Archives of Developmental Biology*, 193(5), 296–307. <https://doi.org/10.1007/BF00848158>
70. Wieschaus, Eric, & Nüsslein-Volhard, C. (2016). The Heidelberg Screen for Pattern Mutants of Drosophila: A Personal Account. *Annual Review of Cell and Developmental Biology*, 32, 1–46. <https://doi.org/10.1146/annurev-cellbio-113015-023138>

71. Ye, Y. (2006). Diverse functions with a common regulator: ubiquitin takes command of an AAA ATPase. *Journal of Structural Biology*, 156(1), 29–40. <https://doi.org/10.1016/j.jsb.2006.01.005>
72. Zavortink, M., Rutt, L. N., Dzitoyeva, S., Henriksen, J. C., Barrington, C., Bilodeau, D. Y., Wang, M., Chen, X. X. L., & Rissland, O. S. (2020). The E2 Marie Kondo and the CTLH E3 ligase clear deposited RNA binding proteins during the maternal-to-zygotic transition. *ELife*, 9. <https://doi.org/10.7554/eLife.53889>
73. Zeng, Z., de Gorter, D. J. J., Kowalski, M., ten Dijke, P., & Shimmi, O. (2014). Ter94/VCP is a novel component involved in BMP signaling. *PloS One*, 9(12), e114475. <https://doi.org/10.1371/journal.pone.0114475>
74. Zhang, L., Zhou, F., Li, Y., Drabsch, Y., Zhang, J., van Dam, H., & ten Dijke, P. (2012). Fas-associated factor 1 is a scaffold protein that promotes  $\beta$ -transducin repeat-containing protein ( $\beta$ -TrCP)-mediated  $\beta$ -catenin ubiquitination and degradation. *The Journal of Biological Chemistry*, 287(36), 30701–30710. <https://doi.org/10.1074/jbc.M112.353524>
75. Zhang, L., Zhou, F., van Laar, T., Zhang, J., van Dam, H., & Ten Dijke, P. (2011). Fas-associated factor 1 antagonizes Wnt signaling by promoting  $\beta$ -catenin degradation. *Molecular Biology of the Cell*, 22(9), 1617–1624. <https://doi.org/10.1091/mbc.E10-12-0985>

# Copyright Permissions

Home | Help | Email Support | Sign in | Create Account





**SUMO conjugation regulates immune signalling**  
Author: Sushmitha Hegde, , Amarendranath Soory, et al  
Publication: Fly  
Publisher: Taylor & Francis  
Date: Oct 1, 2020  
*Rights managed by Taylor & Francis*

**Thesis/Dissertation Reuse Request**  
Taylor & Francis is pleased to offer reuses of its content for a thesis or dissertation free of charge contingent on resubmission of permission request if work is published.

[BACK](#) [CLOSE](#)

© 2022 Copyright - All Rights Reserved | Copyright Clearance Center, Inc. | Privacy statement | Data Security and Privacy | For California Residents | Terms and Conditions  
Comments? We would like to hear from you. E-mail us at [customer@copyright.com](mailto:customer@copyright.com)

Help | Email Support



**SUMOylation of Dorsal attenuates Toll/NF- $\kappa$ B signaling**  
Author: Hegde, Sushmitha; Sreejan, Ashley  
Publication: Genetics  
Publisher: Oxford University Press  
Date: 2022-05-14  
*Copyright © 2022, Oxford University Press*

**Creative Commons**  
This is an open access article distributed under the terms of the [Creative Commons CC BY](#) license, which permits unrestricted use, distribution, and reproduction in any medium, provided the original work is properly cited.  
You are not required to obtain permission to reuse this article.

© 2022 Copyright - All Rights Reserved | Copyright Clearance Center, Inc. | Privacy statement | Data Security and Privacy | For California Residents | Terms and Conditions  
Comments? We would like to hear from you. E-mail us at [customer@copyright.com](mailto:customer@copyright.com)

## Appendix I: validation of SUMO targets in the 0-3 h embryo

### I.1 Introduction

At the molecular level, since SUMO exerts its effects by altering protein function upon conjugation, efforts have been made to identify these SUMO-modified targets. Mass-spectrometry-based studies have identified SUMO-modified proteins from *Drosophila* in immunity (Handu *et al.* 2015b) and development (Nie *et al.* 2009) in S2 cells and the embryo, respectively, but the modified lysines remain unknown. Seeing that the outcomes of SUMO conjugation are substrate-dependent, general or *a priori* assumptions cannot be made regarding SUMO conjugation as yet, and it needs to be studied at the individual protein level.

A proteomics screen identified nearly 150 integral SUMOylated proteins, part of the cell cycle and developmental patterning, in the 0-3 h embryo (Nie *et al.* 2009). From this list, a subset of proteins involved in embryonic patterning was chosen to study the effect of SUMOylation.

We set out to demonstrate the SUMOylation of Ubc9, the SUMO-conjugating E2 enzyme, and the adaptor 14-3-3 proteins to understand their roles in cell cycle and embryonic patterning. Ubc9 SUMOylation has been demonstrated in mammalian cells and yeast. Auto-SUMOylation of Ubc9 in mammalian cells regulates target discrimination (Knipscheer *et al.*, 2008), while it is involved in SUMO chain formation in budding yeast (Klug *et al.*, 2013). Studying SUMOylation of the conserved *Drosophila* ortholog dUbc9, encoded by the gene *lesswright* (*lwr*), will shed light on its physiological role in the animal.

The 14-3-3 family of proteins is well conserved across phyla. They are characterized by their ability to bind various proteins in signaling cascades, such as the Ras (Li *et al.*, 1997) and the Hippo pathway (Dong *et al.*, 2007). The *Drosophila* genome encodes two 14-3-3 proteins: 14-3-3ζ (*leonardo*) and 14-3-3ε. The 14-3-3 proteins are maternally deposited and have distinct and overlapping functions in the embryo. They are essential for mitotic progression (Su *et al.*, 2001; Tien *et al.*, 1999), and 14-3-3ζ, in particular, is required for terminal patterning as part of the torso signaling network in early embryos (Li *et al.*, 1997). Interestingly, several proteomics studies identify SUMOylation of the 14-3-3 proteins (Handu *et al.* 2015b; Hendriks and

Vertegaal 2016b; Pirone *et al.* 2017). Hence, SUMOylation could enhance the potential interactions of this adaptor molecule, aiding in its function.

## I.2 Results

### I.2.1 RNAi-based knockdown of SUMO cycle components

Loss of function alleles of dUbc9 and hypomorphs of SUMO result in a loss of anterior structures (Epps & Tanda, 1998) and DV patterning defects (Nie *et al.* 2009), respectively. Despite these studies, the contribution from the maternal and zygotic SUMO is not very clear. In recent years, the Transgenic RNAi Project (TRiP) has generated VALIUM (Vermilion-AttB-Loxp-Intron-UAS-MCS) fly lines that can be used specifically for maternal or zygotic knockdowns or both. Knockdown of SUMO or components of the conjugation pathway using the VALIUM20 and VALIUM22 RNAi lines and MTD-Gal4 (BDSC 31777) or  $\alpha$ -tubulin-Gal4: VP16 (mat-gal4; BDSC 7062/BDSC 7063) would reduce these transcripts in the female germline (Fig. I.1). Loss of maternal SUMO transcripts would allow us to gain additional insight into the maternal contributions of SUMO and pathways most sensitive to the loss of SUMO in the embryo.

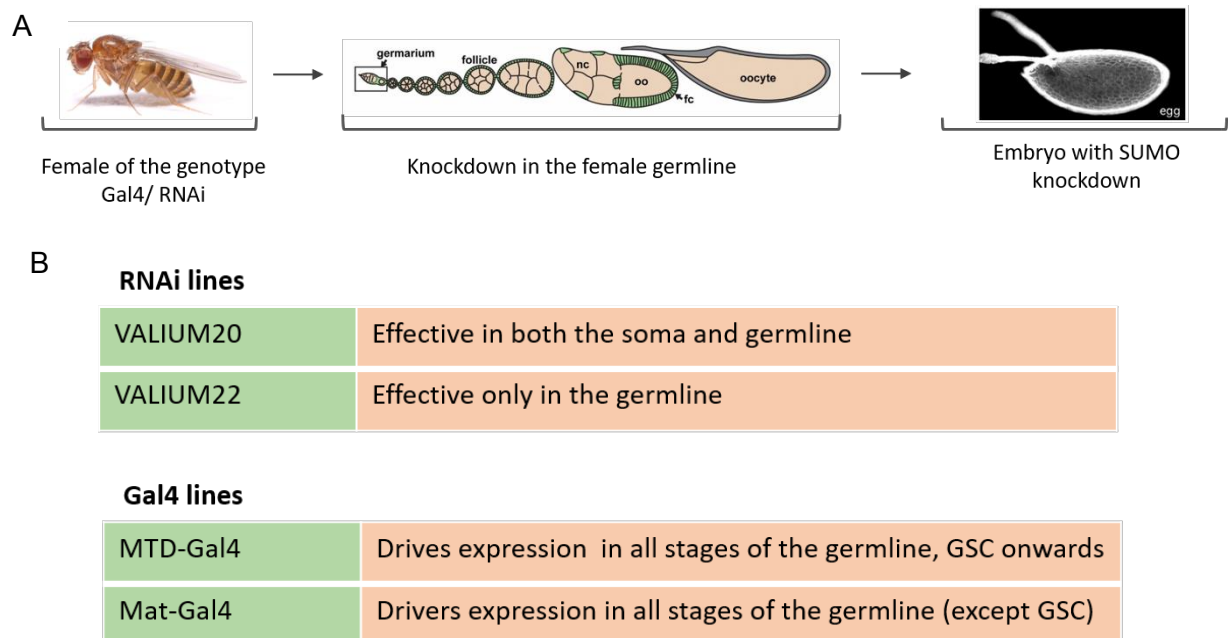


**Fig. I.1. Maternal knockdown of SUMO components.** A schematic of the maternal knockdown is described in (A). Adapted from (Staller *et al.*, 2013). (B) depicts the RNAi and GAL4 lines used.

The following lines were available through the Bloomington *Drosophila* Stock Center (BDSC) to assess knockdown phenotypes and were procured for testing.

**Table 1: Lines tested for Maternal knockdown of SUMO cycle elements.**

	<b>Stock</b>	<b>Source, Stock number, Genotype</b>	<b>Notes</b>
<b>A</b>	<b>Gal4 lines</b>		
1	<i>MTD-Gal4</i>	BDSC 31777 [P[w[+mC]=otu-GAL4::VP16.R]1, w[*]; P[w[+mC]=GAL4-nos.NGT]40; P[w[+mC]=GAL4::VP16-nos.UTR]CG6325[MVD1] (I,II,III)]	Maternal Triple Driver
2	<i>α-tubulin-Gal4:VP16</i>  ( <i>Mat-Gal4</i> )	BDSC 7062 [P[matα4-GAL-VP16]V2H (II)];  BDSC 7063 [P[matα4-GAL-VP16]V37 (III)]	Does not express in the female stem cells. Expresses in the cystoblasts and late stages.
4	<i>Nos-Gal4:VP16</i>	BDSC 4937 [w[1118]; P[w[+mC]=GAL4::VP16-nos.UTR]CG6325[MVD1] (III)]	Nanos promoter
5	<i>C587-Gal4</i>	BDSC 67747 [P[w[+mW.hs]=GawB]C587, w[*] (I)]	Expresses in most somatic cells of the ovary
<b>B</b>	<b>Maternal RNAi lines</b>		
5	<i>SUMO/ Smt3</i>	BDSC 36125 (VALIUM20); BDSC 28034 (V10)	VALIUM10 uses a double-stranded hairpin strategy. The lines are usually co-expressed with UAS-Dicer2.
6	<i>SAE1/Aos1 (E1 enzyme)</i>	BDSC 36074 (VALIUM22); BDSC 28972 (V10)	VALIUM20 uses a shRNA for knockdown.
7	<i>SAE2/Uba2 (E1 enzyme)</i>	BDSC 63986 (VALIUM20); BDSC 28569 (V10)  BDSC 35806 (VALIUM22)	

8	<i>Ubc9/Lwr (E2 conjugase)</i>	BDSC 37506 (VALIUM20); BDSC 37481 (V22); BDSC 31396 (V1)	VALIUM1 constructs are 1 <sup>st</sup> generation and use a double-stranded hairpin strategy. The lines are co-expressed with UAS-Dicer2.
9	<i>PIAS (E3 ligase)</i>	BDSC 32915; BDSC 32956 (VALIUM20)	

**Note:** The Perrimon lab shRNA-based RNAi lines, the VALIUM series, has been designed for effective zygotic and maternal knockdowns. The VALIUM22 series are meant exclusively for maternal knockdowns, while the VALIUM20 lines function effectively in zygotic knockdowns and work, though with lower efficiency, for maternal knockdowns.

*sumo* and components of the SUMOylation machinery available were knocked down in the early embryo using a maternal driver (*MTD-Gal4* or *Mat-Gal4*) to assess the role of SUMOylation in early development. The components knocked down are indicated below.

**Table 2: Lines tested for knockdown of SUMO/ SUMO cycle components in the embryo.**

Gene	RNAi Stock	Gal4	Lethality at 25 °C	Lethality at 29 °C
<i>smt3</i>	BDSC 36125 (VALIUM20)	<i>MTD-Gal4</i> and <i>Mat-Gal4</i>	None	None
<i>dUbc9</i>	BDSC 37506 (VALIUM20); BDSC 37481 (VALIUM22);	<i>MTD-Gal4</i> and <i>Mat-Gal4</i>	None	None
<i>Uba2</i>	BDSC 35806 (VALIUM22)	<i>Mat-Gal4</i>	100%	100%
<i>Aos1</i>	BDSC 36074 (VALIUM22)	<i>Mat-Gal4</i>	100%	100%

Maternal knockdown of *smt3* and *ubc9* did not yield lethality or embryonic defects, as assessed by the cuticle preparation of aged (24 h) embryos. The lack of an apparent

phenotype is most likely due to inefficient knockdown, since mutant alleles of *dUbc9* and *smt3* have previously exhibited lethality and embryonic defects (Epps and Tanda 1998; Nie *et al.* 2009). In contrast, the maternal knockdown of *aos1* and *uba2* led to lethality, highlighting a role for SUMO components in early development (Fig. I.2). Since cell cycle processes were affected in the early stages, patterning defects could not be uncovered, but the importance of SUMO in development was re-established.

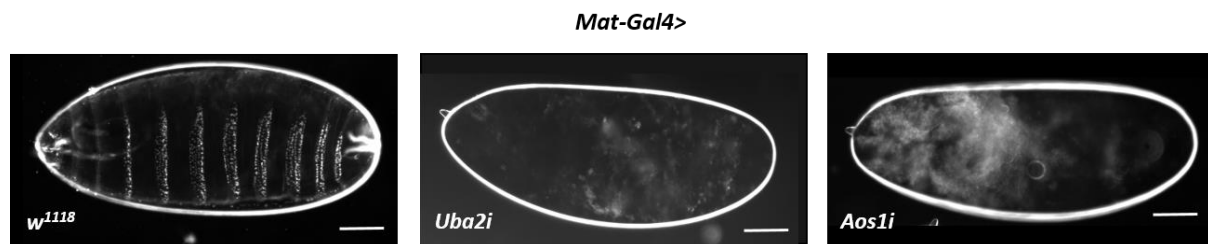


**Fig. I.2. Early embryonic lethality was observed upon the knockdown of SUMO cycle components.** Cuticle preparation of embryos with an intact vitelline membrane is presented for the genotypes indicated. The *w<sup>1118</sup>* embryos display a regular arrangement of denticle bands. They are markedly absent in *Uba2i* and *Aos1i* embryos. Embryos are oriented with the anterior to the left. n = 100.

### I.2.2 Proteins in *Drosophila* axis patterning events as potential SUMO targets

The presence of patterning defects in 0-3 h *Drosophila* embryos indicates the SUMOylation of critical molecules involved in either the patterning system (AP, DV, or terminal) or cell division. Based on the earlier proteomics experiment (Nie *et al.*, 2009) and a literature survey of published SUMO targets in *Drosophila* and mammalian systems, we generated a list of candidates that may be involved in early embryonic patterning (Table 3). These are listed below in order of their priority. Higher priority was assigned to proteins that have known functions in embryonic development.

**Table 3: Potential SUMO Targets in early *Drosophila* development.**

A	AP, DV and Terminal GRNs	Function, Network and Signaling Module	SUMO Site ( <u>Known</u> , Predicted)
	Dorsal (DL)	Transcription Factor, Dorsal GRN, Toll Signaling	<u>K382</u>



	Hunchback (hb)	Transcription Factor, Anterior GRN	K28 (Ac Switch), K264, K551, K568, K591,
	Caudal (Cad)	Transcription Factor, Posterior GRN	K359 (Ac Switch)
	Pumilio (Pum)	Transcription Factor, Germline Development	K489, K513, K1423
	Groucho (Gro)	Transcription Co-repressor, Terminal GRN, MAPK signaling	K32, K46, K279 (SC-SUMO), K516
<b>B</b>	<b>Signaling and Adaptor Proteins</b>	<b>Function, Network and Signaling Module</b>	<b>SUMO Site (<u>Known</u>, Predicted)</b>
	14-3-3 $\epsilon$	Adaptor, Hippo signaling	K78, K118, K125
	14-3-3 $\zeta$	Adaptor, Hippo signaling, Terminal GRN (Torso signaling).	K118, K125
<b>C</b>	<b>Protein Complexes</b>	<b>Function, Network and Signaling Module</b>	<b>SUMO Site (<u>Known</u>, Predicted)</b>
	Tsu, mago	mRNA related Complexes	Mago K42 (weak) Tsu K159 (weak)
	PCNA, RCF2	DNA related Complexes	PCNA K254 (High) RCF2 K187, K293 (low)

SUMOylation preferentially targets disordered regions of proteins for modification. Around 50% adhere to the consensus motif,  $\psi$ KXE/D, where  $\psi$  is a large hydrophobic residue, K is the modified lysine, and X is any amino acid, followed by a glutamate or aspartate residue. The SUMO prediction software JASSA (Beauchair *et al.* 2015) predicts probable lysine targets for SUMOylation based on the consensus motif and published literature. An *in-bacto* SUMOylation assay (described in (Nie *et al.* 2009) was utilized to demonstrate SUMOylation and identify modified lysines of the chosen proteins. Presented in the following sections is the data for SUMO conjugation of 14-3-3 and Ubc9.

### I.2.3 14-3-3ε is SUMOylated *in bacto*

14-3-3ε was one of the initial targets tested for SUMOylation *in bacto*. The SUMO targets predicted by JASSA as well as a published list of SUMO-modified 14-3-3ε lysines in HeLa cells were used to conduct a mutagenesis study to determine the SUMOylated lysine (Fig. I.3).

The bacterial SUMOylation assay was carried out as follows: HA-tagged proteins expressed in a pET45b (+) vector were used in combination with a vector expressing His-SUMO, and the enzymes of the *Drosophila* SUMO machinery. Q<sup>ΔGG</sup> expresses non-conjugatable His-SUMO-ΔGG, which acts as a control, while the Q<sup>SUMO</sup> vector

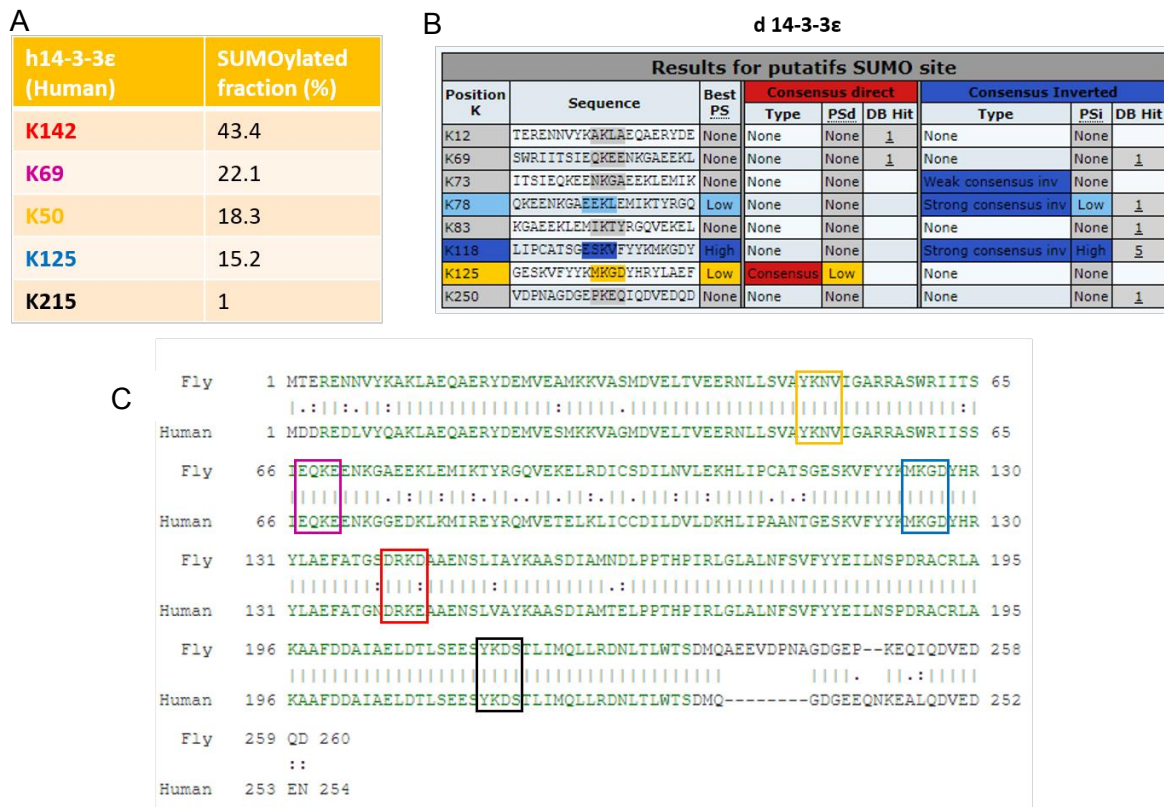


**Fig. I.3. SUMOylation predictions for 14-3-3ε.** The 14-3-3ε SUMOylation sites experimentally validated via mass-spectrometry in HeLa cells, and the relative abundances of the SUMOylated species are tabulated in (A). SUMO site predictions for *Drosophila* 14-3-3ε and the associated confidence scores from JASSA are indicated in (B). Sequence alignment of fly and human 14-3-3ε shows 90% sequence similarity (C). DIOPT (*Drosophila* RNAi Screening Center Integrative Ortholog Prediction Tool) sequence alignment (Hu *et al.*, 2011) was used. The conserved SUMO consensus sequences are highlighted.

expresses mature His-SUMO. Anti-His affinity purification with Ni-NTA enriches the SUMOylated protein fraction, which is detected on a western blot (Fig. I.4).

Mutations of lysines 50, 69, 125, 142, and 142/69 in combination did not show a loss of SUMOylation of 14-3-3 $\epsilon$  (Fig. I.4). Hence, more lysine residues need to be targeted to determine the site of SUMOylation.

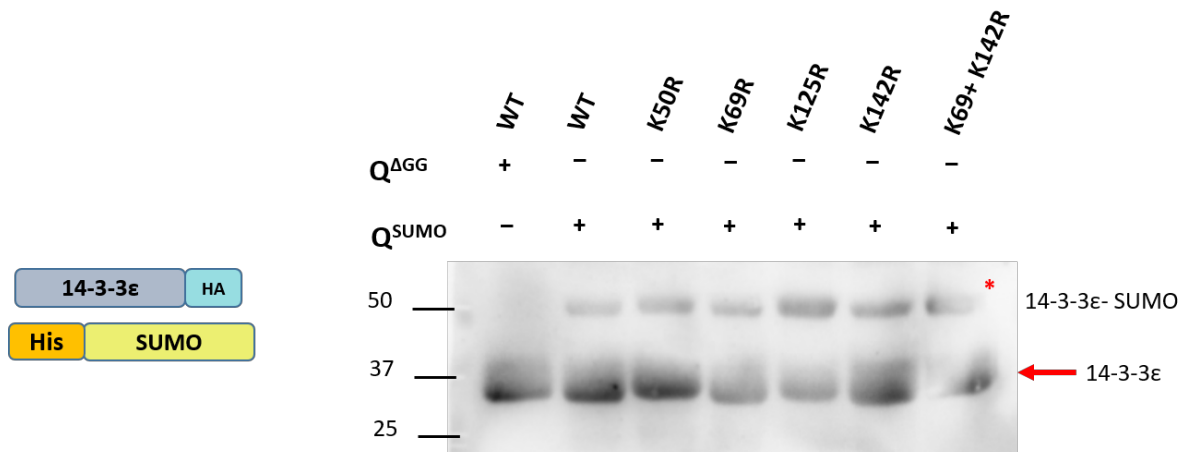


**Fig. I.4. 14-3-3 $\epsilon$  is SUMOylated in a bacterial SUMOylation assay.** The tags on 14-3-3 $\epsilon$  and SUMO are indicated in the schematic on the left. Arrow indicates the unmodified protein, while asterisks denote the SUMO-conjugated form, which migrates ~20 kDa higher after a Ni-NTA affinity purification. Mutations of lysines 50, 69, 125, 142, and a 69/142 double mutant do not abolish SUMOylation.

#### I.2.4 dUbc9 is SUMOylated *in bacto*

A strategy similar to 14-3-3 $\epsilon$  was used to identify and mutate lysines for dUbc9. dUbc9 has a conserved active cysteine at position 93, which is conjugated to SUMO (henceforth denoted as Ubc9\*SUMO) during transfer to the target. Also, conserved lysines at positions 14 and 49, identified to be SUMOylated (henceforth denoted as Ubc9-SUMO) in mammals and K65, predicted by JASSA, were mutated to arginines *in-bacto* (Fig. I.5).



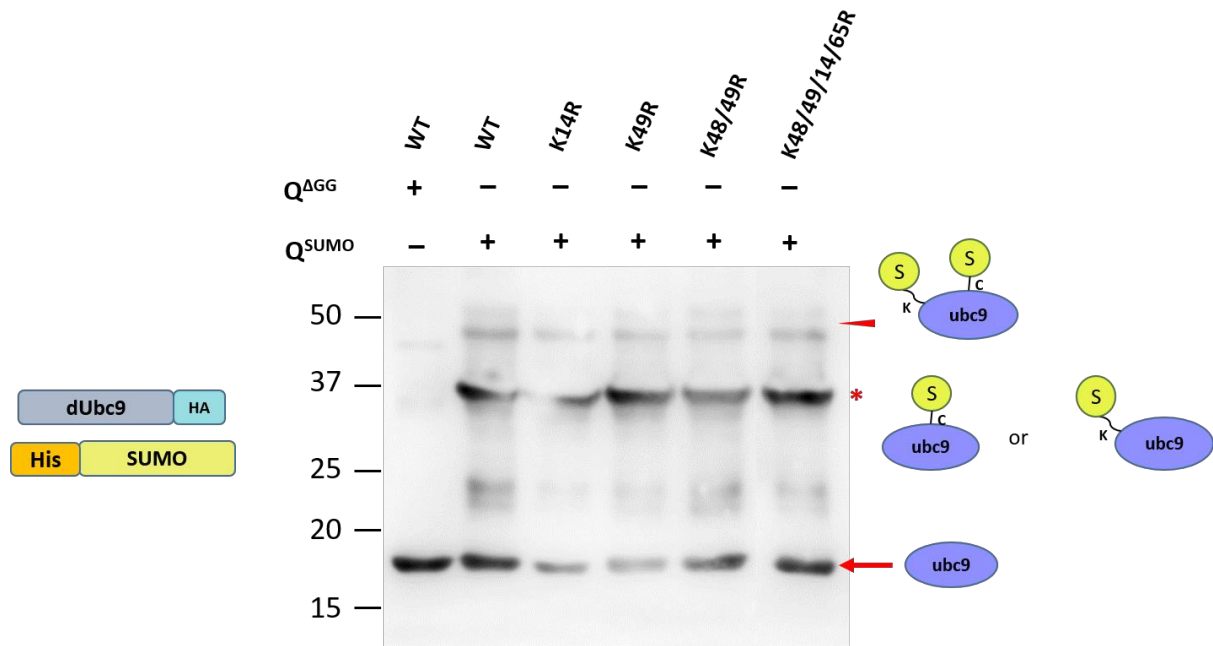


**Fig. I.6. dUbc9 is SUMOylated in a bacterial SUMOylation assay.** Arrow indicates unmodified protein, while asterisk denotes the SUMO- conjugated form (Ubc9-SUMO or Ubc9\*SUMO), which migrates ~20 kDa higher, after a His-affinity purification. Additional higher molecular species indicated by an arrowhead, represent putative SUMOylation at lysines. Mutations of lysines 14, 49, 48/49 and a 14/48/49/65 quadruple mutant does not abolish SUMOylation.

### I.3 Discussion

This study reinforces the importance of SUMO-cycle components in early development. We attempted to identify the SUMOylation sites for two proteins, 14-3-3 $\epsilon$  and Ubc9 experimentally using an *in bacto* assay system following an *in silico* prediction. Unfortunately, despite mutating the predicted lysines, we were unable to detect a loss of SUMOylation for the proteins studied. Though we can proceed with the mutants we have generated, in our experience the effects of SUMO conjugation are subtle. Thus, in the absence of a SUMO-conjugation resistant variant of the protein, the possibility of clearly defining a role for SUMO conjugation of a protein falls. In an organismal model, which is our usual goal, the time-component for discovery is ~2 years, which also deters us from proceeding with mutants that do not lose SUMO conjugation.

Alternate means of identifying SUMO conjugated lysines can include the use of a Mass spectrometer. Mass spectrometry-based identification of modified lysine residues remains challenging due to the presence of a large SUMO fragment after tryptic digestion, occluding the identification of the modified lysine. To overcome this challenge, modified, exogenously supplied SUMO has been used, and SUMOylated proteins and their lysine residues identified in HeLa cells (Hendriks *et al.* 2017). But in this scenario, promiscuous SUMOylation of proteins due to overexpression remains a concern.

Recently, efforts have been made to identify endogenously modified lysine residues, in mouse tissues (Hendriks *et al.* 2018). This strategy employs a SUMO antibody-based enrichment of modified proteins, followed by sequential action of proteases to yield fragments amenable to mass spectrometric analysis. The same strategy can be adapted for *Drosophila* to identify modified proteins with lysine residues in the context of development and immunity. The lysines can then be mutated, to study the function of SUMOylation.

Moreover, the lysines identified by the *in-bacto* SUMOylation assay may not be the lysines that undergo SUMOylation under physiological conditions, in the fly. To overcome the problem of context-specific SUMOylation, SUMOylation needs to be confirmed in the fly, and lysines need to be identified, by mass-spectrometry-based studies. Alternatively, loss of SUMOylation needs to be demonstrated in a putative SUMO-resistant mutant, to attribute observed phenotypes to loss of SUMOylation.

#### **I.4 Materials and methods**

##### *Embryonic lethality and cuticle preparation*

0-3 h embryos were transferred to a new sugar-agar plate, aligned in grids, counted and unhatched larvae were scored after 48 hours to determine viability.

Embryos were collected for three hours, aged for 22 hours at 25 °C, and dechorionated in a 4% sodium hypochlorite solution for 2 minutes. Dechorionated embryos were washed thoroughly under running tap water and transferred to a scintillation vial containing 1:1 methanol: heptane. The vial was shaken vigorously for a few minutes, and de-vitellinized embryos in the lower methanol phase were transferred to a new vial with fresh methanol. A fraction of non-devitellinized

embryos was retained to observe early defects otherwise not visible in devitellinized embryos. Embryos were transferred onto a slide, mounted in 85% lactic acid, and incubated overnight at 55 °C on a slide warmer. Cuticles were imaged on a Zeiss Axio Imager Z1 microscope, using dark field illumination with a 10X objective.

#### *Cloning and generation of constructs*

14-3-3 $\epsilon$  (FBgn0020238) and Ubc9 (FBgn0010602) CDS were PCR-amplified from a cDNA library generated from 0-3 h embryos via reverse transcription of mRNA. The CDS was independently cloned into the pET45b (+) vector for the *in bacto* SUMOylation assay using the modified Seamless Ligation Cloning Extract (SLiCE) protocol (Zhang et al., 2012). The SLiCE protocol enables homologous recombination in an *E. coli* strain termed PPY, harboring the Red recombination system. The putative SUMO-conjugated lysines were mutated to arginines using site-directed mutagenesis with mutagenic primers and constructs transformed in PPY cells for restriction-free cloning. All wild-type and mutant plasmids were verified via sequencing. The PPY cells were a gift from Dr. Winfried Edelmann.

#### *In bacto SUMOylation assay*

The bacterial SUMOylation assay adapted from Nie et al was modified. A 'quartet' vector expressing components of the *Drosophila* SUMOylation machinery was co-transformed into a BL21DE(3) *E. coli* strain with a pET45b(+) vector harboring the C-terminal HA-tagged CDS of 14-3-3 $\epsilon$  and Ubc9. All wild-type and mutant plasmids were verified via sequencing. Bacterial cultures were induced with 1 mM Isopropyl  $\beta$ -D-1-thiogalactopyranoside (IPTG) at 25 °C for 6 hours.

#### *Pulldown and western blotting*

For the pulldown assay, 10 mL of the bacterial culture was pelleted and re-suspended in 1 mL denaturing lysis buffer (8 M Urea, 100 mM NaH<sub>2</sub>PO<sub>4</sub>, 100 mM TrisCl pH 8, 10 mM Imidazole). The samples were sonicated for 1 min (10 s on, 10 s off) and centrifuged at 10,000g for 30 min at room temperature. The supernatant was added to 50  $\mu$ L of Ni-NTA superflow resin (Qiagen, #30430), equilibrated with the denaturing lysis buffer, and incubated at room temperature for 2 hours on a nutator. The supernatant was preserved after the pulldown, and the beads were washed four times with the denaturing wash buffer (8 M Urea, 20 mM Sodium Phosphate, pH 6.0,

500 mM NaCl) for 10 min each. Beads were made free of the wash buffer and reconstituted with 70  $\mu$ L of 1X PBS and 20  $\mu$ L of 5X SDS loading dye.

The input and IP fraction were resolved on a 10% polyacrylamide gel and transferred onto a PVDF membrane (Immobilon-E, Merck). The membrane was blocked with 5% milk in TBS containing 0.1% Tween20 (TBS-T) for an hour, followed by incubation with the primary antibody diluted in 5% milk in TBS-T. Following three washes with TBS-T, the membrane was incubated with the secondary antibody diluted in 5% milk in TBS-T for an hour at room temperature. The membrane was washed thrice with 0.1% TBS-T, incubated with Immobilon Western Chemiluminescent HRP substrate (Merck), and visualized on a LAS4000 Fuji imaging system. The following antibodies were used: Rabbit anti-14-3-3, 1:5000 (Pan, #51-0700, Invitrogen); Rabbit anti-FLAG, 1:5000 (#H3663, Sigma); Goat anti-rabbit HRP secondary antibody at 1:10000 (Jackson ImmunoResearch).

**I.5 Contributions/Notes:** Other projects were initiated for maternal roles for proteins that are SUMO conjugated. Groucho is a SUMO target and there are ongoing attempts to generate Groucho SCR variants. Similarly, Dorsal has SIM sites; these sites are interesting targets for mutations. These projects will be taken forward by subsequent graduate students.



## I.6 References

1. Beauclair, G., Bridier-Nahmias, A., Zagury, J.-F., Saïb, A., & Zamborlini, A. (2015). JASSA: a comprehensive tool for prediction of SUMOylation sites and SIMs. *Bioinformatics*, *31*(21), 3483–3491.  
<https://doi.org/10.1093/bioinformatics/btv403>
2. Dong, J., Feldmann, G., Huang, J., Wu, S., Zhang, N., Comerford, S. A., Gayyed, M. F., Anders, R. A., Maitra, A., & Pan, D. (2007). Elucidation of a Universal Size-Control Mechanism in *Drosophila* and Mammals. *Cell*, *130*(6), 1120–1133.  
<https://doi.org/10.1016/j.cell.2007.07.019>
3. Epps, J. L., & Tanda, S. (1998). The *Drosophila* semushi mutation blocks nuclear import of Bicoid during embryogenesis. *Current Biology*, *8*(23), 1277-S2.  
[https://doi.org/10.1016/S0960-9822\(07\)00538-6](https://doi.org/10.1016/S0960-9822(07)00538-6)
4. Handu, M., Kaduskar, B., Ravindranathan, R., Soory, A., Giri, R., Elango, V. B., Gowda, H., & Ratnaparkhi, G. S. (2015). SUMO-Enriched Proteome for *Drosophila* Innate Immune Response. *G3*, *5*(10), 2137–2154.  
<https://doi.org/10.1534/g3.115.020958>
5. Hendriks, I. A., Lyon, D., Su, D., Skotte, N. H., Daniel, J. A., Jensen, L. J., & Nielsen, M. L. (2018). Site-specific characterization of endogenous SUMOylation across species and organs. *Nature Communications*, *9*(1), 2456.  
<https://doi.org/10.1038/s41467-018-04957-4>
6. Hendriks, I. A., Lyon, D., Young, C., Jensen, L. J., Vertegaal, A. C. O., & Nielsen, M. L. (2017). Site-specific mapping of the human SUMO proteome reveals co-modification with phosphorylation. *Nature Structural & Molecular Biology*, *24*(3), 325–336. <https://www.nature.com/articles/nsmb.3366>
7. Hendriks, I. A., & Vertegaal, A. C. O. (2016). A comprehensive compilation of SUMO proteomics. *Nature Reviews. Molecular Cell Biology*, *17*(9), 581–595.  
<https://doi.org/10.1038/nrm.2016.81>
8. Hu, Y., Flockhart, I., Vinayagam, A., Bergwitz, C., Berger, B., Perrimon, N., & Mohr, S. E. (2011). An integrative approach to ortholog prediction for disease-focused and other functional studies. *BMC Bioinformatics*, *12*, 357.  
<https://doi.org/10.1186/1471-2105-12-357>
9. Klug, H., Xaver, M., Chaugule, V. K., Koidl, S., Mittler, G., Klein, F., & Pichler, A. (2013). Ubc9 Sumoylation Controls SUMO Chain Formation and Meiotic

- Synapsis in *Saccharomyces cerevisiae*. *Molecular Cell*, 50(5), 625–636.  
<https://doi.org/10.1016/j.molcel.2013.03.027>
10. Knipscheer, P., Flotho, A., Klug, H., Olsen, J. V., van Dijk, W. J., Fish, A., Johnson, E. S., Mann, M., Sixma, T. K., & Pichler, A. (2008). Ubc9 Sumoylation Regulates SUMO Target Discrimination. *Molecular Cell*, 31(3), 371–382.  
<https://doi.org/10.1016/j.molcel.2008.05.022>
  11. Li, W., Skoulakis, E. M., Davis, R. L., & Perrimon, N. (1997). The *Drosophila* 14-3-3 protein Leonardo enhances Torso signaling through D-Raf in a Ras 1-dependent manner. *Development (Cambridge, England)*, 124(20), 4163–4171.  
<https://www.ncbi.nlm.nih.gov/pubmed/9374412>
  12. Nie, M., Xie, Y., Loo, J. A., & Courey, A. J. (2009). Genetic and proteomic evidence for roles of *Drosophila* SUMO in cell cycle control, Ras signaling, and early pattern formation. *PLoS One*, 4(6), e5905.  
<https://doi.org/10.1371/journal.pone.0005905>
  13. Pirone, L., Xolalpa, W., Sigurðsson, J. O., Ramirez, J., Pérez, C., González, M., de Sabando, A. R., Elortza, F., Rodriguez, M. S., Mayor, U., Olsen, J. V., Barrio, R., & Sutherland, J. D. (2017). A comprehensive platform for the analysis of ubiquitin-like protein modifications using in vivo biotinylation. *Scientific Reports*, 7, 40756. <https://doi.org/10.1038/srep40756>
  14. Staller, M. V., Yan, D., Randklev, S., Bragdon, M. D., Wunderlich, Z. B., Tao, R., Perkins, L. A., DePace, A. H., & Perrimon, N. (2013). Depleting Gene Activities in Early *Drosophila* Embryos with the “Maternal-Gal4–shRNA” System. *Genetics*, 193(1), 51–61. <https://doi.org/10.1534/genetics.112.144915>
  15. Su, T. T., Parry, D. H., Donahoe, B., Chien, C.-T., O’Farrell, P. H., & Purdy, A. (2001). Cell cycle roles for two 14-3-3 proteins during *Drosophila* development. *Journal of Cell Science*, 114(19), 3445 LP – 3454.
  16. Tien, a. C., Hsei, H. Y., & Chien, C. T. (1999). Dynamic expression and cellular localization of the *drosophila* 14-3-3epsilon during embryonic development. *Mechanisms of Development*, 81(1–2), 209–212. [https://doi.org/10.1016/S0925-4773\(98\)00238-X](https://doi.org/10.1016/S0925-4773(98)00238-X)

## Appendix II: SUMOylation of DL; a contrasting tale of the UAS-GAL4 system

### II.1 Introduction

Dorsal (DL) was one of the earliest *Drosophila* proteins identified as a target for SUMO conjugation at lysine 382, in S2 cells (Bhaskar *et al.* 2000, 2002). Since DL was also identified to be SUMOylated in the 0-3 hr embryo (Nie *et al.* 2009), it was chosen to investigate the outcome of SUMOylation.

Before proceeding with a CRISPR/Cas9 based genome-editing strategy (outlined in Chapter 2), we used the conventional UAS-GAL4 system (Brand and Perrimon 1993; Duffy 2002; Elliott and Brand 2008) to drive maternal expression of a SUMO-conjugation resistant DL<sup>K382R</sup> variant in a DL null background. A similarly expressed DL<sup>WT</sup> was used as a control. We hypothesized that altering the SUMOylation status of DL would perturb DL activity and affect dorsoventral (DV) patterning. Using this traditional *null; rescue* system, we observed that DL<sup>K382R</sup> fails to enter the nucleus and activate target genes. Moreover, it is unstable in the 0-3 embryo but retains its function in the presence of wild-type DL. Therefore, we concluded that SUMOylation of DL is essential to regulate its stability and function in the early *Drosophila* embryo. This conclusion was however at odds with the results we had with the DL<sup>K382R</sup> mutant generated via CRISPR-Cas9 (Chapter 2). After careful consideration, we choose to publish the CRISPR based data.

### II.2 Results

#### II.2.1 Validation of transgenic constructs

To uncover roles for DL SUMOylation in the early embryo, *dl<sup>WT</sup>* and *dl<sup>K382R</sup>* coding sequences were cloned into the pUASp vector (Rørth, 1998) to generate multiple transgenic fly lines (Mithila/Srija) that could be expressed both maternally and in the zygote. The *pUASp-dl<sup>WT</sup>* and *pUASp-dl<sup>K382R</sup>* lines were further recombined with a null allele for DL, *dl<sup>1</sup>* (Isoda *et al.* 1992). Expression was tested by driving the transgenes in the dorsal compartment of the wing imaginal disc using *apterous-GAL4* (Fig. II.1). Antibody staining against DL indicates that both DL<sup>WT</sup> and DL<sup>K382R</sup> are expressed to

similar levels in the wing imaginal disc (Fig. II.1). These lines were used for further experiments.

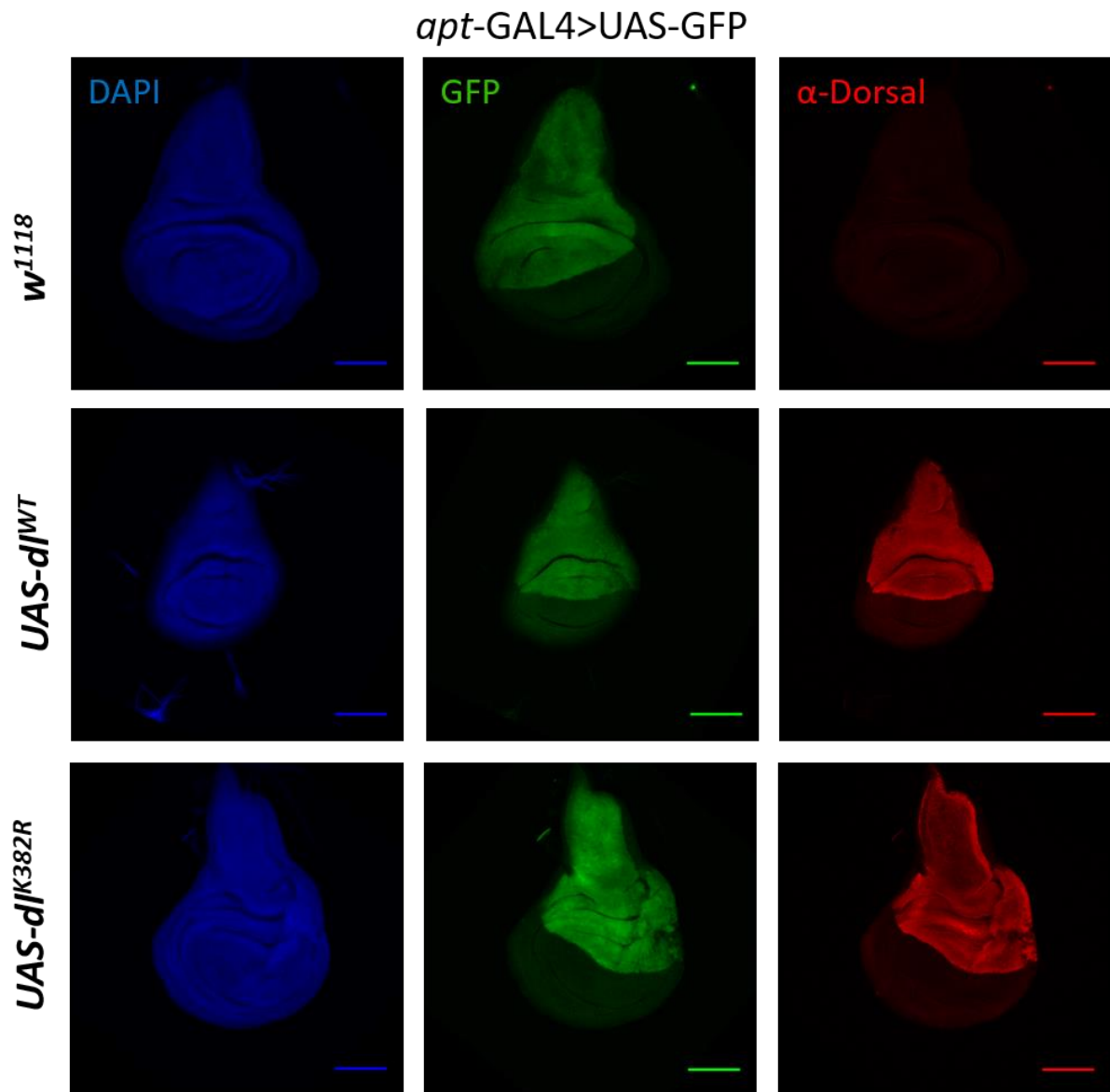


**Fig. II.1. Validation of *UAS-dl* constructs.** Expression of DL transgenes in the wing imaginal disc driven by *apt-GAL4*, detected by an antibody against DL. GFP marks the GAL4 expression domain, while DAPI is used to visualize wing disc nuclei.

### II.2.2 *DL<sup>K382R</sup>* mutants are defective in DV patterning

*dl<sup>1</sup>/dl<sup>1</sup>* animals lack functional DL and as a consequence, fail to specify the embryonic mesoderm, resulting in embryonic lethality (Isoda *et al.* 1992). Embryos derived from *dl<sup>1</sup>/dl<sup>1</sup>* mothers present as a dorsalized tube in cuticle preparations, with a marked absence of regularly spaced, ventral denticle bands unlike the wild-type

embryo (Fig. II.2). In this background, we wanted to test the behaviour of the  $dl^{WT}$  and  $dl^{K382R}$  transgenes. Expression was driven maternally using the *13.4 Mat-GAL4* driver, a line with transgenic insertions on the 2<sup>nd</sup> and 3<sup>rd</sup> chromosomes, as previously described (Ratnaparkhi et al., 2006). Embryos were derived from mothers of the genotype:  $dl^1, pUASp-dl^{WT}/dl^1; Mat-GAL4/+$  and  $dl^1, pUASp-dl^{K382R}/dl^1; Mat-GAL4/+$ , and are henceforth referred to as  $dl^{WT}$  and  $dl^{K382R}$  respectively. Cuticle preparations indicate that maternally deposited  $DL^{WT}$  rescues the dorsalized cuticle phenotype of  $dl^1/dl^1$ , re-establishing the denticle bands (Fig. II.2). In contrast,  $DL^{K382R}$  failed to rescue the phenotype, and 100% of the embryos phenocopy the  $dl^1/dl^1$  cuticles. These experiments suggest that SUMOylation of DL is critical for specifying the DV axis.

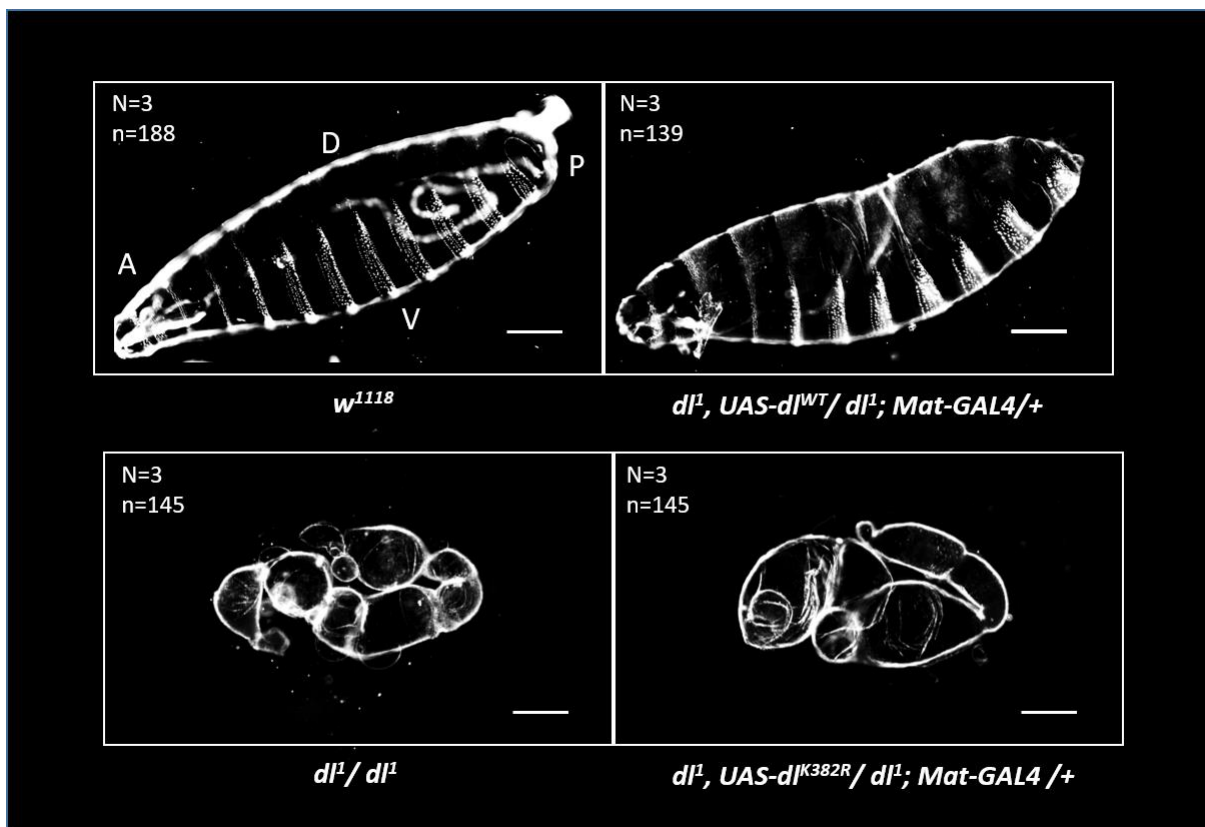


**Fig. II.2.  $DL^{K382R}$  animals are defective in DV patterning.** Cuticle preparations of first instar larvae (aged for 22-24 hrs post-egg lay). Top left panel shows a wild-type cuticle.  $UAS-dl^{WT}$  rescues the lethality of  $dl^1/dl^1$  embryos (top right panel), while  $UAS-dl^{K382R}$  (bottom right panel) phenocopies the  $dl^1/dl^1$  phenotype (Severe dorsalization, D0, bottom left panel) and is lethal. Embryos are oriented anterior to the left and ventral side down.

### II.2.3 DL<sup>K382R</sup> fails to enter the nucleus

The failure of DL<sup>K382R</sup> in patterning the DV axis could be due to a variety of reasons. Nuclear import, stability, or transcriptional activity could be compromised in the SUMO-conjugation deficient DL<sup>K382R</sup>. To distinguish between these possibilities, we first wanted to observe the localization of DL. 0-3 hour embryos were stained with an antibody against DL and visualized on a confocal microscope. In wild-type syncytial blastoderm embryos, DL translocates to the ventral nuclei in response to a graded Toll signal (Fig. II.3). Embryos rescued with DL<sup>WT</sup> also display nuclear localization of DL in the ventral side. In *dl<sup>1</sup>/dl<sup>1</sup>* embryos, no DL is detected in the ventral nuclei (Fig. II.3). Similarly, DL<sup>K382R</sup> is not imported to the nucleus, and downstream targets of DL like *twi* and *sna* are not activated, explaining the dorsalized (D0) cuticular phenotype.

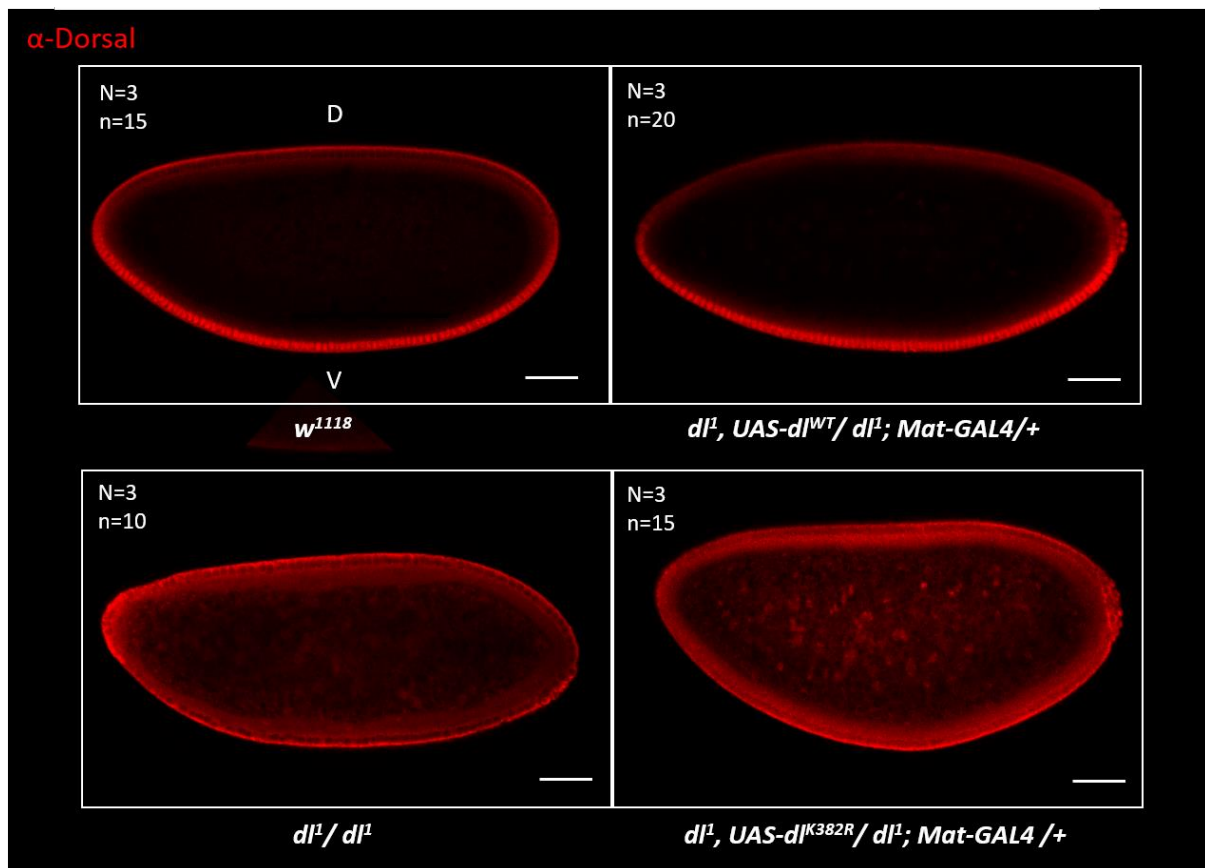


**Fig. II.3. DL<sup>K382R</sup> is undetectable in the ventral nuclei.** Sagittal sections of cell cycle 13/14 (syncytial blastoderm/cellular blastoderm) embryos showing DL (anti-DL antibody) localization. DL localizes to the ventral nuclei in the wild-type (top left panel) and in the *UAS-dl<sup>WT</sup>* rescue embryos (top right panel), while it is absent in the *dl<sup>1</sup>/dl<sup>1</sup>* and *UAS-dl<sup>K382R</sup>* embryos.

## II.2.4 DL<sup>K382R</sup> is unstable in the 0-3 hr embryo

We next wanted to check DL protein levels in the *dl<sup>WT</sup>* and *dl<sup>K382R</sup>* rescue embryos. A western blot for DL indicates that 0-3 hour embryos laid by *dl<sup>1</sup>/dl<sup>1</sup>* mothers lack detectable levels of DL, compared to *w<sup>1118</sup>*. DL levels were significantly lower in the DL<sup>WT</sup> rescue embryos, in comparison to *w<sup>1118</sup>* embryos, but sufficient to rescue embryonic patterning. Surprisingly, DL was undetectable in *dl<sup>K382R</sup>* embryos (Fig. II.4). The DL inhibitor Cact is known to be stabilized by its interaction with DL (Kidd 1992; Kubota and Gay 1995); hence levels of cactus also serve as a proxy for DL stability. Cact is absent in the embryos of *dl<sup>1</sup>/dl<sup>1</sup>* and *dl<sup>K382R</sup>* mothers (Fig. II.4), indicating that the loss of SUMOylation destabilizes DL and subsequently Cact in the early embryo.

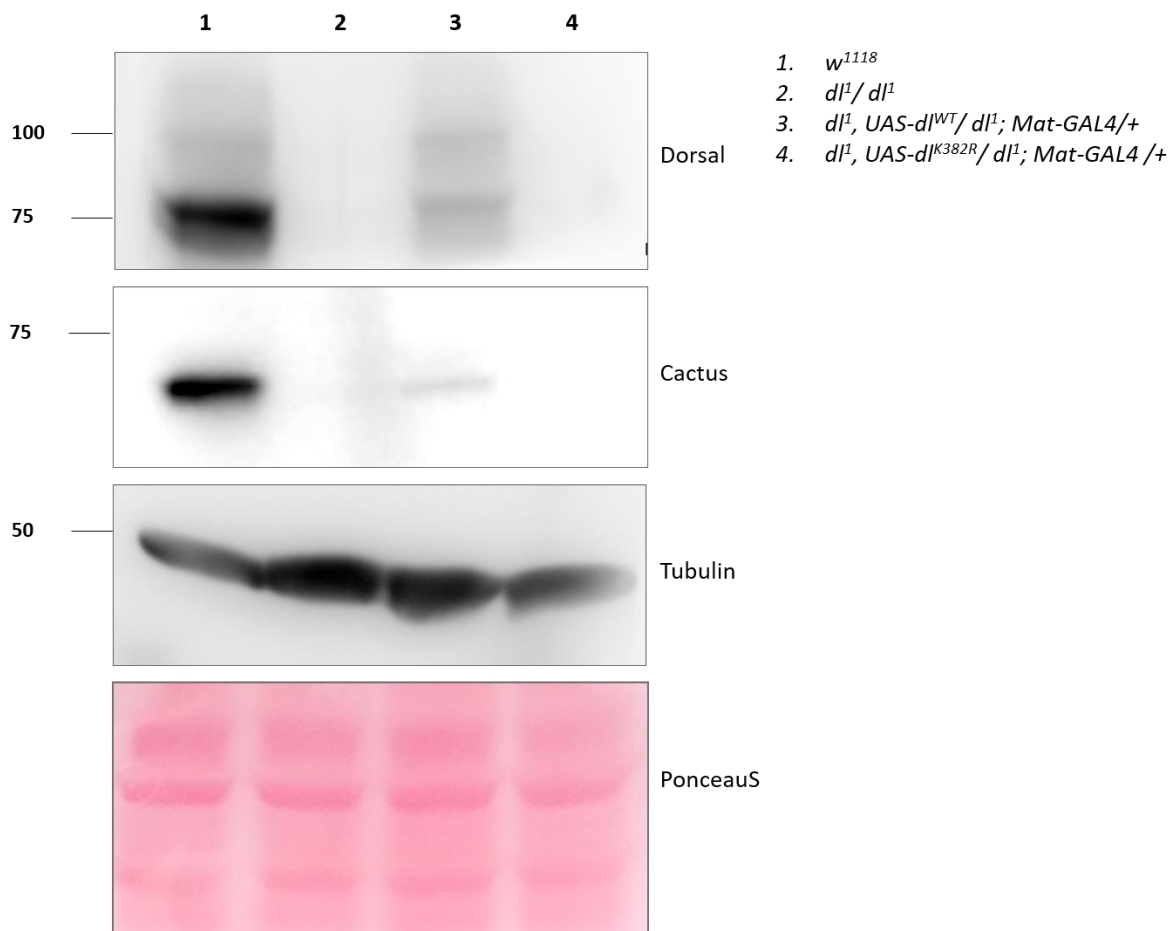


**Fig. II.4. DL<sup>K382R</sup> is degraded in the embryo.** Western blot of 0-3 hr embryo lysates, probed with anti-dorsal and anti-cactus antibodies. DL is not detected in the *UAS-dl<sup>K382R</sup>* embryo lysate (lane 4). Cactus, interacting partner of dorsal is also absent, indicating that DL is unstable in the 0-3 hr embryo. Tubulin and PonceauS are used as loading controls.

### II.2.5 DL<sup>K382R</sup> retains its function in the presence of a wild-type Dorsal

The developmental paradigm is robust in *Drosophila* embryos and is buffered against environmental factors perturbing morphogen distribution. In the context of DV patterning, Cact is present in excess of DL, curbing aberrant translocation of DL into the nucleus (Govind *et al.* 1993). A two-fold or greater increase in DL levels is known to saturate the inhibitory effect of Cact, leading to the expansion of the DL gradient and subsequent ventralization of embryos (Govind *et al.* 1993). We wanted to test the behaviour of DL<sup>K382R</sup> in the presence of wild-type DL. First, we over-expressed DL<sup>WT</sup> in the presence of a single copy of endogenous DL using a *Mat-GAL4* driver. As expected, embryos laid by *dl<sup>1</sup>, pUASp-dl<sup>WT</sup>/+; Mat-GAL4/+* mothers showed a wide range of phenotypic abnormalities, ranging from near wild-type to severely ventralized (V1) cuticles (Fig. II.5). To our surprise, embryos derived from *dl<sup>1</sup>, pUASp-dl<sup>K382R</sup>/+; Mat-GAL4/+* females also displayed a similar proportion of ventralization phenotypes. These have been classified on the basis of their severity as V1 to V4 (Fig. II.5), as described previously (Roth *et al.* 1991). Thus, DL<sup>K382R</sup> is stable and functional in the presence of endogenous DL. In this background, DL<sup>K382R</sup> retains its ability to dimerize and activates ventral targets like its wild-type counterpart. In contrast, an absence of any wild-type DL renders DL<sup>K382R</sup> non-functional.



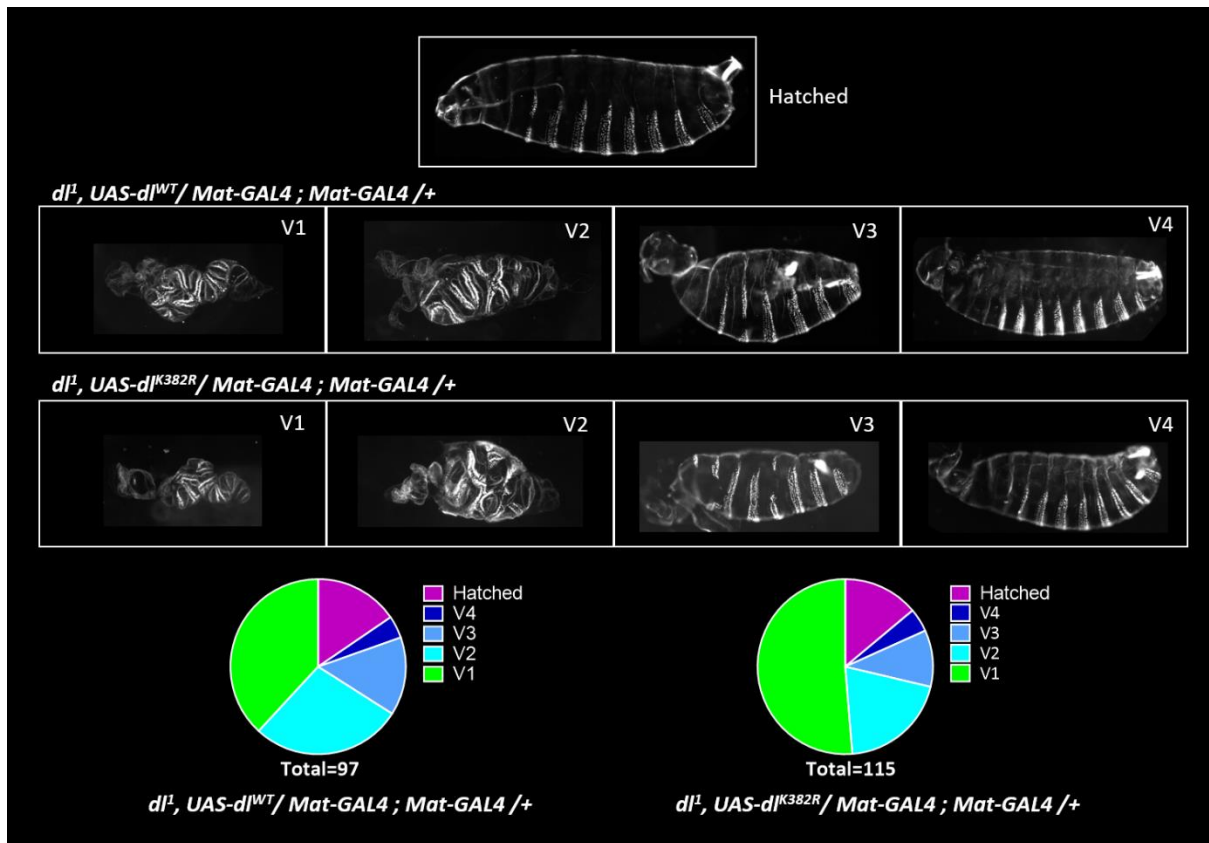


**Fig. II. 5. DL<sup>K382R</sup> can carry out its function in the presence of wild type Dorsal.** Cuticle preparations of first instar larvae (aged for 24 hrs post egg lay). Overexpression of both DL<sup>WT</sup> and DL<sup>K382R</sup> leads to the formation of ventralized embryos (V1- most severe to V4-mild severity).

### II.3 Discussion

In this study, we have explored the role for SUMOylation of DL using the UAS-GAL4 system. We observe that maternally expressed DL<sup>WT</sup> rescues DV cuticular patterning in DL<sup>null</sup> embryos. In contrast, SUMOylation-deficient DL<sup>K382R</sup> mothers lay embryos that phenocopy DL<sup>null</sup>, failing to specify the mesoderm. Immunostaining for DL<sup>K382R</sup> indicates that it does not enter the nucleus. Surprisingly, western blot analysis shows an absence of DL and its interacting partner Cact in DL<sup>K382R</sup> embryos. When over-expressed in the presence of wild-type DL in the background, DL<sup>K382R</sup> is functionally similar to DL<sup>WT</sup>, causing ventralization of the embryos. Therefore, SUMOylation of DL seems to be critical for the stability of DL in the developing embryo.

A caveat of this study is the insertion of the *pUASp-dl<sup>WT</sup>* and *pUASp-dl<sup>K382R</sup>* transgenes at random, non-identical locations on the second chromosome. This could potentially influence the transcript levels and protein expression. Additionally, western blot analysis suggested that the *pUASp-dl<sup>WT</sup>* allele expresses at a lower level in a DL null background than in the homozygous wild-type condition. There is a strong likelihood that the *pUASp-dl<sup>K382R</sup>* allele, by virtue of its expression levels, is causing an artefactual phenotype. Achieving endogenous expression levels of the mutant protein would entail precise editing of the genomic locus. CRISPR-Cas9-based genome editing was the perfect candidate for this approach, and we proceeded to use this toolkit to create a genomic K382R mutation in the DL locus to understand the function of SUMOylation.

## II.4 Materials and methods

### *Fly husbandry and stocks*

Flies were raised on standard cornmeal agar at 25 °C unless stated otherwise. The 13.4 Mat-GAL4 driver, encoding Gal4-VP16 under the control of the maternally active  $\alpha$ -*Tubulin* promoter was a kind gift from the Courey lab, USA (Ratnaparkhi et al., 2006). Transgenic flies of the following genotypes were used: (1) *dl<sup>1</sup>, pUASp-dl<sup>WT</sup>/dl<sup>1</sup>; Mat-GAL4/+*; (2) *dl<sup>1</sup>, pUASp-dl<sup>K382R</sup>/dl<sup>1</sup>; Mat-GAL4/+*; (3) 13.4 *Mat-GAL4*. The *dl<sup>1</sup>/CyO* (3236) line was procured from the Bloomington *Drosophila* Stock Centre.

### *Cuticle preparation*

Embryos were collected for three hours, aged for 22 hours at 25 °C, and dechorionated in a 4% sodium hypochlorite solution for 2 minutes. Dechorionated embryos were washed thoroughly under running tap water and transferred to a scintillation vial containing 1:1 methanol: heptane. The vial was shaken vigorously for a few minutes, and de-vitellinized embryos in the lower methanol phase were transferred to a new vial with fresh methanol. Embryos were transferred onto a slide, mounted in 85% lactic acid, and incubated overnight at 55 °C on a slide warmer. Cuticles were imaged on a Zeiss Axio Imager Z1 microscope, using dark field illumination, with a 10X objective.

### *Immunostaining of wing imaginal discs*

Wing imaginal discs were dissected from wandering third instar larvae of the appropriate genotypes in ice-cold 1X Phosphate-buffered saline (PBS). The samples were fixed in 4% formaldehyde in PBS for 20 minutes, followed by three 15-minute washes with 1X PBS containing 0.1% Triton X-100 (0.1% PBS-T). After blocking with 2% Bovine serum albumin (BSA) in 0.1% PBS-T, the samples were incubated overnight at 4 °C with the primary antibody. Following three 15-minute washes with 0.1% PBS-T, they were incubated with the secondary antibody for an hour at room temperature. Samples were washed thrice in 0.1% PBS-T, and DAPI was added in the penultimate wash. Samples were mounted in SlowFade Gold mountant (Invitrogen) and imaged on a Leica Sp8 confocal microscope under a 20X oil-immersion objective. The antibodies used were: Rabbit anti-Dorsal, 1:1000 (Courey Lab) and goat anti-rabbit Alexa568 secondary antibody, 1:1000 (Invitrogen).

### *Immunostaining of embryos*

0-3 hour embryos were dechorionated in 4% sodium hypochlorite for 2 minutes. Embryos were rinsed and fixed in a 1:1 solution of 4% formaldehyde in 1X Phosphate-buffered saline (PBS): heptane for 20 minutes. The aqueous phase containing formaldehyde was removed, and embryos were devitellinized by adding an equal volume of ice-cold methanol followed by vigorous shaking. Devitellinized embryos were washed thrice in methanol. Embryos were re-hydrated and permeabilized by giving six 15-minute washes in 1X PBS containing 0.3% Triton X-100 (0.3% PBS-T). After blocking with 2% Bovine serum albumin (BSA) in 0.3% PBS-T, embryos were incubated overnight at 4 °C with the primary antibody. Following four 15-minute washes with 0.3% PBS-T, embryos were incubated with the secondary antibody for an hour at room temperature. Embryos were washed thrice in 0.3% PBS-T, and DAPI was added in the penultimate wash. Embryos were mounted in SlowFade Gold mountant (Invitrogen) and imaged on a Leica Sp8 confocal microscope under a 20X oil-immersion objective. The antibodies used were: Mouse anti-Dorsal, 1:1000 (DSHB 7A4-c) and goat anti-mouse Alexa568 secondary antibody, 1:1000 (Invitrogen).

### *Western blotting*

0-3 hour embryos were dechorionated in 4% sodium hypochlorite and washed thoroughly with distilled water. Embryos were crushed in lysis buffer (1% Triton X-100, 50 mM Tris-HCl (pH 8.0), 150 mM NaCl, and 1X PIC) and cleared by centrifuging at 21,000g for 30 minutes. Total protein was estimated by BCA assay (Pierce) and samples were boiled in 1X Laemmli buffer. Equal amounts of protein (50-70 µg/sample) were resolved on a 10% polyacrylamide gel and transferred onto a PVDF membrane (Immobilon-E, Merck). The membrane was blocked with 5% milk in TBS containing 0.1% Tween20 (TBS-T) for an hour followed by incubation with the primary antibody diluted in 5% milk in TBS-T. Following three washes with TBS-T, the membrane was incubated with the secondary antibody diluted in 5% milk in TBS-T for an hour, at room temperature. The membrane was washed thrice with 0.1% TBS-T, incubated with Immobilon Western Chemiluminescent HRP substrate (Merck), and visualized on a LAS4000 Fuji imaging system. The following antibodies were used: Rabbit anti-Dorsal, 1:5000 (kind gift from the Courey laboratory); Mouse anti- $\alpha$ -Tubulin, 1:10000 (T6074, Sigma-Aldrich); Mouse anti-Cact, 1:100 (3H12, DSHB), Goat anti-rabbit HRP and Goat anti-mouse HRP secondary antibodies, each at 1:10000 (Jackson ImmunoResearch).

**II.5 Contributions/Notes:** The initial characterization of phenotypes of *dIK<sup>382R</sup>* mutants was carried out by Srijia Bhagvatula as a MS thesis project (Bhagavatula, S. (2012). *Development of Threshold sensitive NF- $\kappa$ B reporters for Live Imaging of NF- $\kappa$ B transcription in Drosophila melanogaster* (Doctoral dissertation)) and was a collaboration with Dr. Richa Rikhy's group. I repeated and extended the data in my initial years as a graduate student before shifting completely to the CRISPR mutant.

## II.6 References

1. Bhaskar, V., Valentine, S. A., & Courey, A. J. (2000). A functional interaction between dorsal and components of the Smt3 conjugation machinery. *The Journal of Biological Chemistry*, 275(6), 4033–4040. <https://doi.org/10.1074/jbc.275.6.4033>
2. Bhaskar, Vinay, Smith, M., & Courey, A. J. (2002). Conjugation of Smt3 to dorsal may potentiate the Drosophila immune response. *Molecular and Cellular Biology*, 22(2), 492–504. <https://doi.org/10.1128/MCB.22.2.492-504.2002>

3. Brand, A. H., & Perrimon, N. (1993). Targeted gene expression as a means of altering cell fates and generating dominant phenotypes. *Development* , 118(2), 401–415. <https://www.ncbi.nlm.nih.gov/pubmed/8223268>
4. Duffy, J. B. (2002). GAL4 system in *Drosophila*: a fly geneticist's Swiss army knife. *Genesis* , 34(1–2), 1–15. <https://doi.org/10.1002/gene.10150>
5. Elliott, D. A., & Brand, A. H. (2008). The GAL4 System. In C. Dahmann (Ed.), *Drosophila: Methods and Protocols* (pp. 79–95). Humana Press. [https://doi.org/10.1007/978-1-59745-583-1\\_5](https://doi.org/10.1007/978-1-59745-583-1_5)
6. Govind, S., Brennan, L., & Steward, R. (1993). Homeostatic balance between dorsal and cactus proteins in the *Drosophila* embryo. *Development* , 117(1), 135–148. <https://www.ncbi.nlm.nih.gov/pubmed/8223244>
7. Isoda, K., Roth, S., & Nüsslein-Volhard, C. (1992). The functional domains of the *Drosophila* morphogen dorsal: evidence from the analysis of mutants. *Genes & Development*, 6(4), 619–630. <https://doi.org/10.1101/gad.6.4.619>
8. Kidd, S. (1992). Characterization of the *Drosophila* cactus locus and analysis of interactions between cactus and dorsal proteins. *Cell*, 71(4), 623–635. [https://doi.org/10.1016/0092-8674\(92\)90596-5](https://doi.org/10.1016/0092-8674(92)90596-5)
9. Kubota, K., & Gay, N. J. (1995). The dorsal protein enhances the biosynthesis and stability of the *Drosophila* IκB homologue cactus. *Nucleic Acids Research*, 23(16), 3111–3118. <https://doi.org/10.1093/nar/23.16.3111>
10. Nie, M., Xie, Y., Loo, J. A., & Courey, A. J. (2009). Genetic and proteomic evidence for roles of *Drosophila* SUMO in cell cycle control, Ras signaling, and early pattern formation. *PLoS One*, 4(6), e5905. <https://doi.org/10.1371/journal.pone.0005905>
11. Ratnaparkhi, G. S., Jia, S., & Courey, A. J. (2006). Uncoupling dorsal-mediated activation from dorsal-mediated repression in the *Drosophila* embryo. *Development* , 133(22), 4409–4414. <https://doi.org/10.1242/dev.02643>
12. Rørth, P. (1998). Gal4 in the *Drosophila* female germline. *Mechanisms of Development*, 78(1), 113–118. [https://doi.org/10.1016/S0925-4773\(98\)00157-9](https://doi.org/10.1016/S0925-4773(98)00157-9)
13. Roth, S., Hiromi, Y., Godt, D., & Nüsslein-Volhard, C. (1991). cactus, a maternal gene required for proper formation of the dorsoventral morphogen gradient in *Drosophila* embryos. *Development* , 112(2), 371–388. <https://www.ncbi.nlm.nih.gov/pubmed/1794309>

## Appendix III: SUMOylation of DL and the stress response in adults

### III.1 Introduction

SUMO is known to play a cytoprotective role during conditions of stress. Global SUMOylation is largely upregulated in response to various stressors like heat, osmotic stress, starvation, and immune stress (Golebiowski *et al.* 2009; Enserink 2015; Drabikowski 2020; Ryu *et al.* 2020).

Dorsal (DL), in concert with Dorsal-related immune factor (Dif) mediates the innate immune response to gram-positive bacteria and fungi in *Drosophila*. The NF- $\kappa$ B factors migrate to the fat body nuclei to transcribe antimicrobial peptides that mitigate the infection (Ip *et al.* 1993; Lemaitre *et al.* 1995; Petersen *et al.* 1995; Gross *et al.* 1996; Dushay and Eldon 1998; Wu and Anderson 1998; Meng *et al.* 1999; Govind 2008). Dif and DL are redundant in the third instar larvae but Dif is the pre-dominant Toll-specific NF- $\kappa$ B factor in adult immunity (Rutschmann *et al.* 2000, 2002).

Interestingly, activation of the Toll pathway also affects nutrient storage. Mounting the energy-intensive immune response promoted catabolism of the stored triglycerides, via the insulin signaling pathway (DiAngelo *et al.*, 2009; Roth *et al.*, 2018; Suzawa *et al.*, 2019).

Earlier (Chapters 2 and 3), I have described roles for SUMO conjugation in DV patterning and larval immunity. Here I evaluate the phenotypic effects of the *d<sup>SCR</sup>* mutation in the adult, focusing on starvation stress and immune challenge. The lifespan of adult flies was monitored in response to these stresses.

### III.2 Results

#### III.2.1 Toll signaling in adult *d<sup>SCR</sup>* animals

Larvae expressing a SUMO-conjugation deficient allele, *d<sup>SCR</sup>*, generated via CRISPR-Cas9 gene editing (Chapter 2) showed a higher expression of Toll-specific AMPs in larvae. To assess whether these results hold true in adults, we performed a qRT-PCR for AMPs downstream of the Toll pathway: *Drosomycin* (*Drs*) and *Metchnikowin* (*Mtk*). Transcript levels were assayed in uninfected 5–7 day old males.

In the absence of an immune challenge, both *Drs* and *Mtk* were upregulated (Fig. III.1A), indicating a basal state reminiscent of inflammation. To evaluate whether the inflammation translated to any detriments in the fly, a survival assay was performed. Analysis of the lifespan suggested the absence of survival defects in uninfected males (Fig. III.1B).

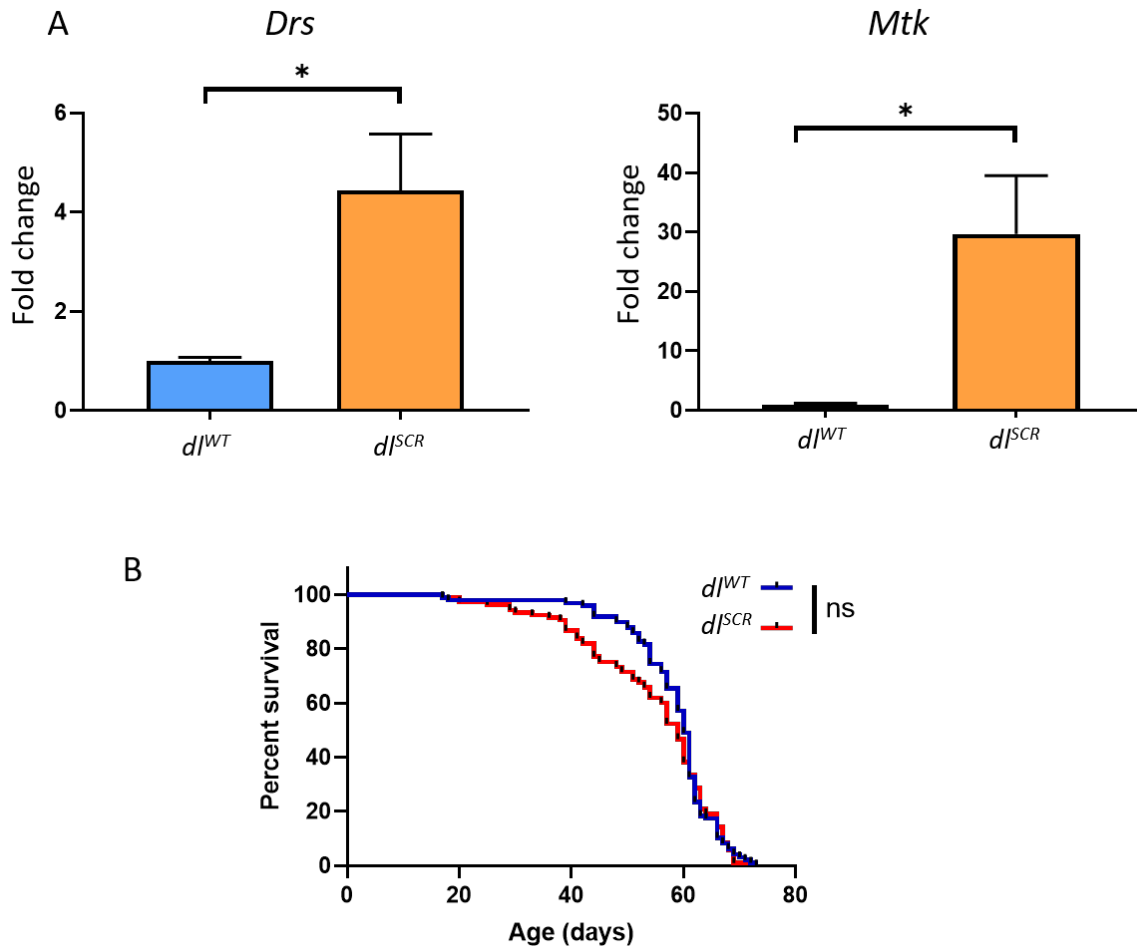


**Fig. III.1. Toll signaling in  $dl^{SCR}$  animals.** Transcript levels of *Drs* and *Mtk* assayed by qRT-PCR for  $dl^{WT}$  and  $dl^{SCR}$  are presented in (A). N = 3, mean  $\pm$  SEM, Ordinary one-way ANOVA, (\*)  $P < 0.05$ . (B) shows survival of unchallenged males in  $dl^{WT}$  and  $dl^{SCR}$ . Kaplan-Meier survival curves were plotted and significance was analyzed using the Mantel-Cox test on GraphPad Prism 8. n = 100, (ns)  $P < 0.05$ .

### III.2.2 $dI^{SCR}$ animals succumb to infection

To gauge the response of SUMO-deficient flies to infection, adult males were infected with the Gram-positive pathogen *Staphylococcus saprophyticus* and survival was monitored daily. At 29 °C,  $dI^{SCR}$  males succumb to infection faster than their wild-type counterpart (Fig. III.2B). The survival of unchallenged males was comparable between  $dI^{SCR}$  and  $dI^{WT}$  at 29 °C. These results indicate an immune deficit in the  $dI^{SCR}$  males, despite an upregulation of AMPs in the unchallenged state. The heightened AMP response is not sufficient to offer a survival advantage in *S. saprophyticus*-infected adults.

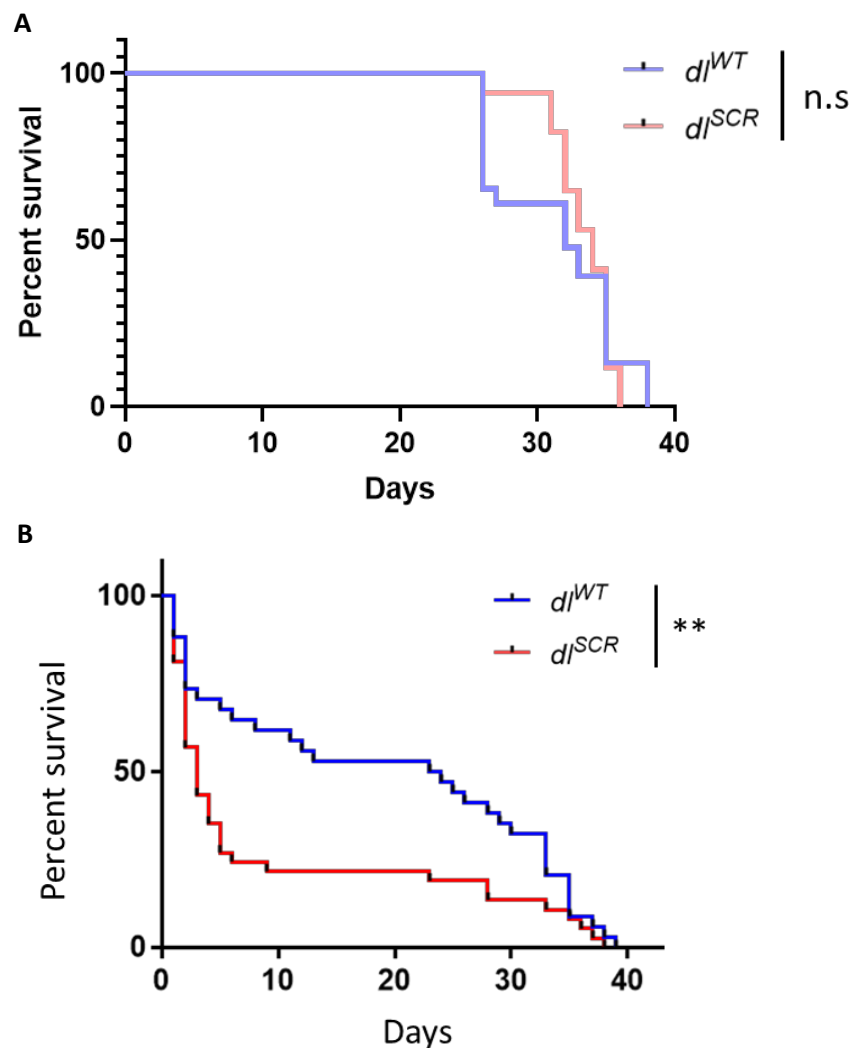


**Fig. III.2.  $dI^{SCR}$  animals are susceptible to infection.** Survival curves for uninfected animals at 29 °C is plotted in (A), for  $dI^{SCR}$  and  $dI^{WT}$ . Survival after *S. saprophyticus* infection was monitored, and is plotted in (B). Gehan-Breslow-Wilcoxon test,  $n = 3$ ,  $n = 30$ , (ns)  $> 0.05$ , (\*\*)  $P < 0.01$ .



### III.2.3 $dI^{SCR}$ animals are sensitive to starvation

The fat body is the seat of the primary immune response modulated by AMPs. It also integrates metabolic signals in the fly and facilitates the storage of nutrients. Since the increase in AMPs in the unchallenged state could possibly lead to a diversion of energy and resources, we wanted to test the response of these animals to starvation. 3–4 day old flies raised on normal media were deprived of both amino acids and sugars and their survival was monitored once every 12 hours.  $dI^{SCR}$  flies were significantly more sensitive to starvation in comparison to  $dI^{WT}$  and succumbed earlier than  $dI^{WT}$  flies (Fig. III.3). Therefore, the absence of SUMOylation of DL in these flies renders them more susceptible to starvation stress.

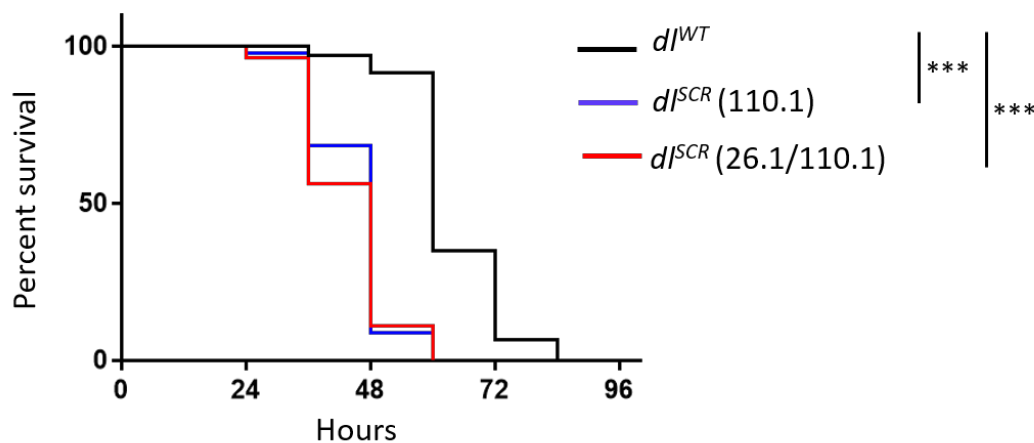


**Fig. III.3.  $dI^{SCR}$  animals are susceptible to starvation.** Kaplan-Meier survival curves for  $dI^{WT}$  and  $dI^{SCR}$  animals under starvation are shown.  $N = 3$ ,  $n = 30$ , Mantel-Cox test, (\*\*\*)  $P < 0.001$ .

### III.3 Discussion

Here, we looked at possible roles for SUMOylation of DL in the adult stress response. SUMOylation of DL was assessed under conditions of both immune and starvation stress. In  $dI^{SCR}$  animals, the Toll-responsive AMPs *Mtk* and *Drs* were upregulated in the absence of an immune challenge. Moreover,  $dI^{SCR}$  animals showed an increased susceptibility to infection with the gram-positive bacteria *Staphylococcus saprophyticus*.  $dI^{SCR}$  animals deprived of amino acids and sugar succumbed faster than  $dI^{WT}$ , indicating a lower resistance to starvation stress. Taken together, these results indicate that SUMOylation of DL may have evolved as a mechanism to confer a survival advantage to flies under immune and starvation

stress. Absence of SUMOylation of DL under basal conditions is also undesirable, mimicking a state sterile inflammation.

Previously, we have established that *dl<sup>SCR</sup>* is a stronger transcriptional activator in the haploinsufficient condition (Chapter 2) and in the larval immune response (Chapter 3). Animals lacking zygotic DL survive into adulthood and do not present with any apparent defects, indicating that DL is dispensable beyond the stages of early embryonic development (Meng *et al.* 1999). The zygotic roles of immunity for NF- $\kappa$ B are largely performed by Dif. Though the lack of DL is well tolerated, over-activation can lead to adverse effects including melanotic tumor formation (Qiu *et al.* 1998; Govind 1999). Therefore, it is conceivable that the low levels of DL in the adult are subjected to regulation via SUMOylation, to keep its activity in check. DL is known to dimerize with Dif (Gross *et al.*, 1996), and the DL<sup>SCR</sup>-Dif heterodimer may confer hyper-activity. In conclusion, SUMOylation of DL restores the fine balance of NF- $\kappa$ B factors in *Drosophila*.

### **III.4 Materials and Methods**

#### *Fly husbandry and stocks*

Flies were raised on standard cornmeal agar at 25 °C unless stated otherwise. *dl<sup>1</sup>/CyO* (3236) and *dl<sup>4</sup>/CyO* (7096) were procured from the Bloomington *Drosophila* Stock Centre.

#### *Starvation sensitivity assay*

3–4 day old mated males were transferred to a 1% agar media in batches of ~20 per vial. Survival was monitored every 12 hours. Survival curves were plotted using Graphpad Prism8.

#### *Infection and survival assays*

An overnight culture of *S. saprophyticus* adjusted to OD<sub>600</sub> = 100 was used to infect 5–7 day old males. Flies were infected at the sternopleural plate with insect pins dipped in the bacterial culture. They were allowed to recover, and survival was monitored daily at 29 °C (Dead flies after 3 hours of pricking were excluded from the analysis).

### Quantitative PCR

RNA was extracted from adult males (n = 10 /sample) using the RNeasy Plus Universal mini kit (Qiagen) according to the manufacturer's instructions. 1 µg of total RNA was used to generate cDNA using the High-Capacity cDNA Reverse Transcription kit (Thermo Fisher Scientific). The qPCR reaction was performed on a qTOWER<sup>3</sup> real-time thermal cycler (Analytik Jena) with KAPA SYBR FAST master mix (Sigma-Aldrich). Gene expression was monitored using gene-specific primers. Transcript levels were calculated using the comparative Ct method to obtain fold change values. Relative mRNA levels were calculated using the delta Ct values. Rp49 was used as a reference gene. The following primer pairs were used (Forward primer, F and reverse primer, R):

*rp49* F: GACGCTTCAAGGGACAGTATC, *rp49* R: AAACGCGGTTCTGCATGAG;

*mtk* F: GCTACATCAGTGCTGGCAGA, *mtk* R: TTAGGATTGAAGGGCGACGG;

*drs* F: CTGTCCGGAAGATACAAGGG, *drs* R: TCGCACCAGCACTTCAGACT

**III.5 Notes:** Role for DL in the adult are not well characterized.

### III.6 References

1. DiAngelo, J. R., Bland, M. L., Bambina, S., Cherry, S., & Birnbaum, M. J. (2009). The immune response attenuates growth and nutrient storage in *Drosophila* by reducing insulin signaling. *Proceedings of the National Academy of Sciences of the United States of America*, *106*(49), 20853–20858.  
<https://doi.org/10.1073/pnas.0906749106>
2. Drabikowski, K. (2020). Ubiquitin and SUMO Modifications in *Caenorhabditis elegans* Stress Response. *Current Issues in Molecular Biology*, *35*, 145–158.  
<https://doi.org/10.21775/cimb.035.145>
3. Dushay, M. S., & Eldon, E. D. (1998). *Drosophila* immune responses as models for human immunity. *American Journal of Human Genetics*, *62*(1), 10–14.  
<https://doi.org/10.1086/301694>

4. Enserink, J. M. (2015). Sumo and the cellular stress response. *Cell Division*, 10, 4. <https://doi.org/10.1186/s13008-015-0010-1>
5. Golebiowski, F., Matic, I., Tatham, M. H., Cole, C., Yin, Y., Nakamura, A., Cox, J., Barton, G. J., Mann, M., & Hay, R. T. (2009). System-wide changes to SUMO modifications in response to heat shock. *Science Signaling*, 2(72), ra24. <https://doi.org/10.1126/scisignal.2000282>
6. Govind, S. (1999). Control of development and immunity by rel transcription factors in Drosophila. *Oncogene*, 18(49), 6875–6887. <https://doi.org/10.1038/sj.onc.1203223>
7. Govind, S. (2008). Innate immunity in Drosophila: Pathogens and pathways. *Insect Science*. <https://onlinelibrary.wiley.com/doi/abs/10.1111/j.1744-7917.2008.00185.x>
8. Gross, I., Georgel, P., Kappler, C., Reichhart, J.-M., & Hoffmann, J. A. (1996). Drosophila Immunity: A Comparative Analysis of the Rel Proteins Dorsal and Dif in the Induction of the Genes Encoding Diptericin and Cecropin. *Nucleic Acids Research*, 24(7), 1238–1245. <https://doi.org/10.1093/nar/24.7.1238>
9. Ip, Y. T., Reach, M., Engstrom, Y., Kadalayil, L., Cai, H., González-Crespo, S., Tatei, K., & Levine, M. (1993). Dif, a dorsal-related gene that mediates an immune response in Drosophila. *Cell*, 75(4), 753–763. [https://doi.org/10.1016/0092-8674\(93\)90495-c](https://doi.org/10.1016/0092-8674(93)90495-c)
10. Lemaitre, B., Meister, M., Govind, S., Georgel, P., Steward, R., Reichhart, J. M., & Hoffmann, J. A. (1995). Functional analysis and regulation of nuclear import of dorsal during the immune response in Drosophila. *The EMBO Journal*, 14(3), 536–545. <https://www.ncbi.nlm.nih.gov/pubmed/7859742>
11. Meng, X., Khanuja, B. S., & Ip, Y. T. (1999). Toll receptor-mediated Drosophila immune response requires Dif, an NF-kappaB factor. *Genes & Development*, 13(7), 792–797. <https://doi.org/10.1101/gad.13.7.792>
12. Petersen, U. M., Björklund, G., Ip, Y. T., & Engström, Y. (1995). The dorsal-related immunity factor, Dif, is a sequence-specific trans-activator of Drosophila Cecropin gene expression. *The EMBO Journal*, 14(13), 3146–3158. <https://www.ncbi.nlm.nih.gov/pubmed/7621828>
13. Qiu, P., Pan, P. C., & Govind, S. (1998). A role for the Drosophila Toll/Cactus pathway in larval hematopoiesis. *Development*, 125(10), 1909–1920. <https://www.ncbi.nlm.nih.gov/pubmed/9550723>

14. Roth, S. W., Bitterman, M. D., Birnbaum, M. J., & Bland, M. L. (2018). Innate Immune Signaling in *Drosophila* Blocks Insulin Signaling by Uncoupling PI(3,4,5)P3 Production and Akt Activation. *Cell Reports*, 22(10), 2550–2556. <https://doi.org/10.1016/j.celrep.2018.02.033>
15. Rutschmann, S., Jung, A. C., Hetru, C., Reichhart, J. M., Hoffmann, J. A., & Ferrandon, D. (2000). The Rel protein DIF mediates the antifungal but not the antibacterial host defense in *Drosophila*. *Immunity*, 12(5), 569–580. [https://doi.org/10.1016/s1074-7613\(00\)80208-3](https://doi.org/10.1016/s1074-7613(00)80208-3)
16. Rutschmann, Sophie, Kilinc, A., & Ferrandon, D. (2002). Cutting edge: the toll pathway is required for resistance to gram-positive bacterial infections in *Drosophila*. *Journal of Immunology*, 168(4), 1542–1546. <https://doi.org/10.4049/jimmunol.168.4.1542>
17. Ryu, H.-Y., Ahn, S. H., & Hochstrasser, M. (2020). SUMO and cellular adaptive mechanisms. *Experimental & Molecular Medicine*, 52(6), 931–939. <https://doi.org/10.1038/s12276-020-0457-2>
18. Suzawa, M., Muhammad, N. M., Joseph, B. S., & Bland, M. L. (2019). The Toll Signaling Pathway Targets the Insulin-like Peptide Dilp6 to Inhibit Growth in *Drosophila*. *Cell Reports*, 28(6), 1439-1446.e5. <https://doi.org/10.1016/j.celrep.2019.07.015>
19. Wu, L. P., & Anderson, K. V. (1998). Regulated nuclear import of Rel proteins in the *Drosophila* immune response. *Nature*, 392(6671), 93–97. <https://doi.org/10.1038/32195>